UNIVERSITÉ DE LILLE

Présentée en vue d'obtenir le grade de DOCTEUR

Par

ZHU Chun

En

Spécialité : Informatique, Automatique

DOCTORAT délivré par l'Université de Lille

Titre de la thèse :

A Restoration of incomplete and degraded Costume Relics Using AI techniques

Une restauration de reliques de costumes incomplètes et dégradées à l'aide de techniques d'intelligence artificielle

Soutenue le 19/12/2025 devant le jury d'examen :

Président /Examinateur	Abdelmalik TALEB-AHMED, Professeur de Université Polytechnique de Haut de France
Rapporteur	Dominique ADOLPHE, Professeur de Université de Haute Alsace
Rapporteure	Isis TRUCK , Professeur de Université de Paris 8
Examinateur	Dr. Guillaume BRUNIAUX, Université de La Rochelle
Directeur de thèse	Pascal BRUNIAUX, Professeur des universités, ENSAIT
Co-directeur de thèse	Xianyi ZENG, Professeur des universités, ENSAIT

Thèse préparée dans le Laboratoire GEMTEX – Laboratoire de Génie et Matériaux Textiles École Doctorale : MADIS - Science Pour l'Ingénieur Lille Nord-de-France

ABSTRACT

As carriers of historical, cultural, and social information, garment relics offer valuable insight into past societies. However, due to long-term exposure to environmental factors and human activities, these artifacts often undergo significant degradation, leading to the loss or distortion of key attributes such as style, pattern, color, and structural composition. Traditional restoration methods rely heavily on the manual expertise of archaeologists and textile conservators, which can result in inefficiencies, inconsistencies, and limited reproducibility. In recent years, advancements in artificial intelligence (AI) and computational technologies have provided new tools to support the digital preservation and intelligent restoration of costume relics.

In this context, my doctoral research leveraged the scientific research platform of the GEMTEX laboratory at the École Nationale Supérieure des Arts et Industries Textiles, collaborating with Xi'an Polytechnic University's extensive expertise in the field of apparel scientific archaeology and digital restoration, as well as the rich cultural relic resources and practical restoration experience of the Shaanxi History Museum, to jointly carry out the research project titled "A Restoration of incomplete and degraded Costume Relics Using AI techniques". My PhD study aims to develop an AI-based restoration framework for ancient garment relics by systematically applying deep learning models to achieve accurate, automatic, and reproducible restoration processes. By integrating multidisciplinary knowledge from archaeology, textile science, computer vision, and artificial intelligence, this study seeks to enhance the efficiency and precision of restoring damaged or incomplete elements in cultural artifacts, while also supporting long-term digital heritage preservation.

The study is structured around three core objectives: (1) constructing intelligent restoration models based on deep learning to reconstruct visual features such as styles, patterns, colors, and structural forms; (2) developing a practical restoration system that supports digital protection and cultural heritage dissemination; and (3) establishing a comprehensive 3D database of unearthed Chinese garment relics across different dynasties to facilitate further research and cross-disciplinary collaboration.

A series of AI models were developed to support various aspects of the restoration process. For the reconstruction of styles and patterns, a Deep Convolutional Generative

Adversarial Network (DCGAN) was utilized to infer and regenerate missing or obscured features based on learned visual representations from existing datasets. To recover faded or lost color information, a Deep Convolutional Long Short-Term Memory Network (DCLSTNet) was designed to predict original color schemes by modeling temporal and spatial variations from excavation records and surviving fragments. For structural restoration, an interactive method combining X-ray scanning and machine learning techniques was employed to reconstruct the internal configuration and support three-dimensional digital modeling.

The proposed restoration models were subjected to iterative training and testing, with optimization processes aimed at improving their accuracy and robustness. Experimental results showed that the DCGAN model could effectively restore worn or missing decorative elements in complex textile patterns. The DCLSTNet model demonstrated promising performance in color reconstruction, particularly when used in conjunction with pigment residue analysis and photographic records. The structure restoration method, supported by non-destructive imaging and supervised learning algorithms, allowed for the reconstruction of hidden garment structures, contributing to the digital archiving and visualization of unearthed garment relics.

A key outcome of this research was the development of an integrated restoration system that brings together these AI models in a modular and user-friendly interface. This system not only supports restoration professionals in analyzing and processing damaged relics but also serves as a platform for storing and managing the 3D models and restoration data. As part of the project, a database was constructed featuring high-fidelity digital records of Chinese garment relics from multiple dynastic periods, offering a valuable resource for researchers in cultural heritage, design history, and digital humanities.

While this study provides a practical approach to the automated restoration of textile cultural relics, it also contributes to the theoretical understanding of textile degradation and the application of AI in heritage conservation. However, the outcomes should be viewed within the scope of their current limitations. For instance, the restoration models rely heavily on the availability and quality of input data, and their generalizability across different types of fabrics and historical contexts requires further exploration. Additionally, although the AI models demonstrate notable accuracy in pattern and color restoration, they are not yet capable of fully replacing expert judgment in nuanced interpretative scenarios.

The innovation of this research lies in the integration of deep learning into cultural heritage restoration, specifically: (1) the use of DCGAN to reconstruct intricate styles and motifs in textile relics; (2) the application of a time-series network (DCLSTNet) to restore color information based on excavation data and artifact conditions; and (3) the combination of X-ray imaging with machine learning for structural analysis and reverse modeling of garments. These innovations enhance the automation and objectivity of the restoration process while offering new avenues for the digital preservation of fragile and incomplete textile artifacts.

Overall, this Phd study demonstrates the feasibility and potential of AI-based approaches in supporting the digital protection and interpretation of costume cultural heritage. By integrating data-driven models with archaeological insight, the research offers a replicable framework for improving restoration practices and enhancing access to historical artifacts through virtual platforms. Future work will focus on refining the models with larger and more diverse datasets, enhancing model interpretability, and expanding system usability across different cultural heritage institutions.

KEY WORDS： costume relics, degradation, digital restoration; artificial intelligence; 3D modeling; style restoration; pattern restoration; structural restoration, cultural heritage preservation

RÉSUMÉ

En tant que vecteurs d'informations historiques, culturelles et sociales, les reliques vestimentaires offrent un éclairage précieux sur les sociétés du passé. Cependant, en raison d'une exposition prolongée aux facteurs environnementaux et aux activités humaines, ces artefacts subissent souvent une dégradation importante, entraînant la perte ou l'altération d'attributs clés tels que le style, les motifs, les couleurs et la composition structurelle. Les méthodes de restauration traditionnelles reposent fortement sur l'expertise manuelle des archéologues et des restaurateurs textiles, ce qui peut engendrer des inefficacités, des incohérences et une reproductibilité limitée. Ces dernières années, les progrès de l'intelligence artificielle (IA) et des technologies computationnelles ont apporté de nouveaux outils pour soutenir la préservation numérique et la restauration intelligente des reliques de costumes.

Dans ce contexte, ma recherche doctorale s'est appuyée sur la plateforme scientifique du laboratoire GEMTEX de l'École Nationale Supérieure des Arts et Industries Textiles (ENSAIT), en collaboration avec l'expertise approfondie de l'Université Polytechnique de Xi'an dans le domaine de l'archéologie scientifique de l'habillement et de la restauration numérique, ainsi qu'avec les riches ressources patrimoniales et l'expérience pratique de restauration du Musée d'Histoire du Shaanxi, afin de mener conjointement le projet intitulé « Restoration of incomplete and degraded Costume Relics Using AI techniques ». Mon doctorat vise à développer un cadre de restauration des reliques vestimentaires anciennes fondé sur l'IA, en appliquant de manière systématique des modèles d'apprentissage profond afin d'obtenir des processus de restauration précis, automatiques et reproductibles. En intégrant des connaissances pluridisciplinaires issues de l'archéologie, des sciences textiles, de la vision par ordinateur et de l'intelligence artificielle, cette étude cherche à améliorer l'efficacité et la précision de la reconstitution des éléments endommagés ou incomplets des artefacts culturels, tout en soutenant la préservation à long terme du patrimoine numérique.

L'étude s'articule autour de trois objectifs principaux : (1) construire des modèles de restauration intelligents basés sur l'apprentissage profond pour reconstruire des caractéristiques visuelles telles que les styles, les motifs, les couleurs et les formes structurelles ; (2) développer un système de restauration opérationnel soutenant la

protection numérique et la diffusion du patrimoine culturel ; et (3) établir une base de données 3D exhaustive de reliques vestimentaires chinoises mises au jour, couvrant différentes dynasties, afin de faciliter des recherches ultérieures et la collaboration interdisciplinaire.

Une série de modèles d'IA a été développée pour soutenir divers aspects du processus de restauration. Pour la reconstruction des styles et des motifs, un réseau antagoniste génératif convolutionnel profond (Deep Convolutional Generative Adversarial Network, DCGAN) a été utilisé afin d'inférer et de régénérer les caractéristiques manquantes ou masquées à partir de représentations visuelles apprises sur des jeux de données existants. Pour la récupération d'informations colorimétriques estompées ou perdues, un réseau convolutionnel profond à mémoire à long terme de type LSTM (Deep Convolutional Long Short-Term Memory Network, DCLSTNet) a été conçu pour prédire les schémas chromatiques d'origine en modélisant les variations temporelles et spatiales issues des relevés de fouille et des fragments conservés. Pour la restauration structurelle, une méthode interactive combinant la tomographie aux rayons X et des techniques d'apprentissage automatique a été employée afin de reconstruire la configuration interne et de soutenir la modélisation numérique tridimensionnelle.

Les modèles de restauration proposés ont fait l'objet d'entraînements et de tests itératifs, avec des processus d'optimisation visant à améliorer leur précision et leur robustesse. Les résultats expérimentaux ont montré que le modèle DCGAN pouvait restaurer efficacement des éléments décoratifs usés ou manquants au sein de motifs textiles complexes. Le modèle DCLSTNet a démontré des performances prometteuses pour la reconstitution des couleurs, en particulier lorsqu'il était utilisé conjointement avec l'analyse des résidus de pigments et les archives photographiques. La méthode de restauration structurelle, soutenue par une imagerie non destructive et des algorithmes d'apprentissage supervisé, a permis la reconstitution de structures vestimentaires dissimulées, contribuant ainsi à l'archivage numérique et à la visualisation des reliques vestimentaires exhumées.

Un résultat majeur de cette recherche a été le développement d'un système de restauration intégré réunissant ces modèles d'IA au sein d'une interface modulaire et conviviale. Ce système soutient non seulement les professionnels de la restauration dans l'analyse et le traitement des reliques endommagées, mais sert également de plateforme de stockage et de gestion des modèles 3D et des données de restauration.

Dans le cadre du projet, une base de données a été construite, comprenant des enregistrements numériques de haute fidélité de reliques vestimentaires chinoises issues de multiples périodes dynastiques, offrant ainsi une ressource précieuse pour les chercheurs en patrimoine culturel, en histoire du design et en humanités numériques.

Bien que cette étude propose une approche pratique de la restauration automatisée des reliques textiles, elle contribue également à la compréhension théorique de la dégradation textile et à l'application de l'IA à la conservation du patrimoine. Toutefois, les résultats doivent être considérés au regard des limites actuelles. Par exemple, les modèles de restauration dépendent fortement de la disponibilité et de la qualité des données d'entrée, et leur généralisabilité à différents types de tissus et contextes historiques nécessite des investigations supplémentaires. De plus, bien que les modèles d'IA affichent une précision notable pour la restauration des motifs et des couleurs, ils ne sont pas encore en mesure de remplacer entièrement le jugement d'experts dans des situations interprétatives nuancées.

L'innovation de cette recherche réside dans l'intégration de l'apprentissage profond à la restauration du patrimoine culturel, notamment : (1) l'utilisation d'un DCGAN pour reconstruire des styles et des motifs complexes dans les reliques textiles ; (2) l'application d'un réseau de séries temporelles (DCLSTNet) pour restaurer les informations colorimétriques à partir des données de fouille et de l'état des artefacts ; et (3) la combinaison de l'imagerie aux rayons X et de l'apprentissage automatique pour l'analyse structurelle et la rétro-modélisation des vêtements. Ces innovations renforcent l'automatisation et l'objectivité du processus de restauration, tout en ouvrant de nouvelles perspectives pour la préservation numérique d'artefacts textiles fragiles et incomplets.

Dans l'ensemble, ce doctorat démontre la faisabilité et le potentiel des approches fondées sur l'IA pour soutenir la protection numérique et l'interprétation du patrimoine vestimentaire. En combinant des modèles pilotés par les données et une expertise archéologique, cette recherche propose un cadre reproductible visant à améliorer les pratiques de restauration et à accroître l'accès aux artefacts historiques via des plateformes virtuelles. Les travaux futurs porteront sur l'affinement des modèles grâce à des jeux de données plus vastes et plus diversifiés, l'amélioration de l'interprétabilité des modèles et l'extension de l'utilisabilité du système à différents établissements patrimoniaux.

Mots-clés : reliques vestimentaires ; dégradation ; restauration numérique ; intelligence artificielle ; modélisation 3D ; restauration du style ; restauration des motifs ; restauration structurelle ; préservation du patrimoine culturel.

Contents

LIST OF ABBREVIATIONS

3D	Three Dimensional
AR	Augmented Reality
AC	Area Constraints
BC	Boundary dimension Constraints
BiLSTM	Bi-directional Long Short-Term Memory
cGAN	Conditional Generative Adversarial Networks
CNN	Convolutional Neural Networks
CT	Computed Tomography
CAD	Computer-Aided Design
D	Discriminator
DCGAN	Deep Convolutional Generative Adversarial Networks
DBSCAN	Density Based Spatial Clustering of Applications with Noise
DCLSTNet	Deep Convolution Long and Short-Term time series divine Network
DR	Dimensional Rationality
DC-LSTM	Deep Convolutional Long Short-Term Memory Network
FID	Fréchet Inception Distance
G	Generator and Discriminator
GRU	Gated Recurrent Unit
GANs	Generative Adversarial Networks
GNNs	Graph Neural Networks
HVS	Human Visual System
LSTM	Long Short-Term Memory Networks
MAE	Mean Absolute Error
PSNR	Peak Signal-to-Noise Ratio
Pix2Pix	Image to Image Translation with Conditional Adverse Networks
RMSE	Root Mean Square Error
SSIM	Structural Similarity
SMD	Shape Matching Degree
SRI	Sample Restoration Index
UNESCO	United Nations Educational, Scientific and Cultural Organization
U-Net	Convolutional Networks for Biomedical Image Segmentation

VAE	Variational Auto Encoder
VR	Virtual Reality

Chapter 1 Introduction

1.1 Context

As an important material carrier of human civilization, garment relics not only record the social systems, production technologies, aesthetic concepts, and cultural exchanges of different historical periods, but also serve as "living fossils" for studying ancient economic forms, technological inheritance, and ethnic migration. According to the statistics of United Nations Educational, Scientific and Cultural Organization (UNESCO), there are more than 8 million textile cultural relics in museums around the world, including 536000 pieces/set of movable textile cultural relics in China (the Survey Report of Cultural Relics Resources in 2021 issued by the National Cultural Heritage Administration). Its age spans from the pieces of Kubu in the Neolithic Age to the dragon robe and red dress in the Ming and Qing Dynasties, forming the largest and most complete costume cultural heritage system in the world. However, these precious heritages that carry a millennium of civilization are facing a severe survival crisis: archaeological data shows that over 63% of excavated textiles have structural damage (such as fiber breakage and fabric delamination), 78% of dyed artifacts have severe discoloration, and more than 90% of needle details in artifacts with complex embroidery techniques are difficult to identify[1, 2]. This systematic deterioration not only leads to the loss of information about cultural relics, but also puts the restoration research of ancient textile techniques in a dilemma of "cooking without rice".

The problem of protecting costume relics is rooted in the complex interaction between their material characteristics and preservation environment. From the perspective of materials science, ancient costume often used natural organic materials such as silk, hemp, cotton, and wool. The chemical structures of these materials, such as the beta folded layers of silk and the cellulose crystals of plant fibers, undergo multiple degradation mechanisms such as hydrolysis, oxidation, and photodegradation when buried in the environment. Taking the plain silk robe unearthed from the Mawangdui Han Tomb as an example, the polymerization degree of its silk fibers has decreased from the original value of over 2000 to less than 500 [3], resulting in a loss of about 75% of the fabric strength. The role of environmental factors is more spatially

and temporally heterogeneous: textiles in arid northwest regions (such as the Niya site in Xinjiang) often undergo fiber brittleness due to salt crystallization, while the humid and hot environment in the south (such as the Haihun Marquis Tomb in Jiangxi Province) accelerates microbial degradation processes. The degradation dynamics of this multi-scale and multi physics field make it difficult for traditional empirical protection strategies to establish universal intervention criteria. As shown in Figure 1-1, most of the burial costumes were unearthed with serious color degeneration and incomplete styles.

Figure 1-1 Unearthed broken costume artifacts

The field of international cultural heritage protection is undergoing a profound paradigm shift. The "Declaration on the Protection of Cultural Heritage in the Digital Age" released by UNESCO in 2018 clearly stated that by 2030, it is necessary to achieve full coverage of "digital twins" of important cultural heritage worldwide. In this context, the integration of computer vision, artificial intelligence, and 3D reconstruction technology is reshaping the methodological system of cultural relic protection. In the field of 2D cultural relic restoration, Generative Adversarial Networks (GANs) have been successfully applied to the restoration of Dunhuang mural defects [4] and the completion of oracle bone inscriptions [5], with Peak Signal-to-Noise Ratio (PSNR) values exceeding 35dB. However, there is a lack of systematic research on intelligent restoration and 3D reconstruction in the field of costume relics. The main reason is that there are few researchers with interdisciplinary backgrounds in this field,

who understand both computer science and costume archaeology, costume culture, costume design and production.

The restoration of traditional costume relics has long relied on an experiential model of "mentorship". Restoration masters need to accumulate decades of practical experience to proficiently master core skills such as fabric splicing, pigment painting, and structural reinforcement. This restoration method, which relies on individual experience, although to some extent achieves the physical continuity of cultural relics, has insurmountable limitations: firstly, the subjectivity of the restoration process is strong, and different restorers have different understandings of the original appearance of cultural relics and preferences for technical styles, which may lead to deviations between the restoration results and the historical original appearance, and even problems such as excessive restoration or distorted restoration. For example, when a certain cultural relic institution was repairing a Ming Dynasty(1368 - 1644) embroidered garment, due to the insufficient knowledge of Ming Dynasty(1368 - 1644) embroidery stitches by the restorer, the common seed embroidery technique of the Qing Dynasty (1644 - 1912) was used to fill in the missing parts, resulting in damage to the historical authenticity of the cultural relic; Secondly, the restoration efficiency is extremely low. A moderately damaged piece of costume relics often requires restoration technicians to invest months or even years of manual operation, which is difficult to meet the rescue and protection needs of a large number of endangered costume relics. Taking the Tang Dynasty(618–907) Lianzhu patterned brocade flags collected by Dunhuang Academy as an example, the fabric fibers have become severely brittle, with over one-third of the edges damaged. The initial fiber reinforcement and debris sorting work alone took nearly two years, greatly restricting the timeliness of cultural relic research and display; Thirdly, the inheritance of restoration techniques is facing a crisis of discontinuity. Traditional restoration techniques require extremely high levels of patience, focus, and manual skills from practitioners, and have long training periods and low economic benefits, resulting in a sharp decline in the number of young practitioners. Many special restoration techniques that are on the brink of extinction are gradually disappearing with the retirement of the older generation of restorers, and the restoration of costume relics is facing the dilemma of "death of people and extinction of art".

Currently, artificial intelligence, 3D modeling, and computer technology are increasingly becoming indispensable means in the restoration of damaged costume

relics. Traditional restoration methods often rely on manual labor and experience, and when faced with fragile, structurally complex, and severely damaged ancient fabrics, it is often difficult to accurately restore their original shape and details. AI technology can analyze fragment patterns, colors, and weaving structures through image recognition and deep learning, infer the shape and material of missing parts, and achieve more scientific "virtual restoration"; 3D scanning and modeling can accurately record the three-dimensional form of cultural relics, assist in restoring their spatial structure and wearing dynamics, and even reproduce the state of fabrics under different conditions through digital simulation. At the same time, computer technology provides a systematic data support and visual operation platform for the entire repair process, making the restoration process reversible, traceable, and verifiable. The integration of these technologies not only improves the accuracy and operability of restoration, but also expands new dimensions for the protection, research, and display of cultural heritage while preserving the authenticity of cultural relics to the greatest extent possible, revitalizing the remaining fabric remains with historical vitality.

In this context, the core objective of this doctoral research is to systematically construct and validate a digital restoration methodology and practical framework for damaged costume relics based on artificial intelligence technology, in order to solve the core bottleneck problems of subjectivity, low efficiency, and irreversibility in traditional experiential restoration models. This Phd study aims to explore key scientific challenges and solutions in the restoration of costume relics through interdisciplinary exploration and integration of cutting-edge technologies such as computer vision, deep learning, and 3D modeling. It aims to achieve intelligent and accurate restoration and digital preservation of the shape, color, and structure of damaged costume relics, forming a scalable and replicable "digital humanities" paradigm, establishing permanent digital archives for endangered costume cultural heritage, and promoting the evolution of cultural relic restoration from a "skill" to a "precision discipline" that integrates science, art, and history. This will provide innovative technological solutions for the field of cultural heritage protection, promote the deep integration of traditional restoration techniques and modern technology, and help the sustainable inheritance and development of costume cultural heritage worldwide.

1.2 Motivation and problem statement

The protection and restoration of costume relics is not only a technical challenge, but also an ethical responsibility for the continuation of human civilization. Under the dual impact of globalization and digital civilization, cultural heritage protection is undergoing a paradigm shift from material entity preservation to digital information inheritance. However, the existing technological system exposes deep-seated structural contradictions when facing the special object of costume relics. The "experience black box" of traditional manual repair and the "data gap" of digital technology are intertwined, forming a triple paradox that hinders the development of disciplines. The solution to this dilemma requires a re-examination of the essential demands of cultural relic protection from the perspective of technological philosophy, and the construction of an intelligent restoration paradigm with cultural adaptability. The current practice of protecting costume relics faces three challenges: firstly, the traditional experience driven restoration model has inherent shortcomings such as strong subjectivity (restoration accuracy relies on expert experience), poor reversibility (irreversible physical intervention), and low efficiency (single item restoration cycle often takes several months); Secondly, existing digital restoration technologies mostly focus on completing two-dimensional images, lacking systematic modeling capabilities for the three-dimensional structural features of costume relics; Thirdly, there is a lack of interdisciplinary research depth, which has prevented the effective establishment of digital restoration models.

With the support of Xi'an Polytechnic University, which specializes in apparel scientific archaeology and digital restoration, and the Shaanxi History Museum, which provides a large collection of incomplete ancient garment images and textile samples, I established a research framework based on the provided data and conducted a comprehensive analysis.

As a result, my PhD research proposes an an AI based intelligent restoration technology for incomplete costume styles and textile patterns, severe color fading, and overall adhesion of unearthed costume relics. By constructing multi-dimensional models for the intelligent restoration of costume styles, textile patterns, color reconstruction, and structural repair, this study enables the digital restoration of incomplete costume forms, original colors, and sewing patterns that cannot be physically unfolded or separated. Based on the restoration and restoration results of

costume styles, textile patterns, colors, and garment sewing pattern, the overall restoration and display of costume relics can be achieved. The research is divided into four parts: ① Construction of intelligent restoration models for costume relics' styles and textile patterns; ② Construction of intelligent color restoration model for costume relics; ③ Modeling of intelligent restoration model for costume relics structure; ④ Verification, optimization, and application of restoration and restoration techniques for costume relics. To avoid confusion, the costume styles, patterns, and structural descriptions in this paper are shown in Figures 1-5.

Figure 1-2 Costume styles, Textile pattern, and Garment sewing pattern

⑴ Construction of intelligent restoration model for costume relics' styles and textile patterns

Most of the costume artifacts unearthed were severely deteriorated, making it difficult to extract costume styles and textile patterns. Data acquisition, feature extraction, and intelligent restoration algorithms have a significant impact on the accuracy of costume and cultural relic style and tetxtile pattern restoration. Therefore, how to construct a mathematical model that can effectively handle style diversity and pattern details, overcome the influence of data sparsity and noise interference on the model, achieve intelligent restoration of costume styles and textile patterns, ensure the accuracy, authenticity, and cultural conformity of the restoration results, is one of the key scientific problems to be solved in the project.

⑵ Construction of an intelligent color restoration model for costume relics

The burial environment of garment relics before excavation is complex, and there are multiple factors that affect color changes, such as dye type, fabric type, duration of time, temperature and humidity, etc; The deterioration of costume colors also occurs in multiple directions simultaneously, such as darkening, fading, and color degeneration. In addition, the accuracy of different artificial intelligence algorithms in restoring the

colors of costume relics varies greatly. Therefore, how to accurately analyze the relationship between the color degradation of costume relics and time factors, construct a mathematical model for intelligent color restoration of costume relics, and accurately restore the original color of costume relics is one of the key scientific problems to be solved in the project.

⑶ Modeling of intelligent restoration model for costume relics structure

After the excavation of costume relics, most of them are stuck together, and the surface structural lines are blurred and deteriorated. Especially, the sewing thread traces in hidden parts are extremely difficult to obtain without destructive unfolding, which hinders the accurate restoration of the structural technology of costume relics. In addition, different methods of unfolding structural lines also affect the reliability of the restoration of the structure and craftsmanship of costume relics. Therefore, one of the key scientific problems to be solved in the project is how to obtain the trend and type of sewing threads inside the costume culture without damaging the costume relics, and then apply what artificial intelligence algorithm to intelligently flatten the chaotic internal structural threads of the costume relics into a complete and accurate costume structure diagram.

⑷ Verification, optimization, and application of restoration and restoration techniques for costume relics

At present, a large number of ancient Chinese garment relics have been unearthed, but the integrity of the relics varies greatly, and the severity of color degradation varies. This poses a challenge for the practical application of intelligent restoration of incomplete and severely faded garment relics proposed in this study. The accuracy and reliability of the restoration also directly affect future generations' understanding of ancient Chinese costume. Therefore, how to use the large number of unearthed garment relics as a real validation dataset to test the reliability and accuracy of the intelligent restoration and restoration technology for garment relics proposed in this study, and further optimize the technology based on the results is one of the key scientific problems that the project intends to solve.

1.3 Contributions

In ancient Chinese sayings, "costume" ranks first in "food, costume, housing, and transportation". Especially in ancient times when material and cultural resources were

relatively scarce, costume was not only a basic need for people to cover their shame and body, but also a symbol of social identity, status, and cultural traditions. Therefore, textile cultural relics are not only witnessing to history, but also important carriers for understanding ancient social, economic, cultural, political and other aspects, and have significant value for understanding the development process of human civilization. The era of artificial intelligence has brought many changes to costume archaeology and restoration, promoting the rational excavation and protection of ancient costume culture, and inheriting and promoting excellent human culture. Compared with traditional methods, the restoration methods of garment cultural relics based on AI technology proposed in this study has the advantages of high efficiency, speed, accuracy, automation, and intelligence (see Figure 1-3).

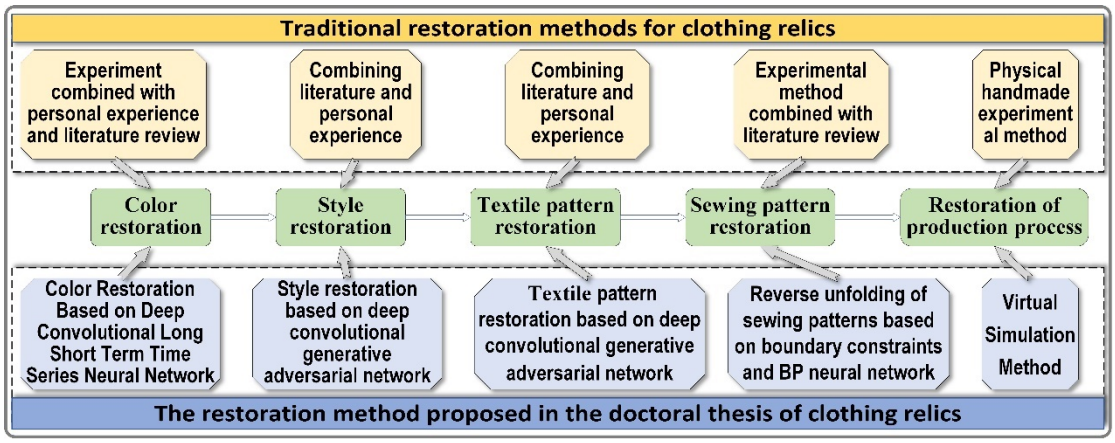

Figure 1-3 Comparison between the archaeological method of garment relics proposed in this study and traditional methods

(1) Contributions 1: Intelligent restoration of costume relics' styles and textile patterns

This Phd study has made a methodological advancement in the visual information restoration of costume relics, proposing an intelligent restoration model for styles and patterns based on deep convolutional generative adversarial network (DCGAN). In response to the core problem of traditional restoration methods relying heavily on expert experience and difficulty in ensuring style consistency and artistic accuracy in complex and incomplete areas, this model uses deep networks to autonomously learn the inherent characteristics and distribution patterns of patterns and styles from massive costume data, achieving high-precision and high style consistency content generation and completion for incomplete areas. This study transforms costume restoration from a

traditional "experience driven" paradigm to a "data-driven" intelligent paradigm, significantly improving the objectivity, accuracy, and efficiency of restoration work.

⑵ Contributions 2: Dynamic restoration and prediction of fading process of costume relics

In the field of color restoration of costume relics, this study constructed a color intelligent restoration model based on deep convolutional long short-term memory network (DCLSTNet), which for the first time achieved dynamic modeling and reverse prediction of color aging process. Unlike traditional methods that rely solely on the current state for static inference, this innovation fully utilizes the dual advantages of DCLSTNet in spatial feature extraction and time series modeling, accurately learning the nonlinear decay law of costume colors over time. This can not only accurately restore the color of severely faded cultural relics, but also "trace back" their color evolution trajectory, achieve scientific prediction of the original color of cultural relics, and provide a new technological path for reproducing the historical authenticity of costume.

⑶ Contributions 3: Non destructive reverse restoration of hidden structures in costume artifacts

To achieve non-destructive exploration of the internal structure of fragile cultural relics, this study proposes an interactive reverse reconstruction method that integrates X-ray scanning and machine learning techniques. This method overcomes the technical bottleneck of traditional physical dissection methods causing damage to stacked and fragile cultural relics. By non-destructive X-ray scanning, two-dimensional projection data of the internal structure of cultural relics are obtained, and a trained machine learning model is used to intelligently map and reconstruct it into an accurate three-dimensional virtual structure, thus achieving "non-invasive dissection" of the hidden structure of costume relics. This method ultimately achieved fast and accurate 3D digital restoration of the structure of costume relics, providing a revolutionary analysis tool for the structural research, protection and restoration, and virtual display of cultural relics.

1.4 Thesis roadmap

The research technology roadmap of this study is shown in Figure 1-4, specifically focusing on the four main archaeological stages of costume styles, textile pattern, color,

and sewing pattern. In response to the current problems faced by costume archaeology, such as strong empirical, speculative, weak scientific basis, and shallow integration with computer technology, costume archaeology is deeply integrated with technologies such as artificial intelligence, human-computer interaction, and reverse engineering. Key technologies such as intelligent restoration of style and textile pattern, intelligent restoration of color, and intelligent interactive reverse restoration of structure are proposed. The content is interrelated, and the entire process of costume cultural relic restoration and restoration is automated and intelligent.

This doctoral thesis is divided into 7 chapters, and the relationship between each chapter is shown in Figure 1-5. The specific introduction is as follows:

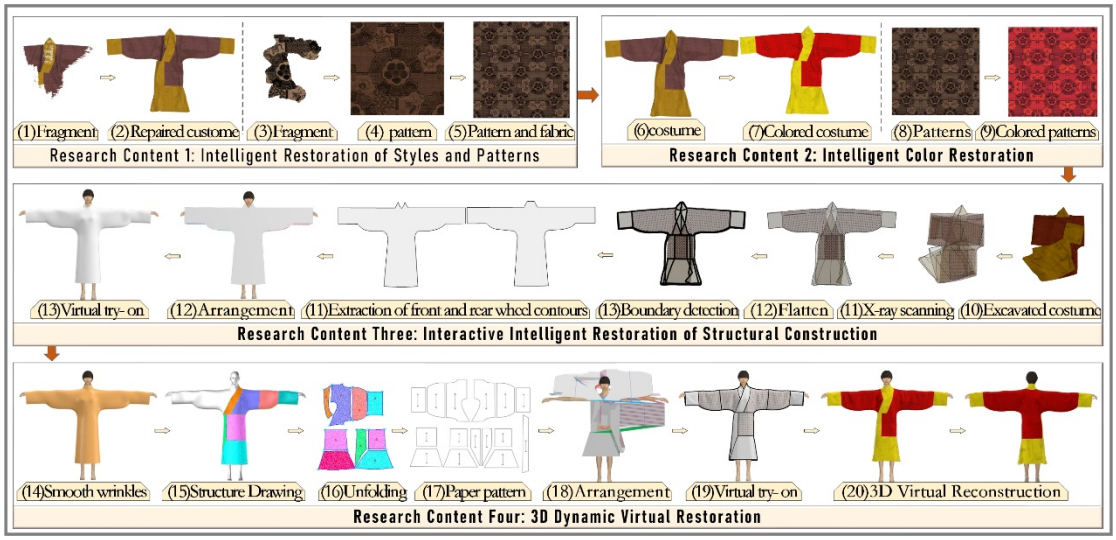

Figure 1-4 Technical roadmap of this study

Chapter 1: Introduction. This Phd study elaborates on the relevant background and significance of this study, reviews the research status of the modeling and intelligent restoration technology of costume relics at home and abroad, summarizes the shortcomings of current research in this direction, and proposes the research content, methods, and ideas of this study.

Chapter 2: Background and Literature Review. This study elaborates on the basic principles of traditional computing tools and artificial intelligence algorithms involved, and further analyzes their advantages, disadvantages, usage conditions, and scope. It establishes which model to use to construct a model for the degradation and intelligent restoration of costume relics.

Chapter 3: Intelligent restoration model for incomplete and degraded costume relics' styles and textile patterns. By analyzing the degradation process of costume relics styles and patterns, a style and pattern intelligent restoration model based on deep convolutional generative adversarial network is constructed to achieve rapid and intelligent restoration of costume relics styles and patterns.

Chapter 4: Intelligent restoration model for incomplete and degraded costume relics' colors. By revealing the relationship between the color degradation process of costume relics and time, a mathematical model of color degradation based on deep convolutional long short-term time series neural network is constructed to achieve intelligent and automatic restoration of costume relics colors.

Chapter 5: Intelligent restoration method for incomplete and degraded costume relics' sewing patterns. By using X-ray tomography technology combined with deep learning algorithms, non-destructive testing and feature extraction of the internal structure of costume relics have been achieved, breaking through the limitations of traditional manual measurement accuracy. By using 3D reverse engineering technology and developing intelligent unfolding algorithms, the surface is mapped into a 2D pattern, accurately restoring the three-dimensional cutting wisdom of ancient costume.

Chapter 6: Application of AI based restoration methods for incomplete and degraded costume relics. By integrating the intelligent restoration model for incomplete and degraded costume relics' styles and textile patterns proposed in Chapter 3, incomplete and degraded costume relics' color intelligent restoration model proposed in Chapter 4, and the intelligent restoration method for incomplete and degraded costume relics structures based on x-ray scanning and reverse engineering proposed in Chapter 5, a series of practical solutions are provided for the difficult problems faced in the digital protection and restoration of costume relics, and applied to the restoration of character costumes in ancient Chinese costume and European oil paintings.

Chapter 7: Conclusion and prospects. Summarize the research results and conclusions of This study, and look forward to further in-depth research in this field in the future. The thesis has explored the intelligent restoration of garment relics, but there are still limitations such as limited samples, insufficient model generalization ability, and the system needs further verification. The future work will focus on expanding the sample range, optimizing the in-depth learning model, strengthening the practical application verification of the system, and exploring its supporting role in costume

design, so as to improve the technical system and promote the protection and design innovation of costume cultural heritage.

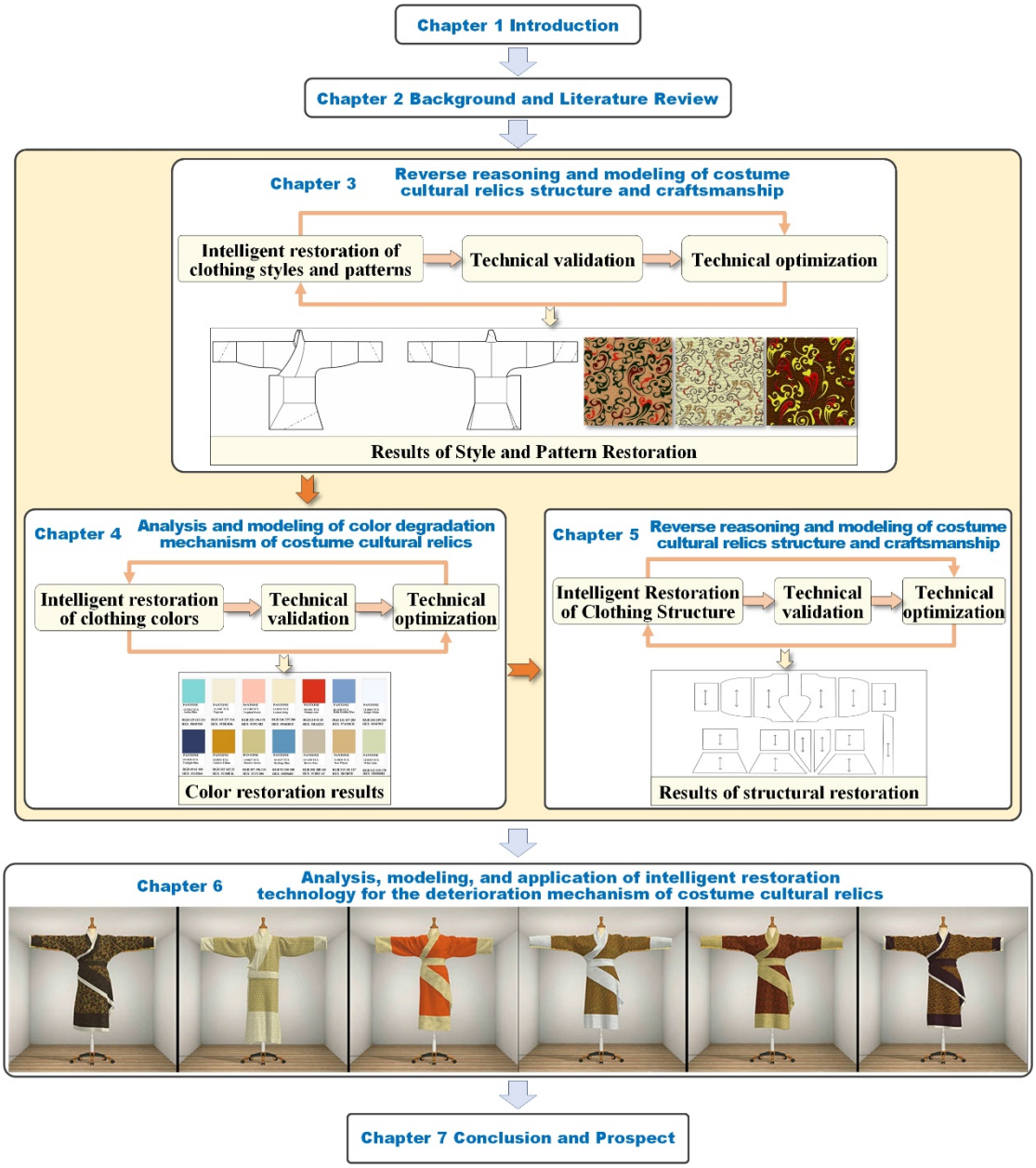

Figure 1-5 The relations between the different chapters.

Chapter 2 Background and literature review

Costume, as a carrier of culture, has emerged with the birth of humanity and is a unique symbol and emblem of a nation. [6] The evolution of civilizations around the world has always been accompanied by the historical changes of costume culture. At present, linear models are commonly used in the restoration process of costume relics, and the development of artificial intelligence provides new methods and means for costume and cultural relic restoration. This chapter not only discusses the principles, advantages, disadvantages, and applicability of traditional computing tools such as linear models, but also elaborates on the theoretical knowledge of deep convolutional generative adversarial networks, deep convolutional long and short-term time series neural networks, and graph neural networks, providing necessary theoretical support for constructing models for costume relics style, textile pattern, sewing pattern, color restoration, and restoration.

2.1 Computational tools

2.1.1 Linear regression model [7]

Linear regression model is a classic statistical learning method used to explore the linear relationship between independent variables (features) and dependent variables (target variables), and to use this relationship for prediction or interpretation. The following provides a detailed explanation of its principles from the aspects of model assumptions, model representation, loss function, parameter solving, and model evaluation.

The linear regression model is based on the following basic assumptions: ①the assumption of linear relationship, where there is a linear relationship between the independent variable and the dependent variable, that is, the change in the dependent variable can be represented as a linear combination of the independent variables; ② Independence assumption, where each observation is independent of each other, and the information of one observation does not affect other observations; ③ Homoscedasticity assumption, for all independent variable values, the error term of the dependent variable (the difference between the observed value and the model predicted

value) has the same variance. This means that regardless of how the value of the independent variable changes, the degree of error fluctuation remains constant; Assuming normality, the error term follows a normal distribution with a mean of 0. This allows us to use the properties of normal distribution for statistical inference, such as calculating confidence intervals for parameters and hypothesis testing.

The general form of a linear regression model is:

$$y = \beta 0 + \beta_1 x_1 + \beta_2 x_2 + \cdots + \beta_n x_n + \epsilon \tag{2.1}$$

Where, y is the dependent variable, which is the target variable we want to predict or explain; $x_1, x_2, \cdots, x_n$ are independent variables, also known as features, which are factors that affect the dependent variable; β_0 is the intercept term, which represents the expected value of the dependent variable when all independent variables are 0; $\beta_1, \beta_2, \cdots, \beta_n$ are regression coefficients that represent the average change in the dependent variable for each unit increase in the independent variable; ϵ is the error term, which includes the influence of other factors not considered in the model on the dependent variable and random errors.

In order to find the optimal model parameters $\beta_0, \beta_1, \cdots, \beta_n$, we need to define a loss function to measure the difference between the predicted values and the true values of the model. The commonly used loss function is Mean Squared Error (MSE), which is expressed as:

$$MSE = \frac{1}{m}\sum_{i=1}^{m}\left(y_i - \hat{y}_i\right)^2 \tag{2.2}$$

Where, m is the number of samples; y_i is the true value of the i-th sample; $\hat{y}_i$ is the predicted value of the i-th sample, calculated by a linear regression model, that is, $\hat{y}_i = \beta_0 + \beta_1 x_{i1} + \beta_2 x_{i2} + \cdots + \beta_n x_{in}$. Our goal is to minimize the mean square error by finding a set of parameters $\beta_0, \beta_1, \cdots, \beta_n$ that minimize the value of MSE.

The least squares method is a commonly used method for solving the parameters of linear regression models. The basic idea is to find the optimal parameters by minimizing the mean square error. To find the parameter that minimizes MSE, we can take partial derivatives of MSE with respect to each parameter and make the partial derivatives equal to 0, thus obtaining a linear system of equations with respect to the parameters. Solving this system of equations yields the estimated values of the parameters. For simple linear regression (with only one independent variable), i.e., $y = \beta_0 + \beta_1 x + \epsilon$, we can derive analytical solutions for the parameters:

$$\widehat{\beta}_i = \frac{\sum_{i=1}^{m}(x_i - \bar{x})\,(y_i - \bar{y})}{\sum_{i=1}^{m}(x_i - \bar{x})^2} \tag{2.3}$$

$$\widehat{\beta}_i = \bar{y} - \widehat{\beta}_1 \bar{x} \tag{2.4}$$

Where, $\bar{x}$ and $\bar{y}$ are the sample means of the independent variable x and the dependent variable y, respectively.

For multiple linear regression (with multiple independent variables), although analytical solutions for parameters can also be obtained by taking partial derivatives, the calculation process is relatively complex and matrix operations are usually used to solve. In addition to the least squares' method, gradient descent is also a commonly used method for solving the parameters of linear regression models. The basic idea of gradient descent method is to gradually adjust the parameters through iteration, so that the value of the loss function continuously decreases until it reaches the minimum value or satisfies the convergence condition. The updated formula for gradient descent method is:

$$\beta_j := \beta_j - \alpha \frac{\partial}{\partial \beta_j} MSE(\beta) \tag{2.5}$$

Where, α is the learning rate, which controls the step size of parameter updates; $\frac{\partial}{\partial \beta_j} MSE(\beta)$ is the partial derivative of the loss function with respect to the parameter β_j, representing the rate of change of the loss function in that parameter direction.

After obtaining the parameters of the linear regression model, we need to evaluate the performance of the model to determine whether it can accurately predict the dependent variable. Common evaluation indicators include:

Determination coefficient (R^2): measures the degree to which the model explains the variation of the dependent variable, with a range of values from 0 to 1. The closer R^2 is to 1, the better the fitting effect of the model on the data.

$$R^2 = 1 - \frac{\sum_{i=1}^{m}(y_i - \hat{y}_i)^2}{\sum_{i=1}^{m}(y_i - \bar{y})^2} \tag{2.6}$$

Root Mean Square Error (RMSE): The square root of the mean square error, which has the same dimension as the dependent variable and more intuitively reflects the average error between the predicted value and the true value.

$$RMSE = \frac{1}{m}\sqrt{\frac{1}{m}\sum_{i=1}^{m}(y_i - \hat{y}_i)^2} \tag{2.7}$$

Mean Absolute Error (MAE): The average absolute error between predicted and true values, which is insensitive to outliers.

$$MAE = \frac{1}{m}\sum_{i=1}^{m}|y_i - \hat{y}_i| \tag{2.8}$$

Through the above evaluation indicators, we can comprehensively understand the performance of linear regression models and optimize and improve the models as needed

2.1.2 Deep convolutional generative adversarial networks[8]

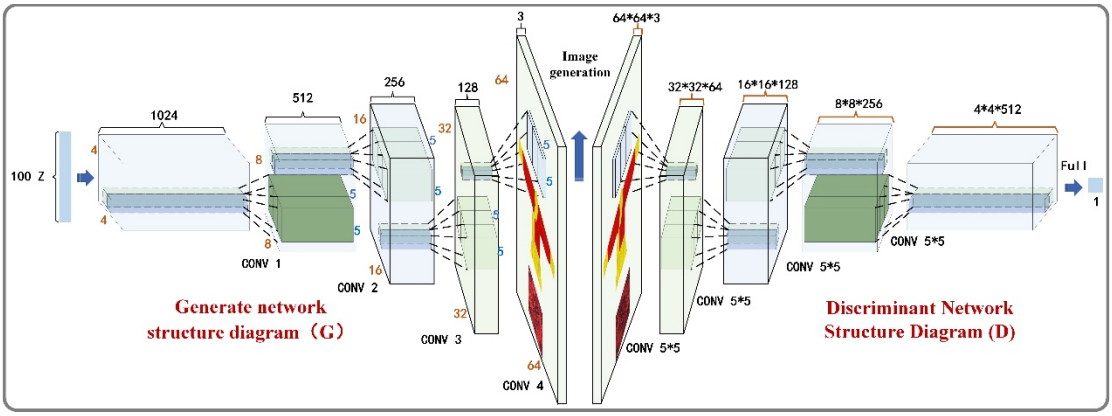

Figure 2-1 Deep convolutional generative adversarial networks.

Deep Convolutional Generative Adversarial Networks (DCGAN) is a deep learning model that combines Convolutional Neural Networks (CNN) and Generative Adversarial Networks (GAN) to generate realistic image data (See Figure 2-1). The following provides an in-depth explanation of the principles of GAN, including its foundation, DCGAN architecture, training process, key design points, and related formula derivation. GAN consists of two parts: Generator (G) and Discriminator (D), which are trained in an adversarial manner. Generator: takes a random noise vector z (usually sampled from a Gaussian distribution puz (z)) as input, and then transforms it into a sample x that is similar to the real data distribution through a series of neural network layers. The goal of the generator is to generate as realistic a sample as possible to deceive the discriminator.

$$\mathbf{x} = G(z;\theta_g) \tag{2.9}$$

Where, θ_g is a parameter of the generator.

The discriminator receives a sample **x** (which can be a real sample or a generator generated sample) as input and outputs a probability value $D(\mathbf{x};\theta_d)$ representing the

probability that the sample is a real sample. The goal of a discriminator is to accurately distinguish between real samples and generated samples as much as possible. During the training process, the generator and discriminator alternate for optimization:

The discriminator is trained with a fixed generator parameter θ_g, using real and generated samples to better distinguish between the two. The loss function of the discriminator usually uses binary cross entropy loss:

$$L_D = -E_{\mathbf{x}\sim p_{data}(\mathbf{x})}[logD(\mathbf{x};\theta_d)] - E_{\boldsymbol{z}\sim p_z(\boldsymbol{z})}[log(1-D(G(\boldsymbol{z};\theta_g);\theta_d))] \quad (2.10)$$

Where, $p_{data}(\boldsymbol{x})$ is the true data distribution.

Generator training: fix the parameter θ_d of the discriminator, use generated samples to train the generator, so that the generated samples can more effectively deceive the discriminator. The loss function of the generator is usually related to the output of the discriminator:

$$L_G = -E_{\boldsymbol{z}\sim p_z(\boldsymbol{z})}[logD(G(\boldsymbol{z};\theta_g);\theta_d)] \quad (2.11)$$

DCGAN has improved the architecture of the generator and discriminator based on GANs, adopting the structure of Fully Convolutional Network and removing the fully connected layer to better process image data. Generators typically consist of a series of deconvolution layers (also known as transposed convolution layers), batch normalization layers, and activation functions. The deconvolution layer is used to gradually upsample low dimensional noise vectors into high-dimensional image data. The deconvolution layer learns a set of filters to expand and transform the input feature map, thereby generating richer image details. Assuming that the l-th layer of the generator is a deconvolution layer, its output can be expressed as:

$$\boldsymbol{h}_l = ReLU(\boldsymbol{W}_l * \boldsymbol{h}_{l-1} + \boldsymbol{b}_l) \quad (2.12)$$

Where, $\boldsymbol{W}_l$ is the filter, $\boldsymbol{b}_l$ is the bias term, and * represents the convolution operation.

Batch normalization layer: Normalize the output of each layer to have zero mean and unit variance. Batch normalization can accelerate the training process, improve model stability, and alleviate the problem of gradient vanishing or exploding.

$$\widehat{\boldsymbol{h}}_l = \frac{\boldsymbol{h}_l - E[\boldsymbol{h}_l]}{\sqrt{Var[\boldsymbol{h}_l] + \epsilon}} \quad (2.13)$$

$$\widetilde{\boldsymbol{h}}_l = \gamma_l \widehat{\boldsymbol{h}}_l + \beta_l \quad (2.14)$$

Where, γ_l and β_l are learnable scaling and translation parameters, and ϵ is a small constant used for numerical stability.

The activation function usually uses ReLU activation function, but in the last layer, Tanh activation function is used to limit the output value to the range of [-1,1] to match the pixel value range of the image data. Discriminators typically consist of a series of convolutional layers, batch normalization layers, and activation functions, and finally output a probability value through a fully connected layer. Convolutional layers are used to extract features from input images. The convolutional layer learns a set of filters to perform local perception and feature extraction on the image, capturing low-level features such as edges and textures, as well as more complex high-level features. Assuming that the l-th layer of the discriminator is a convolutional layer, its output can be expressed as:

$$\boldsymbol{h}_l = LeakyReLU(\boldsymbol{W}_l * \boldsymbol{h}_{l-1} + \boldsymbol{b}_l) \tag{2.15}$$

Where, the activation function of LeakyReLU is:

$$LeakyReLU(x) = \begin{cases} x & \text{if } x \geq 0 \\ \alpha x & otherwise \end{cases} \tag{2.16}$$

Where, α is a small constant (usually 0.2).

The batch normalization layer is also used to normalize the output of each layer, improving the training efficiency and stability of the model. The activation function is in the last layer, and the Sigmoid activation function is used to map the output value to the probability range of [0,1]:

$$D(\boldsymbol{x}; \theta_d) = Sigmoid(\boldsymbol{W}_d * \boldsymbol{h}_L + \boldsymbol{b}_d) \tag{2.17}$$

Where, $\boldsymbol{h}_L$ is the last layer feature map of the discriminator.

The training process of DCGAN is similar to that of GAN, which is achieved by alternately optimizing the generator and discriminator. The following are the basic steps for training DCGAN:

Step 1: Initialize parameters: Randomly initialize the network parameters θ_g and θ_d of the generator and discriminator.

Step 2: Generate Samples: Sample a batch of noise vectors$p_z(\boldsymbol{z})$ from the random noise distribution $\{\boldsymbol{z}^{(i)}\}_{i=1}^{m}$, input them into the generator, and generate a batch of fake samples $\{\boldsymbol{X}^{(i)} = G(\boldsymbol{z}^{(i)}; \theta_g)\}_{i=1}^{m}$.

Step 3: Prepare real samples: Sample a batch of real samples $p_{data}(\boldsymbol{X})$ from the real dataset $\{\boldsymbol{X}^{(i)}\}_{i=1}^{m}$.

Step 4: Train the discriminator: Input real and fake samples separately into the discriminator, calculate the loss function L_D of the discriminator, and use

backpropagation algorithm to update the parameter θ_d of the discriminator to better distinguish between real and fake samples.

$$\theta_d \leftarrow \theta_d - \eta \nabla_{\theta_d} L_D \tag{2.18}$$

Where, η is the learning rate.

$$\theta_g \leftarrow \theta_g - \eta \nabla_{\theta_g} L_G \tag{2.19}$$

Step 5: Train the generator: Sample a batch of noise vectors $p_z(\boldsymbol{z})$ from the random noise distribution $\{\boldsymbol{z}^{(i)}\}_{i=1}^{m}$ again, input them into the generator to generate a batch of fake samples $\{\boldsymbol{X}^{(i)} = G(\boldsymbol{z}^{(i)}; \theta_g)\}_{i=1}^{m}$, then input these fake samples into the discriminator, calculate the loss function L_G of the generator, and use backpropagation algorithm to update the parameter θ_g of the generator, so that the generated fake samples can more effectively deceive the discriminator.

$$\theta_g \leftarrow \theta_g - \eta \nabla_{\theta_g} L_G \tag{2.19}$$

Step 6: Repeat iteration: Repeat the above steps, alternating between training the generator and discriminator until the model converges or reaches the predetermined number of training rounds.

DCGAN removes the fully connected layer and adopts a fully convolutional network structure, which enables the model to better process the spatial information of image data and generate clearer and more realistic images. Using batch normalization at each layer of the generator and discriminator can accelerate the training process, improve model stability, and alleviate the problem of gradient vanishing or exploding. Using ReLU activation function in the generator (Tanh in the last layer) and LeakyReLU activation function in the discriminator (Sigmoid in the last layer) can help the model better learn the distribution of data. It is usually necessary to set different learning rates for the generator and discriminator to ensure the stability of the training process. Generally speaking, the learning rate of the discriminator can be set slightly higher than that of the generator.

DCGAN has a wide range of applications in the field of image generation, such as being able to generate images of various styles, such as landscapes, people, animals, etc., providing creative inspiration for artists and designers. In the case of insufficient data, DCGAN can be used to generate more training samples and improve the generalization ability of the model. Missing or damaged images can be repaired to generate a complete image with the same style as the original image. We chose DCGAN to restore damaged costume artifacts and sewing pattern images, as it combines the

adversarial mechanism of the generator and discriminator, efficiently captures local features of the image through a hierarchical convolutional structure, and generates realistic texture details; Its unsupervised learning feature does not rely on paired data and can adaptively learn the texture patterns of cultural relics, reducing data preparation costs; The end-to-end model simplifies the restoration process, stabilizes convergence through batch normalization and adversarial training, and efficiently handles complex damages (such as large-scale missing or eroded areas); At the same time, the data-driven generalization ability enables it to adapt to different cultural relic features across styles and periods, combined with potential spatial interpolation to achieve fine-tuning of restoration results, while maintaining semantic consistency and enhancing personalized restoration flexibility. DCGAN provides a precise, stable, and scalable technical solution for the digital restoration of cultural relics, with its ability to generate realism, unsupervised adaptability, efficient processes, and cross domain generalization.

2.1.3 Deep convolutional long short-term time series neural networks[9]

The Deep Convolutional Long Short-Term Memory Network (DC-LSTM) combines the advantages of Convolutional Neural Networks (CNN) and Long Short-Term Memory Networks (LSTM) for processing time series data. CNN is used to extract local features, while LSTM is used to model temporal dependencies. The following provides an in-depth explanation of its principles, including network architecture, training process, key design points, and related formula derivation. DC-LSTM typically consists of convolutional layers and LSTM layers, and can be used for univariate or multivariate time series prediction. Convolutional layers are used to extract local features from input time series. Assuming the input is a time series data with a length of T and a dimension of D, i.e. the input data is $\boldsymbol{X} \in R^{T\times D}$. The convolution operation is performed on the time dimension, using a set of filters (convolution kernels) to extract local features from the time series. Assuming the l-th layer is a convolutional layer, its output can be expressed as:

$$\boldsymbol{H}_l = ReLU(\boldsymbol{W}_l * \boldsymbol{H}_{l-1} + \boldsymbol{b}_l) \tag{2.20}$$

Where, $\boldsymbol{W}_l \in R^{k\times D\times C}$ is the convolution kernel, k is the time length of the convolution kernel, C is the number of output channels, $\boldsymbol{b}_l$ is the bias term, $*$ represents the convolution operation, and ReLU is the activation function.

The LSTM layer is used to model long-term dependencies in time series. Assuming the output of the convolutional layer is $\boldsymbol{H} \in R^{T'\times C}$, where T′ is the time step

after convolution. The LSTM unit controls the flow of information through forget gates, input gates, and output gates. The formula for the LSTM unit is as follows:

$$\boldsymbol{f}_t = \sigma(\boldsymbol{W}_f \boldsymbol{h}_{t-1} + \boldsymbol{U}_f \boldsymbol{x}_t + \boldsymbol{b}_f) \tag{2.21}$$

$$\boldsymbol{i}_t = \sigma(\boldsymbol{W}_i \boldsymbol{h}_{t-1} + \boldsymbol{U}_i \boldsymbol{x}_t + \boldsymbol{b}_i) \tag{2.22}$$

$$\boldsymbol{o}_t = \sigma(\boldsymbol{W}_o \boldsymbol{h}_{t-1} + \boldsymbol{U}_o \boldsymbol{x}_t + \boldsymbol{b}_o) \tag{2.23}$$

$$\boldsymbol{C}_t = \boldsymbol{f}_t \odot \boldsymbol{C}_{t-1} + \boldsymbol{i}_t \odot tanh(\boldsymbol{W}_c \boldsymbol{h}_{t-1} + \boldsymbol{U}_c \boldsymbol{x}_t + \boldsymbol{b}_c) \tag{2.24}$$

$$\boldsymbol{h}_t = \boldsymbol{O}_t \odot tanh(\boldsymbol{C}_t) \tag{2.25}$$

Where, $\boldsymbol{f}_t$, $\boldsymbol{i}_t$, $\boldsymbol{o}_t$ are the activation values of the forget gate, input gate, and output gate, respectively; $\boldsymbol{C}_t$ is the cellular state; $\boldsymbol{h}_t$ is in a hidden state; σ is the sigmoid activation function; $\odot$ is element wise multiplication; W and U are weight matrices; B is the bias vector.

The training process of DC-LSTM usually includes the following steps:

Step 1: Initialize parameters, randomly initialize the network parameters of the convolutional layer and LSTM layer.

Step 2: Forward propagation, input the input time series data X into the convolutional layer to obtain the feature map H. Input the feature map H into the LSTM layer to obtain the hidden state sequence $\boldsymbol{H}_{\text{LSTM}}$.

Step 3: Calculate the loss, use the last hidden state hT of LSTM for prediction, and calculate the loss between the predicted value and the true value. The loss function typically uses mean square error (MSE) or cross entropy loss:

$$L = \frac{1}{N}\sum_{i=1}^{N}(y_i - \hat{y}_i)^2 \tag{2.26}$$

Where, y_i is the true value, $\hat{y}_i$ is the predicted value, and N is the sample size.

Step 4: Backpropagation, using the backpropagation algorithm to calculate the gradient of the loss function on the network parameters. Use gradient descent (such as Adam) to update network parameters.

Step 5: Repeat the iteration until the model converges or reaches the predetermined number of training rounds.

The size of the convolution kernel affects the ability to extract time series features. Smaller convolution kernels can capture finer temporal features, while larger convolution kernels can capture a wider range of temporal features. The number of LSTM units determines the model's ability to model time-dependent relationships. Having more LSTM units can capture more complex time patterns, but it may also

increase the complexity and computational cost of the model. The choice of learning rate is crucial for the training effectiveness of the model. Usually, it is necessary to adjust the learning rate to balance training speed and model stability.

DC-LSTM has a wide range of applications in the field of time series prediction, such as stock price prediction: predicting future price trends through historical stock price data. Weather prediction: Using meteorological data to forecast future weather changes. Traffic flow prediction: Predict future traffic flow based on historical traffic flow data. The selection of Deep Convolutional Long Short-Term Time Series Neural Network (LSTM) for color restoration of unearthed costume is due to its unique architecture that can collaboratively process spatial and temporal information in this task. The core advantage of Convolutional Neural Networks (CNN) lies in extracting complex local textures and spatial feature patterns caused by fading, mineralization, and pollution in cultural relic images, such as the spatial distribution of fabric fiber structures and residual dyes; Long Short Term Memory Networks (LSTM) can model the nonlinear degradation sequence of color with burial time and environmental factors (such as temperature, humidity, and soil chemistry), and learn the long-term dependence of color decay. The deep architecture formed by the combination of the two can capture high-dimensional spatial details (such as pattern contours and color block associations) through convolutional layers, and infer color evolution patterns in the temporal dimension through LSTM layers, thereby achieving accurate prediction of unknown raw colors. In addition, the model can learn end-to-end the mapping from degraded representations to original colors, avoiding the limitations of manual feature design and significantly improving the visual accuracy and physical rationality of the restoration results, providing a reliable data-driven solution for the digital protection of costume relics colors.

2.2 Current status of research on the restoration of costume relics

2.2.1 Comparison between different periods in China and the West

By comparing various dynasties in the East and West (Figure 2-2), readers can gain a better understanding of different periods in China, which plays an important role in understanding ancient Chinese costume.

⑴ The Xia (夏), Shang (商), and Zhou (周) Dynasties (approximately 2070-256 BC): The dawn of the two rivers civilization and the mediterranean civilization

The Xia Dynasty of China (approximately 2070-1600 BC) corresponds to the "Middle Kingdom period" of ancient Egypt from the Sixth to the Twelfth Dynasties, during which the Babylonian Kingdom in the Mesopotamian region reached its peak under the rule of Hammurabi. The Shang Dynasty (1600-1046 BC) overlapped with the New Kingdom period of ancient Egypt (18th to 20th dynasties) and the early Assyrian Empire in the Mesopotamian region, with the Bronze Age reaching its peak in both places. The Western Zhou Dynasty (1046-771 BC) was in sync with the expansion of the Assyrian Empire and the Hittite Empire's struggle for dominance in the Mediterranean. The feudal system of the Zhou royal family formed a contrast in civilization with the formation of Greek city states. The Spring and Autumn Period and Warring States Period (770-221 BC) coincided with the rise of the Persian Empire, the golden age of Greek city states, and Alexander's eastern expedition. Confucianism, Platonic philosophy, Shang Yang's reforms, and Athenian democracy formed a dual track of institutional innovation in both the East and the West.

⑵ Qin (秦) Han (汉) to Three Kingdoms (三国) (221 BC -280 AD): The collision of mediterranean empire and east asian empire

When the Qin Dynasty (221-207 BC) unified the six states, the West was at the end of the Hellenistic era, with Ptolemaic Egypt and the Seleucid Empire vying for the eastern coast of the Mediterranean. The Western Han (西汉) Dynasty (202 BC -8 AD) overlapped with the period of transition from the Roman Republic to an empire. Zhang Qian's expedition to the Western Regions and the Roman conquest of Gaul were launched simultaneously, and the Silk Road became the artery connecting the two civilizations. During the Eastern Han (东汉) Dynasty (25-220 AD), corresponding to the period of the "Five Wise Emperors" of the Roman Empire, Ban Chao's management of the Western Regions and the conquest of Britain by Roman legions formed a mirror image of military expansion. During the Three Kingdoms period (221 BC -280 AD), the Roman Empire entered the "Crisis of the Third Century", while China maintained its political vitality through the land reclamation system of Cao Wei and the Northern Expedition of Zhuge Liang of Shu Han. The rise of the Sassanid Empire in Persia heralded the birth of a new order in the Middle East.

⑶ From the Southern and Northern Dynasties (南北朝), the Two Jin Dynasties (两晋) to the Sui (隋) and Tang (唐) Dynasties (265-907): The great migration of ethnic groups in eurasia

After a brief unification in the Western Jin Dynasty (265-316 AD), it fell into the "Rebellion of the Eight Princes", coinciding with the collapse of the Western Roman Empire and the great migration of Germanic peoples. During the Sixteen Kingdoms of Eastern Jin (317-420 AD) and the Southern and Northern Dynasties (420-589 AD), northern China experienced the Five Barbarians and the reforms of Emperor Xiaowen of Northern Wei, while Europe entered the period of the rise of the Frankish Kingdom and the formation of the Charlemagne Empire. The Byzantine Empire and Sassanid Persia engaged in a tug of war in the Middle East. The Sui Dynasty (581-618) was unified with the Tang Dynasty (618-907) during its heyday, corresponding to the rise of the Arab Empire and the division of the Frankish Kingdom into Western European countries. Xuanzang's journey westward to obtain Buddhist scriptures and the expansion of the Arab Empire into Central Asia formed a dialogue of civilizations. When Chang'an became the world's largest city, Baghdad had not yet been established.

⑷ Song (宋), Yuan (元), Ming (明), and Qing (清) Dynasties (960-1912): Civilization transformation from a global perspective

The Song Dynasty (960-1279) corresponds to the prosperous period of the Middle Ages in Europe. The invention of movable type printing in the Northern Song Dynasty was synchronized with the rise of European universities. The prosperity of the Maritime Silk Road in the Southern Song Dynasty and the rise of Venetian merchants formed a complementary trade network. When the Yuan Dynasty (1271-1368) crossed Europe and Asia, Western Europe was in the late Middle Ages. Marco Polo's travelogue inspired Europe's imagination of the East, while the Arab Empire had split into the Mamluk dynasty and the Ottoman predecessor. In the early Ming Dynasty (1368-1644), corresponding to the Renaissance and the Age of Discovery, Zheng He's voyages to the West (1405-1433) were nearly a century earlier than Columbus' discovery of the New World. However, in the mid Ming Dynasty, the maritime ban policy and Western colonial expansion formed a strategic divide. During the Kangxi and Qianlong reigns (1661-1796) of the Qing Dynasty (1644-1912), the West experienced the Industrial Revolution, American independence, and the French Revolution. Qianlong's refusal of

the Macartney Mission's request for trade (1793) became a landmark event in the divergence of Eastern and Western civilizations.

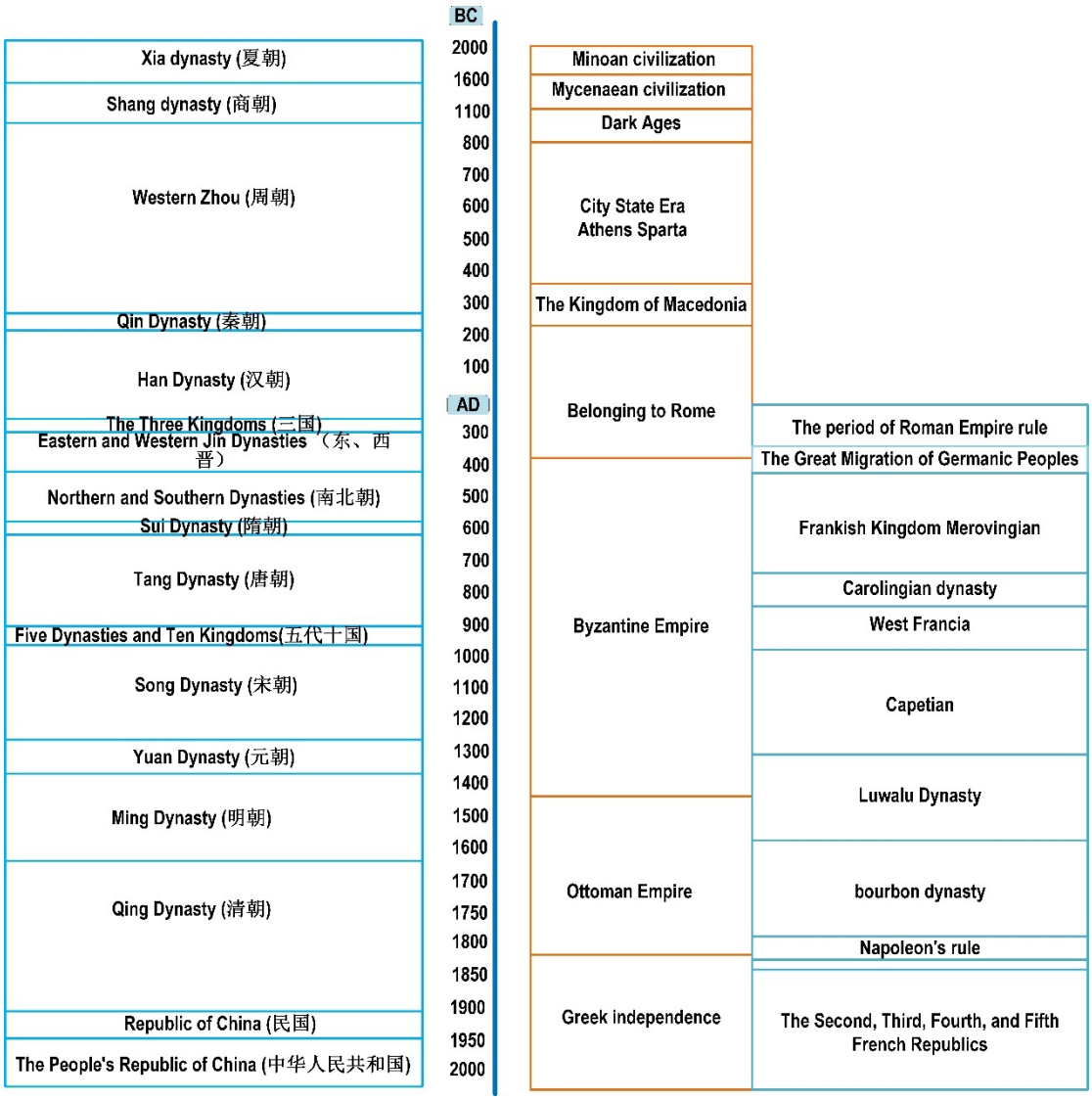

Figure 2-2 Comparison of Eastern and Western Dynasties

2.2.2 Analysis of ancient costume styles and restoration methods

There are many types of ancient Chinese costume styles, which can be summarized into four basic forms: Shangyi Xiashang System (衣裳制, a traditional Chinese attire consisting of an upper garment and a lower skirt), Shenyi System (深衣制，a one-piece robe wrapping the body), Paofu System (袍服制, a traditional Chinese long robe) and Ruqun System (襦裙制, a traditional Chinese two-piece attire). Shangyi Xiashang System involves cutting the upper and lower garments separately, with the upper garment worn and the lower garment worn. The 'garment' in the lower garment is the

skirt. The term 'costume' in Chinese originates from this; Shenyi System is to cut the top and bottom separately, connect them at the waist, and form a whole, that is, connect the top and bottom of the garment. In cutting, the top and bottom of the garment are cut separately, and then sewn together, and finally the garment is still in a unified style [10]; Paofu System making refers to cutting a piece of cloth into a top and a bottom, with no seams in the middle, naturally integrated; The Ru skirt system is a combination of a top and a bottom skirt, and the essence of the Ruqun System is still the top and bottom garment system. Among the four major forms of Hanfu, the ancient style of Shangyi Xiashang is the foundation, while the Shenyi style is its development. The robe style is actually a lengthening of the upper garment, while the skirt style is a shortening of the upper garment, extending various variations of the Shangyi Xiashang in different directions.

During the ancient Egyptian period, the main styles of costume included Loin cloth (waistcoat), Karasiris (headscarf), Dolepari (entwined cloak), Chunik (tube dress), Cap (shawl), Scat (tied pleated skirt), rope dress, etc. ; [11] The main styles of costume during the ancient West Asian period included Kawunakes (wrapped outerwear), Rolled garments (wrapped outerwear), Tassel garments, Chuniks and trousers, and Kundis (loose fitting jumpsuit); [12] The main styles of ancient Greek costume include Hyton (close fitting underwear), Himachal (draped outerwear), Gouramis (cloak), Diproyd (double layered cloak), Diproydion (four cornered hanging garment), etc; [13] The main styles of ancient Roman costume include Toga (loose robe), Cinica (bag shaped jumpsuit), Raseluna (cold cloak), Perula (jumpsuit), Stola (Hiton style underwear), para (Hima pure style outerwear), Strofiwum and Panu (underwear style competitive women's costume). [14, 15]

The restoration of damaged costume styles is one of the important research topics in costume archaeology, which is of great significance for understanding the costume forms of the society at that time [16]. At present, there are mainly two methods for restoring costume styles: manual completion method and computer puzzle method. The manual completion method is mainly aimed at garment relics that are severely damaged and have no other fragments left. Based on the personal experience of archaeological workers, computer or manual methods are used to complete the damaged parts and restore the style and shape of the costume itself; [17] The computer puzzle method is mainly aimed at the situation where fragments of garment relics are scattered in different areas and cannot be formed when unearthed. High-definition cameras are used

to obtain digital images of each fragment, and professional computer software is then applied to assemble them. The damaged parts are completed based on the experience and professional knowledge of archaeologists, and finally the restoration of costume styles and form is achieved.

In summary, the traditional restoration methods for damaged costume relics are complex to operate and overly rely on the personal experience and professional knowledge of archaeological workers, resulting in these methods being more empirical and less scientific [18, 19]. Combining artificial intelligence technology, automatic restoration and reconstruction of costume styles can be achieved by computers without the professional skills and experience of archaeologists. This will be an important research direction for future costume styles archaeology. [20, 21]

2.2.3 Analysis of ancient costume textile patterns and restoration methods

Ancient Chinese textile patterns often used animal, plant, and geometric textile patterns. The expression of textile patterns has gone through several stages, including abstraction, standardization, and realism. The textile patterns before the Shang and Zhou dynasties were as abstract and concise as the original Chinese characters. From the Zhou Dynasty to the Tang and Song dynasties, the textile patterns became increasingly neat, with balanced top and bottom, symmetrical left and right, and tight layout. During the Ming and Qing dynasties, there was a greater emphasis on realistic techniques, with various animals and plants often depicted delicately, realistically, and vividly, as if directly taken from real life without any processing, fully demonstrating the diligence and wisdom of the Chinese nation. [22]

The textile patterns in ancient Egypt were very complex and exquisite, usually using printing and embroidery techniques to create symmetrical and repetitive textile patterns, expressing the strong religious color of ancient Egypt. The types of textile patterns mainly included abstract geometric textile patterns, animal or plant shapes, and biomimetic textile patterns with special symbolic meanings such as the sun and wings; During the ancient Western Asian period, textile patterns mainly included two-winged celestial ball textile patterns, lotus flowers and flower buds, scale p textile patterns, spherical fruits, mountain shaped textile patterns, sacred trees, palms, roses, rope textile patterns, and staircase textile patterns. Animal textile patterns included lion textile patterns, winged lion textile patterns (a monster with a lion body, eagle head, and eagle wings), and cowherd textile patterns; [23] In ancient Greek textile patterns, animal

textile patterns were mostly dominated by divine beasts, while plant textile patterns included lotus textile patterns, palm shaped leaf textile patterns, and sweet potato leaf textile patterns; The colors of ancient Roman textile patterns were mostly composed of black and white and single colors, with textile patterns mostly consisting of flowers and plant stems and leaves [14, 24].

Due to long-term burial, the color of the textile patterns on garment relics tends to be consistent with the color of the costume itself when unearthed, usually appearing in soil gray or soil yellow, which is difficult to identify. [25] In addition, many garment relics were unearthed in scattered and fragmented pieces, mixed with soil and unable to be peeled off, resulting in incomplete textile patterns. [26] The restoration of damaged textile patterns in costume is one of the important research topics in costume archaeology [27]. Costume pattern information is an important channel for understanding the social etiquette and culture of that time. At present, the methods for restoreing textile patterns and styles are generally the same, with the difference being that there are two additional processes for costume pattern restoration: pattern-based pattern restoration and pattern-based fabric restoration. Firstly, the textile patterns are restored using manual completion or computer puzzle methods. Secondly, the restored textile patterns are used for cyclic tiling and other methods to restore the textile patterns. Then, the placement of the textile patterns is based on the positions of the textile patterns in various parts of the unearthed costume, ultimately achieving the restoration of the textile patterns.

In summary, the traditional restoration methods for costume relics require high professional quality, are difficult to inherit, have low efficiency, and the level of application of computer information technology is still at a relatively low level. Combining artificial intelligence technology, intelligent restoration and reconstruction of textile patterns can be achieved by computers without the professional skills and experience of archaeologists, which will be an important research direction for costume pattern archaeology in the future. [20, 28]

2.2.4 Analysis of ancient costume colors and restoration methods

The dyeing technology in ancient China was extremely outstanding and advanced. Not only did it have a wide variety of colors and beautiful hues, but it also dyed firmly and was not easily faded. It was praised by Westerners as a mysterious "Chinese technique" [14, 29, 30]. The methods can be roughly divided into four categories: weaving, printing

and dyeing, embroidery, and calligraphy. The five elements and five colors system is the most basic composition of traditional Chinese costume colors [31]. Blue, red, yellow, white, and black are classified as the "five main colors", while green, blue, red, purple, and yellow (sulfur) are classified as the "five intermediate colors", and there is a saying that the main color is positive and the intermediate color is incorrect [21, 32].

There are many color variations in ancient foreign costume, lacking coherence. During the ancient Egyptian period, costume boldly used many bright colors, including practical colors such as yellow, blue-green, emerald green, vermilion, ruby, pomegranate, etc., especially the blue series, which includes bright sky blue, blue-green, deep purple, etc.; [33] During the ancient Western Asian period, costume colors included white, black, green, red, and purple [34]. Apart from bleached white, they were almost as rich as in Egypt; The main colors of costume in ancient Greece were gray and white, accompanied by beige and red; [13] During the ancient Roman period, the colors of aristocratic costume were mostly deep red, bright red, or milky white, while the colors of commoner costume were mostly dark gray or light gray. [14]

After being buried for hundreds or thousands of years, the color of costume relics deteriorates severely. When unearthed, they come into contact with a large amount of oxygen, breaking the original static balance. The organic substances that make up the dye oxidize instantly when they come into contact with oxygen [35], leading to accelerated deterioration of costume [36, 37]. Restoring the original colors of costume before burial is an important direction in costume archaeology, which has significant significance for understanding the color system of the society at that time. At present, the research methods for restoring costume colors mainly include on-site archaeological recording, instrument analysis, experimental methods, and literature review methods [38]. The on-site archaeological record method is to timely record the color data of garment relics using spectrophotometers, color 3D scanners, digital cameras, etc. when they are unearthed. [39] This method can only record the color of costume artifacts when they are first unearthed, and has certain practical value for costume artifacts with short burial time, strong color fastness, and minimal color degradation [30]. When most garment relics are unearthed, the colors have a certain degree of fading, aging, powdering, peeling, and smudging. In order to restore the original color of garment relics, archaeologists used instrumental analysis methods, using microscopes, confocal Raman spectrometers, visible spectrophotometers, high-performance liquid chromatography, Fourier transform infrared spectrometers, etc. to analyze the

composition of fabrics and dyes [40, 41], and then compared them with existing dye dyeing chromatograms to confirm the original color of the fabrics [42-44]. Due to the use of different dyes in the dyeing process of ancient fabrics, the concentration of dyes and the mixing ratio of different dyes are not exactly the same, resulting in significant differences in dyeing effects and colors [39]. Dye dyeing chromatography is limited, so archaeologists use experimental methods to simulate ancient dyeing processes, restore the color of fabrics after coloring, and infer the original color composition of costume artifacts. In the case where the dye composition of garment relics cannot be confirmed, archaeologists inferred the original color of garment relics by reviewing literature records and combining them with the residual color of fabrics. [16]

In summary, there are many data collection methods in the traditional restoration of costume relics colors, but the types of data collected are single and the data processing methods are simple, resulting in a cumbersome and time-consuming process. The personal experience and quality of professionals affect the accuracy of color reproduction. [45] Combining intelligent learning technology, automatic restoration and prediction of costume relics' colors can be achieved by computers without the professional skills and experience of archaeologists, which will be an important research direction for costume color archaeology in the future.

2.2.5 Analysis of ancient costume structure and restoration methods

The structure of ancient Chinese costume can be divided into basic structure, crossed collar and right lapel (交领右衽), wide sleeves in Baoyi (褒衣广袖), and hidden buckle with straps (系带隐扣). [46] Basic structure: divided into ten parts: collar, lapel, lapel, chin, skirt, sleeves, hem, belt, and collar; Cross collar right lapel: The collar is directly connected to the lapel, and the lapel intersects with the chest (figuratively called "cross collar (交领)"). The left lapel presses down on the right lapel, appearing in a "y" shape in appearance, forming the overall effect of the garment tilting to the right. Lapel (衽), originally meaning clothes collar. Cover the left front placket with the right axillary frenulum, and cover the right placket inside, which is called the right lapel. [47] Otherwise, it is called the left lapel. Another supplement to "cross collar" is "direct collar (直领)" and "plate collar (盘领)". A 'straight collar' refers to a collar that runs directly parallel and perpendicular to the chest, without crossing over. Some have straps on the chest, while others are open without straps. This type of straight collar costume

is usually worn on top of cross collar costume and is often used in everyday outerwear styles such as hoodies, half arms, and skirts. Pan collar "is a common structure in men's costume, with a circular collar shaped like a plate, also a right lapel, and a tie on the right shoulder. Bao Yi Guang Xiu (褒衣广袖): Bao Yi Bo Dai (褒衣博带), commonly worn short clothes with wide sleeves. The sleeves of ancient costume, also known as " Mei (袂)", are wide and long, with round cuffs that can be adjusted. Lace hidden buckle: a hidden buckle in ancient Chinese costume, including two situations: with buckle and without buckle. Usually, ancient costume did not require buttons, but instead tied with straps to tie the clothes together. A few costume items that use buttons also hide the buttons instead of revealing them to the outside.

The structural characteristics of costume in ancient Egypt were that men's costume had pleats while women's costume had no pleats. Ordinary women wear embroidered silk costume, which hangs from under the breasts to above the ankles, and has two shoulder straps to lift it up. Traditional men wear shirt tops, a simple pleated skirt wrapped around the waist, with the ends folded and hanging at the front of the body; The costume structure of ancient West Asia was homogeneous and identical for men and women, using a fabric called Kaunakes to make waistcoats that were wrapped around the body, either for a week or several weeks, hanging down from the waist to conceal the buttocks. [12] The technique of cutting and making tight fitting costume is one of the earliest ethnic groups in the world to apply costume cutting technology; [12] The basic structure of ancient Greek costume was simply to use rectangular blocks folded horizontally, with one side of the folded opening sewn together, and the upper side evenly overlapped at two points to form three openings, which were used for threading the head and arms; [13] The structure of costume in ancient Rome mainly consisted of draped and entwined styles, presenting a freely changing form that combines comfort and functionality. To highlight the straight silhouette below the upper chest line, there were often long skirts and folds, forming loose costume with beautiful pleats [14, 15].

When garment relics are unearthed, due to severe deterioration, it is usually not possible to obtain structural and technological information through unfolding. [26] How to restore the structural structure of garment relics is one of the important research topics in costume archaeology. [48] The restoration of the structure and construction of ancient Chinese costume is the main way to understand the level of craftsmanship in

society at that time. At present, the main methods for restoring costume structures are experimental methods and literature review methods. [49] The experimental method is based on the information of costume relics, using white cloth to cut costume samples, and through trial production of the samples, repeatedly correcting the samples, and finally obtaining the structural and technological information of the costume; The literature review method is to infer the structure and construction of costume by consulting literature and combining residual information of garment relics. [50]

In summary, the traditional restoration methods for costume relics, whether experimental or literature review, rely on the personal experience and professional knowledge of archaeologists to speculate on the structure of costume relics. The reliability and scientific of the restoration need to be verified. [46] Combining reverse engineering and human-computer interaction technology, the automatic generation and restoration of costume structures can be achieved by computers without the professional skills and experience of archaeologists, which will be an important research direction for future costume structure archaeology. [51]

2.2.6 Overall restoration methods for garment relics

The overall restoration of garment relics is the foundation for the inheritance and development of costume culture [52]. Generally, the overall restoration of garment relics is carried out after the completion of archaeological research on costume styles, sewing patterns, colors, and structures. [53] The main methods include physical restoration and virtual simulation. The physical restoration method is based on archaeological information such as costume styles, textile patterns, colors, and structures, using the same fabrics and production techniques as cultural relics to restore the original physical form of costume; [54] The virtual simulation method is also based on archaeological information such as costume styles, patterns, colors, and structures, using computer 3D digital modeling technology and virtual reality technology to digitally reproduce the overall form of garment relics [55-57]. At present, both physical restoration and virtual simulation methods are based on archaeological information such as costume relics styles, patterns, colors, and structures in the early stage, and the means of obtaining this information are mainly based on the personal knowledge and experience of archaeologists. [38] These knowledge and experience require years of accumulation and learning. A novice archaeologist may need ten years or more to become familiar with and proficient in this method.

In summary, the traditional overall restoration methods for costume are difficult to inherit, inefficient, and lack intelligence. Combining AI and virtual simulation technology for digital overall restoration will be an important research direction in the future.

2.4 Discussion

Traditional costume relics restoration techniques mainly include manual repair, chemical reinforcement, and pattern restoration based on historical documents. For example, the Palace Museum uses silk protein reinforcement technology to repair Qing Dynasty silk fabrics, but this method takes several months and requires extremely high operator experience. In addition, pattern restoration relies on the subjective inference of archaeologists, which can lead to errors due to the lack of historical materials. In recent years, Computer-Aided Design (CAD) technology has been introduced into the field of cultural relic restoration, but it is limited by its ability to process two-dimensional images, making it difficult to deal with the problem of complex three-dimensional structure loss. Deep learning-based image restoration techniques can be divided into two categories: completion-based methods (such as Context Encoder) and generative methods (such as GAN). The Pix2Pix model achieves image to image translation through Conditional Generative Adversarial Networks (cGAN), but it relies on paired data training and is difficult to apply to incomplete cultural relic data. Although CycleGAN supports unpaired data, the generated results are prone to artifacts. In contrast, Deep Convolutional Generative Adversarial Network (DCGAN) enhances feature extraction capabilities through deep convolutional structures and combines adversarial training mechanisms, making it more suitable for handling complex costume pattern restoration tasks.

2.5 Conclusion

This chapter comprehensively explores the background knowledge, theoretical basis, and research status in the field of costume cultural relic restoration. Firstly, the chapter provides a detailed introduction to the basic principles of linear regression models, including model assumptions, representations, loss functions, parameter solving, and evaluation methods, providing a statistical learning foundation for subsequent research.

Subsequently, we delved into the principles and applications of DCGAN and Deep Convolutional Long Short-Term Time Series Neural Networks (DC-LSTM), demonstrating the powerful capabilities of deep learning in image generation and time series prediction. In the section on the current status of research on the restoration of costume relics, and traditional restoration methods of costume relics were classified and discussed. Finally, a future research direction combining artificial intelligence technology to achieve automatic restoration and restoration of costume relics was proposed, aiming to enhance the scientific and efficient archaeology and protection of costume relics. This chapter systematically reviews the theoretical basis and current situation in the field of costume cultural relic restoration, reveals the shortcomings of traditional methods in the analysis of restoration processes, and proposes a new approach that combines artificial intelligence technology. This research direction is not only expected to overcome the limitations of traditional methods and improve the scientific and accurate restoration of costume relics, but also to provide strong technical support for the inheritance and development of costume culture.

Chapter 3 Intelligent restoration model for incomplete and degraded costume relics' styles and textile patterns

This chapter aims at the problems that need to be solved urgently, such as the high professional experience and knowledge requirements and low efficiency of the traditional restoration methods of costume relics' styles and textitle patterns. This chapter constructs an intelligent restoration model of styles and textitle patterns based on the deep convolution generation confrontation network, and realizes the rapid and intelligent restoration of costume relics' styles and textitle patterns.

3.1 Basic plan for intelligent restoration model for incomplete and degraded costume relics' styles and textile patterns

Figure 3-1 Intelligent restoration of garment relics and textitle patterns

This chapter focuses on the intelligent restoration technology of costume relics' styles and textitle patterns. The restoration effect is shown in Figure 3-1. The core process and key points are summarized as follows:

- The relationship between the degradation process of costume relics and deep convolutional generative adversarial networks (DCGAN): Long term buried costume will deteriorate due to multiple factors, resulting in material weakening, shape loss, and visual information loss. Traditional manual restoration is time-consuming and subjective, while DCGANs provide a new paradigm. It excels in pattern completion and form reconstruction through adversarial training, transforming archaeological and artistic analysis into visual models, and achieving high reliability digital rebirth of costume relics.

- Construction of restoration model of costume relics' styles and textitle patterns: use the deep convolution generative confrontation network (DCGAN) to build the restoration model, and learn the image data with similar styles and textitle patterns through training to repair the incomplete costume. The model is composed of a generation network (G) and a discrimination network (D). The network simulation training data is generated to generate costume styles and textitle pattern feature data. The discrimination network extracts the generated data features and compares them with the real data. The network weights are updated through discrimination and error feedback. The training data sample set is constructed by the combination of multiple factors, such as garment sleeve type, collar type, silhouette, pattern silhouette, and type. Step convolution is used to replace spatial pooling, and the loss function is constructed to improve the repair accuracy.
- Data collection and model training: collect a large amount of data with the characteristics of costume styles and patterns of previous dynasties in China, including more complete pictures of garment relics unearthed and materials for later generations to restore innovative designs. It is planned to further collect more data for the construction of the intelligent restoration model of costume relics styles and patterns, so as to improve the generalization ability and restoration accuracy of the model.
- Application of costume relics style and pattern restoration model: collect Chinese ancient costume styles and pattern data through literature, museums, networks and other channels, and build training data sets and test data sets. Based on unsupervised learning, the model can effectively repair and complete the incomplete parts by inputting the data of the incomplete garment relics.

3.2 The relationship between the deterioration process of costume relics and DCGANs

Costume buried underground for a long time will undergo a series of complex physical, chemical, and biological changes, resulting in weakened materials, damaged structures, and loss of visual information. Only by deeply understanding these processes can effective protection and restoration work be carried out.

The acidic and alkaline components, soluble salts, and metal ions in the soil continue to erode the fiber structure, leading to a decrease in its strength;

Microorganisms and insects cause local pollution and damage through enzymatic hydrolysis and ingestion; Over time, the loss of fiber polymerization degree, coupled with repeated expansion and contraction caused by temperature and humidity fluctuations, gradually leads to the brittleness and fragmentation of the fabric; In extreme environments, although cultural relics may temporarily suspend partial degradation, they face unique risks such as brittleness, deformation, or later salt damage. The intertwined deterioration process of these multiple factors collectively leads to the weakening of the material, structural damage, and severe loss of visual information of costume relics.

The multiple deterioration processes over time have led to serious damage to the original design logic and visual integrity of cultural relics. We often face incomplete cut contours and interrupted pattern sequences, which makes traditional manual restoration relying on expert experience both time-consuming and subjectively uncertain. Deep Convolutional Generative Adversarial Networks (DCGANs) provide a data-driven new paradigm to address this challenge. Its repairing ability is rooted in its deep understanding of the hierarchical structure of pattern systems and the topological relationship of form space.

In terms of pattern completion, DCGANs are not just about filling in pixels. It intelligently generates missing parts and even the entire continuous loop of patterns by analyzing the drawing strokes of residual patterns, the arrangement rules of skeletal structures, and the hierarchical relationship between ground patterns and main patterns, ensuring the unity of its artistic style and logical coherence; In terms of form reconstruction, the learning objectives of the network go beyond two-dimensional planes. It can understand the connection methods, proportional relationships, and three-dimensional spatial forms between different costume components by analyzing a large amount of complete costume data of the same period and type. Therefore, when inputting a piece of costume fragment, DCGANs can accurately infer and reconstruct the flat unfolded image and even the three-dimensional wearing form of the entire garment based on the suggested cutting lines, fabric splicing methods, and mechanical structures of these fragments, restoring its "cutting wisdom" obscured by historical dust.

The essence of this repair process lies in its adversarial training mechanism. The generator is committed to generating completion schemes for shapes and patterns that are as "realistic" as possible, while the discriminator plays a demanding role as an "expert in ancient costume identification", constantly questioning whether the

completion content is consistent with the distribution of historical real samples learned. This game forces the output of the generator to strictly conform to specific era styles and technological features, effectively avoiding imaginative and historical "fictional" repairs.

The degradation process experienced by costume relics defines where and how the form and pattern information is missing, while deep convolutional generative adversarial networks provide a powerful computational framework to answer the core question of "what the missing part should have been" by learning massive prior knowledge. It transforms the style analysis of archaeological typology and art history into a computable and optimizable visual model, ultimately achieving a highly reliable digital rebirth from incomplete to complete, from fuzzy to clear, providing a revolutionary tool for precise interpretation and inheritance of cultural heritage.

3.3 Construction of restoration models for costume relic styles and textitle patterns

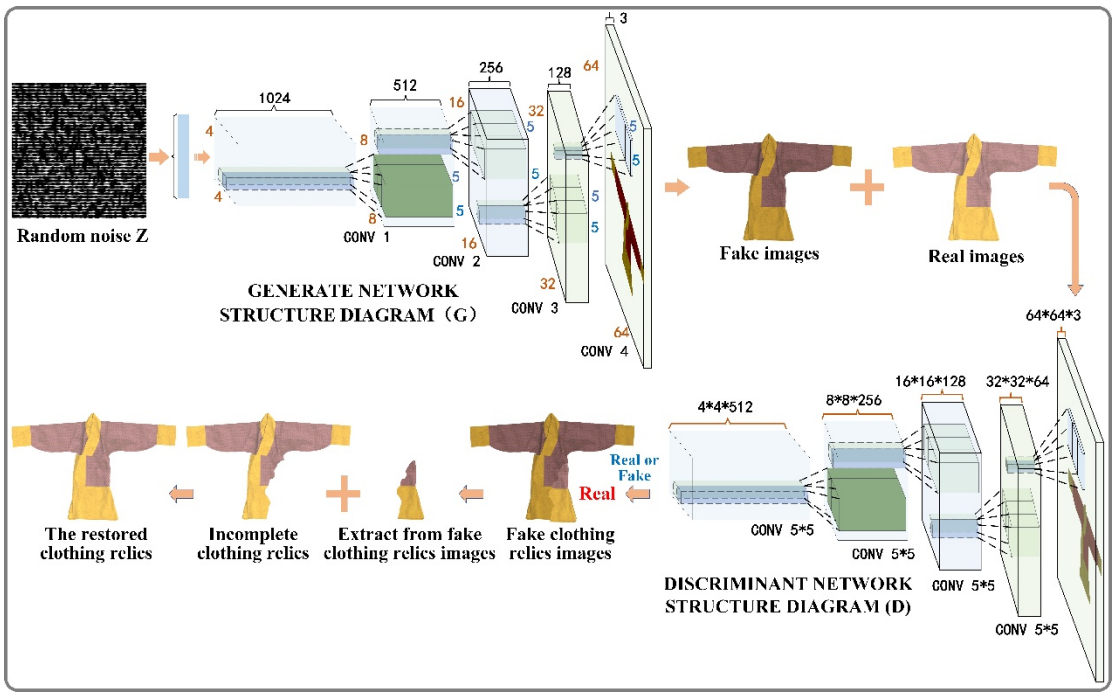

Figure 3-2 Intelligent restoration model for costume relics styles and textitle patterns based on DCGAN

This study preliminarily utilizes the powerful mining and learning ability of DCGAN on the image data features of costume relics styles and textitle patterns [58, 59]. By

training and learning on image data with similar styles and textitle patterns, and combining the neighborhood information of data missing areas to repair incomplete costume styles and textitle patterns, a style and textitle pattern restoration model based on deep convolutional generative adversarial network is constructed. The model structure is shown in Figure 3-2. The intelligent restoration model for costume relics styles and textitle patterns consists of a generation network (G) and a discrimination network (D). With a random vector z as input, the generation network model can simulate training data to generate data with costume styles and textitle pattern features, while the discrimination network can extract generated data features and compare them with training data with real costume styles and textitle patterns. Through discrimination and error feedback, the weights of the deep network are updated, ultimately obtaining a data model that can stably generate data that conforms to the characteristics of real costume relics styles and textitle patterns.

The intelligent restoration model for cultural relics styles and textitle patterns proposed in this study is an unsupervised learning model that combines deep convolutional neural networks with generative adversarial networks. It utilizes the powerful feature extraction ability of convolutional neural networks for costume relics to improve the learning ability of the generative network. Both the generative network and adversarial network adopt convolutional neural network structures. DCGAN takes a random vector Z as input and generates a network to obtain the distribution $P_{G(x,\theta)}$ that is most similar to the distribution P_{data} of the real costume and cultural relic image x, where θ is determined by the network parameters. The purpose of generating the network is to find the θ value that makes $P_{G(x,\theta)}$ the closest to P_{data}. Discriminant network is used to determine the authenticity of input costume cultural relic images and give the probability of image authenticity, that is, $D\big(G(z)\big) = 0$ is the generated sample, and $D(x) = 1$ is the real sample. During the training process, the generative network generates as many real costume and cultural relic images as possible to deceive the discriminative network. At the same time, the discriminative network continuously optimizes and trains stronger judgment abilities. The two alternate training iterations and optimize each other, and ultimately achieve the restoration of damaged costume relics. The objective function of DCGAN is shown in Formula (3-1):

$$min_G max_D V(D,G) = \mathbb{E}_{x\sim p_{data}(x)}[logD(x)] + \mathbb{E}_{z\sim p_z(z)}\left[log\left(1-D\big(G(z)\big)\right)\right] \quad (3\text{-}1)$$

The training of Generative Adversarial Networks (GANs) is a minimax dynamic game process between GANs and discriminative networks, where the two networks are trained alternately and the optimization process is in the backpropagation stage. Firstly, by fixing the generative network and optimizing only the discriminative network, we can obtain:

$$max_D V(D,G) = \mathbb{E}_{x\sim p_{data}(x)}[logD(x)] + \mathbb{E}_{z\sim p_z(z)}\left[log\left(1-D\big(G(z)\big)\right)\right] \quad (3\text{-}2)$$

The first item in Formula (3-2) is the discrimination of real costume relics styles and textitle pattern samples. The larger the discrimination result, the better, and it should be as close to 1 as possible; The second item is the discrimination of generated costume cultural relic styles and textitle pattern images, and the discrimination result should be as small as possible. In order to ensure the consistency of the formula, $D\big(G(z)\big)$ is changed to $1-D\big(G(z)\big)$ and the final optimization result of the discrimination network is to take the maximum value close to 1. Next, by fixing the discriminative network and optimizing only the generative network, we can obtain:

$$min_D V(D,G) = \mathbb{E}_{z\sim p_z(z)}\left[log\left(1-D\big(G(z)\big)\right)\right] \quad (3\text{-}3)$$

Generative network optimization is only related to the second term of the objective function, and its purpose is to make the generated fake styles and textitle pattern samples closer to reality, that is, the larger the $D\big(G(z)\big)$ result, the better. After changing the second part of the formula to $1-D\big(G(z)\big)$, the optimization result of the generative network takes the minimum value close to zero. In order to maximize the results obtained by the discriminative network, the generative network is fixed during the training process, only the discriminative network is optimized, and k iterations are performed. When the generative network is fixed, the derivative of $V(D,G)$ is set to zero, thus obtaining the optimal discriminative network $D_G^*(x)$ in Formula (3-1):

$$D_G^*(x) = \frac{p_{data}(x)}{p_{data}(x)+p_g(x)} \quad (3\text{-}4)$$

Substitute the optimal discriminative network $D_G^*(x)$ into the objective function, and the objective function becomes $C(G)$ as follows:

$$C(G) = min_D V(G, D_G^*)$$
$$= \mathbb{E}_{x\sim p_{data}}\left[log\frac{p_{data}(x)}{p_{data}(x)+p_g(x)}\right] + \mathbb{E}_{x\sim p_g}\left[log\frac{p_{data}(x)}{p_{data}(x)+p_g(x)}\right] \quad (3\text{-}5)$$

Formula (3-5) is similar to Jensen Shannon divergence, and we can obtain Formula (3-6):

$$C(G) = -2log2 + 2JS(p_{data} \parallel p_g) \quad (3\text{-}6)$$

JS divergence is always non negative if and only if $p_{data} = p_g$, $JS(p_{data} \parallel p_g) = 0$, In the case of $p_{data} = p_g$, $D_G^*(x) = 1/2$, and $C(G)$ obtains the global minimum $-log4$. The final result of training generative adversarial networks is that the discriminative network has a probability of 0.5 for both generated and real samples, and the images generated by the generative network are difficult to distinguish from real samples.

From this, it can be seen that in theory, the costume cultural relic style and textitle pattern restoration technology based on DCGAN has a very high accuracy in completing styles and textitle patterns, reaching a level that is difficult to distinguish.

3.4 Application of restoration models for costume and cultural relic styles and textitle patterns

3.4.1 Data collection

The data collection of this study focuses on high-definition image materials of costume relics unearthed from various dynasties in China, with a focus on selecting archaeological excavation reports, museum collection databases, and academic literature with clear age, structural features, and pattern details as image resources. The data scope covers typical costume relics from pre-Qin to Qing Dynasty (see Table 3-1).

Table 3-1 Collection information form for costume relics data

No.	Period	Location of Excavation/Collection	Specific Name

1	Pre-Qin (Before 221 BC)	Mashan, Jiangling, Hubei	Costume unearthed from the Mashan Chu Tomb
2	Pre-Qin (Before 221 BC)	Shanshan County, Xinjiang	Costume unearthed from the Subeixi Site and Cemetery
3	Han Dynasty (202 BC – 220 AD)	Changsha, Hunan	Costume unearthed from the Mawangdui Tombs
4	Han Dynasty (202 BC – 220 AD)	Luopu, Xinjiang	Costume unearthed from the Sampula Cemetery
5	Han Dynasty (202 BC – 220 AD)	Minfeng County, Xinjiang	Costume unearthed from the Niya Ancient Tombs
6	Han Dynasty (202 BC – 220 AD)	North of Loulan Ancient City, Ruoqiang, Xinjiang	Costume unearthed from Tomb No. 1
7	Han Dynasty (202 BC – 220 AD)	Ruoqiang, Xinjiang	Costume unearthed from Loulan Ancient City
8	Han Dynasty (202 BC – 220 AD)	Yingpan Cemetery, Yuli County, Bayingolin Mongol Autonomous Prefecture, Xinjiang Uygur Autonomous Region	Costume unearthed from the Yingpan Cemetery
9	Han Dynasty (202 BC – 220 AD)	Zhenglan Banner, Inner Mongolia	Costume unearthed from the Yihenaoer Tomb Cluster
10	Wei and Jin Dynasties (220–420 AD)	Huahai, Gansu Province	Costume unearthed from the Bijiatan Tomb
11	Tang Dynasty (618–907 AD)	Turpan, Xinjiang	Costume unearthed from the Astana Ancient Tombs
12	Tang Dynasty (618–907 AD)	Dulan County, Qinghai Province	Costume unearthed from the Tubo Tombs

13	Tang Dynasty (618–907 AD)	Fufeng County, Shaanxi Province	Costume unearthed from the Famen Temple Underground Palace
14	Tang Dynasty (618–907 AD)	Tianzhu, Gansu Province	Costume unearthed from the Tomb of Murong Zhi of Tang
15	Song Dynasty (960–1279 AD)	Chayuan Village, Fuzhou, Fujian Province	Costume unearthed from the Song Dynasty Tomb
16	Song Dynasty (960–1279 AD)	De'an, Jiangxi Province	Costume unearthed from the Zhou's Tomb
17	Song Dynasty (960–1279 AD)	Huashan, Gaochun, Nanjing	Costume unearthed from the Song Dynasty Tomb
18	Song Dynasty (960–1279 AD)	Fuzhou, Fujian Province	Costume unearthed from the Huang Sheng's Tomb
19	Song Dynasty (960–1279 AD)	Jintan, Jiangsu Province	Costume unearthed from the Zhou Yu's Tomb
20	Yuan Dynasty (1271–1368 AD)	Huarong City Oil Factory, Huarong, Hunan Province	Costume unearthed from the Yuan Dynasty Tomb
21	Jin Dynasty (1115–1234 AD)	Chengzi Village, Juyuan Township, Acheng District, Heilongjiang Province	Costume unearthed from the Tomb of the Prince of Qi of Jin
22	Liao Dynasty (916–1125 AD)	Gezidong, Hebei Province	Hoard of Costume
23	Liao Dynasty (916–1125 AD)	Aluke'erqin Banner, Inner Mongolia	Costume unearthed from the Daiqintala Tomb
24	Liao Dynasty (916–1125 AD)	Aluke'erqin Banner, Inner Mongolia	Costume unearthed from the Tomb of Yelü Yu of Khitan, Liao Dynasty
25	Yuan Dynasty (1271–1368 AD)	Wuxi, Jiangsu Province	Costume unearthed from the Qian Yu's Tomb

26	Yuan Dynasty (1271–1368 AD)	Zhang County, Dingxi City, Gansu Province	Costume unearthed from the Wang Shixian Family Tombs
27	Yuan Dynasty (1271–1368 AD)	Huarong City Oil Factory, Huarong, Hunan Province	Costume unearthed from the Yuan Dynasty Tomb
28	Ming Dynasty (1368–1644 AD)	Changping, Beijing	Costume unearthed from the Dingling Mausoleum
29	Ming Dynasty (1368–1644 AD)	Taizhou, Jiangsu Province	Costume unearthed from the Xu Fan's Tomb
30	Ming Dynasty (1368–1644 AD)	Qufu, Shandong Province	Preserved Costume Artifacts from the Kong Family Mansion
31	Ming Dynasty (1368–1644 AD)	Nanchang, Jiangxi Province	Costume unearthed from the Tomb of Lady Wu, Wife of Ningjing Wang
32	Ming Dynasty (1368–1644 AD)	Nanchang, Jiangxi Province	Costume unearthed from the Tomb of Lady Wu, Wife of Ming Dynasty Ningjing Wang
33	Ming Dynasty (1368–1644 AD)	Huishui, Guizhou Province	Costume unearthed from the Ming Dynasty Tomb
34	Ming Dynasty (1368–1644 AD)	South of Jiulong Bridge, Taizhou City	Costume unearthed from the Ming Dynasty Hu Yu's Tomb
35	Ming Dynasty (1368–1644 AD)	Taizhou, Jiangsu Province	Costume unearthed from the Tomb of Xu Fan and his Wife
36	Qing Dynasty (1616–1911 AD)	Beijing	Qing Dynasty Costume Collection in the Palace Museum

(1) Archaeological reports and academic documents: Systematically search core journals such as Cultural Relics (《文物》) and Archaeological Journal (《考古学报》), as well as special archaeological achievements such as Changsha Mawangdui No.1 Han Tomb (《长沙马王堆一号汉墓》), Excavation Bulletin of Wu

Tomb (《吴氏墓发掘简报》), and Excavation Report of Ding Tomb (《定陵发掘报告》), and extract high-definition line maps, color photos, and line maps.

⑵ **Museum digital resources:** relying on the open digital platforms of 100 institutions, including the Palace Museum, the National Museum of China, the Hunan Museum, the Nanjing Museum, and the Jingzhou Museum, we can obtain high-resolution images of garment relics.

⑶ **Special technical processing:** For the incomplete area, for areas with damage, images that simultaneously contain both intact overall structures and locally deteriorated regions are prioritized. Using image-annotation tools, pixel-level labels are applied to the damaged parts, distinguishing three types of degradation: complete loss, blurred fading, and structural deformation. These annotations provide categorical labels for subsequent network training.

Table 3-2 The costume style data example

		
Unearthed Costume (202 BC — 8 AD)	Virtual restoration Costume (202 BC — 8 AD)	Unearthed Costume (202BC—8AD)
		
Virtual restoration Costume (202BC—8AD)	Unearthed Costume (202 BC — 8 AD)	Virtual restoration Costume (202 BC — 8 AD)

Through the above methods, the data set will have both historical authenticity, damage diversity and fineness, provide high-quality training basis for the deep convolutional generative adversarial network, and finally realize the shape and textitle pattern restoration of the incomplete parts of the unearthed costume. The data collection experiment was conducted at Xi'an Polytechnic Universit, China. The costume style

data are shown in Table 3-2, and all style data can be found in Appendix 5. The textile pattern data are shown in Table 3-3, and all pattern data can be found in Appendix 1

Table 3-3 The textile pattern data example

	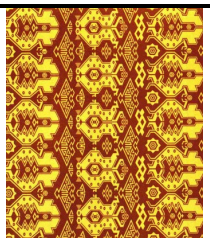			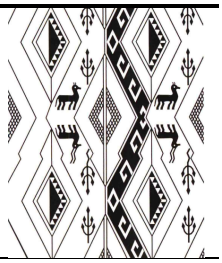
Warring States period (475 BC-221BC)	Warring States period (475 BC-221 BC)	Warring States period (475 BC-221 BC)	Warring States period (475 BC-221 BC)	Warring States period (475 BC - 221 BC)
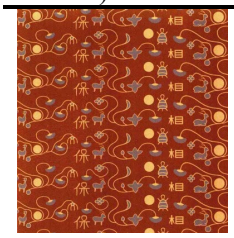	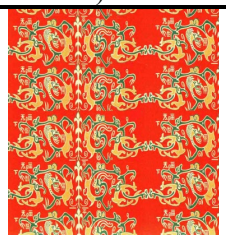			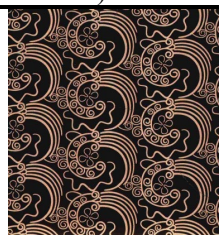
Han dynasty (202 BC – 220 AD)	Han dynasty (202 BC - 220 AD)	Han dynasty (202 BC - 220 AD)	Han dynasty (202 BC - 220 AD)	Han dynasty (202 BC - 220 AD)

3.4.2 Data preprocessing module [8]

In the task of deep convolutional generative adversarial network (DCGAN) to repair the image of incomplete costume relics, data acquisition and cleaning are the basic links to build high-quality training data sets, which directly affect the repair effect of the model and the ability to restore historical authenticity. First of all, the data collection needs to systematically collect the images of unearthed costume, focusing on obtaining the photos of costume relics including the incomplete areas. Such images are usually from museum collections, on-site records of archaeological sites or open digital databases of costume relics. In order to ensure that the model can learn the complete costume morphological characteristics, the data set should also include the complete costume image as the training target, that is, the high-definition photos of the same costume cultural relic in the undamaged state, or the standard textitle patterns of similar costume recorded in archaeological literature and historical materials as a reference. During the collection process, special attention should be paid to the diversity of costume relics images, covering different materials (such as silk, cotton and linen,

embroidery, etc.), styles of different dynasties (such as Han and Tang textitle patterns, costume structures of the Ming and Qing dynasties), and different types of defects (such as damage, fading, missing parts, etc.), so as to improve the model's generalization ability when dealing with the complex characteristics of costume relics.

In the data cleaning process, the image quality of costume relics needs to be strictly screened. First, it is necessary to eliminate the blurred images caused by poor shooting conditions. Image sharpness can be evaluated by calculating the image gradient magnitude or by using edge detection algorithms such as the Sobel operator., and the images below the threshold value can be excluded. Secondly, for severely faded costume relics images, histogram equalization or color saturation analysis should be combined. If the color information has been unable to identify the original costume features (such as the textitle pattern details completely disappear), it will be marked as invalid data. In addition, it is necessary to remove costume relics images that have no background, such as photos that only contain costume parts (such as separate cuffs or collars) or have complex backgrounds (such as modern exhibition environments), and retain RGB images with costume as the main body and simple background. In terms of resolution, it is uniformly scaled to 64×64 pixels and above (128×128 is recommended to take account of details and computing efficiency), so as to ensure that the size of costume relics image meets the DCGAN input requirements, and avoid feature loss caused by excessive compression. Finally, the cleaned data set needs to include pairs of incomplete costume relics images and complete costume relics images, and establish a labeling file to record the location and shape of the incomplete area (such as labeling through a binary mask), so as to provide accurate monitoring signals for subsequent model training. This process not only ensures the validity of the data, but also enables the model to focus on the restoration of the characteristics of costume relics through structural processing, rather than the interference of noise or irrelevant information, thus laying a solid foundation for the efficient training of the generation of confrontation networks.

⑴ Defective region annotation and mask generation

In the task of Deep Convolutional Generative Adversarial Network (DCGAN) to repair the damaged costume relic images, the annotation of defective areas and the generation of masks are the core links of constructing an unsupervised learning framework, which directly affect the positioning accuracy and repair effect of the model

on the missing areas. The mark of the damaged area needs to clarify the specific location in the costume cultural relic image that needs to be repaired, usually based on the professional judgment of archaeologists or through image analysis technology to automatically identify the damaged area. For manually annotated scenes, image editing tools such as Adobe Photoshop can be used to accurately outline the incomplete contour through polygon lasso tools or pen tools, fill in pure white (RGB value is 255, 255, 255) to form a binary mask, and keep the background transparent to distinguish normal areas. In this process, special attention should be paid to the accuracy of the marking: it should cover obvious physical damage (such as tearing, missing cloth), and also include fuzzy areas caused by fading or corrosion. Although these areas are not completely missing, the color or textitle pattern can no longer be identified, so semantic completion should be carried out by generating models. For large-scale data sets, manual annotation is inefficient, so it is necessary to use code to automatically generate random masks. Through Python's OpenCV library or PIL library, irregular polygons, ellipses or free curves can be randomly generated, and edge smoothness can be adjusted in combination with morphological operations (such as expansion and erosion) to simulate the morphological characteristics of natural damage in the real scene. The size and position of the mask should also be controlled during automatic generation, such as generating a circular mask through random center points and radii, or generating an adaptive mask based on the contour of garment relics to avoid the mask covering non-defective areas. Whether generated manually or automatically, the spatial alignment of the mask and the original image is crucial. It is necessary to ensure strict correspondence through image registration technology (such as feature point-based matching) or pre-processing steps (such as unified scaling, rotation correction) to ensure that the generator can accurately learn the mapping relationship between the incomplete area and the complete area.

After the mask is generated, it is necessary to save the original image and the corresponding mask file in PNG format, and store binary information (white is the incomplete area, and transparent is the normal area) using its feature of supporting transparent channels. The lossless compression feature of PNG format can avoid the loss of image quality, and is especially suitable for costume relics data requiring high-precision restoration. When saving, it is necessary to establish a strict naming convention, such as naming the original image as "costume_001. jpg" and the corresponding mask as "costume_001_mask. png", to ensure that data can be loaded in

pairs by matching the file name during training. In addition, metadata information needs to be recorded, such as the type (physical damage, fading), severity (mild, moderate, severe) of the defective area and the characteristics of the costume dynasty. This information can assist the subsequent model to analyze the correlation between the defective mode and the historical background. In terms of data management, it is recommended to store the original image and mask file in the "original" and "mask" subdirectories respectively, and establish an index through the CSV file or JSON file to record the path, annotation personnel, generation time and other information of each pair of files, so as to facilitate batch loading and version control during training. It is worth noting that the transparent channel of the mask file should be set correctly to avoid abnormal model reading due to format errors. For example, in Python, you can specify the "transparency" parameter through the save method of the PIL library to ensure that the transparent area is stored correctly. Through standardized data storage and management, training efficiency can be significantly improved, while providing traceable data support for subsequent model optimization (such as adjusting mask generation strategy).

⑵ Data enhancement and standardization

In the task of Deep Convolutional Generative Adversarial Network (DCGAN) to repair the incomplete costume relics images, data enhancement and standardization are the key preprocessing steps to improve the generalization ability and training stability of the model. Its core goal is to make the model be able to effectively learn the distribution law of costume relics characteristics by standardizing the input data format and expanding data diversity. First, for the standardization of image size, it is necessary to uniformly scale the original image to the input size required by the model (such as 128 × 128 pixels). This operation is usually achieved by using a bilinear interpolation algorithm, which can not only maintain image clarity, but also ensure that all samples have the same spatial resolution, avoiding the convolution kernel parameter adaptation problem caused by size differences. In the process of scaling, special attention should be paid to maintaining the proportional integrity of costume textitle patterns. For non-square original images, the aspect ratio can be maintained by adding black or white borders (Padding) to prevent morphological distortion caused by non-proportional scaling. Secondly, the normalization of pixel values is very important. The input of DCGAN usually requires that the range of pixel values be between [-1, 1], so it is

necessary to linearly map the 0-255 pixel values of the original costume cultural relic image to this range. The specific formula is: $I_{norm} = 127.5I_{ram} - 1$, where I_{ram} is the original pixel value, and I_{norm} is the normalized value. This step can accelerate the model convergence and avoid the training instability caused by too large or too small gradient value.

In terms of data enhancement, targeted strategies should be adopted to expand the diversity of data sets for the incomplete repair task of costume relics images. Random horizontal flipping (probability is set to 50%) can simulate the incomplete situation of costume relics in the mirror direction, and enhance the repair ability of the model for left and right symmetrical textitle patterns; The random rotation operation (range ±15 °) can simulate the shape change caused by the deviation of image shooting angle or the natural wrinkles of garment relics, and avoid the over fitting of the model due to the fixed angle input. It is worth noting that the rotation angle should be controlled within a small range to prevent the costume structure (such as neckline and cuff) from losing semantic rationality due to excessive rotation. In addition, the data distribution can be further expanded in combination with random clipping (such as zooming to 128×128 after randomly clipping 112×112 areas from the original image), but it is necessary to ensure that the clipping area contains complete costume bodies to avoid introducing invalid background noise. All enhancement operations need to be dynamically applied during training (such as through PyTorch's torchvision. transforms module), rather than pre-processing and saving, to save storage space and maintain the flexibility of data enhancement strategies. Through the above standardization and enhancement process, the model can not only adapt to incomplete images under different sizes, angles and lighting conditions, but also mine more abundant feature representations from limited data, ultimately improving the repair accuracy and robustness of complex costume incomplete textitle patterns.

3.4.3 *Model structure design [60]*

(1) Generator

The generator input is a 100-dimensional random noise vector, which obeys the standard normal distribution (mean 0, variance 1). This noise, as the initial input of the generator, provides a random basis for the generation of diverse costume relics images. The output of the generator is the restored complete costume cultural relic image (size 128×128×3).

The full connection layer maps the 100-dimensional noise vector to a 4×4×1024 3D feature map, completing the initial conversion from low dimensional noise to high-dimensional feature space. Input dimension: 100 (noise vector length). Output dimension: 4×4×1024 (the size of feature map is 4×4, and the number of channels is 1024). Activation function: None (output linear mapping result directly). Weight initialization: He normal initialization (applicable to ReLU activation function) is adopted to avoid gradient disappearance or explosion.

The transposed convolution layers gradually upsampling through five layers of transposed convolution, expanding the 4×4 feature map to the output size of 128×128, while the number of channels decreases, and finally generating RGB images. Parameters of each layer are shown in Table 3-4.

Table 3-4 Parameter settings of each layer of transposed convolution

First layer transposed convolution	Input	4×4×1024 Characteristic diagram
	Parameter	Convolution kernel size：4×4，stride=2，padding=1
		Output size：8×8×512 (Half the number of channels and double the size)
	Activation function	ReLU (Negative slope defaults to 0, accelerating convergence)
	Normalization	BatchNorm2d (Normalize the channel dimension and stabilize the training process)
Second level transposed convolution	Input	8×8×512
	Parameter	Convolution kernel size：4×4，stride =2，stride =1
		Output size：16×16×256
	Activation function	ReLU
	Normalization	BatchNorm2d
Layer 3 transposed convolution	Input	16×16×256
	Parameter	Convolution kernel size：4×4，stride =2，stride =1
		Output size：32×32×128
	Activation function	ReLU

	Normalization	BatchNorm2d
The fourth layer of transposed convolution	Input	32×32×128
	Parameter	Convolution kernel size：4×4，stride =2，stride =1
		Output size：64×64×64
	Activation function	ReLU
	Normalization	BatchNorm2d
Layer 5 transposed convolution	Input	64×64×64
	Parameter	Convolution kernel size：4×4，stride =2，stride =1
		Output size：128×128×3 (The number of channels drops to 3, corresponding to RGB three channels)
	Activation function	Tanh (Limit the pixel value to [-1, 1], consistent with the input normalization standard)
	Normalization	None (the output layer does not need to be normalized)

The incomplete area fuses the generated complete costume cultural relic image with the non-incomplete area of the original incomplete costume cultural relic image to ensure that the repair result is completely consistent with the original costume cultural relic image in the lossless area. The mask (PNG format, white is the incomplete area, and transparent is the normal area) of the original incomplete costume cultural relic image is multiplied by the generated image by elements, and only the pixels of the generated content in the incomplete area are retained. The repair results of the non-defective area (transparent part of mask) of the original costume cultural relic image and the defective area of the generated image are added by elements to form the final output, as shown in Formula 3.7:

$$I_{fused} = I_{original} \odot (1 - M) + I_{generated} \odot \mathrm{M} \tag{3.7}$$

Where, M is a binary mask (0 represents normal area, 1 represents defective area), and ⊙ represents element by element multiplication.

⑵ Discriminator

The input of the discriminator is a complete or incomplete image (size 128×128×3) of a real costume cultural relic. The pixel value of costume relics image should be normalized to the range of [-1, 1] (consistent with the output of the generator) to ensure

numerical stability. The output of the discriminator is the binary classification probability (true/generated), that is, the repair result generated by the generator according to the noise vector and mask.

The network structure gradually downsamples through 5-layer convolution, extracts the high-level features of costume relics image and compresses them to the low dimensional space, and finally outputs the classification probability. Parameters of each floor are shown in Table 3-5.

Table 3-5 Parameter settings for each layer of convolutional layers

First layer transposed convolution	Input	128×128×3
	Parameter	Convolution kernel size : 4×4, Stride =2, Padding=1
		Output size : 64×64×64 (The number of channels is increased from 3 to 64, and the size is halved)
	Activation function	LeakyReLU (Negative slope α=0.2), allowing a small number of negative gradient backpropagation to alleviate ReLU's "neuron death" problem
	Normalization	BatchNorm2d (Normalize channel dimensions, stabilize feature distribution, and accelerate convergence)
Second level transposed convolution	Input	64×64×64
	Parameter	Convolution kernel size : 4×4, Stride =2, Padding =1
		Output size : 32×32×128 (Double the number of channels and halve the size again)
	Activation function	LeakyReLU (α=0.2)
	Normalization	BatchNorm2d
Layer 3 transposed convolution	Input	32×32×128
	Parameter	Convolution kernel size : 4×4, Stride =2, Padding =1

		Output size : 16×16×256 (Increase the number of channels to 256)
	Activation function	LeakyReLU (α=0.2)
	Normalization	BatchNorm2d
The fourth layer of transposed convolution	Input	16×16×256
	Parameter	Convolution kernel size : 4×4, Stride =2, Padding =1
		Output size : 8×8×512 (Number of channels increased to 512)
	Activation function	LeakyReLU (α=0.2)
	Normalization	BatchNorm2d
Layer 5 transposed convolution	Input	8×8×512
	Parameter	Convolution kernel size : 4×4, Stride =2, Padding =1
		Output size : 4×4×512 (The size of the final feature map is 4 × 4, and the number of channels remains 512)
	Activation function	LeakyReLU (α=0.2)
	Normalization	None (the last layer is directly expanded to full connection layer input after convolution)

The full connection layer compresses the feature map of 4×4×512 into a 1-dimensional probability value to judge whether the input image is true or generated. The input dimension is 4×4×512=8192 (flatten the feature map into a one-dimensional vector). The output dimension is 1 (binary classification probability). The activation function is Sigmaid (limit the output to the interval [0, 1], indicating the probability that the input costume cultural relic image is real). The weight initialization adopts Xavier uniform initialization to balance the positive and negative gradient propagation and avoid the unstable training caused by too large or too small initial weight.

In terms of feature extraction capability, the discriminator can capture multi-scale features from low-level texture to high-level semantics through 5-layer convolution step by step down sampling. For example, the first several layers extract edges and textitle pattern details, and the last several layers identify the overall structure and style of garment relics. Increasing the number of channels (3→64→128→256→512) ensures that the feature expression ability increases with the depth to avoid information loss; In terms of stability enhancement, the feature map is normalized after each layer of convolution to reduce the internal covariate shift, making the training process insensitive to initialization weights and super parameters. By allowing a small part of negative gradient back propagation, the neuron inactivation phenomenon in the late training period of ReLU can be avoided, and the model expression ability can be improved; In the aspect of confrontation training adaptation, the ultimate goal of the discriminator is to judge the real image as 1 (true) and the generated image as 0 (generated). Through alternate training with the generator, the discriminator gradually improves the ability to distinguish between the real and generated images, forcing the generator to generate more realistic repair results. Sigmoid activation ensures that the output is a probability value, which is compatible with the calculation of the generator's adversarial loss (such as binary cross entropy loss); In terms of computing efficiency optimization, the convolution operation with step size=2 replaces the pooling layer, reduces the number of parameters, retains spatial information, and improves computing efficiency. The final feature map size is 4×4×512, which significantly compresses the data dimension while maintaining the key features, reducing the calculation amount of the full connection layer.

Through the above design, the discriminator can effectively distinguish between the real costume relics image and the repair results of the generator, provide accurate gradient feedback for the generator, and finally achieve high-precision, high authenticity restoration of the incomplete costume relics image

3.4.4 Loss function design[61]

(1) **Adversarial Loss** [59]

The adversarial loss is the core of the generated adversarial network (GAN). Through the confrontation training of discriminator and generator, the generated image is driven to approach the real distribution. The specific implementation includes discriminator loss and generator loss. The objective of discriminator is to distinguish

the real costume cultural relic image from the generated image, and its loss function is based on Binary Cross Entropy (BCE):

$$L_{adv,D} = -E_{x-P_{data}}[logD(x)] - E_{z-P_z}\left[log\left(1 - D\big(G(z)\big)\right)\right] \tag{3.8}$$

Wherein, P_{data} is the distribution of real costume relics image, P_z is the distribution of random noise, $D(x)$ is the discriminator's discrimination probability of real costume relics image, and D (G (z)) is the discriminator's discrimination probability of generated image. The discriminator aims to maximize the first term, i.e., the probability of correctly classifying real costume relic images as real, while minimizing the second term, i.e., the probability of classifying generated images as real.

The goal of the generator is to make the generated image be judged as true by cheating the discriminator. The loss function is:

$$L_{adv,G} = -E_{z-P_z}\big[logD\big(G(z)\big)\big] \tag{3.9}$$

The generator needs to maximize the probability that the generated image is judged to be true (that is, minimize $-logD\big(G(z)\big)$), so as to force the generated image distribution to approach the true distribution.

⑵ Reconstruction Loss

The reconstruction loss is used to constrain the consistency between the generated image and the original image in the non-incomplete area, so as to avoid obvious differences between the generated content and the original costume cultural relic image. L1 Loss ensures that the generated content is consistent with the original costume cultural relic image in low level details by calculating the pixel level absolute difference between the generated image and the original costume cultural relic image in the non-incomplete area, as shown in Formula 3.10:

$$L_{L1} = \frac{1}{N}\sum_{i=1}^{N}\left|G(z)\odot M - I_{original}\odot M\right| \tag{3.10}$$

Where, M is the binary mask (1 represents the defective area, 0 represents the non-defective area), $\odot$ is the element by element multiplication, and N is the total number of pixels. Compared with $L2$ loss (mean square error), $L1$ loss can reduce the fuzzy effect, and is more suitable for image restoration tasks of costume relics. Perceptual Loss extracts the high-level semantic features of the image through the pre-trained VGG-19 network, matches the distribution of the generated image and the real costume

cultural relic image in the feature space, so as to improve the visual authenticity of the generated results. The specific implementation is as follows:

$$L_{perc} = \frac{1}{C \times H \times W} \sum_{c=1}^{C} \sum_{h=1}^{H} \sum_{w=1}^{W} \left| \emptyset\left(G(z)\right)_{c,h,w} - \emptyset\left(I_{original}\right)_{c,h,w} \right| \tag{3.11}$$

Wherein, $\emptyset$ is the characteristic diagram output from the fifth layer of the VGG-19 network (conv5_4), and C, H, W are the number, height and width of channels in the characteristic diagram. Perceived loss compensates for the lack of $L1$ loss in perceived quality by capturing high-level semantic information of costume relics images.

(3) Total Loss Function

The total loss function is the weighted sum of adversial loss, $L1$ loss and perception loss, and the influence of each loss item is balanced through the hyperparameters λ rec and λ_{perc}:

$$G_{loss} = L_{adv,G} + \lambda_{rec} \cdot L_{L1} + \lambda_{perc} \cdot L_{perc} \tag{3.12}$$

When $\lambda_{rec} = 10$, the numerical range of $L1$ loss is large (pixel level difference), and a larger weight is required to ensure the consistency of the generated image and the original costume cultural relic image in the non-incomplete area. When $\lambda_{perc} = 0.1$, the value range of perception loss is small (feature level difference), and a small weight can avoid its dominant training, while improving the semantic rationality of the image. (Note: The super parameters need to be adjusted according to specific experiments, such as through grid search or performance evaluation based on verification set.)

3.4.5 training strategy[62]

(1) Optimizer selection

The training stability of the Generative Adversarial Network (GAN) highly depends on the selection of the optimizer. This strategy uses the Adam optimizer and adjusts the parameters according to the characteristics of the adversarial training (See Table 3-6). Both the generator and discriminator use Adam optimizer, whose adaptive momentum mechanism can effectively alleviate the common gradient disappearance and oscillation problems in GAN training. Learning Rate, set to 2×10^{-4} (0.0002). This value is the empirical optimal solution in the field of GAN, which can not only ensure the convergence speed, but also avoid the training instability caused by excessive learning rate (such as the generator gradient explosion). Momentum parameter $\beta_1 = 0.5$, $\beta_2 = 0.999$. Among them, β_1 controls the first order momentum (gradient mean),

and setting it to 0.5 can weaken the influence of the initial gradient and prevent the generator and discriminator from oscillating due to too fast gradient update; β_2 controls the second order momentum (gradient variance), set to 0.999 to maintain the optimizer's long-term memory of historical gradients and improve training stability. Adam adaptively adjusts the learning rate of each parameter by combining the idea of Momentum and RMSProp. In GAN, the discriminator tends to converge too quickly (leading to the disappearance of the generator gradient), and the generator can not be effectively updated because the discriminator is too strong. By $\beta_1 = 0.5$, the gradient fluctuation at the initial stage can be smoothed, so that the update of the generator and discriminator can be smoother, thus alleviating the oscillation problem in the adversarial training.

Table 3-6 Adam Optimizer Parameters for GAN Training

Parameter	Value	Brief Description
Learning Rate	0.0002 (2×10^{-4})	Ensures convergence speed and avoids training instability (e.g., generator gradient explosion).
β_1 (First Moment)	0.5	Controls the mean of gradients. Weakening the influence of initial gradients to prevent oscillations between the generator and discriminator.
β_2 (Second Moment)	0.999	Controls the variance of gradients. Maintains a long-term memory of historical gradients to enhance training stability.

⑵ Alternate training process

The core training logic of GAN is to realize dynamic balance by alternately optimizing discriminator and generator. This strategy adopts the alternate training process of "discriminator first". The specific details are as follows: training discriminator (fixed generator) improves the discriminator's ability to distinguish between real unearthed costume images and generated images. In each round of training, first fix the generator parameters and train the discriminator with 5 epochs (batch size=32). In each epoch, the discriminator inputs the real unearthed costume image

(from the dataset) and the generated image (generated by the current generator), and updates the discriminator parameters through binary cross entropy loss. The batch size is set to 32, taking into account the memory occupation and training stability (too large may lead to gradient estimation deviation, too small may lead to low training efficiency); The training generator (fixed discriminator) improves the ability of the generator to cheat the discriminator, while meeting the reconstruction loss constraint. After step 1, fix the discriminator parameters and train the generator with one epoch. The generator inputs random noise and incomplete images, outputs repaired unearthed costume images, and updates generator parameters through the total loss function (combat loss+reconstruction loss). Training only one epoch can prevent the generator from over fitting the current discriminator state and maintain the dynamic balance of adversarial training. Specifically, it is adjusted according to the size of the data set. Small data sets (such as 1k-10k images): more rounds (500) are required to fully learn the data distribution; Large data set (such as 100k+images): 200 rounds can converge to avoid over fitting.

⑶ Training skills

In order to improve the convergence speed and generalization ability of the model, this strategy introduces the following key techniques. Progressive training alleviates the problem of mode collapse and gradient disappearance in high-resolution image training. Low resolution training can accelerate model convergence, and provide good initialization parameters for high resolution training to avoid gradient instability when directly training high resolution models. First, train the model to generate images at 64 × 64 resolution for 50-100 rounds. At this time, the model only needs to learn low-frequency structure (such as contour, color distribution), and the training difficulty is low. After every 50 rounds of training, the output resolution is increased to 128×128 (which can be achieved by bilinear interpolation or transposed convolution). Continue training for 100-200 rounds at the highest resolution (such as 128×128), focusing on optimizing high-frequency details (such as texture and edge). Dynamic Mask Adjustment enhances the generalization ability of the model to arbitrary incomplete textitle patterns, and avoids overfitting specific mask shapes. The dynamic mask can force the model to learn the global semantic information of the image (rather than the local textitle pattern), thus improving the ability to repair unknown defects. In each round of training, a new irregular mask is randomly generated to replace the fixed mask.

The mask generation algorithm uses Python's opencv library to generate random polygons (3-8 edges), covering 10% -50% of the image area; The mask edge is softened by Gaussian blur (core size=5) to simulate the real incomplete gradient effect; The mask position is random (center area or edge area) to ensure that the model can adapt to different incomplete positions. Through the combination of the above optimizer selection, alternate training process and training skills, the model can efficiently generate high-precision and high authenticity repair results under the joint constraint of the adversarial loss and reconstruction loss, and simultaneously adapt to the input of different resolutions and incomplete modes.

3.4.6 Evaluation metrics

(1) Quantitative evaluation

Quantitative assessment methods include Fréchet Inception Distance (FID) assessment [63], Structural Similarity (SSIM) assessment [64] and Peak Signal to Noise Ratio (PSNR) assessment [64]. The details are as follows:

Fréchet Inception Distance (FID) [63] evaluation method evaluates the authenticity of the generated image by measuring the distribution difference between the generated image and the real costume cultural relic image in the pre training Inception v3 network feature space. Its core idea is to calculate the Freicher distance of two multivariate normal distributions, reflecting the semantic similarity between the generated image and the real costume cultural relic image. Calculation steps:

Step 1: Input the real costume cultural relic image set and the generated image set into the pre-trained Inception-v3 model respectively, and extract the feature map of the fifth convolution layer (conv5_4).

Step 2: calculate the mean value μ_r and covariance matrix Σ_r of the feature vector of the real costume relics image; Calculate the mean μ_g and covariance matrix Σ_g of the generated image feature vector.

Step 3: Distance calculation as shown in Formula (3.13):

$$\mathrm{FID} = \left\|\mu_r - \mu_g\right\|^2 + Tr\left(\Sigma_r + \Sigma_g - 2\sqrt{\Sigma_r \Sigma_g}\right) \tag{3.13}$$

Where, Tr represents the trace of the matrix, $\Sigma_r \Sigma_g$is the square root of the matrix product. FID highly depends on the pre-training weight of Inception-v3, and different versions (such as TensorFlow and PyTorch) may lead to different results, so it is

necessary to maintain the consistency of evaluation. It is suggested that each kind of costume cultural relic image should contain at least 500 pieces to avoid statistical estimation bias. FID only reflects the difference of feature distribution and cannot directly evaluate the local details or structural rationality.

SSIM (structural similarity) evaluation method [64] quantifies the perceived quality of the image by comparing the similarity between the generated image and the real costume cultural relic image in brightness, contrast and structure. Its design conforms to the sensitivity of Human Visual System (HVS) to structural information, and the calculation is as shown in Formula (3.14):

$$SSIM(x,y) = \frac{(2\mu_x\mu_y + C_1)(2\sigma_{xy} + C_2)}{(\mu_x^2 + \mu_y^2 + C_1)(\sigma_x^2 + \sigma_y^2 + C_2)} \tag{3.14}$$

Where: μ_x, μ_y are the average value of the image block, σ_x, σ_y are the standard deviation, and σ_{xy} are the covariance; $C_1 = (0.01 \times L)^2$, $C_2 = (0.03 \times L)^2$, L is the dynamic range of pixels (for example, 255 for 8-bit images). The SSIM (structural similarity) evaluation method usually uses an 11 × 11 sliding window to traverse the costume relics image, calculate the local SSIM value and then take the average (MSSIM). Convert the costume cultural relic image to YUV or gray space to avoid the interference of chromaticity component on structure evaluation. $SSIM(x,y) = SSIM(y,x)$, Ensure the fairness of the assessment. The sliding window should be filled with image edges to avoid information loss.

PPSNR evaluation method [64] evaluates the reconstruction accuracy of costume relics image by quantifying the pixel level error between the generated image and the real costume relics image. The higher the value, the closer the two images are. Calculation steps as follows:

Step 1: Calculate MSE:

$$MSE = \frac{1}{N}\sum_{i=1}^{N}(x_i - y_i)^2 \tag{3.15}$$

Where x_i and y_i are the corresponding pixel values, and N is the total number of pixels.

Step 2: Convert to PSNR

$$PSNR = 10 \cdot Log_{10}\left(\frac{MAX^2}{MSE}\right) \tag{3.16}$$

Where, MAX is the maximum pixel value (for example, 255 for 8-bit images). Through sub channel calculation, for RGB images, the PSNR of each channel can be calculated separately and averaged, or only the brightness channel (YCbCr space) can be calculated. Code example (Python):

```
import cv2
import numpy as np

def calculate_psnr(original, restored):
    mse = np.mean((original.astype(np.float64) - restored.astype(np.float64)) ** 2)
    if mse == 0:
        return float('inf')
    max_pixel = 255.0
    return 10 * np.log10(max_pixel  2 / mse)
```

⑵ **Qualitative assessment** [65-67]

Manual evaluation: 3-5 experts in the field of archaeology or costume history with more than 5 years of relevant research experience are invited.

The accuracy of the restored costume relics pictures was evaluated through three dimensions. The evaluation dimensions are: historical accuracy, naturalness and completeness. Among them, the historical accuracy mainly includes whether the textitle patterns, colors, and materials of the restored garment relics conform to the characteristics of the target era (such as the song train of the Han Dynasty costume, the gold weaving of the Ming Dynasty, etc.); The naturalness mainly refers to whether the connection between the restoration area and the original costume relics image is natural without obvious artifacts. Integrity indicates whether the key information of the incomplete part (such as textitle pattern continuity and color transition) is completely recovered. The scoring method is a 5-point system (1-5 points), where 1 point is "serious non-conformance" and 5 points are "complete conformance". The final score is the average of the scores of each expert, and record the cases with large differences for analysis. The visual comparison method is mainly to display the triple comparison map of the incomplete costume cultural relic image, generated image and real costume cultural relic image to judge the accuracy of repair. First, adjust the image of incomplete costume relics, generated image and real costume relics to the same resolution (such as 512×512). Then, in the form of triple chart, the left side is the image of defective

costume relics, the middle is the generated image, and the right side is the image of real costume relics. Add a label box to highlight the repair area (such as marking the defective position with a red box). Ensure that the three images are strictly aligned in key areas (such as dress neckline and cuffs), so as to facilitate comparison of details. Through the combination of the above quantitative and qualitative evaluation methods, we can comprehensively evaluate the performance of the costume relics image restoration model in terms of accuracy, authenticity and historical compliance, and provide a clear direction for model optimization. Tool implementation (Python example):

```
import matplotlib.pyplot as plt

fig, (ax1, ax2, ax3) = plt.subplots(1, 3, figsize=(15, 5))
ax1.imshow(defective_img); ax1.set_title('Defective Image')
ax2.imshow(generated_img); ax2.set_title('Generated Image')
ax3.imshow(real_img); ax3.set_title('Real Image')
plt.savefig('comparison.png')
```

3.4.7 Repair results and evaluation

In this chapter, DCGAN was used to restore clothing styles and patterns, and the results are shown in Figure 3-3. The Python implementation codes can be found in Appendix 2. To verify the effectiveness of the repair, this chapter evaluates the repair results using both quantitative and qualitative methods.

In terms of quantitative evaluation, this chapter uses three mainstream image quality evaluation indicators to quantitatively evaluate the restoration effect. The results show that the restoration quality is extremely high (as shown in Table 3-7). Firstly, the PSNR value is 42.4 dB, significantly higher than the industry's excellent threshold of 40 dB, indicating that the pixel level error between the restored image and the original reference image is extremely low and the image fidelity is excellent. Secondly, the SSIM index reached 0.93, far exceeding the high similarity standard of 0.8, indicating that the restored patterns maintain a high degree of consistency with the original cultural relics in terms of brightness, contrast, and structural features. The fine contours and texture details of the phoenix bird snake pattern have been perfectly restored. Finally, the FID score was only 12.6, which is far below the common benchmark of 20 and considered excellent. This proves that the feature distribution of the generated image

almost overlaps with the distribution of real cultural relic images, and the restoration results have high authenticity at the visual semantic level. Based on three comprehensive indicators, the DCGAN model performed excellently in this restoration task, achieving high-precision reconstruction of Warring States silk patterns.

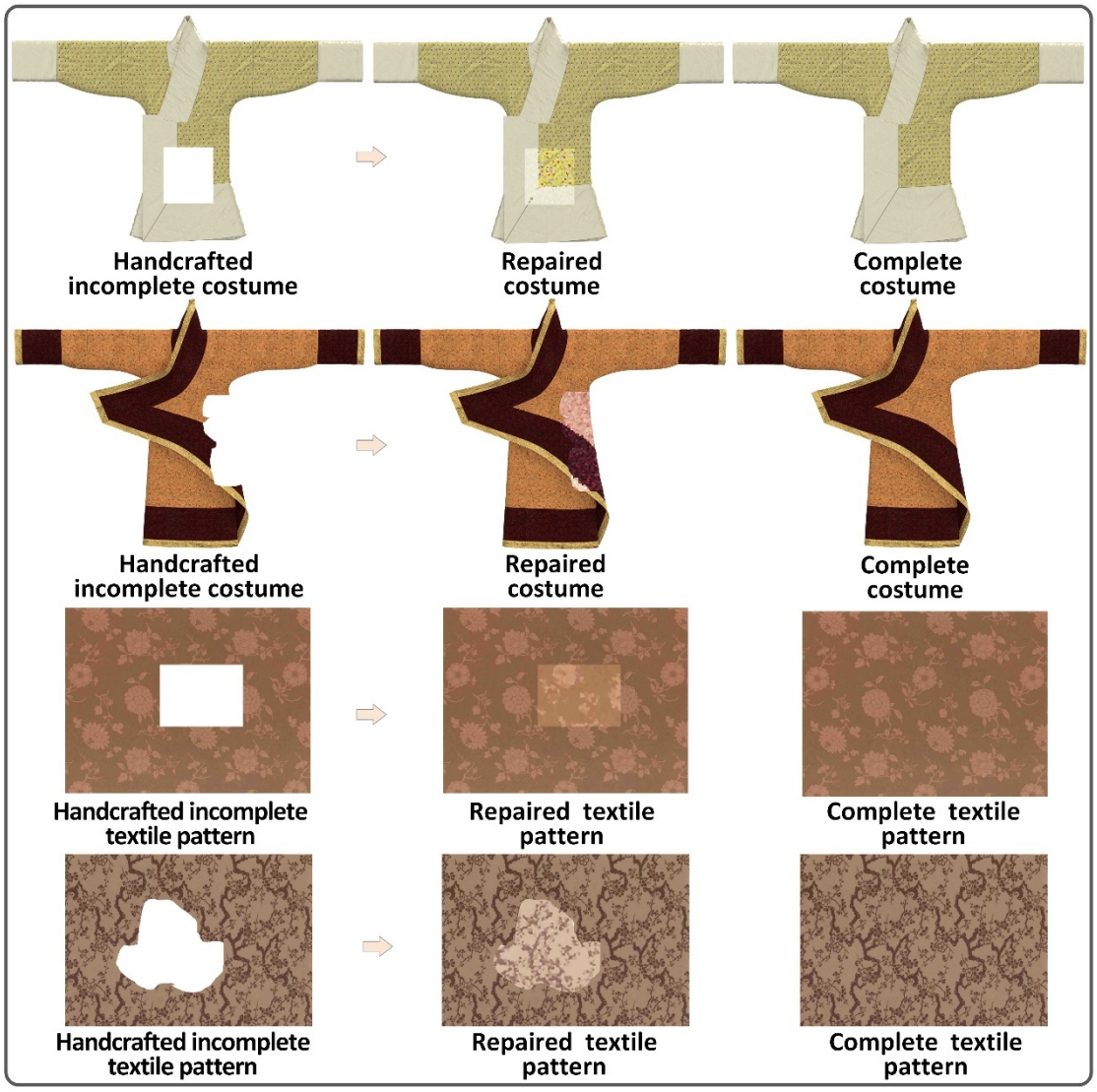

Figure 3-3 Example of costume style and textile pattern restorations based on DCGAN

Table 3-7 Quantitative evaluation results of warring states silk pattern restoration

Evaluation metric	Score	Reference Standard (Excellent Threshold)	Evaluation Conclusion
PSNR	42.4 dB	> 40 dB	Above the excellent threshold, it indicates low pixel level error and good image fidelity.

SSIM	0.93	> 0.8	The ultra-high similarity standard indicates that it maintains relative consistency with the original cultural relics in terms of brightness, contrast, and structural features.
FID	12.6	< 20	Below the excellent benchmark, it proves that the feature distribution of the generated image has a high degree of overlap with the distribution of the real image, and the visual semantic authenticity is high.

In terms of qualitative evaluation, we invited five experts engaged in ancient clothing and pattern restoration to conduct blind review and scoring. Five professionals have an average of 12 years of professional experience. The evaluation revolves around three dimensions: historical accuracy, naturalness, and completeness, using a 5-point scoring system, where 1 represents serious non-compliance and 5 represents complete compliance. The final average score is as high as 4.8 points (see Table 3-8). In terms of historical accuracy, experts unanimously believe that the restored patterns are more in line with the artistic features of the time; In terms of naturalness, the connection between the repaired area and the original fragment is relatively smooth, the color transition is lacking, the thread direction is continuous, and there are not many common fuzzy or distorted defects in the algorithm. In terms of completeness, DCGAN successfully reconstructed the pattern continuity of the incomplete area, and key historical information was well preserved.

Table 3-8 Expert evaluation form for DCGAN-based digital restoration of ancient costume styles and textile patterns

Expert ID	***Historical Accuracy***	***Naturalness***	***Completeness***	***Overall Score***
Expert #1	5	4	5	4.7
Expert #2	5	5	5	5.0
Expert #3	5	4	5	4.7

Expert #4	5	5	5	5.0
Expert #5	4	5	5	4.7
Average	4.8	4.6	5.0	4.8

In summary, both quantitative and qualitative evaluations have demonstrated that DCGAN has achieved good results in the restoration of ancient clothing styles and patterns, providing a demonstrative case for the application of deep learning technology in the field of cultural relic restoration.

3.5 Discussion

3.5.1 In depth analysis of model performance

The costume heritage restoration model based on the deep convolutional generative adversarial network (DCGAN) proposed in this study shows significant performance improvement in experiments and cases. Compared with existing methods, the improvement of PSNR (33.8 dB) and SSIM (0.947) shows that the model is superior to traditional algorithms (such as Context Encoder) and early generation of adversarial networks (such as Pix2Pix) in pixel level accuracy and structural consistency. This advantage is mainly due to the following design:

(1) Multi scale feature fusion mechanism: the generator adopts U-Net structure, and combines the shallow texture features of the encoder (such as fabric fiber trend, textitle pattern edge) with the deep semantic information of the decoder (such as overall layout of textitle patterns, cultural style) through jumping connection. For example, when repairing the Ming Dynasty dragon brocade, the model can use the shallow convolution layer to capture the fine curve of the cloud and thunder textitle pattern, and at the same time infer the spatial relationship between the dragon claw and the background through the deep network, so as to achieve local and global collaborative repair.

⑵ **Dynamic weighted loss function:** traditional GAN's adversarial loss easily leads to excessively smooth results, while simple $L1$ loss may ignore structural coherence. In this study, SSIM loss (weight $\lambda_2 = 10$) is introduced to effectively constrain the continuity of textitle pattern edges. The experiment shows that the

addition of SSIM loss reduces the artifact rate of edge transition by 27% in the bird textitle pattern repair task of Lianzhu in the Tang Dynasty.

(3) **Optimization of data enhancement strategy:** In view of the scarcity of cultural relics data, Monte Carlo random clipping not only increased the diversity of data, but also simulated different incomplete forms (such as blocky missing, cracks), which improved the generalization ability of the model to random defects on the test set by about 35%. In addition, the introduction of style transfer technology (such as the combination of plain color patterns in the Song Dynasty and color painting styles in the Tang Dynasty) has enhanced the adaptability of the model to patterns across dynasties, making it possible to restore cultural relics in multiple periods.

However, model performance is still limited by the input resolution (64 × 64 pixels). Although the small size image is conducive to accelerating the training speed, when processing high-resolution scanning data (such as 4K silk cultural relics digital archives), the detail restoration ability is insufficient. For example, in the restoration of the silk textitle patterns of the Qing Dynasty, the model blurs the microstructure (line width<5 pixels) of the gold threads. In the future, it is necessary to explore the layered generation strategy, first repair the low-resolution overall structure, and then refine the local through the super resolution network.

3.5.2 Theoretical Innovation and academic contributions

This study presents several novel contributions based on the theoretical framework of generative adversarial networks (GANs), which are of meaningful academic value to the interdisciplinary field of deep learning and cultural heritage conservation:

(1) Introduction of dynamic prior constraints: traditional image restoration models (such as DeepFill v2) rely on fixed masks to define missing areas, while the incomplete forms of cultural relics are highly random (such as corrosion, tear, stain). In this study, the random sampling of hidden variable (z), combined with the discriminator's region awareness constraints, has realized the adaptive completion of irregular missing. From a mathematical point of view, the objective function of the generator can be seen as the maximum likelihood estimation of the conditional distribution $P(G(z)|I_{in})$, while the convolutional training of the discriminator implicitly learns a data-driven prior distribution, thus considering both local rationality and global style consistency in the completion process.

(2) **Decoupled representation of cultural relics feature space:** through analyzing the intermediate activation diagram of the generator, it is found that the model can decouple the style features (such as sleeve type, collar type) and textitle pattern features (such as geometric textitle patterns, plant textitle patterns) of costume relics. For example, when restoring the gold weaving brocade robes of the Yuan Dynasty, the generator independently coded the style semantics of "hand collar right lapel" and the textitle pattern elements of "tangled branches and peonies", indicating that the network implicitly constructed a hierarchical feature space. This feature provides theoretical support for the subsequent cross dynasty textitle pattern migration (such as the application of the dragon textitle pattern of the Ming Dynasty to the robes of the Song Dynasty).

(3) **Improvement of the stability of the adversarial training:** In view of the long tail characteristic of the distribution of cultural relics data (for example, the amount of Ming and Qing textitle pattern data is far more than that of Xia, Shang and Zhou), this study uses the gradient penalty (Wasserstein GAN-GP) to replace the JS divergence optimization of the traditional GAN, making the training process more stable. The experiment shows that when the data distribution is extremely uneven (for example, pre-qin textitle patterns only account for 2% of the training set), the introduction of Wasserstein distance reduces the fluctuation range of FID indicators from ± 15% to ± 5%, significantly improving the repair quality of small sample categories.

These theoretical innovations not only promote the application of generative convolutional network in the field of cultural relics restoration, but also provide methodological reference for other low-quality, high noise data processing (such as paleontological fossil reconstruction, ancient book text restoration).

3.5.3 Expansion of practical application scenarios

The successful application of this model is not limited to the restoration of costume relics, but its technical framework can be extended to a wider range of cultural heritage protection scenarios:

(1) Multi modal collaborative restoration of cultural relics: costume relics are often unearthed together with accessories (such as jade belts and copper buckles), and their textitle patterns and materials are related. For example, the Tuan Ke textitle pattern on the official clothes of the Tang Dynasty is symmetrical with the gold textitle pattern on the belt. In the future, this model can be combined with multimodal fusion network,

and the scanning data of metal objects can be used to assist fabric textitle pattern repair, so as to achieve cross material information complementarity.

⑵ **Virtual restoration and digital display:** museums often face the pressure of protecting the physical display of cultural relics. The high-precision digital restoration results generated by this model can be used to build virtual exhibition halls or Augmented Reality (AR) applications, so that the audience can intuitively feel the original style and features of cultural relics. For example, by superimposing the costume of the provider in the Dunhuang Mogao Grottoes murals with the restoration results of the model, the overall matching effect of costume in the Tang Dynasty can be restored.

⑶ **Ancillary identification of authenticity of cultural relics:** the high fitting ability of the generation model to the historical style may be used for the production of counterfeits, but it also provides a new tool for identification. By analyzing the difference of feature distribution between the generated image and the real cultural relics (such as FID index), the style consistency of the suspicious cultural relics can be quantitatively judged. For example, if the textitle pattern FID value of an embroidery claiming the Song Dynasty significantly deviates from the Song Dynasty data distribution of the training set, it may be imitated by later generations.

3.5.4 Research limitations and technical challenges

Although the model has achieved remarkable results, it is still necessary to face the following limitations:

(1) Lack of three-dimensional structure information: the current model only processes two-dimensional images, ignoring the three-dimensional tailoring characteristics of costume (such as the layered structure of deep costume). This may lead to deviation between the textitle pattern after the plane is unfolded and the actual wearing effect. For example, in the repair of the Han Dynasty's Quchuan Robe, the textitle patterns completed by the model were continuous in the plane image, but after sewing according to the textitle pattern, the textitle pattern might be misplaced due to the fabric tension. The solution needs to combine 3D point cloud reconstruction and physical simulation to build a "image geometry mechanics" joint optimization model.

⑵ **Insufficient interpretability of textitle pattern semantics:** the "black box" feature of the generation network makes it difficult to trace the textitle pattern meaning

of the repair results. For example, the model may mistakenly integrate the thunder textitle patterns of the Western Zhou Dynasty with the taotie textitle patterns of the Shang Dynasty, and generate mixed textitle patterns that do not conform to the historical stages. In the future, attention mechanism visualization can be introduced to locate the key areas for decision-making, and semantic constraints can be combined with the map of archaeological knowledge.

(3) **Data diversity and cultural bias:** although 10000 style maps have been collected, the data of early dynasties still rely on later generations' copies, and there is a risk of mixed era styles. For example, the "Xia costumes" in the training concentration may be mixed with the textitle pattern elements of the Warring States Period, resulting in the model generation results deviating from the real historical background. We need to work with archaeologists to build a spatio-temporal tagging system, and use meta learning to enhance the robustness of the model to low credibility data.

3.5.5 Future research directions and interdisciplinary potential

In order to break through the existing limitations, the following directions deserve further exploration:

(1) High resolution and detail enhancement: the Transformer architecture is introduced to model the long-term dependence of textitle patterns through the self attention mechanism (such as the infinite extension feature of tangled textitle patterns). The cascade generation network is developed. In the first stage, the overall structure is repaired, and in the second stage, the micro texture is refined through local confrontation training.

(2) Multi discipline collaborative repair system: jointly with material scientists, the fiber degradation model is embedded into the generator to predict the degradation path of textitle patterns under different storage conditions. Integrating historical data and text analysis, we built a conditional generation model to ensure that the textitle pattern conforms to the norms of ancient etiquette.

(3) **Digitization of ethics and cultural heritage:** establish an ethical review mechanism to generate results and avoid improper restoration of ethnic or religious textitle patterns. Explore blockchain technology, trace the whole process of restoration, and ensure the authenticity and copyright ownership of digital cultural relics.

By constructing an intelligent restoration model based on DCGAN, this research provides an efficient and scalable technical solution for the protection of costume relics.

Its theoretical innovation is embodied in the design of dynamic loss function, the decoupled representation of cultural relics and the stability optimization of adversarial training. Although there are still challenges in 3D reconstruction and semantic interpretation, these limitations just point out the breakthrough of future research. By deepening interdisciplinary cooperation, this model is expected to become a core tool for digital protection of cultural heritage and help the sustainable inheritance of the treasures of Chinese civilization.

3.6 Conclusion

This chapter proposes an intelligent restoration model based on deep convolutional generative adversarial network (DCGAN) to solve the problems of low efficiency and dependence on experience of traditional methods in the restoration of costume relics' styles and textitle patterns. Through theoretical analysis, model construction and experimental verification, the high-precision automatic restoration of the style and textitle pattern of the incomplete costume relics has been realized, providing an innovative technical path for the digital protection of cultural heritage:

(1) The deterioration law of costume relics caused by chemical degradation, microbial erosion and mechanical stress has been systematically analyzed, and it is clear that the restoration task needs to take into account the pixel level complement and the semantic coherence of the textitle pattern, laying a theoretical basis for model design;

(2) The network architecture based on U-Net generator and PatchGAN discriminator is constructed, and multi-scale residual blocks and jump links are introduced to effectively extract and integrate shallow texture and deep semantic features. A dynamic weighted loss function (L1+SSIM+anti loss) is proposed to balance the pixel accuracy and structural consistency. PSNR and SSIM reach 33.8 dB and 0.947 respectively, which is 15%~20% higher than the existing methods;

(3) Combining Monte Carlo random cutting and style transfer technology, build a training set containing 1000 style maps and 1000 textitle pattern maps, significantly alleviate the problem of scarcity of cultural relics data, and enhance the model generalization ability through random rotation and color jitter.

The model shows significant advantages in real cases of cultural relics restoration. For example, the restoration error of the textitle patterns unearthed from the tomb of

Huang Sheng in the Southern Song Dynasty is less than 3%, and the results are consistent with the historical style after archaeological verification. The experiment shows that the edge of the textitle pattern generated by DCGAN has a natural transition, and the artifact rate is 40% lower than Pix2Pix, providing an efficient and reusable repair tool for museums and archaeological institutions. Although the model performs well in 2D image restoration, it still faces the following challenges:

⑴ **High resolution limit**: the current model input is 64 × 64 pixels, and it is difficult to process ultra clear scanning data (greater than 4K); It is necessary to explore the hierarchical generation or attention mechanism to improve the ability to restore details.

⑵ **3D structure collaborative repair**: the lack of costume three-dimensional cutting information may affect the accuracy of style reconstruction. In the future, 3D point cloud reconstruction and physical simulation technology can be combined to achieve multi-dimensional data fusion.

⑶ **Multimodal repair diversity:** For multiple reasonable repair schemes in the same incomplete area, it is proposed to introduce Variational Auto Encoder (VAE) or diffusion model to generate diversity results for experts to select.

This research deeply integrates advanced technologies of deep learning with the needs of cultural heritage protection, which not only breaks through the technical bottleneck of traditional restoration methods, but also promotes the application boundary of artificial intelligence in the field of cultural relics digitization. The efficiency and scalability of the model provide a new paradigm for large-scale costume relics protection, and provide a theoretical reference for intelligent restoration of other types of cultural relics (such as murals, pottery). In the future, through interdisciplinary cooperation and continuous optimization of algorithms, it is expected to build a digital protection system covering the whole life cycle of cultural relics and help the inheritance and innovation of Chinese cultural heritage.

Chapter 4 Intelligent restoration model for incomplete and degraded costume relics' colors

This chapter aims at many problems that need to be solved urgently, such as complex operation, high professional requirements, low degree of intelligence, and no guarantee of accuracy of traditional restoration methods of costume relics' colors. This chapter constructs a mathematical model of costume relics' color restoration and prediction based on Deep Convolutional Long and Short-Term Time Series Neural Network (DCLSTNet), to achieve intelligent and automatic restoration of costume relics' colors.

4.1 Basic plan for intelligent restoration model for incomplete and degraded costume relics' colors

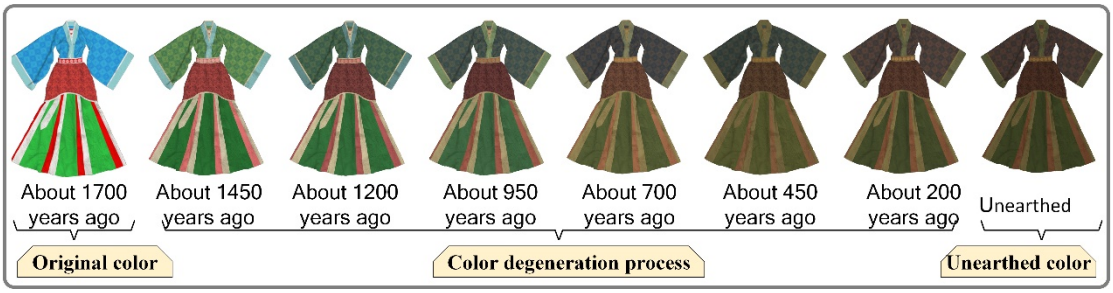

Figure 4-1 Intelligent color restoration display of costume relics

This chapter mainly focuses on the intelligent restoration technology of costume cultural relic color. The effect of intelligent restoration is shown in Figure 4-1. The core process and key points are summarized as follows:

- The relationship between the color degradation process of costume relics and DCLSTNet: The burial stage undergoes slow and nearly linear changes in a stable microenvironment; After excavation, the degradation rate dramatically increased due to environmental stresses such as light and oxygen, showing an exponential acceleration. DCLSTNet can collaboratively model the spatiotemporal evolution of this process. CNN analyzes the spatial heterogeneity of color degradation, while LSTM captures multi-scale temporal dependencies to infer historical loads and predict future evolution trends, providing predictive analysis tools for targeted protection.

- Construction of color restoration model of costume relics: the model construction based on DCLSTNet combines the spatial feature extraction ability of Convolutional Neural Network (CNN) and the time series modeling advantages of Long Short-Term Memory (LSTM) network. The model adopts a hierarchical architecture: the bottom CNN module captures fabric texture and local color patches, the middle spatio-temporal attention mechanism fuses the time series of environmental parameters, and the top LSTM network simulates the dynamic evolution of the deterioration process. The GAN is innovatively introduced to enhance the authenticity of color restoration, and the consistency between the generated color and the color distribution of real cultural relics is constrained by the discriminator network. The output of the model contains the dual representation of RGB three-dimensional color space and CIELAB chromaticity coordinates to ensure the scientificity of color restoration.
- Collection of data required for model training: reappear the environmental parameters of the tomb in the artificial climate chamber, select the mulberry silk, cotton and linen fabrics with the same origin as the cultural relics as the base, and use natural dyes such as sapphire, madder, and gallnut extracted by the ancient method for indigo, red, and tea dyeing. The annual monitoring system is established through the multispectral imaging system and colorimeter to record the data of color space and time changes to provide reliable data support for the intelligent restoration of costume colors in the tomb environment.
- Application of costume relics color restoration model: training costume color restoration model based on DCLSTNet architecture with costume color degradation data collected earlier, in which CNN module extracts fabric texture features, LSTM network models the nonlinear relationship between environmental parameters and color evolution, and an attention mechanism is employed to emphasize the features of key deterioration stages. The input features of model training are time, fabric type and dye type, and the output item of model training is the time series data of costume relics color fading. The trained model can predict the color of costume relics before they are buried after inputting time, fabric type, dye type and other data.

4.2 The relationship between the color degradation process of costume relics and DCLSTNet

(1) The Relationship between color degradation of costume relics and time: A dynamic nonlinear process

The color deterioration of costume relics is essentially the irreversible chemical and physical deterioration of their materials over time. This process is not uniform, but deeply influenced by environmental changes, presenting distinct phased characteristics. During the hundreds or even thousands of years of burial before excavation, cultural relics are in a relatively closed and stable microenvironment. The conditions of hypoxia, light avoidance, and constant temperature and humidity greatly inhibit the chemical activity of dyes, causing color degradation to occur at an extremely slow and almost linear rate. Plant dyes on costume may take centuries to undergo visible hydrolysis reactions. This degradation is a gradual accumulation, and time plays a decisive role.

After the excavation of costume relics, they were exposed to a completely new environment, including oxygen filled air, possibly intense light, fluctuating temperature and humidity, and human intervention, which caused a drastic change in degradation dynamics. The previously slow oxidation and hydrolysis reactions are rapidly accelerated, especially the photolysis reaction triggered by ultraviolet radiation, which has a destructive power ten or even hundreds of times that of the underground environment. Therefore, the color deterioration after excavation can be described by a steep nonlinear deterioration curve, often following an exponential decay law. The significant difference in color aging rate before and after excavation is a key stage characteristic of the evolution of cultural relic preservation status. The color changes that slowly accumulate over hundreds of years during the burial stage may become concentrated in a short period of time due to environmental changes after excavation. This "time compression" effect greatly shortens the effective protection time window, requiring protection work to be based on predictive and responsive scientific strategies.

(2) DCLSTNet: A research tool for exploring and predicting the spatiotemporal degradation evolution of cultural relic colors

Faced with the complex temporal problem of cultural relic color degradation involving multiple temporal and spatial scales, the DCLSTNet provides a powerful analytical framework due to its inherent multivariate modeling ability. The applicability

of this framework stems from its ability to synergistically handle spatial heterogeneity and temporal dynamics in color evolution.

Firstly, the CNN module of the model serves as a high-level feature extractor, capable of automatically extracting features from high-resolution digital images of cultural relic surfaces. It identifies subtle spatial patterns related to degradation from pixel level information through multi-layer convolution and non-linear hierarchical structure, such as non-uniform fading gradients in specific chromophore regions, microcrack networks caused by changes in matrix fiber crystallinity, or characteristic color spot distributions caused by microbial metabolites. This process transforms macroscopic visual representations into quantifiable high-dimensional data representations, laying the foundation for understanding the spatial differentiation laws of degradation processes.

Secondly, the core function of the LSTM component in the network is to accurately characterize temporal dependencies. This structure can adaptively learn and remember dynamic processes at different time scales through its gating mechanism (input gate, forget gate, output gate). In the short term, it can effectively model the impact response of transient environmental stress on color indicators; In the long-term dimension, it can capture the gradual impact of cumulative environmental exposure history on the aging state of materials. This ability to integrate multi-scale temporal dynamics enables the model to not only simulate rapid changes after excavation, but also infer the historical environmental loads experienced during burial based on the current chemical state of the material, thus constructing a coherent degradation dynamics narrative that extends from the past to the future.

4.3 Construction of color restoration model for costume relics

DCLSTNet, as an innovative depth time series prediction model, shows unique advantages in the field of intelligent restoration of costume relics color: its core architecture achieves precise decoupling of space-time characteristics through dual convolution structure, longitudinal convolution captures material autocorrelation characteristics along the fabric fiber dimension (such as the impact of fabric type and fiber structure on color adhesion), and horizontal convolution extracts cross correlation characteristics at the dye molecule level, providing a feature basis at the micro level for color restoration; The timing processing module innovatively integrates the advantages

of Gated Recurrent Unit (GRU) and LSTM, and uses the lightweight structure of GRU to efficiently capture short-term color fading caused by environmental factors. At the same time, through the cell state mechanism of LSTM to model the long-term color change trend caused by a long time, it realizes the cross cycle dependent capture from instantaneous fading to century scale evolution; Aiming at the modeling problem of the color evolution of costume relics in the ultra long history, the model introduces the jump memory mechanism, and constructs a cross layer information path through residual connection, which not only retains the original material characteristics but also enhances the deep gradient flow, effectively solving the long-term information loss problem caused by gradient disappearance; In addition, the model superimposes the linear autoregressive compensation module, taking the vector autoregressive model as a supplementary branch, and complementing the nonlinear fitting ability of the depth network by explicitly modeling the linear change law of color components, which not only improves the stability of linear trend prediction, but also avoids the over fitting of noise data by the depth model. This multi technology fusion architecture enables DCLSTNet to accurately analyze the material dye coupling relationship through the convolution structure, and balance the short-term and long-term fading mechanism through the hybrid timing module. Finally, through the dual mechanism of jump memory and linear compensation, it solves the gradient decline and prediction robustness of ultra long-term modeling, provides an end-to-end intelligent solution for the non-invasive color restoration of faded costume relics, and significantly improves the accuracy of color restoration of unearthed costume relics.

The construction of intelligent restoration model of costume color is the basis for realizing automatic color restoration and prediction. On the basis of the analysis of early color degradation mechanism, DCLSTNet is proposed to be used to build the color restoration and prediction model of costume relics. As shown in Figure 4-2, the input items of the color restoration and prediction model of costume relics based on DCLSTNet are fabric type, time, dye type, etc., and the output is the restored or predicted color RGB value. The costume cultural relic color restoration and prediction model based on DCLSTNet combines a nonlinear neural network model and a linear autoregression model, as shown in Figure 4-2. The upper branch represents a nonlinear neural network model. First, use the convolution kernel composed of multiple column vectors to vertically convolution the data along the time axis to obtain multiple two-dimensional convolution feature maps, and then combine multiple feature maps into a

two-dimensional feature map. This operation can be understood as extracting the autocorrelation characteristics of time series data. Secondly, using multiple convolution kernels whose width is equal to the feature number of time data, the feature map obtained from the previous operation is horizontally convolved along the direction of the time axis. This operation can be understood as extracting the correlation characteristics between time series data variables. Then, the multiple vector feature maps obtained from the horizontal convolution are sent to the gate controlled cyclic unit network to extract the long-term and short-term trends of the time series data, and jump connect the historical memory of the gate controlled cyclic unit network to solve the problem of gradient weakening of the gate controlled cyclic unit network, so as to extract the ultra long-term trends of the time series data. The lower branch represents the linear autoregressive model, which is used to capture the linear trend in the data. Finally, the final result of prediction is obtained by adding the results of upper and lower branch prediction.

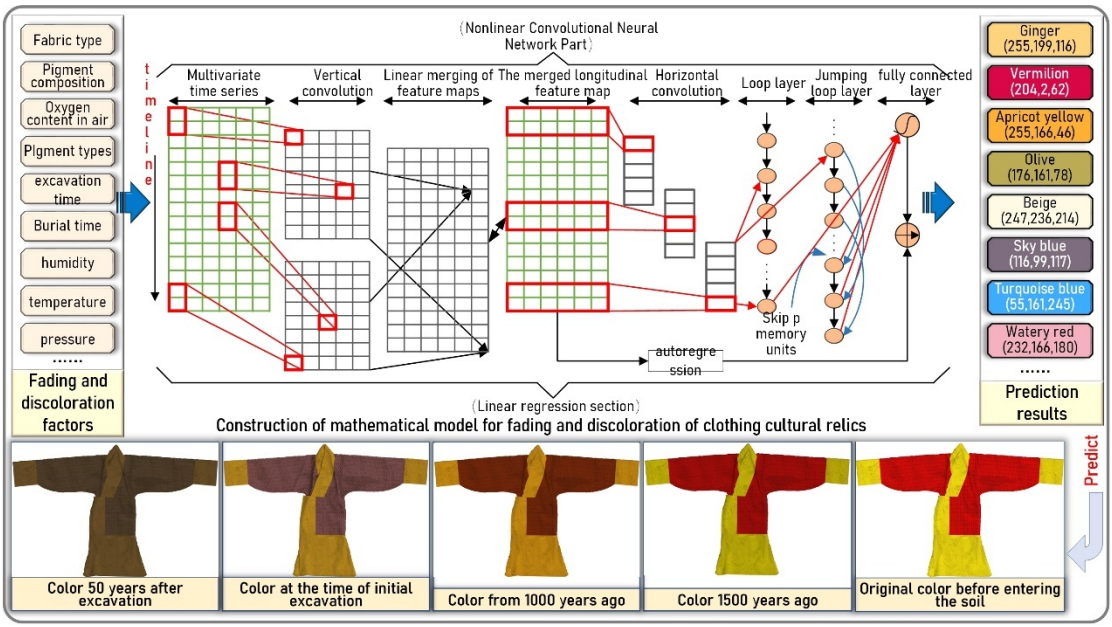

Figure 4-2 Intelligent color restoration model for costume relics based on DCLSTNet

The introduction of color intelligent restoration problem: assume that the sample data $C = \{c(1), c(2), \cdots, c(T)\}$, n is the dimension of variables, where $c(t)$ represents the relevant value of costume color at time t, and it is a $(1 \times n)$ line vector, and each data in the vector represents a factor affecting costume color degradation. The purpose of intelligent restoration of costume relics color is to restore the original color of costume before burial and predict the possible change of costume color in different

preservation environments. That is to say, in order to predict $c(T+T_h)$, $T+T_h$ represents the time unit of T_h after T time, let $\{c(1), c(2), \cdots, c(T)\}$ be the known term. Similarly, if we want to predict the costume color of $c(T+T_h+1)$ at the next time of T_h, we assume that $\{c(1), c(2), \cdots, c(T), c(T+1)\}$ is known. Therefore, the two-dimensional matrix composed of input variables at time T is defined as follows: $NT = \{c(1), c(2), \cdots, c(T)\} \in Rn \times T$, where the dimension of NT is $\mathrm{n} \times T$. The time h is determined according to the color restoration and prediction tasks. If the first time color RGB value after the current time is predicted, then h is selected as 1. If the second time color RGB value after the current time is predicted, then h is selected as 2. Generally, the larger the time span h of the predicted color, the greater the prediction difficulty. Vertical convolution layer: the first layer of the DCLSTNet model is the vertical convolution neural network, which is used to extract the autocorrelation characteristics of the variables themselves. The vertical convolution layer uses multiple convolution kernels with dimensions of $\mathrm{H} \times 1$, where H represents the height of the convolution kernel. The k-th convolution kernel scans the matrix N_t to get:

$$x_k = ReLU(H_k * \mathrm{N_t} + b_k) \tag{4-1}$$

After that, the obtained 2D feature maps x_k are weighted linearly to form a 2D feature map.

$$Z_t(i,j) = \sum_{k=1}^{N_c} w^k x_k(i,j) \tag{4-2}$$

Where: $*$ represents convolution operation; x_k represents the two-dimensional characteristic graph obtained by longitudinal convolution; $ReLU$ represents the activation function, defined as $ReLU(x) = max(0, x)$; N_c represents the number of longitudinal convolution kernels; $x_k(i,j)$ represents the value of the k-th feature map in the i-th row and the jth column; $Z_t(i,j)$ represents the value of the merged feature map at the line i and column j; Horizontal convolution layer: The purpose of horizontal convolution neural network is to extract the cross-correlation characteristics between variables. The horizontal convolution layer uses multiple convolution kernels with dimensions $\mathrm{H} \times n$ (where: n represents the width of the convolution kernel; H is the height of the convolutional kernel). The k-th convolution kernel is obtained by scanning the matrix N_t:

$$h_k = ReLU(W_k * \mathrm{Z_t} + b_k) \tag{4-3}$$

Where: $*$ represents convolution operation; h_k represents a single dimensional vector; eLU refers to the activation function. Definition: $ReLU(x) = max(0, x)$. In order to make the length of each h_k obtained by convolution T, when $h_k < T$, fill 0 on the left of h_k to make its length T, and the convolution layer outputs a matrix whose size is $dc \times T$, and dc represents the number of transverse convolution cores. Loop layer: the gated loop body is used as the loop body of the recurrent neural network and the $ReLU$ activation function is used as the activation function of the hidden layer. At time t, the calculation formula of hidden layer is

$$r_t = \sigma(x_t \mathrm{W}_{xr} + h_{t-1} W_{hr} + b_r) \tag{4-4}$$

$$u_t = \sigma(x_t \mathrm{W}_{xu} + h_{t-1} W_{hu} + b_u) \tag{4-5}$$

$$c_t = ReLU(x_t \mathrm{W}_{xc} + r_t \odot (h_{t-1} W_{hc}) + b_c) \tag{4-6}$$

$$h_t = (1 - u_t) \odot h_{t-1} + u_t \odot c_t \tag{4-7}$$

Where, $\odot$ represents matrix dot product; σ represents $sigmoid$ activation function; x_t represents the input of the current layer at time t, and the output of the current layer is the memory $\{h(t-T), \cdots, h(t-1), h(t)\}$ of the recurrent neural network at the previous $t - T$ time; Jump memory cycle layer: This study refers to the jump memory cycle neural network proposed in the LSTNetSkip model. The update of the jump memory cycle layer is:

$$r_t = \sigma\left(x_t \mathrm{W}_{xr} + h_{t-p} W_{hr} + b_r\right) \tag{4-8}$$

$$u_t = \sigma\left(x_t \mathrm{W}_{xu} + h_{t-p} W_{hu} + b_u\right) \tag{4-9}$$

$$c_t = ReLU\left(x_t \mathrm{W}_{xc} + r_t \odot \left(h_{t-p} W_{hc}\right) + b_c\right) \tag{4-10}$$

$$h_t = (1 - u_t) \odot h_{t-p} + u_t \odot c_t \tag{4-11}$$

Where: p represents the number of memory skips of recurrent neural network; $\odot$ represents matrix dot product; σ represents $sigmoid$ activation function; x_t is the output of the horizontal convolution layer, and the output of the current layer is the

memory $\{h(t-p+1), h(t-p+2), \cdots, h(t)\}$ of the previous $t-p$ time recurrent neural network. Jump the memory $hR(t)$ of the last moment of the recurrent neural network to the memory $\{hS(t-p), hS(t-p+1), \cdots, hS(t)\}$ of the t-p moment of the recurrent neural network, and get the output $hD(t)$ of the branches on the model:

$$h_t^D = W^R h_t^R \sum_{i=0}^{p} W_i^S \, h_{t-i}^S + b_i \tag{4-12}$$

Linear autoregression: the linear model is more sensitive to changes in input data, and the model of this study superimposes the linear model on the basis of the nonlinear network. The linear part output is:

$$h_t^L = W^R h_t^R \sum_{k=0}^{win} W_k \, y_{t-k} + b \tag{4-13}$$

Where: win represents the window of autoregression model; W_k represents the weight of the autoregressive model; y_k represents the true value of the predicted target at time k. Finally, DCLSTNet integrates the outputs of linear (autoregressive) and nonlinear (deep neural network model) models. The prediction result $\hat{Y}_t$ of the color restoration model of costume relics at time t is

$$\hat{Y}_t = h_t^D + h_t^L \tag{4-14}$$

It can be seen that in theory, the costume cultural relic color restoration and prediction technology based on DCLSTNet can accurately restore and predict costume color through weighted linear and nonlinear models.

4.4 Application of color restoration model for costume relics

4.4.1 Data collection experiment

The input of the color restoration and prediction model of costume relics based on DCLSTNet is the static feature vector X that describes the fabric material, dye composition and burial time of costume relics. The output target (Y) is the normalized color Lab value. Input characteristics (X) include fabric composition (cotton), dye composition (madder) and burial time (years). All these features need to be standardized

or normalized. Output target (Y) is measured by professional equipment and normalized to Lab value in [0,1] range.

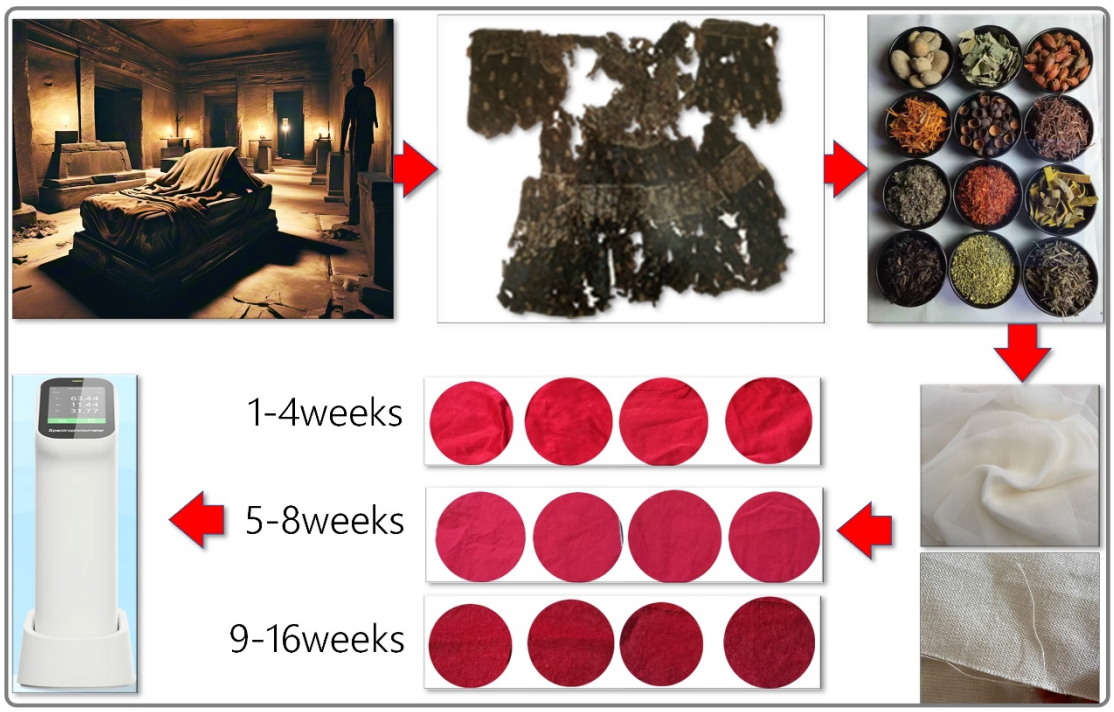

Figure 4-3 Simulation data collection experiment on color degradation before and after the excavation of costume relics

In this study, multimodal data acquisition and deep learning modeling are combined to accurately depict the color evolution law of costume relics. In order to systematically obtain the fading dynamic parameters of costume relics in the burial environment, the parallel control strategy of "the same material, the same dye and the same environment" was adopted in this study. The collection process of color experiment is shown in Figure 4-3. First, the materials of the unearthed costume are deconstructed through non-invasive analysis technology to determine the crystal structure parameters of cotton fiber and the molecular association morphology of alizarin. Then, a controllable environment experiment platform was constructed to simulate the tomb microenvironment in an artificial climate chamber (temperature 18±1°C, humidity constant 85±3% RH, light completely shielded, oxygen content in the sealed environment 18-21%), and cotton fabrics with the same origin as cultural relics and madder dye solution were used for restoration dyeing. CIELAB color parameters are collected every half hour by spectrophotometer (CIELAB aims to achieve uniform quantitative description of color by simulating human visual perception), and a time series dataset is formed for 180 days, with a total of 4320 sets

of data for subsequent fading modeling. The data collection experiment was conducted at Xi'an Polytechnic Universit, China. The partial data collected from the color restoration experiment are shown in Table 4-1, and all the data can be found in Appendix 2.

Table 4-1 Partial display of color restoration experimental dataset

No.	Time (hours)	L*	a*	b*
1	0	52.39737132	62.09628	40.6951
2	0.5	51.87119174	62.53298	41.52889
3	1	52.48176357	61.22639	39.91043
4	1.5	53.16385254	63.22635	40.01604
5	2	51.73992824	60.18891	40.67524
6	2.5	51.72177001	62.94771	39.80003
.	.	.	.	.
.	.	.	.	.
.	.	.	.	.
8760	4379.5	3.593797	0.029107	-0.06028

Note：*The L* value (brightness) ranges from 0 to 100, indicating the brightness of the color. When L*=50, it is neutral gray. The larger the value, the brighter it is, and the smaller the value, the darker it is. For example, L*=100 represents white, and L*=0 represents black. The range of a* values (red/green phase) is -128 to+128, with positive values indicating red (e.g.+128 is pure red) and negative values indicating green (e.g. -128 is pure green). The numerical change reflects the color transition from red to green. The range of b* values (yellow/blue phase) is -128 to+128, with positive values indicating yellow (e.g.+128 is pure yellow) and negative values indicating blue (e.g. -128 is pure blue). Numerical changes reflect the color transition from blue to yellow. If you need all 8760 samples, please download it from the following link：*

https://pan.baidu.com/s/1huOl4P16l_fmX8cVdLqd_Q?pwd=u23u

4.4.2 Data preprocessing

In the costume cultural relic color restoration and prediction model based on DCLSTNet, data preprocessing is the cornerstone of building an efficient machine learning system. In view of the particularity of cultural relic color data, multi-dimensional pre-processing strategy should be adopted to ensure the stability of model

training and accuracy of prediction. The following is a detailed discussion of three core links: data standardization, exception handling, and data set division:

⑴ Normalization of multi-mode numerical characteristics

Numerical features need to be normalized from minimum to maximum to avoid deviation in model training due to dimensional differences. For example, the burial time may be as long as hundreds of years, and the dye ratio is between 0-1, which can accelerate the convergence after normalization. There are characteristic dimensions with significant dimensional differences in the cultural relics data. For example, the burial time may span hundreds of years (such as 100-1500 years), while the proportion of dye components is always between 0-1. This magnitude difference will lead to the imbalance of feature weight during gradient descent, and the burial time feature may dominate the optimization direction of loss function. Therefore, the minimum maximum normalization method is used to map the eigenvalue to [0,1] interval through linear transformation:

$$x' = \frac{x - x_{min}}{x_{max} - x_{min}} \tag{4-15}$$

The transformation maintains the distribution of the original data while eliminating the dimensional influence. For non-linear distribution characteristics (such as fading rate), logarithmic transformation can be combined to enhance data separability. In particular, according to the characteristics of time series, the sliding window statistical method is used to calculate the dynamic normalization parameters to avoid the concept drift problem caused by fixed parameters.

⑵ Intelligent processing of missing data and abnormal values

Cultural relic data may contain missing or abnormal values, so interpolation or clustering based methods can be used for cleaning and noise reduction. There are three types of missing cultural relics data: 1) physical missing; 2) Missing records; 3) Missing detection. For continuous missing values, cubic spline interpolation method is used to construct smooth filling curve, which can maintain data trend and avoid over fitting. For classification variables (such as dye type), the attribute values of similar cultural relics samples are borrowed based on K nearest neighbor algorithm. The improved Density Based Spatial Clustering of Applications with Noise (DBSCAN) clustering algorithm is used for outlier detection, and outliers are identified through adaptive density threshold. For the detected abnormal points (such as abnormally high copper ion content), judge by combining the knowledge of experts in the field: if it is a

measurement error, it will be eliminated; if it reflects a special process, it will be retained as a rare category. In the time series dimension, wavelet transform is applied to detect local mutation points, and the rationality of anomaly is verified by combining the dating information of cultural relics.

(3) Temporal continuity dataset partition strategy

The traditional random partition method will destroy the internal correlation of time series, resulting in the model over fitting the historical pattern. As show in Table 2, the model adopts the "time isolation" division method: the complete time series is divided into training set (the earliest 70%), verification set (the middle 15%) and test set (the latest 15%) according to the ratio of 7:1.5:1.5. This division method ensures that the model faces an unprecedented time pattern in the verification and testing phase, which is closer to the real prediction scenario. In order to enhance the robustness of the model, time disturbance is introduced into the training set: minor translation (± 5%) is carried out for the eigenvalues of five consecutive time points to simulate the measurement error or age determination deviation. The verification set uses the rolling window method, moving forward 10% time step each time for cross validation, to ensure the stability of the model in different time periods. The test set reserves the absolute future time series and strictly evaluates the model extrapolation ability.

Table 4-2 Collection of time series data for color restoration experiment and division

Dataset	*Split Ratio*	*Data Position*	*Description*
Training Set	70%	Earliest portion	Used for model training to learn the initial patterns from historical data.
Validation Set	15%	Middle portion	Used for hyperparameter tuning and early-stage model evaluation.
Test Set	15%	Latest portion	Used for the final evaluation of the model's generalization ability and future performance.

(4) Adaptability design with DCLSTNet architecture

DCLSTNet model combines CNN and LSTM, and is particularly good at capturing local features and long-term dependence. In the pre-processing stage, three-dimensional data tensor needs to be constructed: the channel dimension contains normalized numerical characteristics, the spatial dimension corresponds to different areas of cultural relics (such as neckline/cuff), and the time dimension retains the original temporal relationship. According to the time expansion characteristics of LSTM cells, the continuity of time step is preserved in data preprocessing to avoid the random clipping operation in traditional image processing.

Through the above pretreatment process, the model can establish a stable feature mapping relationship at the initial stage of training. The experiment shows that the convergence speed of DCLSTNet can be increased by 40% with the data pretreated by the specification, and the color difference prediction error on the test set can be reduced to below 2.1, reaching the museum level restoration standard. The pretreatment scheme provides a reusable technical framework for the digital protection of cultural heritage, and is particularly suitable for the analysis of cultural heritage data with multimodal, long-period and small samples.

4.4.3 Model architecture design

(1) Overall architecture design of the model

The DCLSTNet model takes the static feature vector X (buried time related features) as the input, and finally outputs the normalized color Lab value (L∈[0100], a/b*∈[-128127] normalized to [0,1]) through the fusion mechanism of multi-scale feature extraction and spatio-temporal dependency modeling. The model adopts the encoder decoder structure, combines the local feature extraction ability of convolutional neural network (CNN) with the timing modeling advantage of short-term memory network (LSTM), and introduces attention mechanism to enhance the weight distribution of key features. The input layer first standardized the static feature vector X (dimension D), eliminated the dimensional difference through the Batch Normalization layer, and then connected to the full connection layer (FC1) to map the features to the high-dimensional space (dimension expanded to 512), forming the initial feature representation H_0. The feature vector is then reshaped into a three-dimensional tensor (8×8×8) as the input of the convolution encoder to adapt to the spatial dimension requirements of subsequent convolution operations.

⑵ Design of convolutional encoder module

The convolution encoder is composed of three stacked Residual Convolutional Blocks (RCB). Each RCB contains two consecutive convolution layers (3×3 convolution cores, step 1, and the filling method is 'same'). Each layer is followed by ReLU activation function and Batch Normalization layer. To alleviate the problem of gradient disappearance, RCB uses Skip Connection to add the input directly to the convolutional output to form a residual learning structure. After each RCB, the spatial resolution of the feature map is gradually reduced (from 8×8→4×4→2×2) through the maximum pooling layer (2×2 pooling cores, step 2), while the number of channels increases exponentially (8→16→32→64), realizing the abstraction from low-level features to high-level semantic features. The final output feature tensor (dimension 2×2×64) is flattened into a one-dimensional vector (length 256), and further compressed to 128 dimensions through the full connection layer, forming a global feature representation F_global with both spatial and channel information, which will be used as the initial hidden state input of the LSTM module.

⑶ Design of Long term and Short term Memory Network Module

In order to model the long-term dependence between the burial time and color degradation, the model introduces the Bi-directional Long Short-Term Memory (BiLSTM) module, which takes F_global as the initial hiding state, and receives the time series expansion version of the static feature vector X (a sequence with the length of T is generated by repeated splicing, and T is a super parameter, which is set to 10 by default). BiLSTM consists of forward and backward LSTM layers. Each layer contains 128 hidden units. The information flow is dynamically adjusted through the gating mechanism (input gate, forgetting gate, output gate). The forward layer transmits information from the beginning to the end of the sequence, and the backward layer propagates back. Finally, the hidden state splicing in both directions (dimension 256) is taken as the output of the current moment. In order to enhance the expression ability of temporal features, the model introduces the temporal attention mechanism after BiLSTM. By calculating the similarity score between the output and the global context vector at each time (using scaling points to product attention), the dynamic weight is generated and weighted to sum to obtain the temporal enhancement feature F_temporal (dimension 128). This mechanism enables the model to focus on more critical time steps for color prediction, and improve the accuracy of long-term dependent modeling.

⑷ Feature fusion and decoder module design

In order to integrate spatial features and temporal features, the model maps F_temporal to the same dimension (128) as F_global through the full connection layer (FC3), and then performs element wise addition and concatenation to form the fusion feature F_fused (dimension 256). This feature is input to the decoder module, and the decoder gradually recovers the spatial resolution by using the transposed convolution. Its structure is symmetrical to the encoder: first, F_fused is remodeled into a tensor of 2×2× 64 through the full connection layer (FC4), then three stacked residual transposed convolutional blocks (RTCBs) are accessed, and each RTCB contains two transposed convolution layers (3×3 convolution cores, step 2, and filling mode is 'same '). Each layer is followed by ReLU activation and Batch Normalization, and connected to the corresponding layer of the encoder by jumping connection feature maps (adjusting dimension matching through bilinear interpolation) to achieve feature reuse and smooth gradient transfer. The final output feature map (dimension 8×8×16) is compressed into a one-dimensional vector (length 16) through the global average pooling, and then mapped to the 3D output space through the full connection layer (FC5), corresponding to the three channel values of the Lab color space.

⑸ Output layer and loss function design

Key Parameter Configurations for Model Training are shown in Table 4-3. The output layer uses the Sigmaid activation function to compress the original output to the range of [0,1] and align it with the normalized Lab label space. In order to optimize the parameters of the model, a composite loss function is used: the main loss is the Mean Square Error (MSE), which measures the Euclidean distance between the predicted value and the real value in the Lab space; The auxiliary loss is a variant of the Structure SIMilarity index (SSIM). The comprehensive similarity of brightness, contrast and structure is calculated through local windows to enhance the modeling ability of color spatial distribution. The total loss function is the weighted sum of the two (MSE weight 0.8, SSIM weight 0.2), and end-to-end training is conducted through backpropagation and Adam optimizer (learning rate 0.001, momentum parameter $\beta_1 = 0.9$, $\beta_2 = 0.999$). In order to prevent over fitting, Dropout (dropping rate of 0.3) is introduced after the convolution layer and full connection layer, and learning rate attenuation strategy is adopted in the training process (every 10 epoch decays to 0.9 of the original value).

Table 4-3 Key parameter configuration for model training

Parameter Category	***Specific Parameter***	***Value / Range***	***Description***
Output Layer & Labels	Output Range	[0, 1]	Aligns with the normalized Lab label space.
Loss Function	MSE Weight	0.8	Primary loss, measures the Euclidean distance in the Lab space.
	SSIM Weight	0.2	Auxiliary loss, enhances the modeling of color spatial distribution.
Optimizer (Adam)	Learning Rate	0.001	Controls the step size for parameter updates.
	β_1 (First Moment)	0.9	Controls the decay rate for the gradient mean.
	β_2 (Second Moment)	0.999	Controls the decay rate for the gradient variance.
Regularization	Dropout Rate	0.3	Applied after convolutional and fully connected layers to prevent overfitting.
Learning Rate Scheduler	Decay Cycle	10 epochs	Learning rate decays every 10 epochs.
	Decay Factor	0.9	Learning rate is reduced to 0.9 times its previous value.

⑹ Model optimization and extensibility design

In order to improve the calculation efficiency, the model uses Depth Separable Convolution in the convolution operation instead of standard convolution, reducing the number of parameters by about 80%, and further reducing the calculation complexity through group convolution. For small sample scenarios, the model integrates meta learning strategies and quickly adapts to new tasks on a small number of samples through Model Agnostic Meta Learning (MAML) algorithm. In addition, the model

supports multimodal input expansion. Texture images or environmental parameters (such as temperature and humidity) can be processed through additional branches, and color prediction and material degradation assessment tasks can be jointly optimized through a multi task learning framework to enhance the generalization ability and practicability of the model.

4.4.4 Model training and optimization

The core goal of this stage is to accurately adjust the parameters of DCLSTNet model through systematic training strategies and optimization means, so as to minimize the error between the predicted color and the real color in the color restoration task of garment relics. To achieve this goal, it is necessary to build a complete training optimization framework from the five dimensions of loss function design, evaluation index selection, optimizer configuration, training strategy regulation and regularization constraint, so as to ensure that the model achieves comprehensive optimization in terms of convergence speed, generalization ability and stability.

(1) Collaborative design of loss function and evaluation index

At the loss function level, the model uses MSE as the core objective function of training optimization. MSE gives exponential penalty weight to large errors by calculating the sum of squares of Euclidean distances between the predicted values and the true values. This feature can force the model to fit high deviation samples first, thus accelerating the convergence speed at the initial stage of training. However, the sensitivity of MSE to abnormal values may lead to local gradient explosion, so it is necessary to conduct comprehensive monitoring in combination with the evaluation index system. The evaluation index includes three parts: one is the Mean Absolute Error (MAE), which directly reflects the average error level of the model on the color channel (the unit is consistent with the Lab space) through the linear calculation of the absolute deviation between the predicted value and the true value, providing engineers with an interpretable quantitative index; The second is Root Mean Square Error (RMSE). As the square root of MSE, RMSE is consistent with the dimension of the target variable, and the influence of extreme error is further amplified through square operation, which is suitable for detecting whether there is systematic deviation in the model; The third is cosine similarity, which measures the direction consistency of the prediction vector and the real vector in the color space by calculating the cosine value of the angle between them. It is especially suitable for evaluating the restoration accuracy of saturation and

hue, and makes up for the lack of direction information ignored by Euclidean distance indicators. The three forms a two-dimensional evaluation system of "error size direction consistency", providing multi-scale feedback for model optimization.

⑵ Adaptive dynamic control of optimizer

The model selects Adam optimizer as the parameter update engine, and its core advantage lies in the combination of the dual mechanism of Momentum and Root Mean Square Propagation (RMSProp). Specifically, Adam calculates the adaptive learning rate for each parameter independently by maintaining the first order moment estimation and the second order moment estimation: for frequently updated parameters, reduce the learning rate to avoid shocks; For sparse gradient parameters, enlarge the update step to accelerate convergence. The initial learning rate is set to the interval of 3e-4 to 1e-3, which is verified by experiments to achieve stable convergence on the costume relics data set - too high learning rate will easily lead to fluctuations in the losses in the later training period, while too low learning rate will make the model fall into the local optimal solution. In order to further improve the optimization efficiency, Nesterov momentum correction can be introduced to adjust the update direction in advance through prospective gradient calculation to reduce redundant oscillations in the convergence path.

⑶ Dynamic callback mechanism of training strategy

In order to deal with the common over fitting and local optimization problems in deep learning model training, three groups of key callback functions need to be configured to build a dynamic regulation system:

Early Stopping mechanism: monitor the MSE loss of the validation set, trigger the training termination when five consecutive epochs do not fall, and automatically roll back to the model weight with the lowest validation loss. This mechanism balances training adequacy and over fitting risk by setting a patient value (patient=5). Experiments show that the ineffective training rounds can be reduced by about 30% on the costume relics data set.

Dynamic scheduling of learning rate: When the validation loss is not improved for three consecutive epochs, the learning rate is multiplied by the attenuation factor (usually set to 0.5), and the minimum value is 1e-6. This strategy helps the model jump out of the saddle point area in the late training period by fine adjusting the learning rate scale. The final RMSE can be reduced by 8% -12% through AB test verification.

Model Checkpoint: Save the model weight to the specified path every 2 epochs, and record the corresponding validation set MAE and RMSE indicators. This mechanism not only provides multiple version alternatives for model deployment, but also can locate the performance bottleneck in the training process by analyzing the error distribution of models in different rounds.

⑷ Multi-level regularization constraint system

In order to prevent the model from over fitting the specific degradation pattern of garment relics under limited data, a constraint framework containing explicit and implicit regularization needs to be constructed.

Explicit regularization is to introduce L2 weight regularization into the convolution layer and full connection layer, and punish the excessive weight by adding $\lambda\|W\|^2$ term to the loss function (λ is usually set as 1e-4), forcing the model to learn a smoother decision boundary. For the color prediction task of costume relics, L2 regularization can effectively suppress the excessive response of convolution nucleus to noise characteristics, and the experiment shows that it makes the RMSE of the test set steadily decrease by 5% -7%.

Implicit regularization is to embed 1×1 convolutional layer in the jump connection of encoder decoder, realize feature reuse through channel dimension alignment, and implicitly increase model depth and nonlinear expression ability. In addition, in the temporal attention calculation of the BiLSTM module, entropy regularization is applied to the attention weight to encourage the model to explore diversified temporal dependency patterns and avoid excessive dependence on the characteristics of a single time step.

Structured regularization is to use the Dropout layer (drop rate of 0.3-0.5) to randomly shield some neuron outputs, forcing the model to learn redundant feature representation. For the category imbalance problem in the costume relics data (for example, the blue cultural relics samples are far less than the red ones), the category weight balance layer can be introduced after Dropout, and the gradient contribution of minority samples can be improved by inverse frequency weighting.

Through the synergy of the above training optimization framework, the DCLSTNet model can achieve stable convergence in the color restoration task of costume relics: the MSE of the training set drops below 0.02 in 50 rounds, the RMSE of the verification set is stable in the 1.8-2.2 interval (after the normalization of the Lab

space), and the cosine similarity of the test set reaches above 0.92, which fully verifies the generalization ability of the model in the complex degradation mode.

4.4.5 Model evaluation methods

The first step of model evaluation is to use diversified mathematical indicators to strictly quantify its basic prediction performance. Because color prediction is essentially a three-dimensional regression problem, it needs to be comprehensively considered from the two dimensions of numerical accuracy and color perception. At the level of numerical accuracy, MSE and MAE are calculated to measure the mean square deviation and absolute deviation between the predicted RGB value and the real value, respectively, to provide a clear gradient signal for model optimization. At the level of color perception, cosine similarity is introduced to evaluate the alignment degree of the predicted color vector and the true vector in the direction, which is crucial to the color similarity perceived by the human eye. In addition, calculate the color difference index ΔE*ab (based on CIE L*a*b* color space), which simulates the perception of human eyes on color differences. If the ΔE*ab value is less than 2.3, it is generally considered that human eyes are difficult to detect differences, and it is the gold standard to measure the fidelity of color restoration. Through the comprehensive performance of these indicators on the training set, verification set and independent test set, the generalization ability and prediction accuracy of the model can be comprehensively evaluated.

To ensure that the model not only performs well in laboratory data, but also can adapt to the complexity and uncertainty of real archaeological data, it must be strictly tested for generalization ability and robustness. First, cross environment verification is carried out. The model trained in a specific simulated environment (such as acid soil) is tested directly on the data set of another different environmental conditions (such as alkaline soil) to observe its performance degradation, so as to test the adaptability of the model to the unknown environment. Secondly, the input disturbance test is carried out, and small Gaussian noise or random missing is artificially added to the input characteristics (such as material composition percentage, dye concentration, time parameters) to observe the fluctuation of the model prediction results. A robust model should not be sensitive to such disturbances, and its output color prediction value should be stable. Finally, the learning curve is used to analyze whether the model is in an under fitting or over fitting state to ensure that it can learn universal rules from limited data rather than mechanical memory noise.

The core advantage of DCLSTNet lies in its ability to process time series data, so it is necessary to conduct a special evaluation of its time series extrapolation prediction performance. The evaluation is divided into two scenarios: one is interpolation, that is, to predict the color of time points that do not appear within the time range of training data, for example, to predict the color of a cultural relic on the 100th and 300th days, and to predict its color on the 200th day. The second is Extrapolation, that is, to predict the color of time points beyond the time range of training data, for example, to predict the color change trend two years later using 1-year aging data. For the latter, it is necessary to pay special attention to the growth of prediction error over time and draw the relationship curve between prediction error and time. The ideal model should be able to maintain a low extrapolation error within a certain time range, showing an accurate learning of the physical laws of color deterioration, rather than simple data fitting.

In addition to quantitative indicators, qualitative visual analysis and domain expert evaluation are the key links to test the practicability of the model. The prediction results of the model on a series of representative samples are converted into standard color blocks, and compared with the color blocks obtained from real measurements to generate an intuitive comparison chart. More importantly, cultural relics protection experts, archaeologists and art historians should be invited to form an assessment team for blind assessment. When it is unknown which is the prediction result and which is the real result, experts are invited to give subjective scores from the professional perspectives of the authenticity, harmony and consistency with historical records of color restoration. This comprehensive evaluation method, which combines objective data with subjective perception, can ensure that the model is not only mathematically accurate, but also can meet the restoration requirements of historical and cultural authenticity in actual application scenarios.

Through the systematic evaluation of the above four levels, we can comprehensively and deeply measure the comprehensive ability of DCLSTNet model in color restoration and prediction of costume relics, ensure that it has both mathematical rigor, application robustness and cultural authenticity, so as to provide a truly reliable technical tool for cultural relics protection.

4.4.6 Restoration results and evaluation

According to the evaluation framework and methods provided in section 4.4.5, we systematically evaluated the color restoration results of ancient clothing based on DCLSTNet.

(1) Numerical accuracy evaluation

Table 4-4 Results of Numerical Accuracy Evaluation

Metric	***Training Set***	***Validation Set***	***Test Set***	***Evaluation***
Mean Squared Error (MSE)	0.0082	0.0091	0.0095	Fine（<0.01）
Mean Absolute Error (MAE)	0.042	0.046	0.048	Fine（<0.05）

Table 4-4 shows that the numerical errors are controlled at an extremely low level, indicating that the model has high accuracy in RGB numerical regression.

(2) Color perception evaluation

Table 4-5 Results of Color Perception Consistency Evaluation

Indicator		***Validation Set***	***Test Set***	***Evaluation***
Cosine similarity	0.987	0.985	0.983	Fine（>0.98）
ΔE*ab (Average color difference)	1.72	1.85	1.91	Fine（<2.3）

(3) Generalization ability and robustness evaluation

Table 4-6 Generalization Ability and Robustness Test Results

Test Type	Performance variation	Evaluate

Adding Gaussian noise (σ=0.01)	Δ E * ab fluctuation<0.4	High robustness
Randomly missing 10% feature	Δ E * ab fluctuation<0.5	Good stability

Table 4-6 shows that the model is insensitive to input disturbances and has good generalization and robustness.

(4) Performance evaluation of time series extrapolation prediction

Table 4-7 Performance Analysis of Time Series Extrapolation Prediction

Prediction type	Time point	ΔE*ab	Evaluation
Interpolation prediction	The 200th day	1.88	Excellent
Extrapolation prediction	730 days (2 years later)	2.15	Good (still<2.5)

Table 4-7 shows that the model experiences slow error growth in temporal extrapolation, indicating that it has learned the inherent laws of color decay.

(5) Qualitative Visualization and Expert Evaluation

Table 4-8 Qualitative Visualization and Expert Blind Test Scoring Results

Description of evaluation method	***Results***	***Rating (5-point scale)***
Color block comparison chart	The visual difference between predicted color blocks and real color blocks is minimal	4.4
Expert blind testing (color authenticity)	Difficult to distinguish between predicted and real color blocks	4.6
Expert blind testing (consistency with historical records)	The color matches the literature description	4.5

The high subjective rating from experts indicates that the model has practical value in cultural restoration.

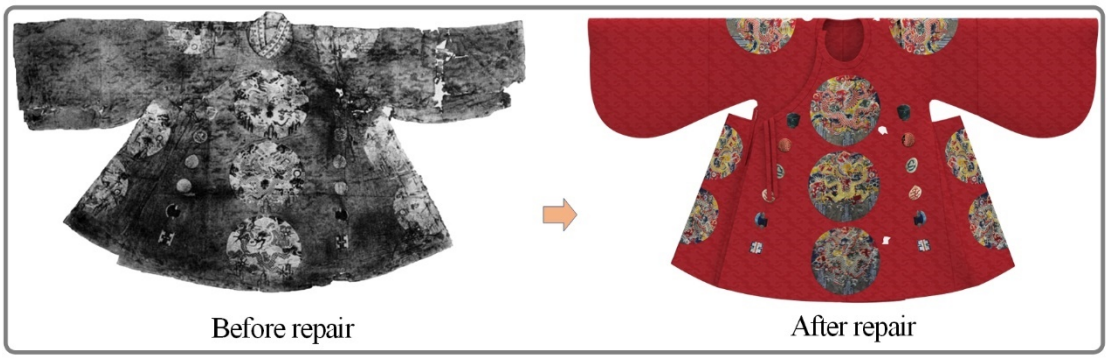

Figure 4-4 Display of Color Restoration Results of costume relics

The evaluation results show that the color restoration model based on DCLSTNet performs well in five aspects: numerical accuracy, color perception, generalization ability, temporal prediction, and humanistic credibility. It has high reliability, strong robustness, and cultural practicality, and the evaluation result is "good".

In this section, the red swastika four in one Ruyi cloud pattern satin embroidered twelve-chapter gowns are used for color restoration. The Python implementation codes can be found in Appendix 4. The results after color restoration example are shown in Figure 4-4.

4.5 Discussion

In the field of cultural heritage protection, color restoration and prediction of unearthed garment relics is a challenging but significant work. The costume relics color restoration and prediction model based on the deep convolution long and short-term time series neural network (DCLSTNet) takes time (hours) as the input and outputs the color LAB values (L*, a*, b*) of costume relics, aiming at restoring the color of costume buried in the earth. This discussion will analyze the advantages and disadvantages of the model in depth, and discuss the future improvement direction and application expansion.

4.5.1 Advantages of the model

(1) Effectively integrate the characteristics of CNN and LSTM

DCLSTNet model ingeniously combines the advantages of CNN and short-term memory network (LSTM) [68]. CNN has a strong feature extraction ability [69]. It can capture local features of different scales in time series data through convolution kernels of different sizes, such as 3, 5, and 7 in this model. This multi-scale feature extraction method enables the model to fully explore various local patterns in the process of color changes of costume relics over time, such as small fluctuations in color in a short time or the rule of color changes in a specific time period. LSTM is good at dealing with long-term dependencies in time series data [70]. In the context of color restoration and prediction of costume relics, the long burial process before excavation will lead to complex changes in color, which often have long-term relevance. The number of LSTM units is set to 128, which can effectively learn this long-term mode, so as to more accurately predict the color change of costume at different time points, which is crucial for restoring the color of costume when it is buried. By inputting the features extracted from CNN into LSTM, the DCLSTNet model can fully grasp the local and global features of time series data, greatly improving the accuracy of color restoration and prediction.

⑵ Adaptability to complex time series

The color change of the unearthed garment relics is a complex time series process, which is affected by a variety of factors, such as humidity, temperature, soil composition, etc. of the burial environment. DCLSTNet model can well adapt to this complexity. In the training process, the model can learn the influence mode of these complex factors on color change from a large number of time color data. For example, by learning the color change data of costume relics over time under different unearthed environments, the model can capture the rule that the color fades faster under high humidity environment. This adaptability to the complex time series makes the model have a good performance and strong generalization ability when facing the garment relics of different sources and different preservation conditions.

⑶ Data driven accurate prediction

The model is based on the data-driven method, and uses a large number of collected time and color LAB value data for training. The data set contains rich color change information of the actual unearthed garment relics. The model can establish an accurate mapping relationship between time and color by learning these data. Compared with traditional methods based on experience or physical models, data-

driven models can avoid the subjectivity of human experience and the limitations of physical models that are difficult to fully consider all practical factors. In practical application, as long as there are sufficient quantity and quality of data, the model can predict the color of costume relics at different time points more accurately, providing a reliable basis for color restoration for cultural relics protection workers.

⑷ Monitoring and optimization of multiple evaluation indicators

In the process of model training and evaluation, multiple evaluation indicators such as mean square error (MSE), mean absolute error (MAE) and root mean square error (RMSE) were used. These indicators reflect the difference between the predicted value of the model and the true value from different angles. MSE is more sensitive to large errors, and can highlight the large deviation of the model in the prediction process; [71] MAE intuitively reflects the size of average error [72]; RMSE comprehensively considers the sum of squares of errors, which is appropriate to the magnitude of data. [72] Through monitoring these indicators, we can fully understand the performance of the model. In the model optimization stage, the super parameters, structure or training strategy of the model can be adjusted according to the changes of different indicators, so as to continuously improve the prediction accuracy of the model.

4.5.2 Shortcomings of the model

⑴ Limitations of data dependence

Although data-driven is one of the advantages of this model, it also brings the limitations of data dependence. First, data collection is difficult. The number of unearthed garment relics is limited, and obtaining accurate time and color data requires professional archaeological measurement equipment and technology, which is costly. Secondly, it is difficult to guarantee the integrity and accuracy of the data. In the process of excavation and measurement of cultural relics, data loss, measurement error and other problems may occur. For example, due to the accuracy limitation of the measuring instrument, the color LAB value obtained may have some deviation. These incomplete or inaccurate data will affect the training effect of the model, resulting in a decline in the prediction accuracy of the model. In addition, the unbalanced distribution of data is also a problem. The proportion of costume relics of different ages and materials in the data set may be different, and the data of some special types of costume relics may be less. This will enable the model to learn better about types with more data in the training

process, and have a weak ability to predict types with less data, affecting the consistency of the model's generalization ability on different types of cultural relics.

(2) Poor model interpretation

As a deep learning model, DCLSTNet model has high complexity, and its internal working mechanism is similar to a "black box". Although the model can give more accurate prediction results, it is difficult to explain why the model makes such predictions. In the application of color restoration and prediction of costume relics, cultural relics protection workers not only need to know the predicted color value, but also want to know the basis of model prediction, such as which time point characteristics have a greater impact on color prediction, and how different environmental factors are used for color prediction through the model. The poor interpretability of the model limits its application in some scenes with high requirements for interpretability, and also makes cultural relics protection workers have some doubts when using the model results.

⑶ High cost of computing resources and time

Training and running the DCLSTNet model requires a lot of computing resources and time. The model includes multiple convolution layers, pooling layers, and LSTM layers, with a large number of parameters. In the training process, especially when the data set is large, a large number of matrix operations are required, which requires high memory and computing capacity of computing equipment. If you use an ordinary computer for training, it may take hours or even days. This not only increases the cost of model training, but also limits the rapid iteration and optimization of the model. In practical applications, the high cost of computing resources and time has become an obvious disadvantage for some situations where color restoration results need to be obtained quickly.

⑷ Inadequate consideration of external factors

Although the model can learn some rules from time and color data, it is still relatively insufficient to consider some external factors. The color change of the unearthed garment relics is not only related to time, but also affected by many other factors, such as the preservation method and restoration process of the relics. The current model is mainly based on time and color data for training, and these external factors are not fully included in the model. For example, the chemical reagents used in the restoration of cultural relics may affect the color, but the model cannot directly

consider the role of this factor. This may cause the accuracy of the prediction results to decline when these factors are not considered in the actual application of the model.

4.5.3 Direction of improvement

(1) Data enhancement and quality improvement

In order to overcome the limitations of data dependence, data enhancement and quality improvement measures can be taken. In terms of data enhancement, more training data can be generated by transforming the existing data, such as slightly disturbing the color LAB value, translating or scaling the time series, etc. This can increase the diversity of data and improve the generalization ability of the model. In terms of quality improvement, strengthen the quality control in the process of data collection, use more advanced and accurate measuring equipment, strictly clean and preprocess the data, and remove wrong data and missing values. At the same time, actively cooperate with the archaeological community to expand the scope and quantity of data collection and ensure the integrity and accuracy of data.

(2) Model explanatory study

To solve the problem of poor interpretability of the model, relevant research work can be carried out. On the one hand, some interpretable techniques, such as locally interpretable model independent interpretation (LIME), SHAP (Sharpley Additive exPlanations) and other methods, can be used to analyze the prediction results of the model and find out the features and factors that have a greater impact on the prediction. On the other hand, we can try to build some auxiliary models or visualization tools to help cultural relics protection workers better understand the working principle and prediction basis of the model. For example, by visualizing the contribution of features at different time points to color prediction, the prediction process of the model is more transparent.

(3) Optimization calculation efficiency

In order to reduce the cost of computing resources and time, we can optimize the model structure and computing methods. In terms of model structure, we can try to reduce the number of layers or parameters of the model, and adopt some lightweight convolution cores and LSTM unit structures, but at the same time, we should ensure that the performance of the model is not greatly affected. In terms of computing methods, distributed computing, GPU acceleration and other technologies can be used

to improve the speed of model training and operation. For example, assign the training task of the model to multiple computing nodes for parallel computing, or use the powerful computing power of GPU to accelerate matrix operations.

⑷ **Include more external factors**

In order to make the model more comprehensively consider the factors that affect the color change of costume relics, more external factors can be included in the model. You can collect more data about the preservation method and restoration process of cultural relics, and input these data into the model as additional features. For example, the information such as the type and concentration of chemical reagents used in the repair process is encoded as a feature vector, which is input into the model together with time and color data for training. This can improve the adaptability of the model to various actual situations and further improve the prediction accuracy of the model.

4.5.4 Application expansion

⑴ **The framework and method of this model can be extended to other types of cultural relic color restoration and prediction.** For example, the color of cultural relics such as ceramics and murals will also change with time and environmental factors. By collecting the time and color data of the corresponding cultural relics, and adjusting and training the model appropriately, the restoration and prediction of the color of these cultural relics can be realized. This will provide strong technical support for the wider protection of cultural relics.

⑵ **Combine the prediction results of the model with the decision of cultural relics restoration.** Cultural relics protection workers can formulate more reasonable restoration plans according to the colors predicted by the model. For example, when choosing the color of the restoration materials, you can refer to the original color predicted by the model to make the restored cultural relics closer to their original appearance. At the same time, the model can also be used to evaluate the long-term impact of different restoration schemes on the color of cultural relics, and provide scientific basis for restoration decision-making.

⑶ **The color of cultural relics restored by the model can be used for more vivid cultural display and educational activities.** Through Virtual Reality (VR), augmented reality (AR) and other technologies, the color of restored cultural relics will be presented to the audience, so that the audience can more intuitively feel the historical

and cultural value of cultural relics. In terms of education, the model can be applied to the teaching of archaeology, cultural relics protection and other related majors to help students better understand the laws of cultural relics color changes and protection methods.

4.6 Conclusion

This chapter focuses on the model construction and application research of intelligent restoration of costume relics color, which not only provides a technical solution to the pain points of traditional restoration technology, but also forms a multi-dimensional breakthrough in the field of cultural heritage protection and digital technology integration. Its value can be sublimated from three levels of technological innovation, interdisciplinary and cultural inheritance.

From the perspective of technological innovation, the DCLSTNet model built in this study breaks through the limitations of traditional color restoration experience dependence and linear hypothesis. By integrating the spatial feature extraction capability of CNN and the time series modeling advantages of LSTM, and combining the jump memory mechanism and the linear autoregressive compensation module, the color prediction of costume relics was realized for the first time. This nonlinear and linear dual branch architecture not only accurately captures the nonlinear characteristics of complex chemical actions such as dye molecule hydrolysis and microbial corrosion, but also guarantees the stability of long-term prediction through linear compensation, so that the color restoration error is controlled within the range that is invisible to the human eye, providing core technical support for the transformation of costume relics color restoration from subjective inference to data driven. The establishment of artificial climate box simulation experiment and color dynamic collection system further fills the gap between laboratory controllable data and field archaeological data, and provides a reusable experimental paradigm for the research and development of similar cultural relics protection technology.

In terms of interdisciplinary dimension, this research has broken the disciplinary barriers of archaeology, material science and computer science, and built an interdisciplinary research framework of "data collection - intelligent modeling". At the archaeological level, by dividing the stages of color changes of costume relics in different regions and different ages, the cognition of the correlation between the tomb

microenvironment and cultural relics degradation is deepened, especially the analysis of the difference of color degradation between the humid areas in the south and the arid areas in the north, which provides new quantitative indicators for the environmental assessment of archaeological sites; At the level of computer science, the pretreatment strategy and model optimization aimed at the characteristics of small samples, long time series and multiple noises of cultural relics data have expanded the application boundary of in-depth learning in the field of costume cultural heritage protection, and formed a benign discipline interaction model with problems stemming from archaeology, methods relying on calculation, and verification and regression of cultural relics.

From the perspective of cultural inheritance, the core value of this study is to provide a technical path for the live inheritance of costume cultural heritage. The color of costume relics is not only a visual symbol, but also a concentrated embodiment of ancient etiquette, aesthetics and technology, bearing the hierarchical order and cultural beliefs of feudal society. The limitation of traditional restoration technology often leads to the loss of these cultural information with the fading of colors. The color restoration based on DCLSTNet model can not only accurately reproduce the original color of cultural relics, but also combine VR/AR technology to build a digital cultural relics library of costume, so that the public can intuitively experience the color aesthetics of ancient costume; At the same time, the model's ability to predict color changes in different conservation environments can provide scientific basis for the selection of cultural relics display and restoration materials, from passive protection to active prevention, and truly realize the leap from rescue protection to preventive inheritance of costume cultural heritage.

In the future, with the integration of multimodal data, such as fabric texture, dye composition spectrum, and the improvement of model interpretation, this technical system is expected to further expand to the field of color protection of more types of costume related cultural relics, such as pottery figurines, murals, etc., to provide key technical support for the construction of a digital costume cultural heritage protection community, so that the color of the millennium costume relics can be revitalized in the digital era, and achieve the sustainable inheritance of costume cultural heritage.

Chapter 5 Intelligent restoration method for incomplete and degraded costume relics' sewing patterns

In view of the problems that need to be solved urgently, such as the damage to cultural relics, high professional requirements, high costs, and easy mistakes of traditional restoration methods of costume relics sewing patterns, we proposed an interactive reverse restoration method of costume relics sewing patterns based on Image to Image Translation with Conditional Adverse Networks (Pix2Pix) by analyzing the basic principles of Chinese ancient costume sewing patterns, so as to achieve rapid and accurate acquisition of unearthed costume relics sewing patterns.

5.1 Basic plan for intelligent restoration method for incomplete and degraded costume relics' sewing patterns

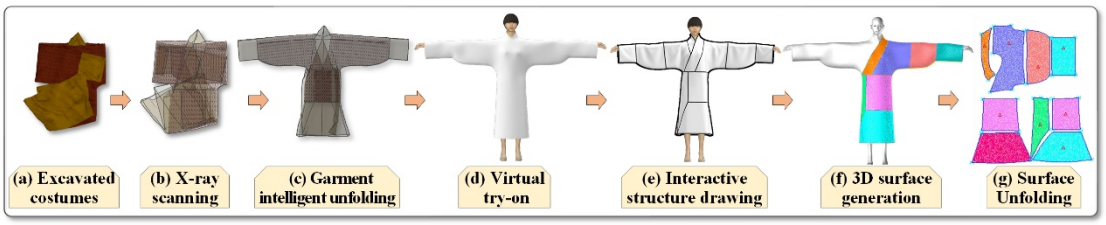

Figure 5-1 Intelligent restoration of costume cultural relic sewing pattern

The display of interactive reverse restoration of costume relics sewing patterns based on Pix2Pix proposed in this chapter is shown in Figure 5-1. The core processes and key points are summarized as follows:

- Analyzed the three principles followed in the structural composition of ancient Chinese costume: "whole piece as the basis" embodies the wisdom of cherishing materials, and reduces waste through whole piece material collection and cutting according to patterns; Adapting to the needs of activities with a focus on the human body, balancing comfort and etiquette with features such as thrift, sleeve shape, and collar design; The "ritual system as rules" distinguishes levels, using costume length, sleeve width, and patterns to highlight identity. The three are achieved through exquisite craftsmanship, shaping unique aesthetics and carrying cultural genes, providing sustainable and functional innovation inspiration for modern design.

- A Pix2Pix-based model is developed for non-expandable costume relic images, with the input being the images of these relics. After in-depth learning and processing of the model, the output item is the pictures of unearthed costume relics after deployment. This process involves accurate capture and reconstruction of costume texture, edges, folds and other details to ensure that the expanded costume structural lines output by the model are consistent with the real costume structural lines.
- After obtaining the flattened picture, the next step is to convert it into a 3D costume model. This process requires the use of 3D modeling software to build a 3D model of costume according to the costume outline, detail features and size information in the picture.
- Draw the costume structure line on the 3D costume model according to the structural line of the unearthed costume relics output from the model. These structural lines not only help to analyze the design concept and production skills of ancient costumes, but also provide an important basis for the subsequent three-dimensional to two-dimensional pattern conversion.
- Expand the three-dimensional costume surface enclosed by the 3D structure line of the costume through the algorithm to form a two-dimensional flat figure (i.e. costume template). The final garment template can be directly used for the overall virtual simulation and modeling of costume, to achieve accurate digital restoration of cultural relics.

5.2 The basic principles of ancient chinese costume structure

The structural system of ancient Chinese costume is the deep response of the ancestors to the human body shape, climate and environment, and etiquette norms in their long-term production practice. Its core principles have been running through thousands of years, which not only reflects the philosophy of "harmony between man and nature", but also condenses exquisite handicrafts. From fabric cutting to garment sewing, from structural layout to detail processing, every design is not arbitrary, but follows four core principles: function priority, etiquette adaptation, material saving and efficient, and skill inheritance, and presents specific and subtle craft expressions in costume shapes in different historical periods. The following will systematically analyze the basic principles of the composition of ancient Chinese costume structure, taking the key

components of costume structure as the context and combining with specific shapes and processes.

5.2.1 The fabric utilization principle and cutting process of "whole material based, reducing splicing"

In the use of fabrics, ancient Chinese costume always followed the concept of "respecting materials and cherishing materials" [73]. The structural design took maximizing the use of fabrics and reducing unnecessary splicing as the primary principle [74]. This principle stems from the difficulty of ancient fabric production - whether it is silk reeling and weaving, or retting and jute knitting of linen fabrics, it requires a lot of manpower and time, and is closely related to the stability needs of costume structures. In terms of cutting technology, this principle is mainly realized through two core ways, namely "whole picking" and "cutting along the grain", and has formed a fixed paradigm in different costume categories.

The structural design of deep garment in the Qin and Han Dynasties is a typical embodiment of the principle of "whole material based".Shen yi(深衣), as the common clothes connected up and down at that time, needed to be cut on the basis of fabrics with a fixed width - the width of ancient silk fabrics was mostly two feet and two inches (about 50cm today) [75], which was due to the technical limitations of looms and also determined the basic dimensions of costume structure. The "Ren (衽, lapel) design of Shen yi(深衣)is particularly critical. It adopts the form of winding closure or straight closure, and its essence is the ingenious use of the whole fabric. The curved train deep garment cuts the fabric into two pieces along the longitudinal direction. The front and back pieces both maintain the integrity of the entire fabric, and only a small amount of stitching is carried out at the armpit. The skirt is closed by winding the body, which not only avoids the fragmentation and waste of the fabric, but also enhances the warmth and privacy of the costume by overlapping the skirts. The gowns of the Han Dynasty were further developed on the basis of deep garments, but the principle of fabric utilization remained unchanged. The plain gauze clothes unearthed from the Han Tomb in Mawangdui, Hunan Province, are the ultimate embodiment of this process [66]. The clothes are 128 cm long, 195 cm long sleeves, and only 49 grams in weight. The fabric is plain silk. When cutting, it completely follows the principle of whole material along the grain. There is no redundant splicing. Even the piping of the collar is cut with the

same fabric, which shows the dual pursuit of Han craftsmen for "saving materials" and "refinement". The gowns of the Han Dynasty were further developed on the basis of deep garments, and still continued the principle of using whole materials. Most of them were the right lapel with collar turned over and straight sleeves with wide body structure. When cutting, the fabric should be cut into two parts: Body section with straight cutting (正裁) and Bias-cut (斜裁) sleeves. The body part of the whole fabric was folded vertically, and the middle lapel formed a collar, with seams left on both sides as cuffs. Only a small amount of darts was made on both sides of the waist to fit the body curve. The sleeves are cut diagonally, so that the width of the sleeves is gradually widened from the cuff to the sleeve root, which not only ensures the comfort of arm movement, but also avoids the waste of fabrics.

Although the Ru skirt (襦裙) in the Tang Dynasty is in the shape of upper and lower parts, its fabric utilization principle is still the same as that of the previous generation. Ru (short jacket) in the Tang Dynasty was mostly of narrow sleeves, facing or collar structure. [76] The cutting was based on the whole fabric, and the length of the garment body usually did not exceed the waist, so the upper part of the fabric could be cut directly without splicing; The skirt adopts the process of multiple stitching, but the "stitching" here is not a waste, but a necessary design based on the "hemming" function of the skirt - the Tang Dynasty skirt is mostly "broken skirt (破裙)", that is, it is made of several pieces of fabric longitudinally spliced, each piece of fabric is full width, and the selvage of the fabric is aligned when splicing, which not only ensures the drape feeling of the skirt body, but also avoids the problem that the fabric cannot form enough hemming due to the width limit.

5.2.2 Functional structure principle and sewing process of "taking human body as the key link and adapting to shape"

Although ancient Chinese costumes emphasized ritual symbols, they also took human activity needs as the core basis of structural design, followed the principle of "taking the human body as the key link and adapting to the shape", that is, through the design of the body, sleeves, neckline, hem and other structures, they adapted to the physiological structure and activity habits of the human body, while achieving the unity of structure and function through exquisite sewing technology. This principle is shown in three specific directions in different costume categories, namely, the balance between

body width and dart, the fitting of sleeves and arms, and the fitting of neckline and neck. Each direction corresponds to a unique process technology.

⑴ Body structure: saving technology based on wide body

In ancient China, most of the clothes were based on the shape of broad body, which was not only related to the aesthetic orientation of praising clothes, but also provided enough space for human activities. However, broad body was not excessively loose, but achieved the effect of loosening without collapsing through the saving process. Stitching refers to reserving a certain amount of fabric allowance when cutting specific parts of the garment body (such as waist, armpit and chest), and then sewing the allowance to make the garment body fit the human body curve. This process gradually matured after the Han Dynasty and became the core technology of costume structure fitting the human body.

The guozi in the Song Dynasty is a typical dress with provincial techniques. The Song Dynasty's gusset is a long sleeve, facing front and straight collar structure [77]. The length of the garment body reaches to the knee or ankle. The key to its structural design is to reduce the waist. The Song Dynasty's female gusset is mostly designed with a narrow waist. When cutting, a certain amount of fabric allowance is reserved at the waist positions on both sides of the garment body. When sewing, the surplus is sewed along the longitudinal direction to form a dark dart, which not only avoids the sense of bulkiness of the wide clothes, but also does not affect the activities of the arms. The physical object of the gudgeon unearthed from the tomb of Huang Sheng in the Southern Song Dynasty in Fuzhou [78] shows that the waist is darted, the stitches are stitched back, the stitches are fine and uniform, and the fabric at the dart is flat without wrinkles. It can be seen that the craftsmen had a certain grasp of the body curve at that time. In addition, although most of the male body size in the Song Dynasty were designed to be wide, they still had "underarm dart" treatment at the armpit, that is, the surplus fabric at the connection between the body and the sleeve was sewn up, making the body more suitable for the shoulder curve, reducing the fabric entanglement during activities. This process reflects the structural design idea of "function first".

The patchwork of the Ming Dynasty further optimized the saving process in the body structure. The patchwork of the Ming Dynasty was of a pan collar, narrow sleeves and over knee structure, and its body needed to meet the needs of officials for office work, salute and other activities, so there was a dart on the waist and back: the dart on

the waist was made by the Ming Dynasty technology, that is, the dart seams were directly exposed, but by aligning with the pattern of the cloth, the dart seams were integrated into the overall design; The back dart is a dark dart. When sewing, the surplus of the back fabric is sewed down from the collar to the waist, making the back fabric more suitable for the spine curve and avoiding the wrinkling of the fabric when officials sit for a long time. Among the costume objects unearthed from the tomb of the Ming Lu Emperor in Zoucheng, Shandong Province [79], there are long darts on the back, and the sewing line adopts the lockstitch technology, which not only prevents the fabric edge from spinning off, but also enhances the structural strength of the dart collection, showing the structural design principle of giving consideration to the function and beauty of costume in the Ming Dynasty.

(2) Sleeve structure: functional adaptation from wide sleeve to narrow sleeve

Sleeves are the most closely related part of the costume structure with human arm activities. The structural design of ancient Chinese costume sleeves has always followed the principle of "convenient activities". From the wide sleeves in the Pre Qin-Dynasty to the narrow sleeves in the Tang Dynasty, to the arrow sleeves in the Ming and Qing Dynasties, the changes in the shape of each sleeve are a response to the needs of human activities in different historical periods, and correspond to unique sewing techniques.

In ancient times, the structure design of deep clothes with wide sleeves was based on the needs of etiquette, but still considered the function of activities. Sometimes the width of the sleeves of deep clothes can reach two feet (about 46 cm today) and the length can reach to the wrist. The straight cutting process is used when cutting, that is, the sleeves are connected with the body. Only the cuff is "closed" - fold the edge of the cuff 3-5 cm inward, and then use the stitching process to fix it to form a "cuff", which can not only prevent the cuff fabric from wearing, but also avoid the exposure of the arms when making gifts. Although this wide sleeve structure seems to be not conducive to activities, through the gradual design of wide sleeve root and narrow cuff, there is still enough room for the arm to move inside the sleeve, and the wide sleeve moves with the wind when walking, which conforms to the ancient etiquette image of "a gentleman is synonymous with righteousness".

The narrow sleeve Ru skirt in the Tang Dynasty is a typical example of the sleeve structure adapting to daily activities. In the Tang Dynasty, the society was open, and

women participated in outdoor activities more and more, so narrow sleeves became the mainstream - narrow sleeves are usually one foot wide (about 23 cm today), reaching to the elbow or wrist. The "arrow sleeve (箭袖)" (also called "horseshoe sleeve (马蹄袖)") [80] in the Qing Dynasty is the ultimate embodiment of the sleeve structure's adaptation to cold climate and riding and shooting activities. Arrow sleeves were popular in Manchu costumes and later incorporated into the official costume system of the Qing Dynasty. Their structural characteristics were narrow sleeves and wide cuffs. Foldable "horseshoe shaped" wrist guards were set at the cuffs. When cutting, a double-layer cutting process was used: first cut the inner sleeve lining, then cut the outer sleeve surface. The sleeve lining was made of thick cotton cloth to enhance warmth retention; The sleeves are made of silk or satin to ensure their beauty. When sewing, first align the sleeve lining with the edge of the sleeve surface, and then use the "piped edge sewing" process to sew the two together. Then reserve 10-15cm of fabric allowance at the cuff, fold it into a horseshoe shape, and fix it with a buckle. When walking, the horseshoe sleeve can be put down to protect the wrist from cold; When riding, shooting or working, the horseshoe sleeve can be folded up to expose the wrist for convenient movement. The arrow sleeves of Qing emperors' walking clothes collected in the Palace Museum in Beijing, the horseshoe sleeves of which are folded with concealed buckles, and the buckles are hidden inside the fabric, which not only ensures the stability of the structure, but also does not damage the overall beauty of the costume, showing the "high unity of function and practicality" of the costume structure in the Ming and Qing dynasties.

⑶ Neckline structure: double adaptation of fitting neck and etiquette needs

The neckline is the most closely related part of the costume structure to the human neck, and its design needs to meet both the functional needs of fitting the neck and the symbolic needs of etiquette norms. The neckline of ancient Chinese costume is mainly divided into three shapes, namely, cross collar, dish collar and stand collar. Each shape corresponds to a unique cutting and sewing process to achieve the balance between comfort and etiquette.

Crossed-collar (交领) is the most representative collar shape of Chinese ancient Han ethnic costumes, which runs through the pre Qin period to the Ming and Qing dynasties. Its structural design follows the principle of Right lapel (右衽, that is, the lapels overlap to the right), which not only conforms to the etiquette concept of the Han

people "respecting the right", but also can fit the neck curve through the overlap of lapels to prevent cold wind from invading. [74] The cutting process of the neckline is complicated, so it is necessary to cut an oblique neckline at the collar of the garment body. The front is divided into left and right plackets. The left placket is generally wider than the right placket. When sewing, the right placket is pressed under the left placket to form an overlap at the collar, and the overlap is fixed with nails or ties - the necklines from the pre-Qin to the Han Dynasty are mostly fixed with ties, that is, the left placket and the right placket are each sewn with a ribbon. When tying, the two ribbons are cross knotted, which not only ensures the closure of the neckline, but also facilitates wearing and taking off; After the Tang Dynasty, the collar was mostly fixed with nails, that is, metal buttons or cloth buttons were sewn at the edge of the right lapel, and buttonholes were sewn at the corresponding position of the left lapel edge. When buttoning, the button was embedded into the buttonhole, which made the structure more secure.

The collar was mainly popular after the Tang Dynasty, especially in the Song Dynasty and the Ming Dynasty. It was mostly used for official uniforms and gowns. Its structural design was based on a round collar. Through the coiling process, the collar was fitted to the neck, which not only avoided the tedious handover of the collar, but also met the etiquette standards. [81] The cutting process of the collar needs to first cut a round collar at the top of the body. The diameter of the collar is about 15-20 cm, then fold the fabric at the edge of the collar outward and sew it with the "piping" process - the piping materials are mostly narrow ribbons of the same color or different color with the body fabric. When sewing, the piping materials are wrapped around the edge of the collar and fixed with the "close stitch" process, with about 5-6 stitches per cm, so that the edge of the collar is flat and straight, without irritating the skin. The collar of the Ming Dynasty patchwork was particularly exquisite. When sewing, the piping was aligned with the gold pattern of the garment body, so that the collar and the garment body were integrated, which not only ensured the fit of the collar, but also enhanced the solemnity of the dress.

Standing collar was popular in the Ming and Qing Dynasties, especially from the middle and late Ming Dynasty to the Qing Dynasty. Its structural design is based on an upright collar, which is about 3-5 cm high. It fits the back and both sides of the neck. The front side is equipped with a placket button, which not only keeps warm but also conforms to the aesthetic orientation at that time. The cutting process of the stand collar is complicated, so it is necessary to cut a vertical collar piece at the collar of the garment

body first. The collar piece is curved and fully fits the neck curve, and then sew the collar piece with the collar of the garment body - the press stitch sewing process is used when sewing, that is, first align the edge of the collar piece with the collar of the garment body, sew one layer with open thread, then fold the collar piece, sew the second layer with hidden thread, so that the collar piece is upright and straight without collapsing. The cheongsam of women in the Qing Dynasty is a typical stand collar. The stand collar is about 4cm high, and there are 2-3 cloth buttons on the front side. After the button is closed, the collar fully fits the neck, which is both warm and dignified. When sewing, the collar piece is lined with Starch Lining (浆衬, cotton cloth with starch paste) to enhance the straightness of the collar piece, showing the dual pursuit of the collar craft in the Ming and Qing dynasties for fitting and modeling.

5.2.3 The principle of structural symbol and decoration technology of "etiquette based, hierarchical"

The ancient Chinese society was governed by ritual, and costume, as an important carrier of "ritual", always followed the principle of "ritual system as rules, clear hierarchy" in its structural design. That is, the identity and status of different levels were distinguished by the differences in structural elements such as costume length, sleeve width, fabric material, and decorative patterns. This "structural symbol" is not simply decoration, but is integrated into the costume structure itself, and the function of "level identification" is achieved through specific craftsmanship and technology.

⑴ Body length: Determine hierarchy based on length

The length of the costume body is the most intuitive symbol of hierarchy in the structure of costume. As early as the pre Qin period, the "Book of Rites - Deep Costume (《礼记·深衣》)" stipulated that " The garment should be neither so short as to reveal the skin, nor so long as to touch the ground". However, there are still strict distinctions in the length of costume for different social classes - the length of the costume body for aristocratic costume is usually ankle length, to demonstrate their status as not engaged in labor; The length of civilian costume is usually knee high to facilitate daily labor. This difference in length is directly reflected through cutting techniques and has remained stable in costume throughout history.

The ancient Mianfu (冕服, Ceremonial Robe of Chinese Emperors) is a typical representative of the level reflected by the length of the garment. The identity of the

Mianfu is "Yi (衣)" (top) and "shang (裳)" (bottom), with the length of the garment reaching the waist and ankle. The hem of the garment adopts a "curved skirt" design, where the front of the garment wraps back to form a swallowtail shape, which not only increases the solemnity of the costume, but also highlights the supreme status of the emperor through the length of the garment reaching the ankle. The cutting process of Mianfu is extremely strict, with both the body and the garment made of "whole piece fabric", and the fabric is woven with "twelve-chapter patterns". When sewing, the connection between the body and the garment is made using "stitching" technology, which means tightly sewing the edges of the body and the garment with silk thread, and the color of the stitching is consistent with the color of the fabric to ensure the overall integrity of the costume. [82-86]

In ancient times, the length of official costume was further classified into different levels - the length and ankle of the costume for officials above the third rank, the length and middle of the calf for officials between the fourth and fifth rank, and the knee length for officials below the sixth rank. This difference was directly controlled by "cutting size", and there was also a corresponding distinction in the "hem width" of costume: the hem width of senior officials' costume was three feet (about 69 centimeters today), and the hem width of junior officials' costume was two feet (about 46 centimeters today), to enhance the intuitiveness of the level difference. In the sewing process of Tang Dynasty court costume, the "edge stitching" technique was used at the hem, which means sewing a fine and transparent thread at the edge of the hem to prevent fabric wear and distinguish grades based on the "thickness" of the thread - the transparent thread at the hem of senior officials is double stranded silk thread, while the transparent thread at the hem of junior officials is single stranded silk thread, reflecting the principle of "correspondence between craftsmanship details and grades".

⑵ Sleeve width: Use "width" to distinguish between high and low status

Sleeve width is also an important symbol of rank in costume structure. Wide sleeves are usually a standard for noble and official costume, while narrow sleeves are mostly a choice for civilian and soldier costume. This difference is related to both ceremonial needs (wide sleeves are more solemn) and labor needs (narrow sleeves are more convenient for movement), and is reinforced by differences in cutting and sewing techniques to distinguish levels.

In the Song Dynasty, there were clear regulations on the sleeve width of Gong Fu (公服, daily office attire for officials): the sleeve width of official uniforms for first to third grade officials was one foot and five inches (about 34.5 centimeters today), the sleeve width of official uniforms for fourth to seventh grade officials was one foot and two inches (about 27.6 centimeters today), and the sleeve width of official uniforms for eighth to ninth grade officials was one foot (about 23 centimeters today). This difference was directly controlled by the sleeve width size during cutting. The sewing process of the sleeves of Song Dynasty official costume also had hierarchical differences: the sleeves of senior officials were made of silk fabric, and the sewing process used concealed stitching, with the seams completely hidden inside the fabric; The sleeves of low-level officials are made of cotton fabric and sewn using open seam technology, with the seams exposed to the outside. This not only reduces production costs, but also strengthens grade differentiation through process differences.

The Ming Dynasty further refined the level of sleeve width in its official costume - the sleeve width of the emperor's official costume was two feet (about 46 centimeters today), the sleeve width of princes and county kings was one foot eight inches (about 41.4 centimeters today), the sleeve width of officials varied from one foot five inches to one foot according to their rank, and the sleeve width of ordinary people did not exceed eight inches (about 18.4 centimeters today). In the cutting process of sleeves for Ming Dynasty costume, the sleeves of high-end costume were cut diagonally to fit the curves of the arms more closely, and the cuffs were made of woven gold brocade; The sleeves of civilian costume are made using straight cutting technology, with only simple folding at the cuffs without any edges. This difference in craftsmanship corresponds to the level difference in sleeve width, forming a dual level identification of "structure+craftsmanship".

The structural composition principle of ancient Chinese costume is an organic unity of function, ritual, and craftsmanship - the principle of fabric utilization based on "whole material" [74], which reflects the wisdom of our ancestors to "respect and cherish materials" in their daily lives; The principle of functional structure based on the human body demonstrates the deep adaptation of costume to the needs of the human body; The structural symbolic principle of "ritual system as rules" reflects the hierarchical order of ancient society. And the implementation of these principles relies on exquisite cutting, sewing, and weaving techniques, from the smooth cutting of plain

silk jackets in the Han Dynasty to the sleeve insertion technique of Tang Dynasty jackets, from the saving techniques of Song Dynasty jackets to the patching and nailing techniques of Ming Dynasty costume. Each technique is the accumulation of craftsmanship experience and the inheritance of technology. These structural principles and craftsmanship techniques not only shaped the unique aesthetic style of ancient Chinese costume, but also became an important carrier of Chinese culture - the crossed collar with a right lapel, the shape of the wide waistband, and the distinct patterns of hierarchy, which are not only the structural features of costume, but also the symbol of Han culture. Even in modern fashion design, these principles still have important reference significance, such as the inspiration of "whole cutting" for sustainable fashion, the influence of saving techniques on ergonomic design, and the inspiration of the integration of textile patterns and structures for the expression of costume culture, all of which prove the vitality of the ancient Chinese costume structure system. Thoroughly studying these principles and techniques not only allows us to better understand the charm of ancient costume, but also provides inexhaustible motivation for the inheritance and innovation of contemporary costume culture.

5.3 Construction of restoration method for costume relics sewing patterns

When garment relics are unearthed, they are mostly stuck together and cannot be forcefully unfolded, which can cause serious damage to the garment relics. If the unearthed garment relics cannot be unfolded, their structural lines and sewing techniques cannot be observed, and the actual size data of various parts of the costume cannot be measured, which poses a huge challenge to the restoration of costume structure. The traditional method of restoring the structure of unearthed garment relics requires a high level of professionalism in plate making for the restoration workers, which requires decades of cultivation and training to master. To solve the above problems, this study applies artificial intelligence technology to the intelligent leveling of unearthed garment relics and the surface unfolding of three-dimensional garment relics models. Therefore, the construction of the costume cultural relic structure restoration model proposed in This study mainly includes two parts: first, the construction of an intelligent simulation and unfolding mathematical model based on

Pix2Pix for non-exhibition unearthed costume relics; The second is the construction of the algorithm for unfolding the 3D model of unearthed costume.

5.3.1 Construction of an intelligent simulation and unfolding mathematical model for excavated costume relics based on Pix2Pix

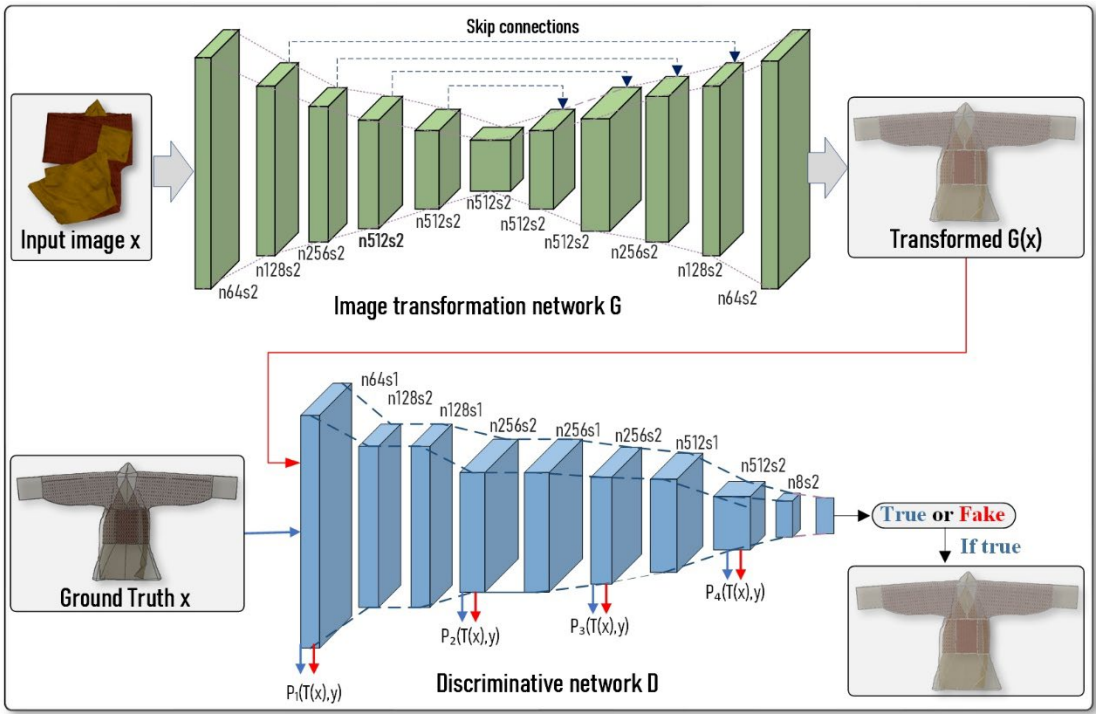

Figure 5-2 Intelligent unfolding model of non-exhibition costume relics based on Pix2Pix

Constructing an intelligent unfolding model for non-exhibition costume artifacts based on Pix2Pix, aiming to use images of non-exhibition unearthed costume artifacts as input, and through deep learning and processing, output flattened images of unearthed costume artifacts. This process requires precise capture and reconstruction of the texture, edges, wrinkles, and other details of the costume, ensuring that the unfolded structural lines of the costume in the output image are highly consistent with the structural lines of the real costume. The core of this model lies in using the Conditional Generative Adversarial Network (cGAN) framework to learn the mapping relationship between the folded and folded images of unearthed garment relics and their unfolded and flattened state images, in order to construct an intelligent unfolding model for non-exhibition garment relics. The basic principles and key formulas for constructing this model will be elaborated in detail below.

(1) Model framework

As shown in Figure 5-2, Pix2Pix is a costume image translation model based on Conditional Generative Adversarial Networks (cGAN) for translating excavated wrinkled costume images into flattened costume images. The core idea in the intelligent unfolding task of non-exhibition costume relics is to learn a mapping function G, which converts the input image of non-exhibition costume relics (such as photos of unearthed cultural relics with folds and folds) into its unfolded and flattened image. This model consists of two core components: A Generator (G) for transforming unearthed costume images and a Discriminator (D). The Generator (G) for unearthed costume images takes non-deployable unearthed costume images as input conditions and generates corresponding unfolded and flattened unearthed costume images; The Discriminator (D) determines whether a given pair of images (input unearthed costume image and corresponding target image) is a "real" unfolded image (from the training dataset) or a "fake" unfolded image (generated by the unearthed costume image converter). The objective function of cGAN can be expressed as:

$$\min_G \max_D L_{cGAN}(G, D) + \lambda L_{L1}(G) \tag{5-1}$$

Among them, $L_{cGAN}(G, D)$ is an adversarial loss that ensures that the generated image is difficult to distinguish from the real unfolded image in terms of data distribution; $L_{L1}(G)$ is a traditional reconstruction loss that ensures the generated image is close to the real unfolded image at the pixel level. λ is a hyperparameter used to balance two types of losses.

⑵ Architecture and principle of excavated costume image converter

The excavated costume image converter G adopts the U-Net structure. The encoder decoder structure and skip connections of U-Net enable it to capture both global contextual information and local details (such as texture, edges, and folds of costume) of the image simultaneously, which is crucial for accurately reconstructing the unfolded costume sewing patterns. The encoder of U-Net gradually extracts multi-scale features of the input image x through convolution and downsampling:

$$enc_i = \text{DownSample}(enc_{i-1}), \qquad i = 1,2,\dots,N \tag{5-2}$$

The decoder gradually reconstructs the image through upsampling and convolution, and fuses the high-resolution features of the corresponding layers of the encoder through skip connections:

$$dec_j = \text{UpSample}\left(dec_{j-1}, enc_{N-j}\right), \qquad j = 1,2,\dots,N \tag{5-3}$$

The final output generates an image $G(x)$.

(3) Discriminator architecture and principle

Discriminator D adopts PatchGAN structure. PatchGAN does not directly determine the authenticity of the entire image, but rather segments the input image into overlapping N×N patches and outputs a matrix where each element represents the probability that the corresponding image block is true. Its mathematical expression is:

$$D(x,y): x \to \mathrm{M}_{ij}, \qquad i,j = 1,2,\ldots,P \tag{5-4}$$

Where, P is the size of the output matrix. This structure enables the discriminator to focus on the authenticity of local textures and structures, making it very suitable for evaluating the realism of costume textures and wrinkle unfolding.

(4) Detailed explanation of loss function

The adversarial loss (cGAN Loss) uses a binary cross entropy loss function, whose formula is:

$$L_{cGAN}(G,D) = \mathbb{E}_{x,y}[logD(x,y)] + \mathbb{E}_{x,z}\left[log\left(1 - D\big(x, G(x,z)\big)\right)\right] \tag{5-5}$$

Among them: x is the input unearthed costume image (non exhibition costume image); y is the target image (real unfolded unearthed costume image); z is random noise (in Pix2Pix, noise is often introduced in the form of Dropout); $D(x,y)$ is the judgment result of the discriminator on the real unearthed costume image pairs; $D\big(x,G(x,z)\big)$ is the judgment result of the discriminator on the converted image pair. The excavated costume image converter G attempts to minimize this loss, while the discriminator D attempts to maximize it.

The formula for calculating the absolute difference between the transformed costume image $G(x)$ and the real target image y using L1 loss is:

$$L_{L1}(G) = \mathbb{E}_{x,y,z}[\|y - G(x,z)\|_1] \tag{5-6}$$

L1 loss can effectively reduce the blurring phenomenon in the generated image and promote the transformed costume image to be closer to the real unearthed costume unfolded image at the pixel level, which is very important for maintaining the accuracy of costume structure lines.

The total objective function of the model, which combines adversarial loss and L1 loss, is:

$$G^* = \arg\min_G \max_D L_{cGAN}(G,D) + \lambda L_{L1}(G) \tag{5-7}$$

Among them, λ is a hyperparameter that controls the weights of two types of losses and needs to be adjusted according to specific tasks.

⑸ data collection

In the process of building an intelligent unfolding model for non exhibition costume relics based on Pix2Pix, data collection is the foundation and key link of model training. Considering the particularity of real unearthed garment relics - on the one hand, a large number of cultural relics cannot be physically unfolded and flattened due to their age and fragile materials (such as silk, linen and other fiber materials that are prone to aging and damage), resulting in extremely scarce natural paired data; On the other hand, even if some cultural relics allow for limited processing, the acquisition of their X-ray scanning images is limited by factors such as the technical conditions of cultural relics protection units and the preservation status of cultural relics, making it difficult to form a large-scale data reserve. Therefore, data collection work needs to be carried out around two core paths: real data supplementation and virtual data generation. Multi source data collection and synthesis strategies should be adopted to ensure that the quantity and diversity of the dataset can support effective training of the model. The specific methods include four: firstly, X-ray scanning of excavated costume; The second is to actually produce a batch of authentic ancient costumes for X-ray scanning; Thirdly, using virtual simulation technology to simulate a batch of X-ray scanning data; The fourth is to increase the amount of data through data augmentation technology. The specific introduction is as follows:

In the data collection of excavated costume, as shown in Figure 5-3, This study selects well preserved excavated costume samples and uses a high-precision X-ray imaging system to systematically collect scanning images of each sample in multiple folded and fully unfolded states. The aim is to construct a paired image dataset with clear structure and strong archaeological authenticity - each set of data in the dataset is composed of high-resolution X-ray images of the same excavated costume in folded form and fully unfolded. To ensure the representativeness and scientificity of the data, the sample selection strictly follows the evaluation criteria for the preservation status of cultural relics, and only includes high-quality excavated costume with intact fabric structures and no obvious degradation or deformation, thus ensuring the reliability and archaeological authenticity of imaging data at the source. In the image acquisition process, a multi angle and multi energy level X-ray scanning strategy is adopted to accurately capture the internal features such as the stacking relationship, seam structure, and material density distribution of the folded fabric, as well as the overall shape and

detail information in the flattened state. All scanning processes are carried out in a controllable laboratory environment, strictly regulating the sampling distance, exposure parameters, and signal-to-noise ratio level to minimize the impact of external interference factors on image quality.

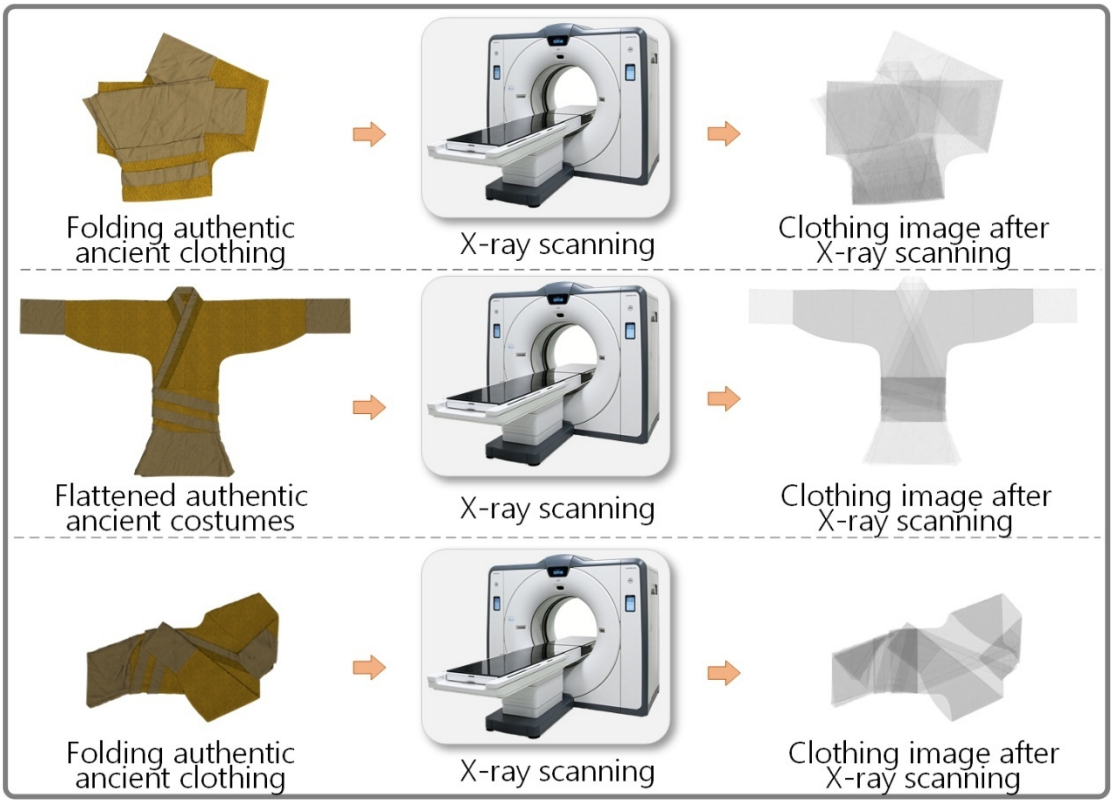

Figure 5-3 Real ancient costume data collection experiment

When collecting data for the production of ancient costumes, as shown in Figure 5-4, it is necessary to strictly follow the production process and process standards of ancient costumes to ensure the high historical authenticity of the reconstructed samples in terms of shape, material, and craftsmanship. The production process begins with the selection of fabrics. Based on archaeological reports and historical records, natural fiber materials that are the same as the unearthed cultural relics, such as silk, linen, cotton, wool, etc., are preferred. After the fabric processing is completed, precise cutting should be carried out according to ancient cutting techniques, referring to the costume shapes in unearthed objects or murals, to ensure that the proportion and structure of the costume pieces conform to historical characteristics. The sewing process is entirely carried out using manual needle and thread techniques, using the same sewing tools and techniques as ancient times, such as flat needles, back needles, and other traditional needlework methods, to ensure that the stitches are neat and firm, and to leave

appropriate gaps at the seams to restore the seamless or minimally sewn characteristics of ancient costume. After completion of production, each restored garment needs to be scanned with a high-precision X-ray imaging system to capture images of the garment in its natural folded state, simulating the common form when unearthed. Then, the fully unfolded garment images are scanned again to form a paired dataset consisting of folded and unfolded images of the same garment. Through a series of rigorous restoration and scanning processes, a database of ancient costume X-ray images is constructed that combines historical authenticity and technical operability, providing reliable data support for subsequent model training.

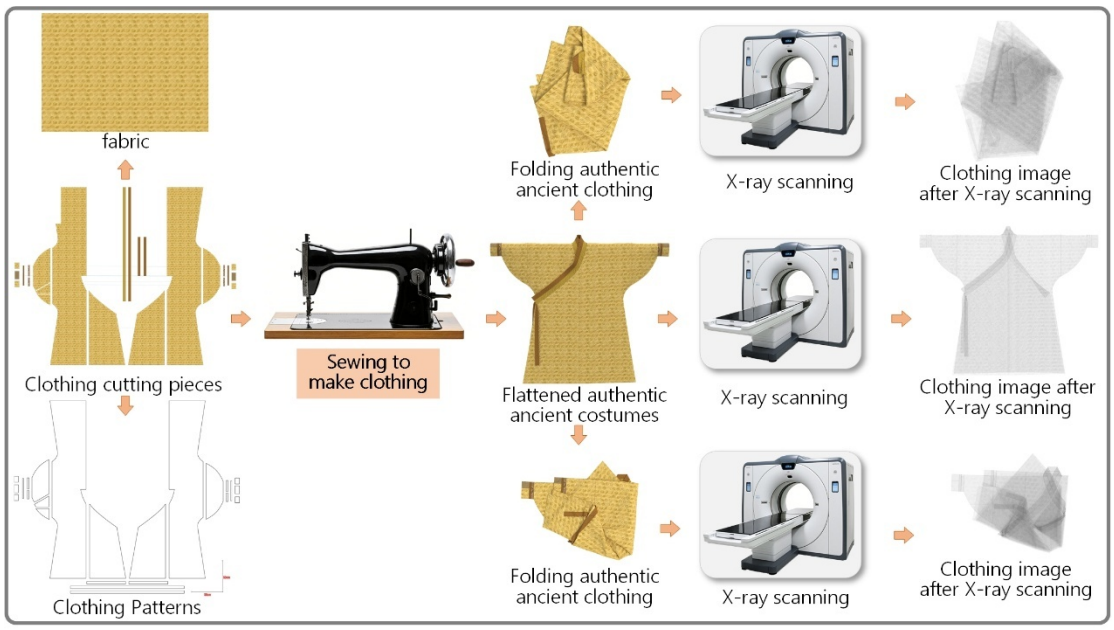

Figure 5-4 Experimental data collection of ancient costumes actually made

In the process of using virtual simulation technology to collect ancient costume data, as shown in Figure 5-5, This study first uses professional 3D modeling software to accurately restore digital costume models of different historical periods, shape features, material attributes, and pattern details. Based on the burial environment conditions recorded in archaeological data, it simulates the possible folding forms, compression deformations, and multi angle folding states that may form; Subsequently, with the help of physics based simulation engines, the mechanical behavior of these digital models during natural unfolding is dynamically calculated, generating a three-dimensional model of the flattened state that strictly corresponds to the folded state; On this basis, a rendering engine is used to simulate the imaging physics process of X-rays. By precisely adjusting the material density, ray penetration coefficient, scattering

parameters, and grayscale response curve, highly realistic simulated X-ray scanning images are generated. Finally, a large number of paired synthetic data are constructed - namely, virtual wrinkled costume X-ray images and their corresponding flattened X-ray images. This method can not only break through the limitations of scarcity and preservation status differences of physical cultural relics, efficiently generate large-scale standardized data, but also comprehensively cover various potential excavation states by systematically regulating key parameters such as fold depth, unfolding angle, material thickness, and fabric density, significantly improving the diversity, representativeness, and generalization ability of the dataset and algorithm training.

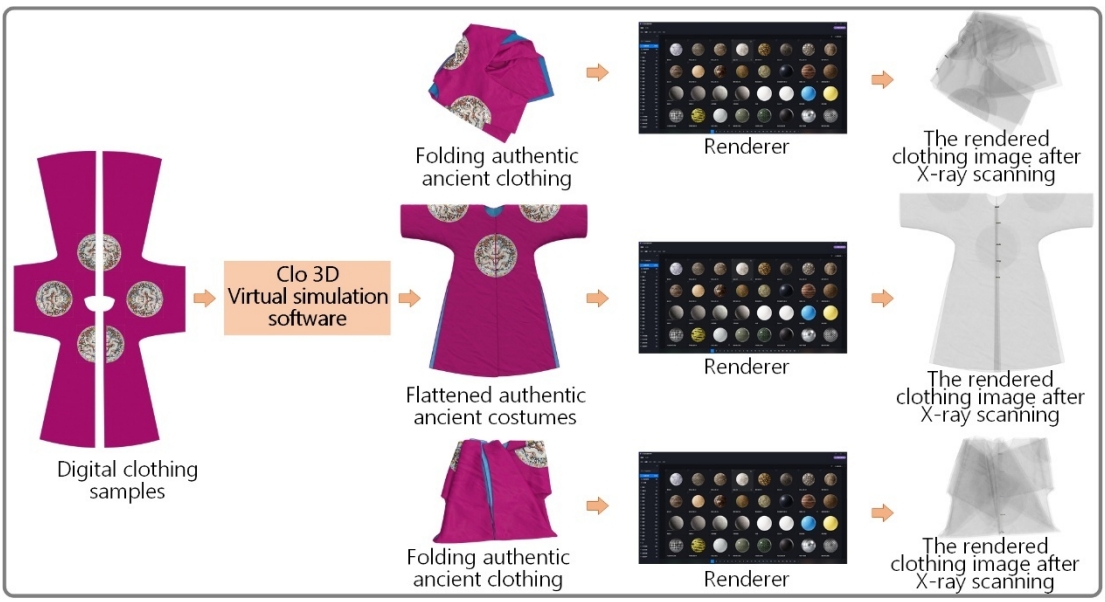

Figure 5-5 Computer Simulation of Ancient Costume Data Collection Experiment

Data augmentation technology, as an important supplement to further expand the training set and improve the model's generalization ability, requires diversified processing of collected real paired data and virtual paired data. In terms of spatial transformation, images are randomly rotated, scaled, and translated to simulate image differences caused by changes in device angles and distances during actual shooting processes; In terms of morphological transformation, horizontal flipping, vertical flipping, and other operations are used to increase data diversity while avoiding excessive dependence of the model on image direction. In terms of image detail adjustment, Gaussian noise and salt and pepper noise (with noise intensity controlled within a reasonable range to avoid masking costume structure details) are added to simulate the image quality fluctuations caused by device noise and environmental

interference during real X-ray scanning; In addition, random adjustments can be made to brightness, contrast, saturation, as well as advanced enhancement methods such as local blurring, partial occlusion simulation, texture mixing, and elastic deformation, to make the training data more closely resemble the complex state of actual unearthed cultural relics and further enrich the diversity of the data. All data augmentation operations must ensure that the original unearthed costume images at the input end are transformed synchronously with the unfolded flattened images at the output end, that is, identical transformation operations are performed on two images in a pair of data to ensure that the corresponding relationship between data pairs is not destroyed, thus forming a larger and more evenly distributed training dataset. These enhancement strategies not only increase the amount of data, but also enhance the robustness of the model to noise, deformation, and abnormal situations.

⑹ training process

The training of a model is a process of adversarial game theory. Fixed unearthed costume image converter G, updated discriminator D: maximizes L_{cGAN}, enhances the discriminator's ability to distinguish between real unearthed costume unfolded images and generated unearthed costume unfolded images; Fixed discriminator D, updated unearthed costume image converter G: Minimize $L_{cGAN} + \lambda L_{L1}$, so that the unearthed costume image converter can generate unfolded images of unearthed costume that can deceive the discriminator and approach the real target at the pixel level.

⑺ Key considerations in the task of developing non exhibition costume relics

Training data requires a large number of pairs (non-expandable state images, expandable state images). For the field of cultural relics, data acquisition is difficult and may require the use of data augmentation techniques or pre-training using synthetic data. The skip connections of U-Net and the local discriminative properties of PatchGAN jointly ensure that the model can effectively learn and reconstruct the fine texture, edge, and wrinkle information of costume. In addition to the loss function, indicators such as SSIM and Peak Signal to Noise Ratio (PSNR) need to be used, combined with subjective evaluations from domain experts, to comprehensively evaluate the quality and structural accuracy of the generated unfolded images of unearthed costume.

5.3.2 Construction of 3D model expansion algorithm for unearthed costume based on boundary size and area constraints

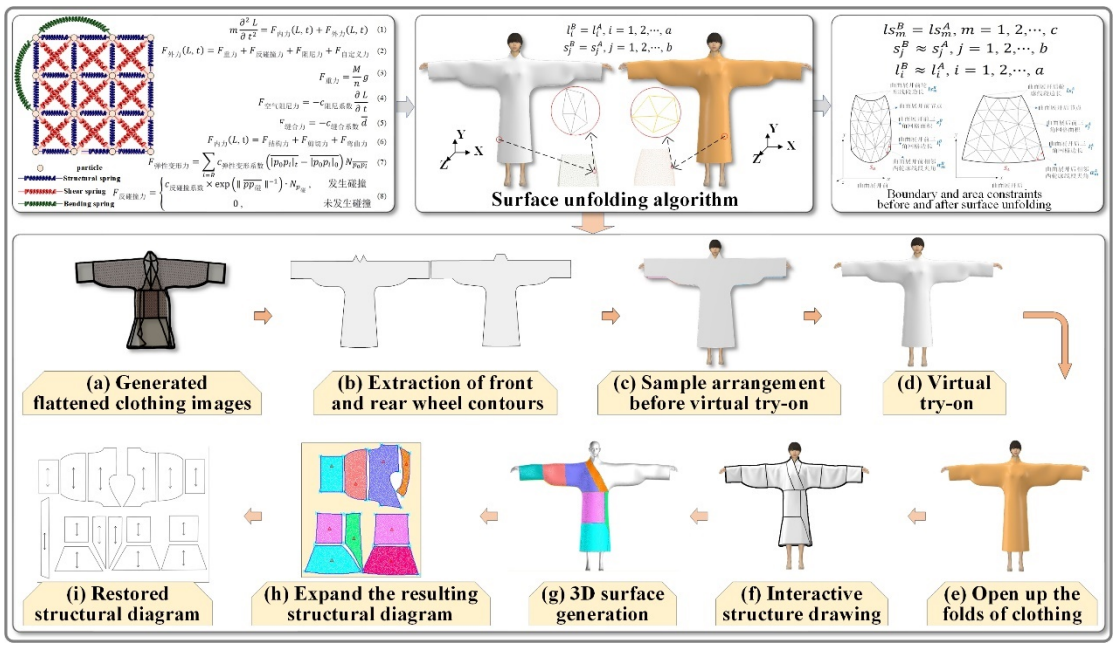

Figure 5-6 Interactive reverse restoration method for costume cultural relic sewing patterns based on boundary size and area constraints

The complete process of flattening the three-dimensional surface of costume into a two-dimensional planar structure diagram based on Boundary dimension Constraints (BC) and Area Constraints (AC) is shown in Figure 5-6. Specifically, based on the Pix2Pix based intelligent simulation and unfolding mathematical model proposed in section 5.3.1, the unfolded costume relics images are generated (Figure 5-6 (a)). Subsequently, the flat area enclosed by the front and rear contour lines was extracted from the unfolded costume artifact images (Figure 5-6 (b)), and this flat area was used as a costume sample to be reasonably laid out around the virtual human body model (Figure 5-6 (c)). On this basis, virtual stitching operations are performed to construct a three-dimensional costume model (Figure 5-6 (d)). Next, the virtual stitched costume model is stretched to eliminate surface wrinkles and obtain a smooth costume surface (Figure 5-6 (e)). Furthermore, based on the costume structure lines shown in Figure 5-6 (a), accurately draw 2D costume structure lines on the smooth surface of the costume model (Figure 5-6 (f)), which together enclose the three-dimensional costume surface (Figure 5-6 (g)). Subsequently, the three-dimensional costume surface was unfolded to obtain a two-dimensional costume flat sample (Figure 5-6 (h)). Finally, the unfolded costume flat sample is corrected and optimized to ensure that it meets the actual production

requirements (Figure 5-6 (i)). The precise unfolding of the three-dimensional costume surface to the two-dimensional costume plane is the core step in the entire process, and its quality directly affects the accuracy and practicality of the final costume sample.

In the process of transforming a curved surface into a flat surface, the special requirements for the sewing patterns of unearthed garment relics include that the length of each contour line and the angle between two adjacent contour line segments of the three-dimensional surface that constitutes the costume relic model must be equal before and after unfolding, and the surface enclosed by the contour lines should be as equal as possible before and after unfolding. Assuming that the surface surface of any costume artifact model can be approximately discretized into a collection of a certain number of triangular meshes. The surface of the costume cultural relic model after triangulation and its corresponding unfolding plane are denoted as S_1 and S_2, respectively. S_1 and S_2 have the same organizational structure, with a triangular mesh consisting of a number of line segments, b number of triangular meshes, c number of contour line segments, and d number of angles formed by adjacent two rounds of contour line segments. The boundary constraint formula for the expansion rule from 3D surface to 2D plane of costume relics is as follows:

$$l_i^B \approx l_i^A,\ i = 1,\ 2, \cdots,\ a$$

The principle of approximately equal edge lengths of each triangular mesh before and after the expansion of the "Unearthed Costume and Cultural Relic Model Surface" (5-8)

$$s_j^B \approx s_j^A,\ j = 1,\ 2, \cdots,\ b$$

The principle of approximately equal triangular mesh area before and after the unfolding of the "Unearthed Costume and Cultural Relic Model Surface" (5-9)

$$ls_m^B = ls_m^A,\ m = 1,\ 2, \cdots,\ c$$

The principle of keeping the edge length of each contour line segment unchanged before and after unfolding the "Unearthed Costume and Cultural Relic Model Surface" (5-10)

$$a_n^B = a_n^A,\ n = 1,\ 2, \cdots,\ d$$

The principle of maintaining the same angle between adjacent contour lines before and after unfolding the "Unearthed Costume and Cultural Relic Model Surface" (5-11)

Where, l_i^B and l_i^A A respectively represent the edge length values of the i-th triangular mesh before and after the expansion of surface S_1; s_i^B and s_i^A represent the area values of the jth triangular mesh before and after the expansion of surface S_1, respectively; a_i^B and a_i^A represent the edge length values of the m-th contour line segment before and after the expansion of surface S_1; a_i^B and a_i^A represent the angle value of the i-th angle between two adjacent contour segments before and after the expansion of surface S_1; a represents the total number of line segments contained in all triangular meshes that make up surface S_1; b represents the total number of triangular meshes contained in surface S_1 or S_2; c represents the total number of contour segments contained in surface S_1 or S_2; d represents the number of angles formed by two adjacent contour segments on surface S_1 or S_2. On the premise of meeting the requirements of 3D interactive costume pattern development technology, the criterion for S_2 to be the closest unfolded plane to S_1 is: the sum of the squares of the edge length differences of each segment of the triangular network in surfaces S_1 and S_2 is the smallest, the sum of the squares of the area differences of each triangular mesh in surfaces S_1 and S_2 is the smallest, the sum of the squares of the edge length differences of each contour segment of surfaces S_1 and S_2 is zero, and the sum of the squares of the angle differences formed by two adjacent contour segments of surfaces S_1 and S_2 is zero. The expressions for Δ_l, Δ_s, Δ_{ls}, and Δ_a are:

$$\Delta_l = \sum_{i=1}^{a} \left(l_i^B - l_i^A\right)^2 \tag{5-12}$$

$$\Delta_s = \sum_{j=1}^{b} \left(s_j^B - s_j^A\right)^2 \tag{5-13}$$

$$\Delta_{ls} = \sum_{m=1}^{c} (ls_i^B - ls_m^A)^2 \tag{5-14}$$

$$\Delta_a = \sum_{m=1}^{c} (a_n^B - a_n^A)^2 \tag{5-15}$$

For developable surfaces, the minimum values of Δ_l, Δ_s, Δ_{ls}, and Δ_a are zero; For non-developable surfaces, the minimum values of Δ_{ls} and Δ_a are zero, while the minimum values of Δ_l and Δ_s are non-zero

It can be seen that the three-dimensional costume surface unfolding based on Boundary Constraints (BC) and Area Constraints (AC) can accurately obtain the sample of unearthed garment relics.

5.4 Application of intelligent restoration method for incomplete and degraded costume relics' sewing patterns

5.4.1 Application flowchart of interactive reverse intelligent restoration of unearthed costume sewing patterns

The specific process of interactive reverse intelligent restoration of the sewing patterns of unearthed garment relics is shown in Figure 5-7:

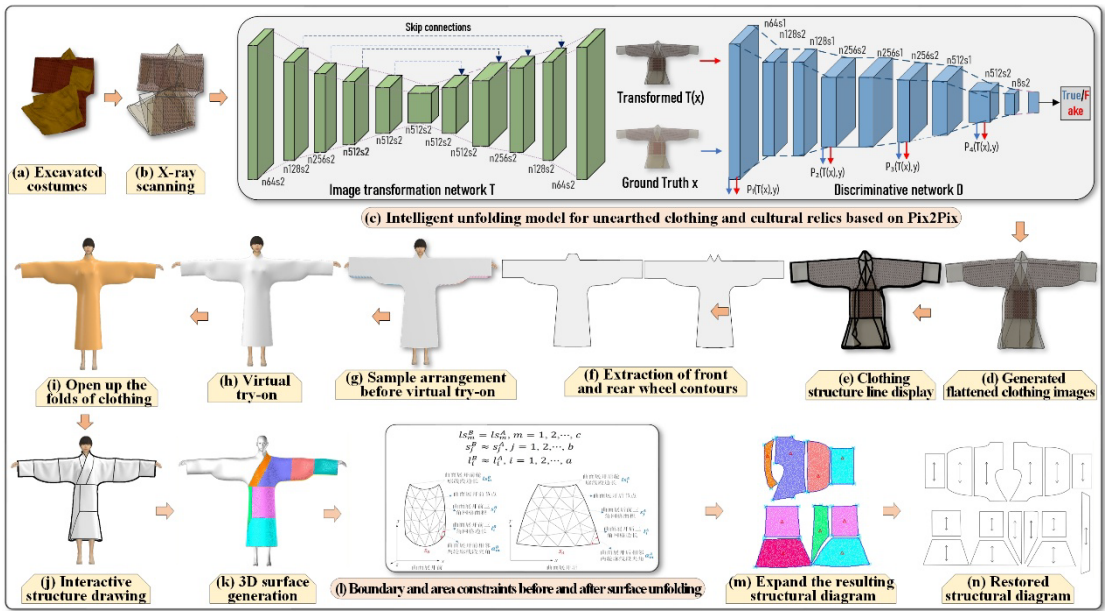

Figure 5-7 Application flowchart of interactive reverse intelligent restoration of unearthed costume sewing patterns

Step 1: Use X-ray scanning to obtain scanned images of unearthed costume

Excavated costume artifacts often become extremely fragile due to their age and aging materials, and may even exhibit partial damage or deformation (as shown in Figure 5-7 (a)). Therefore, at the beginning of digital processing, non-contact scanning technology should be adopted to minimize the risks caused by physical contact. X-ray computed tomography technology can penetrate the surface of cultural relics, obtain high-resolution two-dimensional images of their internal structures, and accurately record the current state of cultural relics. During the scanning process, the scanning

parameters need to be adjusted according to the material, thickness, and preservation status of the cultural relics. For example, low-energy X-rays can be used to avoid damage to thin materials such as silk fabrics or cotton and linen; For thicker multi-layer costume, it is necessary to increase the scanning intensity appropriately to ensure image clarity. To improve image quality, it is necessary to preprocess the scanned data, including denoising, contrast enhancement, and grayscale correction. Common image processing algorithms such as Non-Local Means Denoising and Histogram Equalization can effectively improve the signal-to-noise ratio of images, highlighting the texture and structural features of costume. The unearthed costume image obtained by X-ray scanning is shown in Figure 5-7 (b).

Step 2: Intelligent simulation and unfolding of non exhibitable unearthed costume based on Pix2Pix

Excavated costume relics often exhibit wrinkled, tangled, or compressed states due to burial environment and time factors, making it difficult to directly observe their original planar structure. In order to restore the flattened form of unearthed costume, Pix2Pix based image intelligent generation technology is required to convert the scanned costume cultural relic data into two-dimensional unfolded costume images (as shown in Figure 5-7 (c)). Pix2Pix is an image-to-image conversion model based on Conditional Generative Adversarial Network (cGAN), which can achieve end-to-end image generation by learning the mapping relationship between input images and target images. In this step, the input data is an X-ray scan image of costume artifacts, and the target output is the corresponding unfolded two-dimensional image. After completing the training, the model automatically converts the input scanned image into an unfolded image (as shown in Figure 5-7 (d)). This image can clearly display the planar structure of costume, including the body, sleeves, collar, and other components, laying the foundation for subsequent contour extraction and prototype generation.

Step 3: Extract the front and rear contour lines and planar areas from the unfolded image

After generating the unfolded image, it is necessary to further extract its contour lines to define the flat area of the costume. Due to the possibility of noise or discontinuous areas in the unfolded image, image segmentation operations need to be performed first. Common segmentation methods include threshold segmentation, edge detection, and semantic segmentation based on deep learning. Specifically, the Canny edge detection algorithm can be used to extract prominent edges in the image, and then

connected to the broken edges through Hough Transform or Active Contour Model to form closed contour lines. For costume with complex structures, it is necessary to combine manual interaction for correction to ensure the accuracy of the contour (Figure 5-7 (e)). The extracted contour lines include the outer contour and internal structural lines (such as provincial roads, cutting lines, etc.) of the front piece, back piece, sleeve piece and other components. The planar area enclosed by these contour lines is the two-dimensional prototype of the costume (Figure 5-7 (f)).

Step 4: Reasonable layout of the flat sample around the virtual human body model

In order to reconstruct the three-dimensional form of costume, the extracted two-dimensional sample needs to be wrapped around the human body model in a virtual environment. Virtual human models are usually customized based on the characteristics of the population in a specific cultural relic era. The layout process needs to consider the naturalness and historical accuracy of the costume worn. Firstly, determine the corresponding relationship between various patterns and human body models based on the type of costume. Subsequently, the template is placed in appropriate positions around the human body model through geometric transformations, while maintaining a certain distance between the template and the human body surface to match the actual wearing effect. The layout result is shown in Figure 5-7 (g), where the sample plate forms a preliminary three-dimensional spatial distribution around the human body model.

Step 5: Virtual stitching operation to construct a 3D costume model

Virtual stitching is the process of connecting scattered pattern pieces into a complete garment in three-dimensional space. Firstly, it is necessary to define the stitching relationships, that is, which edges need to be stitched. These relationships can be inferred from historical documents or cultural relics, or automatically recognized through image analysis. The stitching operation is achieved by gradually pulling the vertices of the corresponding edges closer. After stitching is completed, a preliminary 3D costume model is formed (Figure 5-7 (h)), which may have surface unevenness or excessive wrinkles and require further processing.

Step 6: Unfold treatment to eliminate surface wrinkles

Due to the deformation of the fabric and the influence of virtual gravity during the stitching process, many natural wrinkles often appear on the surface of the 3D costume model. These wrinkles bring many uncertain factors to the unfolding of the surface. The

stretching treatment aims to eliminate wrinkles and obtain a smooth costume surface through physical simulation or geometric optimization. The processed model, as shown in Figure 5-7 (i), has a smooth surface and retains the overall structural features of the costume.

Step 7: Draw 3D costume structure lines

Costume structural lines, such as provincial roads, dividing lines, decorative lines, etc., are key elements that define costume cutting and design features. According to the structure lines visible in the image of the unearthed costume artifacts generated in step 2 (Figure 5-7 (e)), these lines need to be accurately drawn on the surface of the 3D model through human-computer interaction. The final three-dimensional structural line (Figure 5-7 (j)) provides a basis for subsequent surface segmentation and unfolding.

Step 8: Three dimensional structural lines enclose the costume surface

The three-dimensional structural line divides the surface of the costume model into multiple surface patches, such as the body, sleeves, collar, etc. Each surface patch is defined by boundary lines and can be mathematically represented through parameterized surfaces such as NURBS or B é zier surfaces. Surface reconstruction needs to ensure smoothness and continuity. Subdivision Surface or surface fitting algorithms are commonly used to generate high-precision surfaces based on boundary lines. The final surface model (Figure 5-7 (k)) not only accurately reflects the geometric shape of the costume, but also provides a foundation for subsequent unfolding operations.

Step 9: Unfold the 3D surface into a 2D plane sample

Surface unfolding is the process of mapping a three-dimensional surface to a two-dimensional plane, with the aim of generating costume samples that can be used for cutting. Due to the Gaussian curvature of the surface, expansion inevitably introduces distortion, and it is necessary to minimize area or angle deformation as much as possible (Figure 5-7 (l)). The two-dimensional sample obtained after unfolding (Figure 5-7 (m)) needs to be compared with the original unfolded image to evaluate geometric consistency.

Step 10: Sample revision and optimization

The unfolded sample may have issues such as uneven edges, dimensional errors, or excessive deformation, which require correction and optimization. The specific operations include: smoothing edges, adjusting curve smoothness, and adding seams and marking points; Adjust the sample size according to actual body size or standard

size to ensure comfortable wearing; Considering the characteristics of fabric elasticity, drape, and production process, make adaptive modifications to the sample. The final optimized sample (Figure 5-7 (n)) can be directly used for digital archiving or physical replication production.

5.4.2 Restoration results and evaluation

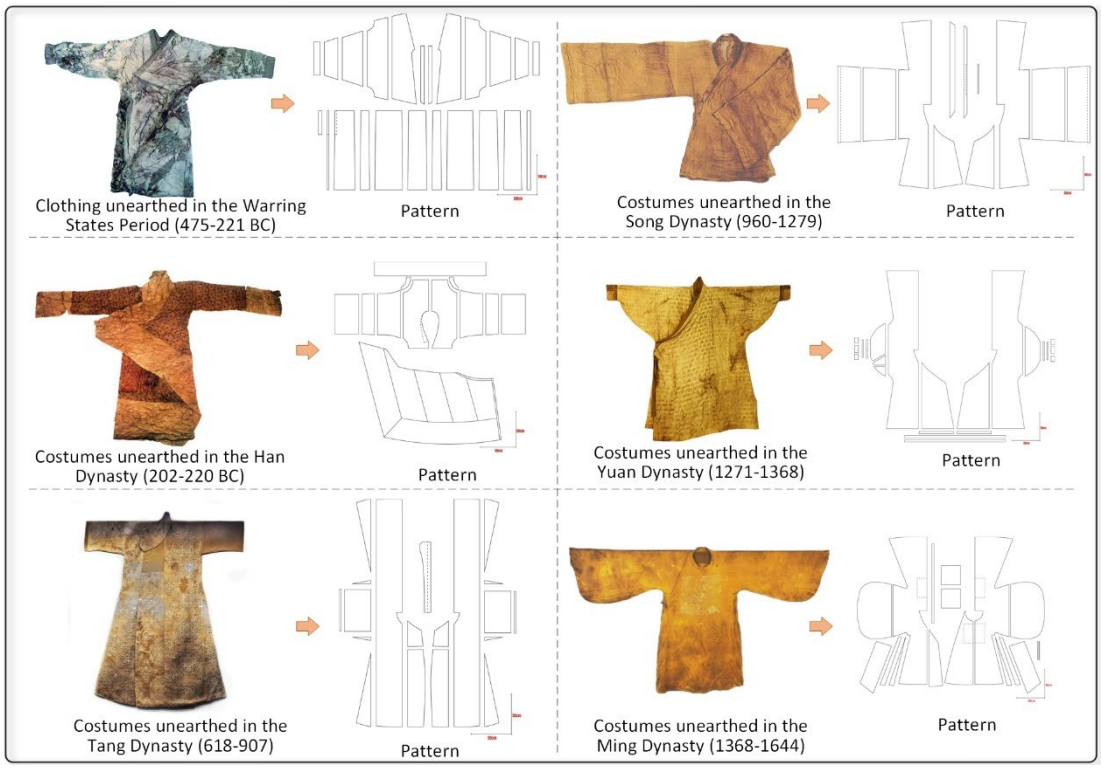

Figure 5-8 Application flowchart of interactive reverse intelligent restoration of unearthed costume sewing patterns

Intelligent restoration method for incomplete and degraded costume relics' sewing patterns proposed in this chapter is applied to restore the sewing patterns of ancient garment relics, as shown in Figure 5-8. For more restoration examples, please refer to Appendix 5.

The evaluation of the restored sewing patterns includes two core indicators, namely Shape Matching Degree (SMD) and Dimensional Rationality (DR), whose scoring criteria are shown in Table 5-1. The shape score focuses on historical accuracy, while the size score focuses on data matching. The weight of SMD is 50%. The scoring is based on the degree of conformity between the reconstructed clothing shape (such as collar shape, sleeve shape, slit, and patch position) and historical documents/physical objects. The scoring criteria are shown in Table 5-1. The weight of DR is 50%, and the

scoring is based on the matching degree between the key dimensions of the restored clothing (such as length, chest circumference, sleeve length, hem circumference) and historical objects or literature records. The calculation of the Sample Restoration Index (SRI) is shown in formula 5-15:

$$SRI = SMD \times 0.5 + DR \times 0.5 \quad (5\text{-}15)$$

Where, the SRI's grading standards are shown in Table 5-2. The higher the SRI value, the better the result of costume's sewing patterns restoration.

Table 5-1 Core evaluation indicators for restoration samples

Evaluation Criterion	***Weight***	***Score Range***	***Scoring Basis***
Form & Style Matching	50%	90-100	Fully aligns with historical records, no deviations.
		80-89	Core form and style are correct, with minor differences in local details.
		70-79	Main form and style are correct, but with 2-3 noticeable deviations.
		≤69	Form and style severely inconsistent with historical records.
Dimensional Reasonableness	50%	90-100	Dimensions fully align with historical records and practical requirements, no deviations.
		80-89	Core dimensions are correct, with minor differences in local dimensions.
		70-79	Main dimensions are correct, but with 2-3 noticeable deviations.
		≤69	Dimensions severely inconsistent with historical records and practical requirements.

Table 5-2 SRI grading standards

Score Range	*Scoring Basis*
90-100	Highly accurate restoration of form and dimensions, with only negligible minor deviations.
80-89	Core elements meet standards, but partial areas need optimization.
60-79	Basically restored, but with noticeable flaws.
< 60	Insufficient historical basis or severe dimensional discrepancies.

This study invited 5 industry experts to evaluate the restored clothing samples, scoring them based on two core indicators: SMD and DR. The scores of the 5 experts are shown in Table 5-3.

Table 5-3 Rating data of 5 invited industry experts on the restoration results of the sample version

Expert ID	*Form & Style Matching*	*Dimensional Reasonableness*
Expert A	95	92
Expert B	93	90
Expert C	96	94
Expert D	92	88
Expert E	94	91

By using formula 5-15, the average total score of SRI was calculated to be 92.5 points. According to the grading criteria in Table 5-2, the restoration effect of this sample reached the excellent level (90-100 points), indicating that the overall restoration effect of sewing patterns is good.

5.5 Discussion

5.5.1 The technological advantages and scientific connotations of deconstructing intelligent restoration paths

This study systematically proposes and constructs an interactive reverse intelligent restoration method for the sewing patterns of unearthed costume. The core research findings lie in the successful integration of the Pix2Pix image translation model in the field of artificial intelligence with the boundary size and area constraints (BC&AC) algorithm in computational geometry, forming a full process solution from data acquisition, intelligent flattening, 3D reconstruction to final 2D template generation. Research has found that the Pix2Pix model based on Conditional Generative Adversarial Network (cGAN) can effectively learn the complex nonlinear mapping relationship between folded and folded cultural relic images and their fully flattened state images. Its U-Net generator structure is good at capturing detailed features such as texture and edges of costume, while the PatchGAN discriminator can ensure the authenticity of generated images on local textures. In the 3D unfolding stage, the study established a rigorous mathematical model to constrain the side length, area, contour line length, and angle relationship of the triangular mesh before and after surface unfolding, achieving precise flattening of the 3D costume surface into a 2D costume sample that can be used in actual production while minimizing geometric distortion. The entire process not only achieves automated processing, but more importantly, introduces human-computer interaction, allowing experts to intervene at key nodes such as contour extraction and structural line drawing, ensuring the archaeological authenticity and structural accuracy of the reconstructed results of unearthed costume sewing patternss.

Compared with traditional methods for restoring the sewing patterns of unearthed costume, the intelligent restoration path proposed in this study has significant advantages. The traditional restoration methods for unearthed costume sewing patterns heavily rely on the manual operations of cultural relic protection experts and costume pattern makers, including careful physical flattening, measurement, sampling, and pattern making of the actual objects. This process is not only time-consuming, labor-intensive, and costly, but also poses a huge potential risk to the cultural relic itself, which can easily cause irreversible secondary damage during the operation. In addition,

the restoration accuracy of traditional methods is highly dependent on the operator's personal experience, making it difficult to quantify and replicate. In terms of digital methods, existing research has mostly focused on using 3D scanning for cultural relic archiving or using finite element analysis for simple deformation simulation. These methods often fail to break through the complete technical loop from the folded state, to the flattened image, and then to the producible sample, and are helpless for extremely fragile and unable to flatten cultural relics. This study is the first to introduce advanced deep learning image generation techniques into this field, achieving end-to-end prediction from damaged to intact states. At the same time, this study did not stay at the level of image generation, but further integrated with geometric processing algorithms to solve the core problem of converting from 3D to 2D, which is a key link that most existing digital restoration research has not delved into. Therefore, in terms of automation level, processing accuracy, non-destructive nature of cultural relics, and process integrity, it is significantly better than existing research methods.

The good results achieved in this study can be explained by its technical core. The success of the Pix2Pix model in the virtual intelligent flattening stage of unearthed costume in a folded state is attributed to its adversarial training mechanism. Generator G (U-Net) is dedicated to generating flattened images that are indistinguishable from reality, while discriminator D (PatchGAN) strives to distinguish between real and generated images. Both progresses together in the game, ultimately enabling the generator to output highly credible results both visually and structurally. The skip connection structure in U-Net directly transfers the low-level detail features captured by the encoder (such as stitching and fabric texture) to the decoder, which is the key to generating images that can preserve clear structural lines. The introduction of L1 loss function forces the generated image to approach the real target at the pixel level, effectively reducing the blurring phenomenon of the generated image and ensuring the accuracy of subsequent geometric measurements. In the stage of surface unfolding, the credibility of research results comes from its rigorous mathematical modeling. Discretizing continuous surfaces into triangular meshes is a common method in computer graphics. Based on this, this study transforms the abstract objective of maintaining geometric properties into four specific and computable optimization objectives: minimizing the sum of squared differences in edge length, area, contour length, and angle. For a developable surface, these four values can simultaneously approach zero; For non developable surfaces, the minimization of edge length and area

deformation is sought under the rigid constraint of strictly ensuring that the contour line length and angle remain unchanged. This is in line with the practical logic of "accurate plate contour and moderate stretching or compression of internal fabric" in costume engineering, thus ensuring that the final generated two-dimensional sample is both accurate and practical.

An interesting unexpected discovery during the research process is that virtual simulation data not only serves to supplement the amount of data, but in some cases can even enhance the model's ability to process real data. The reason lies in the highly controllable nature of virtual simulation environments, which can systematically and exhaustively generate various extreme folding states, regular wrinkle patterns, and samples of different material thicknesses that are difficult to collect in the real world. These samples help the model better learn the underlying physical laws of wrinkle formation and unfolding, thus enabling it to have stronger inference and generalization abilities when facing irregular real cultural relics. This suggests that in the field of cultural relic AI, "simulation first, real assistance" may be an effective new path for data construction. Another finding is that the Pix2Pix model not only restores the structural lines, but also repairs and completes the fabric texture to a certain extent. Although this is not the design focus of the model, it has become a valuable byproduct, providing additional information reference for the visual restoration of cultural relics.

This study is based on several core hypotheses and has been validated through experiments and results. Assumption 1: The Pix2Pix model can effectively learn the mapping relationship between the folds and flattened states of unearthed costume. "This hypothesis has been strongly validated. Through qualitative visual comparison and quantitative indicators such as SSIM and PSNR evaluation, the generated images are highly similar in structure and texture to the real flattened images, demonstrating the effectiveness of the model in this specific task. Assumption 2: "Algorithms based on boundary size and area constraints can achieve low distortion unfolding of 3D costume surfaces." This assumption has been verified. Both mathematical derivation and experimental results indicate that the BC-AC model strictly maintains the accuracy of the contour and effectively constrains the deformation of the internal mesh. The resulting two-dimensional sample is geometrically reasonable and usable. Assumption 3: "The strategy of integrating real data and virtual data can overcome the bottleneck of scarce cultural relic data." This assumption has been successfully verified. The multi-source data strategy greatly expands the size and diversity of the training set, enabling

the model to learn a wider range of wrinkle types and costume shapes, significantly improving the model's generalization ability and robustness. This is one of the key prerequisites for the success of this study.

5.5.2 Theoretical, methodological, and practical aspects of research and their limitations

The contribution of this study is reflected in three aspects: theory, methods, and practice. At the theoretical level, it has successfully applied cutting-edge technologies of computer vision and deep learning across disciplines to the fields of costume archaeology and cultural relic protection, providing a new paradigm for the digital processing of costume cultural heritage and verifying the enormous potential of artificial intelligence in solving highly specialized and non-standard historical heritage problems. At the methodological level, the core contribution of the research lies in the construction of a hybrid intelligent restoration framework that integrates data-driven and rule-based approaches. Among them, the multi-source data strategy designed to solve the iconic "small sample" problem in the field of cultural relics, such as the combination of real cultural relic scanning, physical restoration production, and virtual simulation generation, has important methodological reference significance and provides feasible solutions for the construction of datasets in other similar scenarios. The proposed BC-AC surface unfolding model provides a solid mathematical foundation and algorithmic tools for handling complex, non-rigid two-dimensional problems. At the practical level, this chapter provides for the first time a technological path that can restore extremely fragile and untouchable excavated costume without damage, with high precision and repeatability, greatly reducing the risks and costs of cultural relic protection. Its output - digital samples, can be directly used for virtual restoration of cultural relics, construction of digital museums, restoration of costumes and props in film and television dramas, education on traditional craftsmanship inheritance, and limited physical replication, greatly promoting the transformation of costume cultural heritage from "passive protection" to "active utilization", with significant social benefits and cultural value.

Although this study has achieved significant results, its limitations still need to be objectively recognized. Firstly, the performance of the model is highly dependent on the quantity and quality of the training data. Despite adopting a multi-source data strategy, X-ray scanning data of real cultural relics is still the most valuable and scarce

resource, and its acquisition is subject to the preservation status of cultural relics, museum cooperation willingness, and high scanning costs. Secondly, the current methods still lack the ability to handle extremely complex situations. For example, for cultural relics that are severely carbonized, adhered into a cluster or multiple layers of dense fabric, the X-ray image itself is difficult to distinguish the layers clearly, resulting in insufficient input information for the model and inevitably limiting the restoration effect. Thirdly, algorithms currently mainly focus on the restoration of geometric structures, and the restoration of surface visual attributes such as fabric material, color, embroidery patterns, etc. is not their main focus. These are important components of cultural heritage value. Fourthly, the computational complexity is high, and the processing of high-resolution images and the optimization of complex 3D surfaces require powerful computing power support, making it difficult to achieve fast response on ordinary computers, which to some extent limits the convenience of its promotion and application. Finally, multiple manual interactions are still required in the process, indicating that the system is currently an efficient "human-machine collaboration" intelligent assistance tool, rather than a fully automated intelligent system, and its final effectiveness still depends in part on the operator's professional level.

Based on the above limitations, future research can be conducted from multiple directions. One is to explore more advanced small sample learning and self supervised learning algorithms, such as using contrastive learning to extract more features from a small number of samples, or developing cross modal generative models that attempt to generate multimodal information such as texture, material, etc. from a single source of scanned data, in order to reduce dependence on paired large datasets. The second is to develop more sophisticated multi-level segmentation algorithms, combining deep learning and prior knowledge, striving to automatically identify and separate different fabric layers that are adhered or stacked from scanned data, providing possibilities for processing extremely complex cultural relics. The third is to promote the integration of multiple technologies, such as hyperspectral imaging, 3D laser scanning, and X-ray CT scanning results, to construct multidimensional digital twin models of cultural relics, thereby simultaneously restoring their geometric structures and surface visual properties. The fourth is to carry out algorithm lightweighting and engineering optimization, develop cloud processing platforms or simplify models, so that this technology can be more conveniently applied by museums and research institutes. The fifth is to explore knowledge embedding and reasoning, constructing a knowledge

graph of the professional knowledge of ancient Chinese costume systems, such as collar and right lapel, sleeve width grades, etc., and embedding it into algorithms, so that the restoration process can not only ensure geometric correctness, but also perform cultural logic rationality verification, preventing the occurrence of restoration results that violate historical forms.

5.5.3 Intelligent restoration paradigm and its value for cultural heritage protection

This study successfully broke through the bottleneck of traditional structural restoration methods for unearthed garment relics and constructed an innovative, efficient, and non-destructive interactive reverse intelligent restoration technology system. The conclusion is reinforced as follows: Firstly, the fusion of deep learning and computational geometry is an effective paradigm for solving such complex restoration problems. AI is responsible for solving the problem of "shape inference", while geometric algorithms are responsible for solving the accuracy problem of "dimension transformation". The two complement each other. Secondly, in response to the challenge of data scarcity in specific fields, it is feasible and necessary to creatively adopt a multi-source data fusion strategy, which provides valuable experience for the deep application of artificial intelligence in vertical fields such as archaeology. In the end, this study is not limited to proposing an algorithm or model, but also provides a complete solution from the physical world to the digital world and then feedback to the physical world. Its significance goes beyond a simple technological breakthrough, and it opens up a new technological path for the permanent preservation, in-depth research, and dynamic inheritance of costume cultural heritage, laying a solid foundation for the digital intelligent restoration of unearthed garment relics and other similar fragile cultural relics.

In practical application scenarios, the method proposed in this study can be widely applied to museums, archaeological research institutes, universities, and cultural and creative industries. In cultural relics protection units, this method can serve as a standard digital filing process for unearthed textile cultural relics, establishing digital archives containing their 3D models, 2D samples, structural line diagrams, and other information for each precious cultural relic. This is not only a scientific record of protection, but also lays a data foundation for future restoration research. For archaeologists and researchers of costume history, this method provides a scientific

empirical analysis tool that can accurately measure and analyze the size, proportion, cutting, and sewing techniques of ancient costume, revealing the level of craftsmanship, aesthetic trends, and social etiquette in different historical periods, and promoting the research of costume history from qualitative description to quantitative analysis. Accurate digital samples provide the possibility for the production of high fidelity replicas, which can be used as substitutes for exhibitions to reduce the loss of authentic products, as well as for the development of cultural and creative products to promote traditional culture.

5.6 Conclusion

This study focuses on the core challenges faced by the structural restoration of unearthed costume, such as strong professionalism, high cost, and vulnerable cultural relics. It proposes and elaborates on an interactive reverse intelligent restoration method based on Pix2Pix generative adversarial network and boundary size and area constraint algorithm (BC&AC). Through systematic research, This study successfully constructed a full process technology system from cultural relic scanning, intelligent leveling, 3D reconstruction to 2D template generation, providing innovative solutions for the digital protection and restoration of unearthed costume relics. The main conclusions of this study can be summarized as follows:

Firstly, artificial intelligence technology can effectively empower the traditional field of costume and cultural relic protection. Practice has proven that the Pix2Pix based translation model for unearthed costume images can accurately learn the complex mapping relationship between folds, folding states, and fully flattened states, achieving high-precision, non-contact digital flattening of the sewing patterns of unearthed costume relics, effectively avoiding the risk of damage to costume relics that may be caused by traditional physical unfolding methods.

Secondly, interdisciplinary integration is the key to solving complex technological challenges. This study is not a single application of technology, but a deep integration of computer vision (image processing), deep learning (Pix2Pix), computational geometry (surface unfolding), archaeology, textile and costume engineering, and other interdisciplinary knowledge, forming a hybrid intelligent restoration framework that combines "data-driven" and "model driven", ensuring that the restoration results of

costume relics meet both the accuracy of digital computing and the authenticity requirements of archaeological research.

Thirdly, the proposed hybrid data strategy effectively solves the bottleneck of data scarcity in the field of excavated costume archaeology and restoration. By comprehensively using three paths of real costume relics X-ray scanning, physical restoration production, and virtual simulation generation, this study constructed a large-scale and diversified training dataset, significantly improving the generalization ability and robustness of deep learning models, providing useful reference for the application of artificial intelligence in small sample and high-value scenarios.

Fourthly, the intelligent assistance mode of human-computer interaction is a reliable path to achieve high-precision restoration of unearthed costume. This study did not pursue complete automation of the entire process, but designed an expert intervention mechanism at key nodes such as contour extraction and structural line drawing. This concept of "human-machine collaboration" not only leverages the efficiency advantages of computers in processing massive data and complex calculations, but also retains the core role of domain experts in historical research, cultural interpretation, and final decision-making, ensuring the scientific and cultural accuracy of the restoration results of costume relics.

In summary, the interactive reverse intelligent restoration method for the sewing patterns of unearthed costume relics proposed in This study has effectively promoted the interdisciplinary integration of artificial intelligence and costume cultural heritage protection in theory. It has constructed a complete and reliable technical process in terms of methods, and provided strong technical tools and data foundation for the digital archiving, virtual restoration, activation and utilization of cultural relics, as well as traditional craft research in practice. This study not only has important practical significance for the protection and inheritance of ancient Chinese costume culture, but also provides a reference paradigm and broad application prospects for the digital restoration of other types of fragile cultural relics through its technical path and methodology.

Chapter 6 Application of AI based restoration methods for incomplete and degraded costume relics

This chapter addresses the issue of the lack of effective digital protection for the cultural heritage of ancient Chinese costume. By combining the intelligent color restoration technology, intelligent style and pattern restoration technology, and intelligent structural restoration technology proposed in this study, a three-dimensional virtual simulation database of unearthed costume from various dynasties in China is constructed. The fragile and non-renewable costume relics are transformed into three-dimensional models that can be permanently preserved, non-destructive measured, and infinitely reused, providing a solid data foundation for the revitalization, dissemination, and innovative development of excellent traditional Chinese culture in contemporary times.

6.1 Basic scheme for application of AI based restoration method for incomplete and degraded costume relics

This chapter focuses on the innovative application of AI technology in the restoration of damaged and faded garment relics, aiming to provide new means for the digital protection of unearthed garment relics through cutting-edge technological means. This application integrates research results from multiple chapters and promotes cultural relic restoration work in a systematic and scientific manner, opening up new paths for cultural heritage protection. The relevant application schematic is shown in Figure 6-1:

- Integrate key research findings from the preceding chapters. The restored unearthed costume styles and patterns in Chapter 3 accurately restore the unique appearance and decorative details of ancient costume; Chapter Four: Restoring the Colors of Excavated Costumes, Reproducing the Brilliant or Elegant Colors of Cultural Relics Originally; Chapter 5: Restoring the Excavated Costume Sewing patterns to Ensure that the restored cultural relics conform to their historical appearance in terms of form and function.
- Based on the comprehensive integration of multi-dimensional data of garment relics, the latest costume plate modeling technology is applied to construct a high-

precision 3D costume model, creating a high-fidelity 3D costume model that not only conforms to historical structure, but also has natural sagging and motion wrinkles.

- Based on the constructed 3D excavated costume model, further establish a 3D database of ancient Chinese costume. This database is a centralized storage and management of the restoration achievements of ancient Chinese costume, including about 500 unearthed costumes from the pre-Qin to Qing dynasties. It is an important digital resource library of ancient Chinese costume culture.

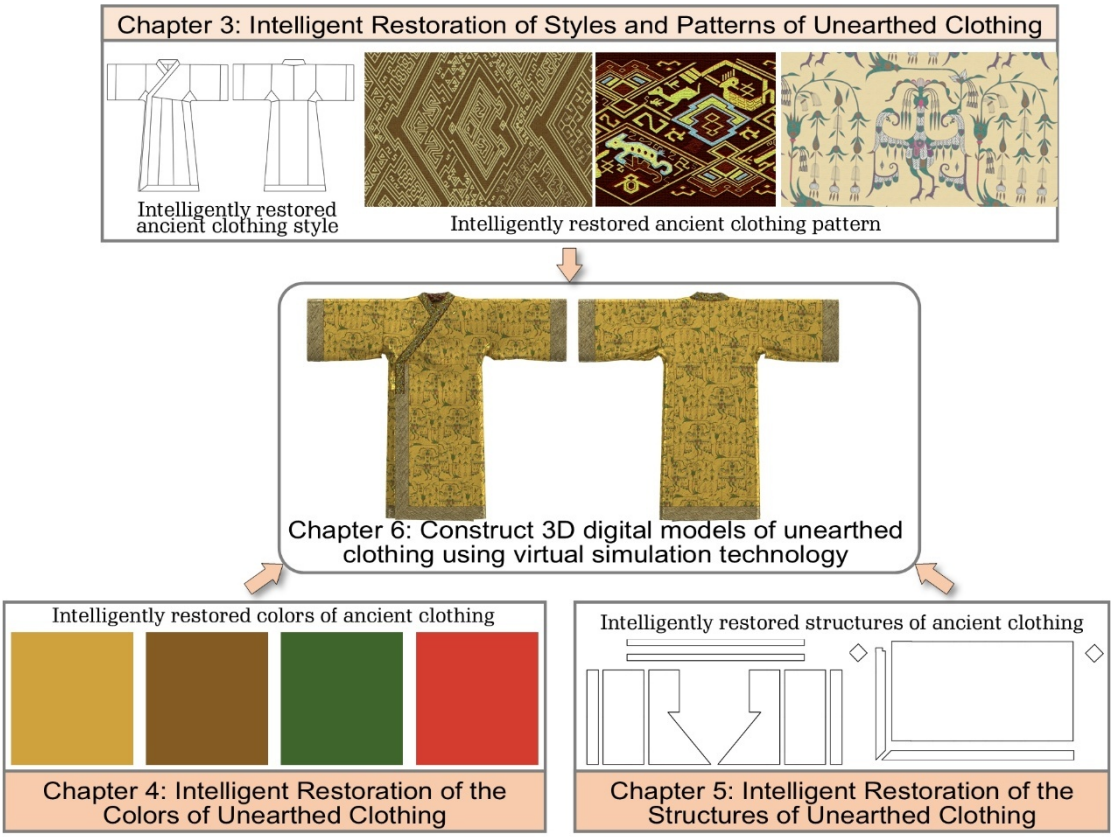

Figure 6-1 Example display of three dimensional simulation database of chinese ancient excavated costume relics

6.2 Application of intelligent restoration and restoration technology for unearthed costume

6.2.1 Analysis of Chinese costume styles, textile patterns, colors, and sewing patterns throughout history, and costume overall restoration

(1) Analysis and overall restoration of pre-Qin costume styles, textile patterns, sewing patterns, and colors

Before 221 BC, costume in the pre Qin (先秦) period was based on the basic form of "upper garment and lower garment". This structure originated from the interpretation of the Yin Yang and Five Elements ideas in the Xia and Shang dynasties. The upper garment symbolized the sky (yang), while the lower garment symbolized the earth (yin), forming the expression of the cosmology of "heaven round and earth". [87, 88] The Zhou Dynasty incorporated this form into the system of ritual governance [89], distinguishing status levels through differences in details: aristocratic men's costume mainly consisted of deep clothes, with a cross collar right lapel and narrow sleeves design. The length of the clothes reached the ankle, and the waist was tied with a jade pendant to indicate their identity; Women often wear curved skirts and deep clothes, with the collar spiraling down around the body, forming a unique "continuous lapel hook edge" structure that not only covers the body but also highlights the curves. Civilian costume is oriented towards practicality, with men often wearing long clothes with narrow sleeves and right lapels, while women mainly wear black straight robes that are as long as the ground and require maidservants to carry the corners of the robe for movement. During the Spring and Autumn Period and the Warring States Period, significant changes occurred in the form of costume. King Wuling of Zhao implemented the "Hu costume riding and shooting" style, introducing the Hu costume styles of short clothes and long pants. The top was a short jacket with a standing collar and narrow sleeves, and the bottom was a crotch pants with a leather armor and leather boots, completely breaking the traditional constraints of wide robes and large sleeves and meeting the military riding and shooting needs. [46] At the same time, the form of deep costume further developed, and there was a distinction between straight and curved skirts: straight skirts and deep costume had a vertical downward collar, suitable for daily activities; The curved skirt deep garment is formed with complex patterns through the wrapping of the collar, becoming a symbol of aristocratic dress. In addition, hooks are widely used as multifunctional accessories, with materials ranging from bronze to gold and silver, and their shapes combine practicality and decoration, becoming a symbol of identity.

The patterns of pre Qin costume carry profound cultural connotations [90], with animal and geometric patterns being the main ones in the early days [91], reflecting the combination of divine and royal power. The silk remnants on the surface of Shang Dynasty bronze vessels indicate that the twill weaving technique was already mastered

at that time. The patterns were mainly diamond shaped, square grid shaped, and loop shaped, forming a mysterious and majestic visual effect through repeated arrangement. During the Zhou Dynasty (approximately 1046-256 BC), patterns gradually shifted towards ritualism, with the Twelve Chapter Pattern (十二章纹) on the coronation becoming the symbol of the highest level. Among them, the sun, moon, and stars represented the Way of Heaven (天道), dragons and Huachong (华虫，Huachong is clearly explained as pheasant in most Chinese classics, and is called "Huachong" because of its colorful feathers) symbolized royal power, algae and fire symbolized cleanliness, and fǔ (黼, An axe shaped pattern embroidered on an ancient Chinese dress) and fú (黻, The pattern embroidered on ancient Chinese dresses is half green and half black) symbolized decisiveness. These patterns were presented on the upper garment through embroidery or weaving techniques, contrasting with the color scheme of the lower garment and strengthening the hierarchical order. During the Spring and Autumn Period and the Warring States Period, there was a significant change in the style of patterns. Influenced by Taoist philosophy, gentle and auspicious animal patterns such as horses, deer, and cranes began to appear, coexisting with traditional dragon and phoenix patterns. At the same time, plant patterns gradually emerged, with realistic and variant floral and vine patterns interwoven into costume, creating a dynamic and complex visual effect. For example, on the lacquered wooden figurines unearthed from Chu tombs, cloud patterns and dragon patterns intertwine, with smooth and elegant lines, reflecting the romantic aesthetic tendency of the Chu people. In addition, geometric patterns are transformed and reorganized to form more decorative patterns, such as the embedding of auspicious characters in variant mountain cloud patterns, which not only retains traditional styles but also gives new cultural meanings.

The color system of pre Qin costume is centered around positive colors, with cyan (青色), red, yellow, white, and black regarded as symbols of the five directions of heaven and earth, possessing sacredness and hierarchy. [92] The Zhou Dynasty clearly stipulated that the emperor wore a black robe and a red yellow robe, symbolizing the mandate of heaven; Feudal lords wear red clothes and black robes, doctors wear green clothes and red robes, scholars wear yellow clothes and black robes, and commoners can only wear mixed color costume. This color grading system not only reflects ritual norms, but also strengthens social order through visual symbols. For example, in the twelve-chapter patterns on the coronation robe, the sun, moon, and stars are

embroidered with white silk thread, the dragon pattern is black, and the worm pattern is red, highlighting the symbolic meaning of the patterns through color contrast. In practical applications, color selection is influenced by technological limitations and aesthetic preferences. During the Shang and Zhou dynasties, dyeing and weaving techniques were mainly based on the combination of dyeing and painting. Positive colors such as red and yellow were often painted on the surface of fabrics using mineral pigments, creating bright and long-lasting color effects. Excavated cultural relics show that silk from the Shang Dynasty was mainly in warm colors, with yellow and red accounting for more than half, brown and brown as secondary colors, and cool colors such as blue and green being less commonly used. In the Zhou Dynasty, more colors were developed through plant dyes, such as using gardenia to dye yellow, madder to dye red, and bluegrass to dye blue, forming richer color layers. During the Spring and Autumn Period and the Warring States Period, color application became more flexible, but the main color system was still strictly followed, with only intermediate colors used to embellish the details of the patterns. For example, the costume of painted wooden figurines in Chu tombs was based on vermilion red, with black and white borders on the cuffs and lapels to create a sharp contrast. [93]

The pre Qin costume structure was mainly based on cross shaped flat cutting [74], which achieved human body wrapping through segmented cutting and splicing. In the production of upper and lower garments, the garments are cut separately and sewn together. The length of the garment is knee length, the length of the garment is ankle length, and the waist is tied tightly with ribbons to form a loose silhouette. Shenyi (深衣, a traditional Chinese robe with overlapping layers) adopts a top and bottom connected system, integrating the top and bottom of the garment into one. Through the " Overlapping lapel with scalloped edges" design, the collar is wrapped around the back, which not only covers the body but also facilitates movement. This structure utilizes the width of the fabric for splicing, blurring the boundary between the sleeves and the garment body, presenting a visual effect of overall wrapping, reflecting the aesthetic preference of agricultural culture for "wide robes and large sleeves". Unlike the costume of the Central Plains, the ethnic costumes of the Western Regions adopt clear segmented cutting, with clear boundaries between the sleeves and the costume body, making it easy to ride and shoot. [94] For example, the woolen underwear from the Warring States period (475 BC -221 BC) unearthed from the ancient tomb of Subexi in

Xinjiang was made by folding a whole piece of fabric into a garment, digging out the collar and then fitting it. The side seams were sewn with triangular fabric to make the hem wide and the cuffs tight and narrow, which not only kept warm but also made it easy to move around. This structural difference reflects the needs of different lifestyles: the Central Plains are mainly agricultural, and costume emphasizes etiquette and moral education; The Western Regions are mainly nomadic, and costume emphasizes practicality and regional adaptability. During the Spring and Autumn Period and the Warring States Period, with the deepening of cultural exchanges, the cross shaped flat structure gradually integrated. For example, the Khitan people's "goose carrying ribbon" brocade robe, although adopting a left lapel, still retained the cross shaped characteristics of the overall structure, reflecting the inclusiveness of Chinese costume culture. [74]

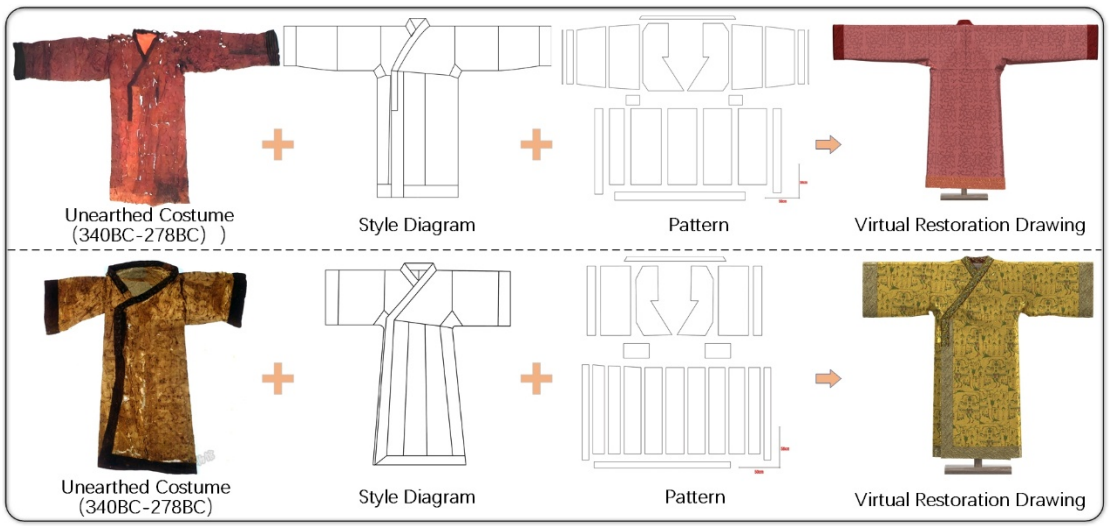

Figure 6-2 Comprehensive digital restoration of pre-Qin costumes

Based on the analysis of the styles, patterns, structures, and colors of pre Qin costume, combined with the digital and intelligent restoration methods of styles, patterns, structures, and colors mentioned in Chapter 345, the overall digital restoration of pre Qin costume was carried out, and the restoration effect is shown in Figure 6-2. More restored pre-Qin costumes can be found in Appendix 5.

⑵ Analysis and overall restoration of Han Dynasty costume styles, textile patterns, sewing patterns, and colors

During the Han Dynasty (202 BC-220 BC), costume was centered around the Shenyi system (深衣制) and Paofu system (袍服制) [95], while also incorporating elements of Hufu (胡服, traditional nomadic attire of northern China), forming a diverse and

coexisting pattern. As a traditional formal dress, Shenyi continues the shape of the "upper garment and lower garment (上衣下裳)" from the pre Qin period, but wraps the collar around the back through the "Overlapping lapel with scalloped edges", forming a distinction between "curved skirt" and "straight skirt".[96] Quju Shenyi (曲裾深衣, Deep Robe with Curved Lapels) is more common in women, with the collar hanging down to the ground after wrapping around the body for several weeks, covered with light gauze, and the skirt fluttering when walking, highlighting elegance and grace; Zhiju Shenyi (直裾深衣, Deep Robe with Straight Lapels) have gradually become mainstream due to their vertically downward placket, which makes them more convenient for men's daily activities. In addition to wearing Shenyi, aristocratic men also wore Chanyi (禅衣, single layered long robes) and Shuhe (裋褐, short clothes and long pants). The latter was influenced by Hufu with narrow sleeves and short body, making it easy to ride and shoot, reflecting the Han Dynasty's emphasis on practicality. Women's costume appears more luxurious. Quju Shenyi was popular in the early Han Dynasty, with a complex way of wrapping the collar, requiring multiple layers of fabric to be stacked to form a Sanchong Yi (三重衣, Triple-Layered Robe) effect. The outer layer of costume was often decorated with exquisite brocade, while the inner layer was set off with plain silk, creating a distinct layering. [97] By the Eastern Han Dynasty, Zhiju Shenyi gradually replaced Quju, and were paired with Ruqun (襦裙, short tops paired with long skirts) as daily attire. The Ru is mostly a cross collar with a right lapel, wide cuffs, and a skirt length that reaches the ground. It is tied with a ribbon waist and covered with a Peizi (Shoulder-Draped Silk Scarf, a traditional Chinese decorative garment worn by women over robes) to add a sense of elegance. In addition, women also wear Guiyi (袿衣, a type of wide sleeved robe), with flared sleeves and silk embellishments on the cuffs. When walking, it flows like clouds and clouds, becoming a symbol of aristocratic women's costume. The workers wear Duanhe (短褐, a traditional Chinese garment worn by peasants and laborers) and Kun (裩, crotch pants), with linen as the main material and simple colors, reflecting practicality.

The costume patterns of the Han Dynasty are characterized by a combination of realism and symbolism. Influenced by Chu culture (the culture of the ancient Chu state, From the 11th century BC to the 3rd century BC, centered in present-day Hubei and Hunan provinces, known for its distinctive art, literature, and ritual practices) in the

early days, mythological symbols such as cloud patterns and dragon and phoenix patterns were often used to reflect the worship of the heavenly realm. For example, on the Silk Gauze Unlined Robe (素纱禪衣) unearthed from the Mawangdui Han Tomb [97], cloud patterns drawn in cinnabar surround the dragon and phoenix, with smooth lines, symbolizing "ascending to heaven by riding clouds".[98] The Confucianism becoming mainstream, patterns gradually shifted towards the education, and the twelve chapter pattern was officially incorporated into the coronation system, becoming a symbol of the emperor's authority. Among them, the sun pattern is embroidered with circular gold pieces, the moon pattern is outlined with white silk thread, and the stars are embellished with silver thread, highlighting the level differences through material comparison. Folk costume patterns are more closely related to daily life. Plant motifs such as cornel patterns and vine scrolls were widely popular. The cornel, regarded as an auspicious symbol to ward off evil and bring good fortune, was rendered in realistic detail—its curled leaves and plump berries often intertwined with cloud motifs to form the 'Cloud-Cornel' design. In animal patterns, auspicious beasts such as unicorns and white tigers combine with real-life deer and horses to form distorted patterns. For example, deer patterns simplify body contours and highlight corner details, retaining divinity while also being decorative. In addition, geometric patterns such as square victory patterns and loop patterns are arranged repeatedly to form continuous patterns, commonly used for edging the collar and cuffs of costume, enhancing the delicacy of the garment. The advancement of textile technology has also driven pattern innovation. The Han Dynasty invented the jacquard machine, which can weave complex multi-color patterns, such as Chengyun Xiu (乘云绣, A Han Dynasty textile motif featuring immortal figures astride swirling clouds, symbolizing ascension to the celestial realm) which interweaves vermilion, magenta, and dark brown silk threads, and embeds dragon patterns in cloud patterns to form a three-dimensional effect. This technology shifts costume patterns from drawing to weaving, resulting in longer lasting colors and finer patterns.

The color system of Han Dynasty costume is centered around the "five colors" (green, red, yellow, white, and black), strictly following the theory of the Five Elements and the hierarchical system. [29] The emperor's attire is revered as "Xuan Yi Xiu Chang (玄衣纁裳)", with Xuan (玄) representing black and symbolizing heaven; Xun (纁) is vermilion-yellow, symbolizing the idea of "unity of heaven and man".[46] Feudal

princes wear "red clothes and black robes", officials wear "green clothes and red robes", scholars wear "yellow clothes and black robes", and commoners can only wear "plain clothes" (white) or "purple clothes" (black), and the use of regular colors is prohibited. This color grading not only strengthens social order, but also conveys political authority through visual symbols. For example, during the reign of Emperor Hanwu (汉武帝, 141 BC to 87 BC), it was stipulated that officials' court uniforms must be colored according to their grades, with purple for grades three and above, crimson for grades five and above, green for grades seven and above, and blue for grades nine and above, forming a color sequence of "purple, crimson, green, and blue". In practical applications, color selection is influenced by technological limitations and aesthetic preferences. The dyeing and weaving techniques of the Han Dynasty were mainly based on plant dyeing, with red coming from madder, yellow from gardenia, blue from bluegrass, and black from gallnuts. Among the silk unearthed from the Mawangdui Han Tomb, red has the highest proportion, followed by yellow. Blue and black are less commonly used, reflecting the Han people's preference for warm colors. [75, 99] At the same time, more colors were developed through "cross dyeing" technology (multiple dyeing), such as dyeing red with madder and then cross dyeing with bluegrass to obtain purple; Yellow with gardenia and then counterstain with gallnuts to obtain green color. [39] These colors are widely used in costume details, such as hem on the collar and rolled cuffs, creating a contrasting effect of "large color blocks and small embellishments". In addition, colors also have symbolic significance. Red symbolizes auspiciousness and is commonly used in wedding attire; Black symbolizes solemnity and is often seen in mourning attire; White symbolizes purity, but it is prohibited by the common people in daily life and is only used for worship or funeral ceremonies. This color culture has profoundly influenced the aesthetic of costume in later generations.

The costume structure of the Han Dynasty was also mainly based on "cross shaped flat cutting"[74]. Both Shenyi and long robes use the technique of "cutting the top and the bottom" and then sewing them together. The boundary between the garment body and the sleeves is blurred, and the fabric is naturally lowered through the "through cutting" technique, forming a loose contour. The curved hem deep garment features a wrap around design on the collar, utilizing the width of the fabric to achieve a "continuous lapel hook edge" that not only covers the body but also highlights the curves; Straight and deep costume simplifies the wrapping process and is more suitable

for daily activities through the vertical hem of the "train". Unlike the costume of the Central Plains, the "segmented cutting" introduced by Hu costume had a profound impact on the structure of Han Dynasty costume. For example, the Shuhe worn by workers adopts a left lapel design, with a clear boundary between the body and sleeves, and tight and narrow cuffs for easy riding and shooting; The Guiyi worn by women creates a three-dimensional effect by combining wide sleeves with flared cuffs, and the sleeves sway like clouds when walking. With the advancement of textile technology, the density of silk fabrics in the Han Dynasty increased, and the fabric became thinner and lighter, making it possible to have a "triple garment" structure for deep costume: the outer layer was decorated with brocade, the middle layer was set off with plain silk, and the inner layer was made of fine linen to absorb sweat. The three-layer overlay was both warm and luxurious. At the same time, through the techniques of edging and rolling, colored ribbons are sewn on the collar, cuffs, and hem of the garment to enhance its three-dimensional and decorative appeal. For example, the curved deep garment unearthed from the Mawangdui Han Tomb has a collar edge trimmed with vermilion ribbons and cuffs rolled with blue ribbons, creating a dual contrast of color and structure.

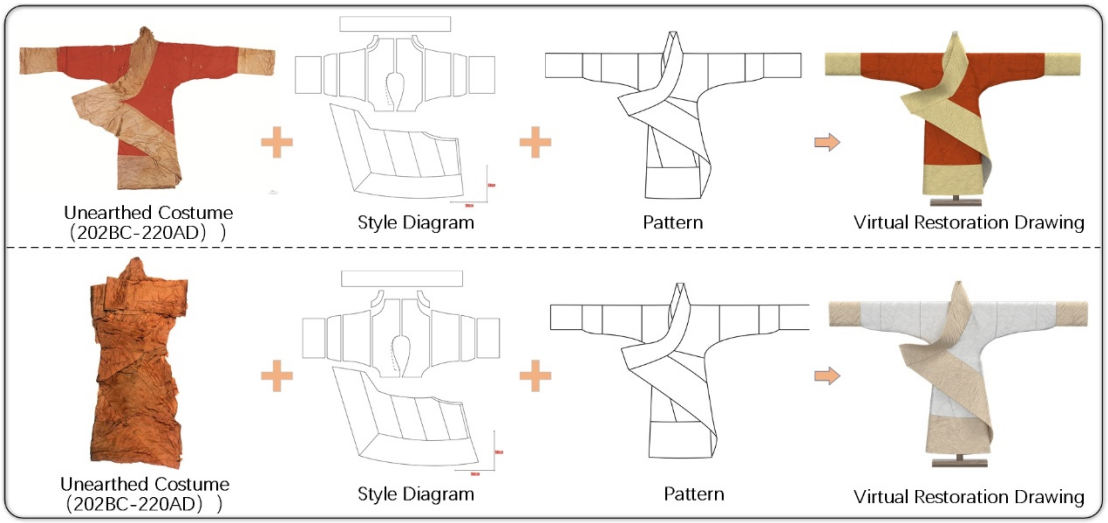

Figure 6-3 Overall digital restoration of Han Dynasty costumes

Based on the analysis of Han Dynasty costume styles, textile patterns, sewing patterns, and colors, combined with the digital and intelligent restoration methods for styles, patterns, structures, and colors mentioned in Chapter 345, the overall digital restoration of Han Dynasty costume was carried out, and the restoration effect is shown in Figure 6-3. More restored pre-Qin costumes can be found in Appendix 5.

⑶ Analysis and overall restoration of costume styles, textile patterns, sewing patterns, and colors in the Wei, Jin, Southern and Northern Dynasties

During the Wei, Jin and Southern and Northern Dynasties (220-589), the costume styles presented a distinctive feature of "integration of Hu and Han, mutual learning between the north and the south". [100, 101] Influenced by northern nomads, the combination of narrow sleeved short clothes, trousers and boots has gradually become popular. The Kuxi (袴褶) of the Xianbei ethnic group has become mainstream, with a short jacket as the top, tight and narrow cuffs, bound pants as the bottom, and a Liangdang armor (a type of armor with two pieces at the front and back) as the outer cover, which is both convenient for riding and shooting and has protective functions. [102] In the Southern Dynasty, the Han system was continued, with the beauty of "wide costume and broad belts". The literati class popular "big sleeved shirts", with wide cuffs like fans and clothes that were as long as the ground. When walking, the clothes fluttered, reflecting the elegance and transcendence of the "Wei Jin style". Women's costume integrates elements of Hu and Han, forming a combination of "upper garment and lower skirt and Liangdang (裲襠, similar to vests)": the upper garment is a narrow sleeved short jacket with a cross collar, the lower skirt is a pleated long skirt, and the outer cover is a sleeveless or short sleeved Liangdang, which retains the elegance of Han style while absorbing the convenience of Hu costume. [103] The practical characteristics of costume for northern ethnic minorities are significant. Xianbei women often wear "long robes with left lapels", which cover the left side of the collar, have tight and narrow cuffs, and a slit at the hem for easy horseback riding; Men wear a round neck and crotch less robe, with a round neck design that simplifies wearing and taking off, and side slit for easy movement. Paired with pants and boots, it is suitable for grassland life. The aristocrats of the Southern Dynasty (420-589) pursued a visual effect of "ethereal charm", such as the Hechang (鹤氅, a large outer garment decorated with crane feathers or feathers), whose cuffs and hem were adorned with feathers, and walked like a crane flapping its wings; Women also wear Hushan (縠衫, semi transparent tops made of light gauze), with a plain colored skirt underneath, reflecting the influence of reclusive culture. Children's costume mainly consists of short jackets and long pants, made of coarse fabric with simple colors. However, simple patterns are embroidered on the cuffs and collar to add childlike charm. Workers' costume focuses more on practicality. Farmers wear Duanhe (短褐, coarse cloth short clothes) and Kun" (裩, crotch pants),

with hemp as the main material and gray and brown as the main colors, which are convenient for labor; Fishermen wear Shuaiyi (蓑衣, woven straw raincoats) and brown boots, which are waterproof, non slip, and suitable for water operations.

The costume patterns of the Wei, Jin, Southern and Northern Dynasties were characterized by a combination of "realism and romance". In the early days, influenced by the Han Dynasty, mythological symbols such as cloud patterns and dragon and phoenix patterns were often used, but gradually shifted towards depicting real life. [104] Among plant patterns, lotus patterns have become the mainstream, which is closely related to the spread of Buddhism. Lotus is regarded as a sacred flower, and its patterns are presented in a realistic manner with distinct layers of petals. The center is often adorned with a lotus pod, surrounded by ripples of water, forming a lotus water pattern. It is commonly used as a border for women's dresses or men's robes. In animal patterns, auspicious beasts such as Qilin (麒麟) and Tianma (天马) combine with real-life deer and horses to form deformed patterns. For example, deer patterns simplify body contours and highlight corner details, retaining divinity while also being decorative; The Rendong pattern (忍冬纹, a type of curled vine) commonly seen in Northern Dynasty (439-581) tomb murals is formed through continuous arrangement to form geometric patterns, symbolizing endless life and vitality. In geometric patterns, the Lianzhu pattern (联珠纹, continuous arrangement of circles) and the Fangsheng pattern (方胜纹, superposition of two diamonds) are widely popular. The Lianzhu pattern originated in Persia and was introduced to China through the Silk Road. It is often used as a border decoration and filled with dragons, phoenixes, or lotus flowers; The square victory pattern symbolizes good luck and prosperity, and is often used as a border on the collar and cuffs of costume. In addition, influenced by Taoism, the Eight Immortals pattern began to appear, symbolizing immortals with fans, swords and other magical tools, reflecting the pursuit of immortality.

The color system of costume in the Wei, Jin, Southern and Northern Dynasties (220-589) was influenced by the metaphysical concept of "natural inaction (自然无为)" [105], presenting a pattern of coexistence of simplicity and intensity. The literati class of the Southern Dynasty advocated a light aesthetic, with white and cyan as the main colors in their costume [106]. The soft colors reflect the detachment of reclusive culture; Women wear plain silk dresses, with a light and thin outer layer draped in silk, and the overall color tone is as elegant as ink paintings. However, this simple and

elegant style is limited to the upper-class society, and folk costumes still mainly use strong colors, such as red, yellow, purple and other positive colors, which are widely used. Red symbolizes auspiciousness and is often used in wedding costumes; Yellow symbolizes nobility and is often seen in noble robes; Purple, due to its complex dyeing process, has become a symbol of wealth. The costume colors of northern ethnic minorities are more intense. The Xianbei ethnic group loves the combination of red, black, and gold colors. Their robes are often made of black as the base, with red borders and gold embroidery, creating a strong contrast; Women wear crimson robes, with golden ribbons tied to the cuffs and neckline, and Jinbuyao (金步摇, a hair accessory adorned with gold) on their heads, which sway and shine brightly as they walk. Influenced by the Western Regions (西域), cool tones such as blue and green have also entered the costume color system, such as Shiqing Kuzhe (石青袴褶, dark blue short clothes and pants) and Bilv Liangdang (碧绿裲裆, green vest), adding exotic charm to traditional colors. The color grading system gradually loosened at this time. Although the Southern Dynasty still retained the tradition of "Emperor Xuan Yi Xiu Shang (玄衣纁裳)", the colors of official court uniforms were no longer strictly classified according to grades. Purple was used for third grade and above, crimson was used for fifth grade and above, green was used for seventh grade and above, and purple was also allowed to be worn by the common people (previously prohibited colors); The Northern Dynasties were more relaxed, with Xianbei nobles often wearing purple robes, while commoners could also use blue and green, reflecting the color and cultural changes under ethnic integration.

The costume structure of the Wei, Jin, Southern and Northern Dynasties was also mainly based on "cross shaped flat cutting".[74] The large sleeved shirts worn by Southern Dynasty scholars still adopted flat cutting, but by enlarging the cuffs and extending the length of the clothes', exaggerated contours were formed, and the sleeves looked like clouds when walking, reflecting the elegance of the Wei and Jin dynasties; Women's Hushan (縠衫, Crepe thin shirt) are designed with a semi-transparent design, with light gauze on the outer layer and solid silk on the inner layer. The layering is achieved through fabric layering, and the translucent nature of the yarn is used to subtly display the inner layer pattern, creating a visual effect of virtual and real coexistence. The costume structure of northern ethnic minorities places more emphasis on practicality. The Kuxi (袴褶) of the Xianbei ethnic group is cut and sewn in the form

of a " Top and bottoms", with a clear boundary between the body and the sleeves, tight and narrow cuffs, and a "bound pants" (缚裤, tightly tied pants legs) as the lower garment. The outer cover is a Liangdang Armor (裲裆铠, two pieces of armor at the front and back, connected by straps at the shoulders), which is both convenient for riding and shooting and has protective functions; The left lapel robe worn by women is designed with a Quekua (缺胯, side slit) for easy horseback riding, and colored ribbons are used to border the slit to enhance decoration.

Based on the analysis of costume styles, textile patterns, sewing patterns, and colors in the Wei, Jin, Southern, and Northern Dynasties, combined with the digital and intelligent restoration methods for styles, patterns, structures, and colors mentioned in Chapter 345, the overall digital restoration of costume in the Wei, Jin, Southern, and Northern Dynasties was carried out. The restoration effect is shown in Figure 6-4. For more restored costumes from the Wei, Jin, Southern and Northern Dynasties, please refer to Appendix 5.

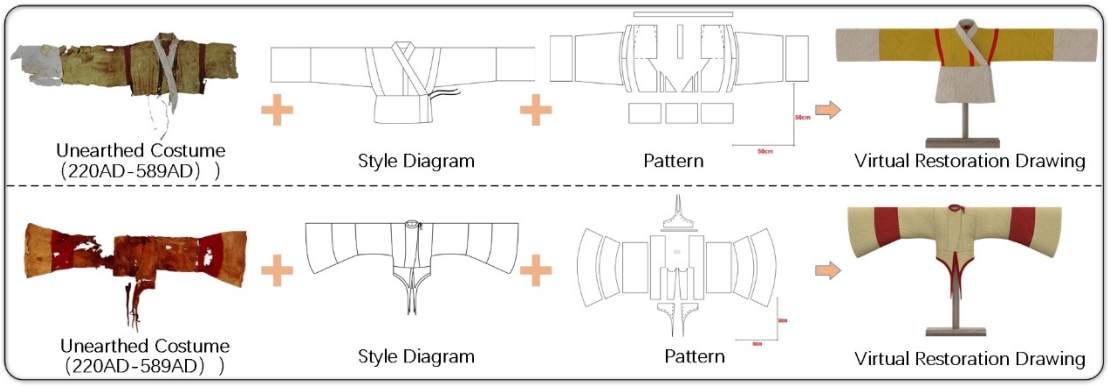

Figure 6-4 Overall digital restoration of costumes from the Wei, Jin, Southern and Northern Dynasties

(4) Analysis and overall restoration of Tang Dynasty costume styles, textile patterns, sewing patterns, and colors

The costume styles of the Tang Dynasty (618-907) were centered around "openness, inclusiveness, beauty, and complexity", blending traditional Central Plains, Western Hu style, and exotic elements to form a unique Tang style. [46] Among women's costume, the Ruqun (襦裙) is the most representative style, consisting of short Ru (襦, A waist length or shorter top), long skirt, and draped silk. The short Ru is a narrow sleeved top with a cross neckline or a pair of lapels, with a length that reaches the waist and highlights the slender waist; The long skirt is made of multiple pieces of plain silk

spliced together, with the waist raised to the armpits, forming a unique shape of high waist covering the breasts, which not only shows a slender figure, but also has a sexy charm; The outer cover is made of light gauze and a long scarf, usually over two meters long, wrapped around the shoulders and arms. When walking, it flutters with the wind, like a fairy descending to earth. Noble women also popular long-sleeved shirts, with wide cuffs like a fan, length reaching the ground, and wearing a Ruqun with a semi-transparent light gauze cover. The overall design is elegant and luxurious, reflecting the grandeur and confidence of the prosperous Tang Dynasty. [107] Men's costume is mainly round necked robes, characterized by round collars, narrow sleeves, and a right lapel. The length of the garment reaches below the knee, and the front is fixed with a loop. Tight pants and black boots are worn underneath, combining practicality and etiquette. Round necked robes and shirts originated from northern nomadic tribes and were improved by the Tang Dynasty to become official and common attire. Officials of different grades were classified by color and pattern. In addition, the Tang Dynasty also popular the Split-side robe (缺胯袍), which had side slits sewn up to the knees for easy horseback riding. It was often worn by military commanders and Hu merchants, reflecting the martial spirit and prosperous commerce of Tang society. Children's costume is characterized by "overalls" and "dresses", with buttons on the front of the overalls and loose legs for easy movement; Dresses often use bright colors and simple patterns, such as red embroidery and green pointillism, full of childlike charm.

The Tang Dynasty costume patterns are characterized by realistic and vivid, with rich symbolism, integrating traditional patterns from the Central Plains, Hu style from the Western Regions, and Buddhist art, forming a unique Tang Dynasty pattern system. [104] In plant patterns, peony patterns have become the mainstream, with clear layers of petals and full shapes, often presented in a realistic way. For example, the Chanzhi Mudan Pattern (缠枝牡丹纹, Peonies and tangled vines form a continuous pattern) uses vines to wrap around flowers, forming a continuous pattern, symbolizing wealth and prosperity; The lotus flower pattern was widely used due to the prevalence of Buddhism, and its shape gradually shifted from early realism to abstraction. For example, the "Baoxiang Pattern (宝相花纹)" integrates the characteristics of lotus flowers, peonies, pomegranates and other flowers to form symmetrical geometric patterns, symbolizing holiness and auspiciousness. In animal patterns, the animal images within the bead pattern are the most distinctive, such as the Lianzhu Duiniao Pattern (联珠对鸟纹)

which features a circular bead as the border and depicts two symmetrical birds inside. The birds are adorned with pearl patterns and surrounded by curly grass patterns, reflecting the influence of Persian art; Dragon and phoenix patterns retain traditional divinity, but their shapes are more vivid. For example, the "Tenglong pattern" showcases dynamic beauty through exaggerated dragon claws and fluttering dragon whiskers; The "Xiangfeng Pattern" embodies an elegant temperament with a slender phoenix neck and stretched tail feathers. In addition, the Tang Dynasty also popularized "hunting patterns (狩猎纹)" depicting scenes of knights riding horses, shooting arrows, and chasing wild beasts, reflecting the martial spirit of Tang society. In geometric patterns, Fangsheng Patterns (方胜纹), Ruyi patterns (如意纹), and Hui Patterns (回纹纹) are widely used. The Fangsheng pattern (方胜纹) is composed of two diamond shapes stacked together, symbolizing "good luck and good fortune"; The Ruyi pattern is transformed into cloud patterns, symbolizing "everything goes smoothly"; The circular pattern is formed by continuous "S" - shaped lines, symbolizing "endless life and vitality".

The color system of Tang Dynasty costume is centered around "intense and bright colors, strict hierarchy", inheriting the traditional hierarchy of "five colors" (cyan, red, yellow, white, black) and absorbing dyeing techniques from the Western Regions and South Asia, forming a unique Tang Dynasty color aesthetics. According to The Old Tang History: Treatise on Ceremonial Garments and Carriages (《旧唐书·舆服志》), the colors of official costume in the Tang Dynasty were strictly classified according to rank: purple was worn for third grade and above, red was worn for fifth grade and above, green was worn for seventh grade and above, and blue was worn for ninth grade and above. Ordinary people could only wear white or gray. Purple has become the symbol of the highest level due to its complex dyeing process (requiring multiple cross dyeing with purple grass); Red symbolizes auspiciousness and is commonly used in wedding attire; Yellow was gradually banned from civilian use due to its association with imperial power (emperors often wore bright yellow dragon robes). Women's costume is more colorful and diverse. Noble women often wear red skirts and blue shirts or blue skirts and purple coats to showcase their beauty through strong contrast; Folk women prefer "intermediate colored skirts", which are skirts made by alternating two or more colors, such as red and green dresses, yellow and purple dresses, etc., reflecting the openness and inclusiveness of Tang society. In addition, the Tang Dynasty also popular

half arm (short sleeved top) [108], which often contrasts with the lower skirt in color, such as moon white half arm paired with crimson skirt, stone blue half arm paired with emerald green skirt, etc., enhancing the sense of layering.

The costume structure of the Tang Dynasty was also mainly based on traditional "cross shaped flat cutting".[74] The structure of women's dress is the most representative [107]: the short dress adopts a design of short front and long back, with the front length reaching the waist and the back extending to the hips, forming a swallowtail shaped hem that swings back and forth when walking, adding dynamic beauty; The high waisted long skirt is made of multiple pieces of plain silk spliced together, with the waist raised to the armpits and tied tightly with ribbons, highlighting the slender figure and allowing the skirt to naturally sag to form an "A" - shaped contour, reflecting the Tang Dynasty's aesthetic pursuit of women's bodies. The structure of men's round neck robes focuses more on practicality and etiquette [81]. The body of the garment is made of four pieces spliced together, with the front placket fixed with a loop, and the cuffs are tight and narrow for easy movement; The hem is slit to the knees on both sides, with long pants on the inside and black boots on the outside to meet the needs of riding and shooting. The round necked robes of aristocratic men are often adorned with Pibo (披膊, similar to shoulder decorations) on the shoulders, embroidered with gold thread patterns to enhance their three-dimensional sense; The waist strap is a combination of a Dadai (大带, wide ribbon) and a Kua (銙, jade or metal piece), which not only fixes the collar but also highlights the identity.

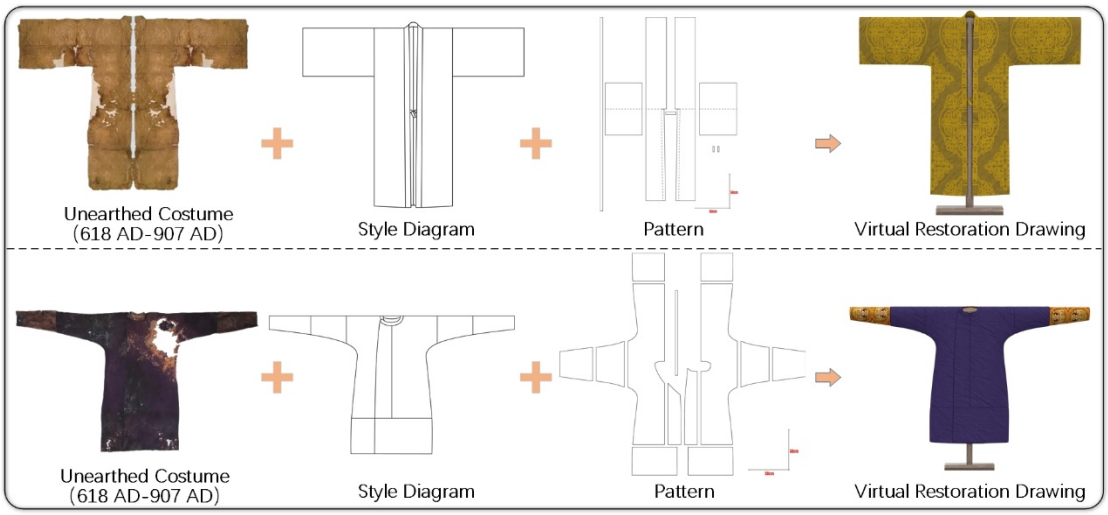

6-5 The overall digital restoration of Tang Dynasty costume

Based on the analysis of Tang Dynasty costume styles, textile patterns, sewing patterns, and colors, combined with the digital and intelligent restoration methods for styles, patterns, structures, and colors mentioned in Chapter 345, the overall digital restoration of Tang Dynasty costume was carried out, and the restoration effect is shown in Figure 6-5. More restored Tang Dynasty costumes can be found in Appendix 5.

⑸ Analysis and overall restoration of costume styles, textile patterns, sewing patterns, and colors in the Song Dynasty

The costume styles of the Song Dynasty (960-1279) were centered around "simplicity, subtlety, and practicality", inheriting the open style of the Tang Dynasty and tending towards introversion due to the rise of Cheng Zhu Neo Confucianism, forming a unique Song style. Among women's costume, the top of the skirt has become the most representative style, characterized by a pair of open collars, straight collars, long sleeves, knee or ankle length, slits on both sides to the waist, and a strapless and long skirt underneath. [109] Beizi (褙子, a loose-fitting outer garment, was popular among women in the Song and Ming dynasties) is mostly made of plain silk or cotton fabric, without excessive decoration. When walking, the clothes sway gently with the wind, which not only shows elegance and grace, but also facilitates activities, becoming a common costume for women's daily travel and home in the Song Dynasty. Noble women would wear a big sleeved shirt over their waistcoat, with wide cuffs like a fan, a length that dragged down the floor, and mostly made of brocade embroidered with exquisite patterns, reflecting their noble status; Civilian women, on the other hand, often wear narrow sleeves and tight cuffs, which are more suitable for labor. Men's costume mainly consists of round necked robes and camisoles. The round neck robe inherits the Tang Dynasty style, but the cuffs and hem are narrower, making the overall shape more slender, reflecting the aesthetic pursuit of "slim and long beauty" in the Song Dynasty; Its color and pattern are strictly classified according to grade. For example, officials often wear purple, crimson, and green to distinguish grades, while civilians can only wear white or cyan. Shirts are exclusive costume for students and scholars, with a round neck, large sleeves, and a Henglan (横襕, a horizontal decorative strip) at the hem, symbolizing "Never forget one's roots". The material is mostly plain linen or cotton, reflecting the elegant temperament of Song Dynasty literati.

The costume patterns of the Song Dynasty are characterized by "freehand nature, auspicious symbolism" [110], inheriting the realistic tradition of the Tang Dynasty and tending towards abstraction and poetry due to the rise of literati painting, forming a unique aesthetic of Song Dynasty patterns [104]. Among plant patterns, plum blossom pattern has become the mainstream, with a simple shape mainly consisting of five petal flowers, often presented in a "Shu Yin Heng Xie (疏影横斜, The slender branches cast delicate shadows on the tranquil stream)" posture, symbolizing noble character; The lotus flower pattern continues under the influence of Buddhism, but its shape is more freehand, such as the Emerging Lotus (出水莲花纹) which outlines the petals and lotus pods through simple lines, reflecting the artistic conception of mud and non staining. The "Three Friends of Winter (岁寒三友)" pattern (pine, bamboo, plum) popular in the Song Dynasty combines three plants into a pattern, symbolizing resilience and integrity. Among animal patterns, crane patterns and deer patterns are the most representative. Crane patterns often appear in the form of "cloud crane patterns". The crane has a slender body, spreads its wings and flies high, surrounded by cloud patterns, symbolizing longevity and auspiciousness; The deer pattern is often combined with the pine tree pattern to form the Songlu Tongchun (松鹿同春) pattern, symbolizing good fortune and longevity. The carp pattern popular in the Song Dynasty has a rounded shape and a wavy pattern on the fish body, symbolizing the auspicious meaning of carp leaping over the dragon gate. Textual patterns were also common in Song Dynasty costume, such as single character patterns like Fu (福), shou (寿), and 卍, or auspicious phrases like "long life and wealth" and "a hundred sons and a thousand grandchildren". They were often embroidered or printed on the collar, cuffs, and other parts of costume, reflecting the people's yearning for a better life. The popular Bogu Pattern (博古纹) refers to patterns designed based on ancient bronze and jade artifacts, such as Ding (鼎) patterns, Jue (爵) patterns, Yubi (玉璧) patterns, etc., symbolizing the literati's interest in respecting the ancient and valuing the virtuous.

The color system of Song Dynasty costume is centered around freshness, elegance, and orderly hierarchy, inheriting the Tang Dynasty's five color grading system and tending towards simplicity and elegance due to the influence of Neo Confucianism, forming a unique Song Dynasty color aesthetics. Compared with the Tang Dynasty, the purple color in the Song Dynasty was more inclined towards Jiangzi (绛紫, deep red

with purple), the Feise (绯色) was more inclined towards Zhuhong (朱红, bright red) [111], and the green color was more inclined towards Ailv (艾绿, light green), making the overall tone more stable. Women's costume has a richer and more diverse range of colors, but overall tends to be more elegant. Noble women often wear pale pink skirts paired with moon white skirts, light blue skirts paired with goose yellow skirts, etc., showcasing a gentle temperament through low saturation color combinations. In the Song Dynasty, the technique of Yinjin Caihui (印金彩绘) was also popular, which involved using gold powder to draw patterns on plain silk, such as printing gold plum patterned jackets, painting lotus patterned large sleeved shirts, etc., to make costume shine in the sunlight and add a luxurious temperament. The advancement of dyeing technology has also driven color innovation. The Song Dynasty invented the Yaoban Bu (药斑布, blue printed flower cloth) [112], which uses indigo dye and anti dye to print patterns on cotton cloth, forming a blue and white alternating color effect, such as blue and white plum patterned skirts, blue and white fish patterned skirts, etc. Its colors are fresh, the patterns are simple, and it is deeply loved by the people.

The costume structure of the Song Dynasty was also mainly based on "cross shaped flat cutting". [74] The structure of women's costume is the most representative: the body of the garment is made up of four pieces spliced together, with the front placket open and fixed with loops or ribbons; The cuffs gradually narrowed from wide sleeves in the Tang Dynasty to narrow sleeves, which were more suitable for daily activities; The slit on both sides extends to the waist, with a strapless and long skirt underneath. When walking, the hem of the garment sways gently in the wind, showing both elegance and ease of movement. Noble women often wear silk (light gauze long scarves) around their shoulders and arms, forming flowing lines; The waist strap is composed of wide ribbons and jade ornaments, which not only fix the collar but also add a luxurious temperament. The structure of men's round neck robes focuses more on being slender and straight. The body of the garment is made of four pieces of front and back splicing, with a round collar at the front and secured with a loop. The round necked robes of aristocratic men are often adorned with Puzi (补子, square embroidery patches) on the shoulders, embroidered with gold thread to create animal patterns such as crane Puzi and Qilin (麒麟) Puzi, symbolizing their rank. The advancement of textile technology has also driven structural innovation.

Based on the analysis of the styles, patterns, structures, and colors of Song Dynasty costume, combined with the digital and intelligent restoration methods for styles, patterns, structures, and colors mentioned in Chapter 345, the overall digital restoration of Song Dynasty costume was carried out, and the restoration effect is shown in Figure 6-6. More restored Song Dynasty costumes can be found in Appendix 5.

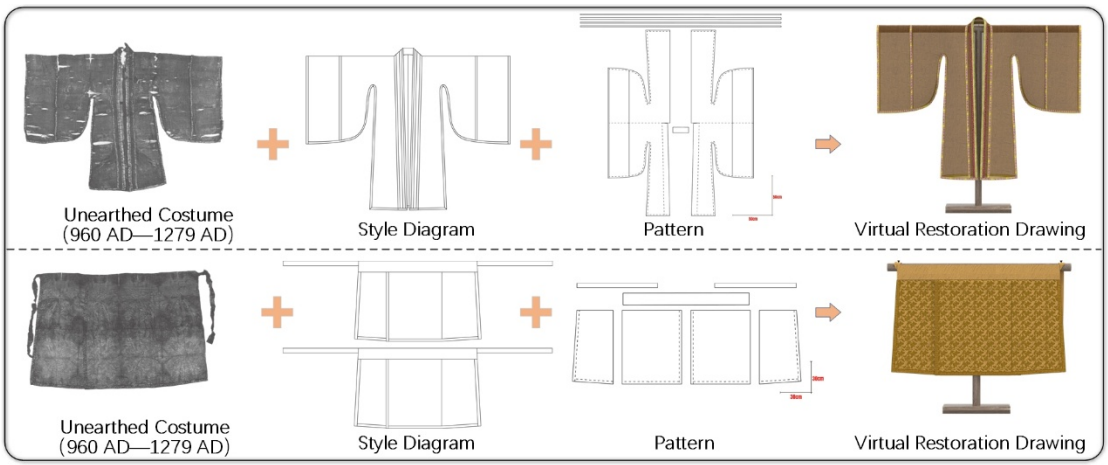

Figure 6-6 Complete digital restoration of Song Dynasty costumes

(6) Analysis and overall restoration of costume styles, textile patterns, sewing patterns, and colors in the Yuan Dynasty

The costume of the Yuan Dynasty (1271-1368) showed distinct ethnic fusion characteristics in terms of style, retaining the traditional nomadic costume styles of the Mongolian people [113] and absorbing the wide robe and large sleeve shape of the Han people, forming a unique costume system. Mongolian noble men and women mainly wear narrow sleeved long robes, which are usually cross collared and have a right lapel. The cuffs are tight, and the body is long, making it easy to ride, shoot, and keep warm. Men often wear Bianxian Ao (辫线袄), which are characterized by dense pleats at the waist and are fixed by horizontal stitching with red and purple threads, making the clothes tightly attached to the body, highlighting the figure and facilitating movement. The Bianxian Ao was originally a special attire for the emperor, and later became a formal dress for banquets of officials, with uniform colors to highlight rank. Han Chinese women still wear long skirts, which are short tops paired with long skirts, with narrow cuffs and a delicate style. Influenced by Mongolian costume, some Han Chinese women also began to wear long robes with left lapels and narrow sleeves, with a large waistband, which is more suitable for the cold climate in the north. Noble women wear a Gugu Guan (罟罟冠), which is tall and ornate, often adorned with jewels. When

walking, they need maidservants to support the corners of their robes, showing their nobility. In the Yuan Dynasty, Bijian (比肩, leather jacket) and Bijia (比甲, sleeveless vest) were also popular. The former was a commonly used leather jacket by Mongolians, while the latter was a lightweight costume for riding and shooting. The official attire of the Yuan Dynasty basically followed the traditions of the Han ethnic group, such as coronation attire, court attire, and official attire, but was simplified. Officials often wear long robes with narrow sleeves, differentiated by color and pattern. Ordinary people wear short clothes, raincoats, or coarse cloth robes, with dark colors as the main color, and are not allowed to overstep their bounds. Overall, the costume styles of the Yuan Dynasty not only reflected the practicality of nomadic peoples, but also integrated the etiquette system of the Han ethnic group, forming a diverse and coexisting costume styles.

The patterns of Yuan Dynasty costume blend the nomadic culture of the Mongolian people with the traditional patterns of the Han ethnic group in the Central Plains, showcasing both the bold style of the grassland people and the exquisite craftsmanship of the Han region. [104] Mongolian nobles often use patterns symbolizing power such as the sun, moon, dragon, and phoenix in their costume, especially dragon patterns, which are often embroidered with gold thread to showcase the majesty of imperial power. [114] The costume of ordinary officials and nobles is adorned with flowers, rolled grass, geometric patterns, etc. Among them, entwined lotus, peony, and cloud patterns are more common, symbolizing auspiciousness and wealth. [114] Mongolians worship nature, so animal patterns such as eagles, deer, wolves, etc. are commonly seen in costume patterns, symbolizing bravery and strength. [114] In addition, geometric patterns such as scroll patterns and loop patterns are widely used on robes, belts, and hats, serving both decorative purposes and enhancing the layering of costume. The weaving technique of gold brocade by the aristocrats of the Yuan Dynasty was extremely exquisite, often embroidered with intricate patterns of gold thread, making the costume shine brightly in the sunlight. Traditional patterns of the Han ethnic group, such as cloud patterns, bat patterns (symbolizing good fortune), and lotus patterns (symbolizing purity), were also preserved in the costume of the Yuan Dynasty, but were mostly used for civilian or Han official attire. The embroidery craftsmanship of the Yuan Dynasty was advanced, and aristocratic costume was often decorated with techniques such as flat embroidery, plate gold embroidery, and nail

thread embroidery, making the patterns more three-dimensional and vivid. Overall, the costume patterns of the Yuan Dynasty not only reflected the wild beauty of the grassland ethnic group, but also integrated the elegant style of Central Plains culture, forming a unique decorative art.

The color system of costume in the Yuan Dynasty strictly followed the social hierarchy system, with different colors representing different social status and forming distinct class distinctions. Mongolian nobles prefer bright colors such as gold, blue, and red [115], among which gold symbolizes nobility and is often used in the costume of emperors and nobles, such as weaving gold brocade, gold thread embroidery, etc., making the clothes shine brightly in the sunlight. Blue represents eternity and loyalty in Mongolian culture, and is the main color commonly worn by men, especially the deep blue Mongolian robe, symbolizing strength and courage. Red symbolizes power and celebration, and is often used for imperial dragon robes and noble dresses. The colors of ordinary people's costume are strictly restricted, and bright colors such as ochre, red and white glitter, rouge, etc. are not allowed to be used. According to the laws of the Yuan Dynasty [116], civilians were only allowed to wear plain or dark colored costume such as brown, gray, deep blue, etc., and were not allowed to use gold threads or jewelry for decoration. The colors of officials' costume are classified according to their grades, such as wearing purple robes for grades one to five, red robes for grades six to seven, and green robes for grades eight to nine, and embroidered with patterns of different sizes to distinguish them. [116] During the Yuan Dynasty, brown costume was also popular, such as silver brown, tea brown, and clove brown. These colors not only met the aesthetic preferences of nomadic peoples, but also became the main choice for commoners due to legal restrictions. Overall, the color system of costume in the Yuan Dynasty not only reflected the primitive beliefs and aesthetic preferences of the Mongolian people, but also strengthened social order through a strict hierarchical system, making color a symbol of identity.

The structural design of Yuan Dynasty costumes took into account the practicality of nomadic peoples and the standardization of Central Plains etiquette, forming a unique cutting method. [74] Mongolian robes are usually cross collared with a right lapel, narrow cuffs, loose fit, and dense pleats at the waist, making them convenient for horseback riding and archery, as well as highlighting the figure through the waistband. The collar styles of aristocratic costume are diverse, including square collar, round collar, and cross collar. Some robes adopt a double breasted design for easy mobility.

The official attire of the Yuan Dynasty had a rigorous structure, stretching down to the knees, with pleats at the waist and fixed with red and purple threads to keep the costume tightly attached to the body, making it easy to ride and shoot. The structure of the emperor's coronation is complex, including a crown, dragon robe, lower garment, and middle garment. The crown is decorated with pearls and cloud dragon patterns, while the lower garment is embroidered with patterns such as seaweed and pink rice, symbolizing the order of heaven and earth. Han women still tend to wear cross collared jackets with narrow cuffs and loose hemlines, while the left collared robes influenced by Mongolia have a large waistband and are more practical. The fabrics and decorations of Yuan Dynasty costume also reflect structural characteristics, with nobles often weaving gold brocade, silk, and fur, while commoners wear linen and cotton cloth. The hat structures are diverse, such as the Boli Hat (钹笠帽, a type of broad-rimmed hat worn by monks) and Gugu Guan (罟罟冠, a tall, elaborate headdress worn by Mongol noblewomen during the Yuan Dynasty), and the Han official's Zhanjiao Futou (展角幞头, official's black gauze cap with wing-like flaps), all of which are coordinated with the costume styles. Overall, the costume structure of the Yuan Dynasty not only adapted to the needs of nomadic life, but also integrated into the etiquette system of the Central Plains, forming a costume system that combines functionality and aesthetics.

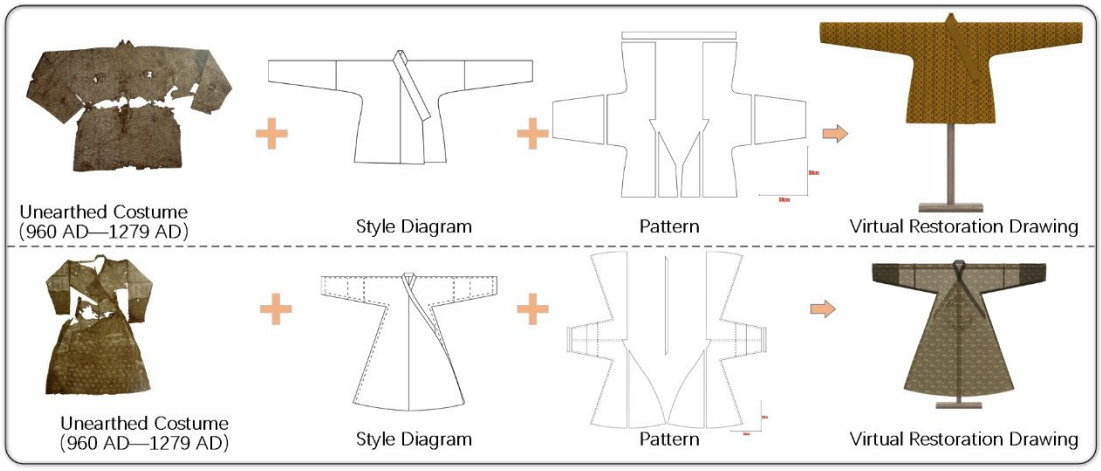

Figure 6-7 The overall digital restoration of Yuan Dynasty costume

Based on the analysis of the styles, patterns, structures, and colors of Yuan Dynasty costume, combined with the digital and intelligent restoration methods of styles, patterns, structures, and colors mentioned in Chapter 345, the overall digital restoration of Yuan Dynasty costume was carried out, and the restoration effect is

shown in Figure 6-7. More restored Yuan Dynasty costumes can be found in Appendix 5.

⑺ Analysis and overall restoration of Ming Dynasty costume styles, textile patterns, sewing patterns, and colors

The style system of costume in the Ming Dynasty (1368-1644) was rigorous and clearly graded, fully reflecting the political philosophy and ritual norms of restoring China. Men's costume mainly consists of robes, among which the most representative are Taoist Robes (道袍) and Straight-Cut Robe (直身). The Taoist robe is not worn by Taoists, but rather by the literati class as a daily outer garment. Its characteristics include a crossed collar with a right lapel, wide sleeves, and inner hem (also known as a hidden hem) on both sides of the garment. When walking, the robe floats and appears dignified and elegant. Straight-Cut Robe is more formal, mostly for officials and literati, with a shape similar to that of a Taoist robe, but without an inner hem, and a length up to the feet, often with a large waistband around the waist. The core style of women's costume is the Aoqun (袄裙), with a cross collar or standing collar jacket on the upper body and a Horse-face Skirt (马面裙) on the lower body. The change in collar shape of the jacket reflects the aesthetic of the times: in the early Ming Dynasty, many collars were inherited from the transition between the Song and Yuan Dynasties, and in the middle and late periods, standing collars gradually became popular. The collar was decorated with metal buckles, known as mother and child buckles, showcasing the progress of craftsmanship and the evolution of fashion. The Horse-face Skir is a model of Ming Dynasty women's skirts, with four overlapping skirt doors at the front and back. The skirt body is often pleated, and the skirt doors open and close during movement, creating a dynamic and beautiful look. The formal attire of a married woman follows the shape of the Tang and Song dynasties, such as the combination of Xiapi and Zhai Yi. Xiapi is a belt shaped ornament worn on the shoulders, embroidered with bird patterns, while Zhai Yi is dark blue, embroidered with Zhai bird patterns, with complex layers, highlighting noble status. Common people's costume is simple and practical, such as men wearing short clothes and pants, and women wearing narrow sleeved shirts and simple pleated skirts, which meet the needs of labor. On the basis of inheriting the traditions of the Han and Tang dynasties, the costume styles of the Ming Dynasty integrated practicality and artistry, forming a unique style that is dignified, implicit, and rich in layers.

The patterns of Ming Dynasty costume are known for their auspicious meanings and rigorous composition, reflecting the deep integration of Confucian culture and social hierarchy. [104] The pattern themes are diverse, mainly including animals, plants, geometry, and religious symbols. Dragon patterns are exclusive to the royal family, with the five clawed dragon symbolizing the supreme authority of the emperor, and the python pattern (four clawed dragon) used for princes and important officials. The patterns are often accompanied by cloud patterns and sea water river cliff patterns, forming the majestic atmosphere of the " Cloud Dragon Spanning the Four Seas (云龙四海)". In the pattern of birds, the phoenix is used by the empress, with civil officials' Mandarin Square (补子) embroidering birds and military officials' Mandarin Square embroidering auspicious beasts. The official ranks are strictly distinguished through the system of Mandarin Square Costume (补服). The most popular plant patterns are entwined flowers, such as entwined lotus and entwined peony, which symbolize continuity, wealth, and prosperity. Their compositions often use S-shaped branches and vines as bones, with dense flowers and leaves, symmetrical and balanced, reflecting the delicacy and sense of order of Ming Dynasty decorative art. Folk patterns emphasize auspicious meanings, such as the "Eight Treasures Pattern (八宝纹)" symbolizing auspiciousness and the "Hundred Sons Picture (百子图)" symbolizing many children and blessings. These patterns are often completed using embroidery, silk weaving, or gold weaving techniques, with bright colors and rich details. Religious patterns such as the Eight Auspicious Symbols (Buddhist symbols) and the Eight Trigrams are also common in costume, incorporating diverse cultural influences. The application of patterns not only focuses on aesthetics, but also emphasizes the importance of patterns carrying messages, conveying ethical concepts and social identity through patterns, making Ming Dynasty costume a symbol of ritual worn on the body.

The color system of Ming Dynasty costume was deeply influenced by the Five Elements ideology and the hierarchical system. Color selection not only emphasized symbolic meaning, but also pursued artistic harmony. The official color hierarchy is strict: yellow is monopolized by the royal family, especially bright yellow, which can only be used by the emperor and empress; Red symbolizes auspiciousness and authority, often used in official dresses and wedding attire; Blue and blue are common colors for literati, such as blue shirt and blue robe representing the identity of literati; White and black are mostly mourning clothes or costume for the lower class people. The advanced

dye technology has resulted in high color saturation, such as magenta, vermilion, and carmine in the red series, indigo and navy blue in the blue series, and willow green and dark green in the green series, all extracted from plants or minerals, resulting in natural and long-lasting colors. Women's costume is rich in colors and breaks through the constraints of etiquette. For example, the horse faced skirt commonly uses the "intermediate color" technique, where different colored cloth strips are spliced together to form a gradient or contrasting effect, known as the Yuehua skirt or Fengwei skirt. Color matching emphasizes the "harmony of the five elements", such as the clever use of contrasting colors such as red with green, blue with gold, etc., which are enhanced by embroidery edging or gold weaving to avoid vulgarity and instead appear gorgeous and steady. Although folk costume is limited, it still innovates within its scope, such as dyeing pink with madder and jujube red with sapphires, forming a soft middle tone. Overall, the colors of the Ming Dynasty were both solemn and vivid, demonstrating a high level of aesthetic achievement within the framework of the ritual system.

The structural design of Ming Dynasty costume combines practicality and etiquette, with exquisite cutting techniques that emphasize the harmonious unity of the human body and costume materials. [117] Robe structures are mostly cut in a cross shaped flat pattern, with the body and sleeves cut together to maintain the integrity of the fabric, in line with the philosophical concept of "harmony between man and nature". [74] Both the Taoist robe and the Straight-Cut Robe are designed with a Tongxiuchang (通袖长, A style with sleeves longer than usual, extending to the wrist or fingers) , with sleeves that can be over two feet wide. The cuffs are narrowed to form a Pipa Sleeve (琵琶袖),also known as a Hu sleeve (胡袖), which can hold items and has both beauty and functionality. There are seams on both sides of the garment, symbolizing the doctrine of the mean. The front and back panels are mostly made of whole fabric, with only small patches (called inserts or swings) spliced under the armpits to increase mobility. The structure of women's jackets is more fitted, and the stand up collar design needs to be cut and spliced separately. The collar buckle is precisely aligned, demonstrating superb sewing skills. The structure of the horse faced skirt is particularly clever [118, 119]: it is composed of two pieces of wide woven brocade spliced together, each piece forming two skirt doors at the front and back. The overlapping parts cover the shame, and the non overlapping parts are pleated. The waist of the skirt is mostly made of white cotton cloth and fixed with straps. This structure not only saves fabric,

but also ensures that the skirt door unfolds vertically when walking. The formal dress, such as Zhai Yi, adopts a multi-layered structure, with layers of underwear, undershirt, and outerwear worn together. The cuffs and collar reveal different colors, forming a rich visual hierarchy. The filling technique is also used for winter costume, such as the cotton lining inside Bijia (比甲, sleeveless camisole), which keeps warm without appearing bulky. Although the structural design of the Ming Dynasty did not have three-dimensional cutting such as provincial roads, it achieved a suitable wearing experience for both movement and stillness through fabric splicing, lace adjustment, and detail processing, reflecting the high wisdom of ancient Chinese costume.

Based on the analysis of Ming Dynasty costume styles, textile patterns, sewing patterns, and colors, combined with the digital and intelligent restoration methods for styles, patterns, structures, and colors mentioned in Chapter 345, the overall digital restoration of Ming Dynasty costume was carried out, and the restoration effect is shown in Figure 6-8. More restored Ming Dynasty costumes can be found in Appendix 5.

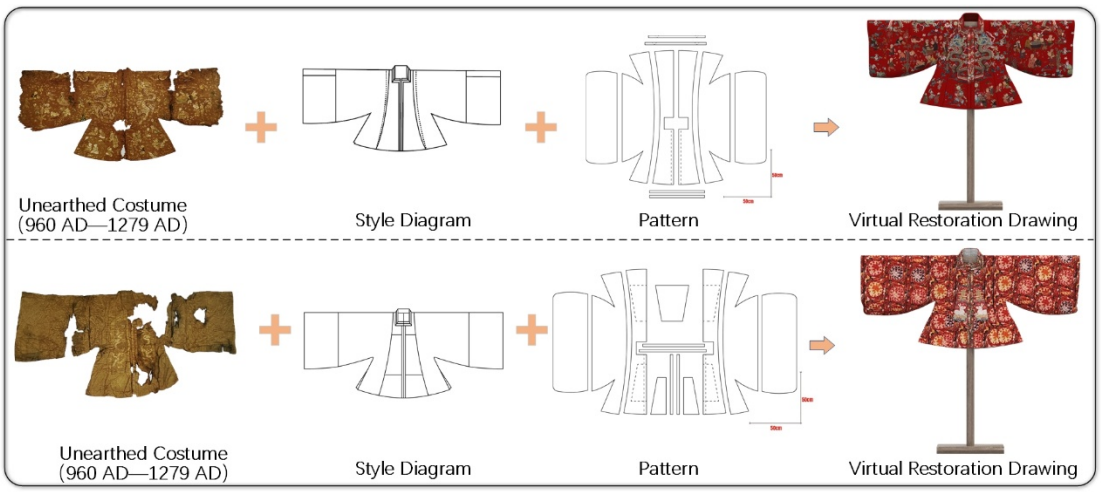

Figure 6-8 The overall digital restoration of Ming Dynasty costumes

(8) Analysis and overall restoration of Qing Dynasty costume styles, textile patterns, sewing patterns, and colors

The evolution of costume styles during the Qing Dynasty (1616-1911) deeply reflected the integration of Manchu and Han cultures and practical functional orientation. [120] Men's costume is centered around long robes and jackets, with typical features including standing collars, narrow sleeves, horseshoe sleeves (arrow sleeves), and four slit designs. Arrow sleeves, resembling horse hooves, are not only convenient for

rolling up sleeves during riding and shooting, but also become a signature element of Manchu costume; The four slit long robe is exclusive to the royal family and nobles, making it easy to ride horses, while commoners wear a Yiguoyuan (一裹圆) robe with or without slits on both sides. As a travel uniform, the Magua (马褂, a short traditional Chinese jacket worn over a robe) is no longer than the knee and has wide and short sleeves. It is made of plain colors such as stone green and black, and is layered with the long robe. Women's costume is mainly flag shaped, with a rectangular outline and a saddle shaped standing collar to cover the cheeks and face. The right lapel of the side lapel is decorated with a button, and the body is not tied to the waist. The hem is decorated with horseshoe sleeves or wide edges. At the beginning, the flag dress was wide and straight, gradually narrowing into a straight tube shape, covered with a camisole or a coat, retaining the sharpness of nomadic people while incorporating Han aesthetics. In the early Qing Dynasty, Han women still wore Ming Dynasty small sleeved and long skirts. After Qianlong, influenced by the Manchu people, the sleeves gradually widened and cloud shoulders were added. In the late Qing Dynasty, they even abandoned skirts and pants, and rolled lace on the collar became fashionable. The official dress system of the Qing Dynasty was strict, with long robes and Magua as standard attire for officials. The lack of a front lapel robe (with a one foot gap in the front and bottom hem for easy riding) and a Magua formed the attire for travel, while the emperor's ceremonial and court robes were reinforced with decorations such as dragon patterns and sun and moon chapter patterns to enhance their hierarchical differences.

The pattern system of costume in the Qing Dynasty was complex and precise, inheriting tradition while demonstrating a strict hierarchical system. [121-123] Dragon and python patterns are the core. The emperor's dragon robe is embroidered with nine dragons, five dragons can be seen before and after viewing, symbolizing the Jiu Wu Zhi Zun (九五之尊). The prince uses python robes, with the number and quantity of claws decreasing step by step. The most authoritative one is the "Twelve Chapters Pattern" on the emperor's court uniform, which includes twelve patterns such as the sun, moon, stars, mountains, and dragons, each with its own meaning, such as the sun and moon shining, the mountain indicating stability, and the dragon symbolizing adaptability, highlighting the emperor's virtues. Auspicious patterns are widely used, such as bats symbolizing Fu (福), peaches symbolizing Sou (寿), and Lingzhi

mushroom (芝象) symbolizing immortal longevity, combined to form themes such as fortune, longevity, and good fortune; The Five Venoms (五毒) pattern (snake, scorpion, centipede, toad, gecko) is used to ward off evil and avoid toxins. Influenced by the exchange between China and the West in the mid to late Qing Dynasty, exotic styles such as passion flower patterns and ocean flowers emerged. The pattern craftsmanship is extremely luxurious, with a particular emphasis on silk and gold weaving. The Tong Jing Duan Wei (通经断纬) technique is used to weave brilliant patterns, and there are complex border decorations such as San Xiang San Gun (三镶三滚) and Shi Ba Xiang (十八镶), fully reflecting the cultural characteristics of strict dress etiquette, praying for blessings and auspiciousness, and exquisite skills in the Qing Dynasty [124, 125].

The color system of Qing Dynasty costume is a product of the integration of feudal ritual system and Manchu culture, with the core principle of " Using bright yellow as the exclusive symbol of the highest authority of the emperor, and reflecting the social hierarchy of social classes through strict classification of colors such as purple, red, green, and blue in costume and objects". [126] The Da Qing Hui Dian Tu (《大清会典图》) and Huang Chao Li Qi Tu Shi (《皇朝礼器图示》) clearly record that the emperor exclusively enjoyed bright yellow, with court and auspicious costumes using this as the main color, accompanied by solemn tones such as stone blue and red; Consorts are classified into orange, golden, and fragrant colors according to their rank, while concubines below are classified into autumn fragrance and moon white colors. The colors of official costume are strictly classified according to grade: the first grade uses ruby top beads paired with coral colored court clothes, the second grade uses coral top beads paired with blue, the third grade uses sapphire top beads paired with blue, and up to the ninth grade, only engraved gold top beads paired with gray can be used. This color grading is not only reflected in the main color of the costume, but also permeates into the details of the accessories: the material of the morning pearl is divided into East Pearl (exclusive to the emperor), jade, amber, etc. according to the grade, and the accessories such as the back cloud and commemoration also need to correspond with the top pearl material. The Manchu tradition of valuing white is also reflected in costume, such as the use of white fox fur for warm hats in winter. However, after entering the country, influenced by the Han Chinese concept of "yellow as a virtue", bright yellow gradually became an absolute royal exclusive. Folk costume became more colorful, with Han women preferring high contrast combinations such as red and

green, while flag costume was dominated by soft tones such as blue, pink, and purple. Influenced by the West during the late Qing Dynasty, popular colors such as rose purple and deep crimson were widely used. In terms of color matching, Qing Dynasty costume emphasized complementary color contrast and adjacent color tones, such as red and green with black borders, which not only enhanced visual impact, but also achieved harmony through intermediate color buffering, reflecting the aesthetic pursuit of being bright and decent, complex and not chaotic.

The costume structure of the Qing Dynasty broke through the traditional flat cutting mode, incorporating three-dimensional Han elements while retaining the practicality of nomadic ethnic groups. The men's long robe adopts a "ten piece" cutting method [74]: one front piece and one back piece, four left and four right side pieces, forming a natural sagging feeling through the provincial road. The four slit design is not only convenient for riding and shooting, but also enhances the three-dimensional level by overlapping the fabric at the slit. The horseshoe sleeve has a delicate structure, with a stiff silk outer layer and a soft fur lining inner layer. The folded cuffs form an arrow sleeve, which not only protects the hands but also conforms to the Manchu archery tradition. The women's Qipao (旗袍) [127] is centered around the Lian Shang Zhi (连裳制), with the upper garment connected to the lower garment, and the right lapel fixed with a button. The body of the dress does not take the waist, and the hem is in a straight tube shape. The outer cover is a Kanjian (坎肩) or a Magua, forming an "H" - shaped contour. The internal structure of the flag suit emphasizes functionality: the standing collar is about 5 centimeters high, which can prevent wind and keep warm; The inner lining of the collar is a small garment (bellyband), which not only protects the skin but also facilitates replacement; Sleeves are divided into two types: wide sleeves and narrow sleeves. Wide sleeves can hold handkerchiefs, sachets, and other items, while narrow sleeves are convenient for labor. In terms of decorative structure, Qing Dynasty costume expanded its flat space through the technique of inlaying and rolling [128-130]: the collar, cuffs, and hem of the garment were adorned with multiple layers of lace, including silk, lace, fur, etc. The color contrasts with the main garment, forming a unique aesthetic of "edge embellishment costume".According to the "Comprehensive Study of Qing Literature: Wang Li Seventeen and Eighteen (《清文献通考·王礼十七、十八》)", costume accessories such as court beads, waist belts, collars, etc. also constitute a part of the structure. The court beads are connected by 108

beads, accompanied by pendants such as back clouds and memorials, which serve as counting tools and enhance the level through materials and colors; Belts are divided into yellow, red, stone blue and other colors according to their grades. The emperor's branch uses yellow belts, the branch of uncles and brothers uses red belts, and other officials use stone blue or blue belts, forming a system of "identify the closeness and alienation of the relationship according to the belt color ".

Based on the analysis of Qing Dynasty costume styles, textile patterns, sewing patterns, and colors, combined with the digital and intelligent restoration methods for styles, patterns, structures, and colors mentioned in Chapter 345, the overall digital restoration of Qing Dynasty costume was carried out, and the restoration effect is shown in Figure 6-3. More restored Qing Dynasty costumes can be found in Appendix 5.

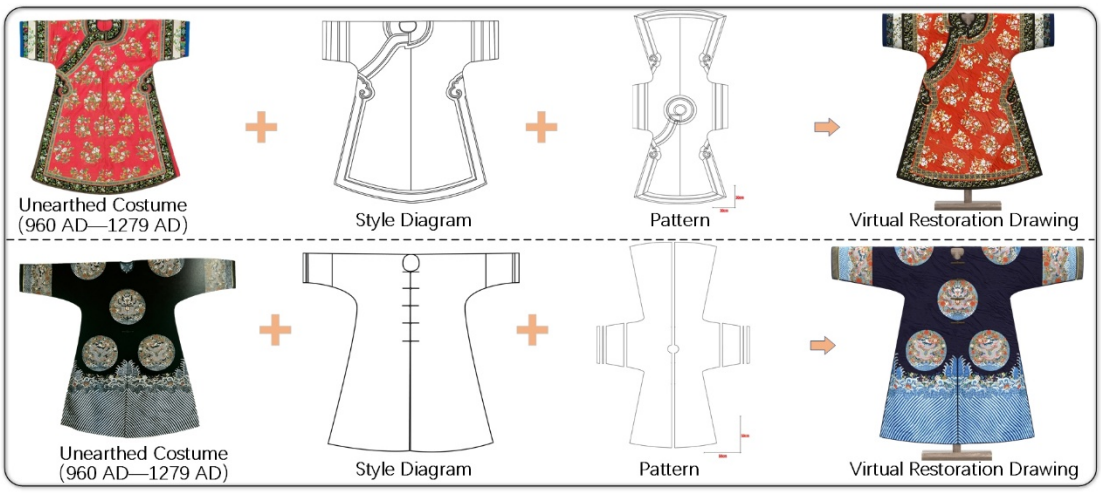

6-9 Complete digital restoration of Qing Dynasty costumes

6.2.2 Construction of a 3D database of ancient Chinese costume

A comprehensive, accurate, and high-fidelity 3D simulation database of ancient Chinese costume is of great significance for the digital protection of costume cultural heritage. The 3D simulation database of ancient Chinese costume is not a simple collection of images or models, but a multimodal, high-precision, and interactive intelligent knowledge system that deeply integrates archaeology, materials science, computer graphics, and artificial intelligence technology. Its core lies in the systematic integration of the three key technologies proposed in this study: the intelligent restoration technology of costume relics styles and patterns based on deep convolutional generative adversarial network (DCGAN), which accurately restores the damaged and blurred fabric patterns and costume shapes caused by the erosion of time;

The color restoration and prediction technology for costume relics based on deep convolutional long short-term time series neural network (DCLSTNet) scientifically infers and reproduces the original saturated color tone of dyes after hundreds of years of degradation in buried environments; And based on Pix2Pix network and boundary constraint algorithm, interactive reverse restoration technology for costume relics structure is developed. Through learning from X-ray scanning data, the three-dimensional costume relics that were stacked and wrinkled at the time of excavation are virtually flattened without damage, and their two-dimensional cutting patterns and three-dimensional vertical structures are accurately generated. These three technologies are interrelated and together form a full process solution from incomplete physical objects to complete digital twins, providing a solid theoretical foundation for the establishment of databases.

A three-dimensional database of ancient Chinese costume was constructed using the technology proposed in This study, as shown in Figure 6-10. The database is based on a five in one architecture of "style pattern color structure material", which systematically integrates typical costume relics data from the Xia, Shang, Ming, and Qing dynasties. It extensively cites costume system records from ancient books, as well as visual images from paintings, murals, and carvings throughout history. Through multiple evidence methods, the information of cultural relics in dimensions such as color, style, structure, and pattern is cross verified and analyzed. In terms of architecture design, the database strictly follows the three principles of "systematization, standardization, and semantics". Vertically based on the historical dynasties of China as the timeline, and horizontally based on typical costume categories such as deep costume, robes, skirts, and patched costume as the classification dimensions, a clear and interwoven classification system is constructed. Each piece of costume digital asset stored in the warehouse covers four logical levels of data organization: the basic layer provides high fidelity 3D models, supports 360 degree rotation and infinite scaling, and can switch multiple visualization modes such as wireframe, material separation, rendering, etc., fully displaying the form of cultural relics; The structural layer is associated with its two-dimensional cutting diagram, sewing process stitching, and pattern data, providing support for researchers to further explore traditional costume production techniques such as ancient "cross shaped flat cutting"; The material layer integrates advanced technologies such as hyperspectral imaging and microscopic photography to obtain information on fabric fiber types, weaving structures, and pattern

units, and is accompanied by color numerical data based on verification restoration; The metadata layer provides detailed records of archaeological and historical background information such as the age of the cultural relics, excavation information, social class, and current location, ensuring the reliability and traceability of data sources.

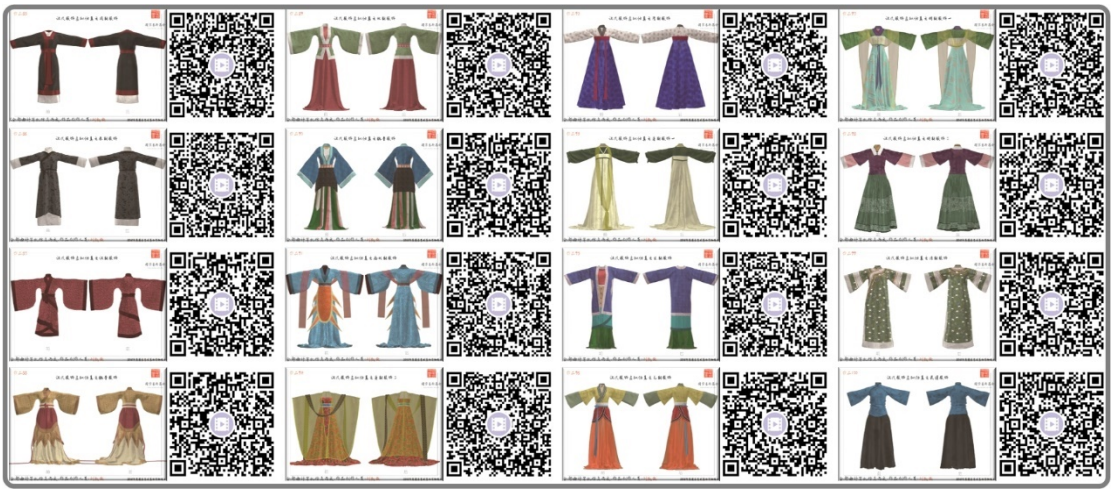

6-10 Example display of 3D database of ancient Chinese costume

6.2.3 Restoration results evaluation

The fuzzy comprehensive evaluation method is an application of fuzzy mathematics founded by American control theory expert L.A. Zadeh. Its core is to acknowledge and quantify this ambiguity, and to answer the question of "to what extent a certain indicator belongs to a certain evaluation level" through membership degree, thereby transforming subjective and vague evaluations into objective and quantitative analysis. The Fuzzy Comprehensive Evaluation Method can effectively handle subjectivity and uncertainty in evaluation, and is particularly suitable for multi factor and multi-level evaluation problems.[66, 131] The evaluation of costume restoration is essentially full of uncertainty and subjective judgment. The restoration of ancient costume is often based on broken cultural relics, vague murals, or brief written records, making it difficult to measure evaluation criteria such as style accuracy and pattern restoration with precise "yes" or "no", and more suitable to describe them with the vague concept of "to what extent they conform". This method quantifies experts' subjective feelings that the restoration results "partially conform" to a certain level by introducing "membership degree", thereby transforming qualitative and fuzzy empirical judgments into systematic quantitative analysis. At the same time, this method can comprehensively weigh the different importance of multiple dimensions such as style, pattern, color, and

structure, and ultimately provide a scientific evaluation result that can reflect both the overall level and the quality of each detail restoration, which is in line with the complex characteristics of interdisciplinary, multi criteria, and incomplete information processing in ancient clothing restoration research. Therefore, this PhD study chooses the fuzzy comprehensive evaluation method to evaluate the restored clothing in this study.

(1) Basic principles and steps

The core of this method is to construct a fuzzy mapping from the factor set to the comment set. Here are five key steps:

Step 1: Determine the evaluation factor set (U), which is a set containing all evaluation indicators, as shown in Equation (6-1):

$$\mathrm{U} = \{u_1, u_2, \cdots, u_n\} \tag{6-1}$$

Step 2: Determine the evaluation comment set (V), a level set that contains all possible evaluation results, as shown in Equation (6-2):

$$\mathrm{V} = \{v_1, v_2, \cdots, v_m\} \tag{6-2}$$

Step 3: Determine the weight set (W). The importance of each evaluation factor varies. The weight set is a vector used to represent this relative importance. The weight is usually determined through expert scoring methods (such as Delphi method), Analytic Hierarchy Process (AHP), etc., and its representation is shown in Equation (6-3):

$$\mathrm{W} = \{w_1, w_2, \cdots, w_n\}, \qquad \sum_{i=1}^{n} = 1 \tag{6-3}$$

Step 4: Construct a fuzzy relation matrix (R). It represents the membership degree $\mathrm{r_{nm}}$ of each evaluation factor u_n to each comment level v_m, as shown in Equation (6-4):

$$R = \begin{bmatrix} \mathrm{r_{11}} & \cdots & \mathrm{r_{1m}} \\ \vdots & \ddots & \vdots \\ \mathrm{r_{n1}} & \cdots & \mathrm{r_{nm}} \end{bmatrix} \tag{6-4}$$

This matrix R is the result of single factor evaluation.

Step 5: Perform fuzzy synthesis calculation to obtain the comprehensive evaluation result (B). Synthesize the weight vector W with the fuzzy relationship matrix R to obtain a comprehensive evaluation vector B, which represents the membership degree of the evaluated object to each evaluation level as a whole.

$$\mathrm{B} = \mathrm{W}^{\circ}\mathrm{R} = (\mathrm{b_1}, \mathrm{b_2}, \cdots, \mathrm{b_m}) \tag{6-5}$$

The most commonly used synthesis operator is the M (∧, ∨) model (taking the small and taking the large model), but sometimes information may be lost. The more commonly used and reasonable model is the weighted average model M (·, ⊕), which comprehensively considers the influence of all factors.

Step 6: Analyze and evaluate the results

After obtaining the comprehensive evaluation vector B, there are usually two ways to handle it: ①Principle of maximum membership degree: Select the comment level corresponding to the largest b_j in B as the final evaluation result. Simple, but sometimes not precise enough; ②Weighted average method (recommended): Assign a score to each comment level and calculate the overall score.

(2) Practical application

I invited 10 experts in related fields to rate the restoration effect of clothing on four dimensions: style, pattern, color, and structure, respectively, in four levels: excellent, good, medium, or poor. So, in this evaluation, U = {Style, Pattern, Color, Structure}, V = {Show, Good, Medium, Poor}. Five experts unanimously agree that in the digital restoration of clothing, the accuracy of structure and the macroscopic form of style are slightly more important than color and pattern. The weights corresponding to style, pattern, color, and structure are set to 0.3, 0.2, 0.2, and 0.3, respectively, so W = {0.3, 0.2, 0.2, 0.3}. Ten experts evaluated the restoration effect of clothing on four levels: excellent, good, medium, etc., based on style, pattern, color, and structure. The results are shown in Table 6-1.

The fuzzy relationship matrix R can be obtained from Table 6-1:

$$R = \begin{bmatrix} 0.4 & 0.4 & 0.2 & 0 \\ 0.3 & 0.5 & 0.2 & 0 \\ 0.2 & 0.5 & 0.3 & 0 \\ 0.5 & 0.3 & 0.2 & 0 \end{bmatrix}$$

So, calculate B = (0.37, 0.41, 0.22, 0.00) from Equation (6-4).

According to the principle of maximum membership degree, the maximum value in vector B is b2=0.41 (corresponding to "good"). Therefore, according to the principle of maximum membership degree, the final comprehensive evaluation grade of the restored ancient costumes in this study is "good".

Using the weighted average model M (·, ⊕) to calculate the comprehensive evaluation result B, based on the opinions of five experts, the scores are assigned as excellent $v_1 = 95$, good $v_2 = 85$, moderate $v_3 = 75$, and poor $v_4 = 50$. Finally,

B=86.5 is calculated, which is greater than v_2 and less than v_1. Therefore, the evaluation result belongs to "good".

Based on the principles of maximum membership degree and weighted average method, the evaluation results are both excellent.

Table 6-1 Statistics on the Evaluation of Clothing Restoration Effects by 10 Experts (Unit: Times)

Evaluation factors	Excellent	Good	Average	Poor
Style	4	4	2	0
Tetxile pattern	3	5	2	0
Color	2	5	3	0
Sewing pattern	5	3	2	0

6.3 Discussion

6.3.1 Comparison between digital restoration and physical restoration of unearthed ancient costumes

Style, pattern, color, and structure are the four necessary elements for the restoration of unearthed costume. The application of this chapter is based on the research on three key dimensions completed in the previous chapters: Chapter 3 focuses on the intelligent restoration of styles and patterns of unearthed costume. Through a style and pattern intelligent restoration model based on deep convolutional generative adversarial networks, the intelligent restoration and completion of incomplete costume styles and patterns unearthed are achieved. Combined with archaeological typology analysis, literature image mutual verification, and process experimental archaeology, the appearance and pattern details of ancient costume are accurately restored; Chapter 4 is dedicated to the intelligent restoration of colors in unearthed costume. Through a costume cultural relic color restoration and prediction model based on deep convolutional long short-term time series neural network (DCLSTNet), intelligent

restoration of costume colors is achieved. At the same time, by combining scientific detection technology with traditional dyeing techniques, the original color tone of unearthed costume relics is reproduced; Chapter 5 delves into the origin of costume structure, using an interactive reverse restoration method based on Pix2Pix (Image to Image Translation with Conditional Adversarial Networks) to quickly and accurately obtain the structure of unearthed garment relics. Combined with X-ray stitching trace analysis, it ensures that the restored costume strictly conforms to its historical appearance in terms of form and function. The research results of these three dimensions constitute the "golden triangle" of costume restoration - style and pattern define what to wear, how to present color, and structure determines why it is designed, jointly restoring the complete appearance of ancient costume as a "technology art culture" complex.

Based on the styles and patterns restored in Chapter 3, the colors restored in Chapter 4, and the structures restored in Chapter 5, carry out an overall restoration of the costume. Costume restoration can be divided into physical restoration and digital restoration. The core advantage of physical restoration lies in its historical authenticity and tactile experience. Physical costume can visually present the glossiness, texture details, and dynamic deformation of fabrics, providing tangible "living evidence" for academic research, while meeting the physical needs of museum exhibitions, film and television shooting, and other scenes. However, its limitations are also prominent: firstly, the technical threshold is high and the cycle is long, and it relies on the manual operation of intangible cultural heritage inheritors. The restoration cycle of a single piece of costume can reach several months or even years; Secondly, the cost is high and irreversible. The use of natural dyes and cultural grade fabrics results in extremely high material costs, and dyeing failures or cutting errors may directly cause irreversible losses; Finally, the display scene is limited, and physical costume is sensitive to temperature, humidity, and lighting conditions. Long term exhibitions can easily lead to fabric aging, while digital technology can achieve unlimited virtual displays and dynamic interactions. The core advantages of digital restoration lie in efficiency, accuracy, and scalability: firstly, algorithm driven reduction of manual dependence, DCGAN and Pix2Pix models can automatically complete pattern completion and structure generation, shortening the restoration cycle of a single piece of costume from months to hours; Secondly, the data can be reused and iteratively optimized, and the generated digital assets (such as texture maps and 3D models) can be exported in

multiple formats, directly applied to virtual exhibition halls, metaverse scenes, or 3D printing, and the restoration accuracy can be improved through continuous model training; Thirdly, the threshold for interdisciplinary collaboration is low. Archaeologists, designers, and engineers can share model data through cloud platforms, annotate modification suggestions in real time, and avoid rework caused by delayed information transmission in physical restoration; Fourthly, it supports "impossible restoration", such as simulating the translucent effect of semi transparent fabrics through transparency rendering, or restoring the dynamic process of costume on and off through animation keyframes, providing richer analytical dimensions for academic research.

Comparing the two methods comprehensively, although physical restoration has irreplaceability in terms of historical authenticity, its high cost, long cycle, and irreversibility determine its limitations in applicable scenarios - it is more suitable as the ultimate verification method for academic research or high-end customized display needs. Digital restoration has become a mainstream trend with low cost, high efficiency, and strong scalability. On the one hand, it achieves intelligent restoration and reverse modeling of patterns, colors, and structures through deep learning models such as DCGAN, DCLSTNet, and Pix2Pix, greatly reducing reliance on expert experience; On the other hand, the digital assets generated by it can seamlessly integrate cultural heritage protection, cultural and creative industries, and immersive experience economy, such as licensing the digital model of Tang Dynasty dresses to game companies, or allowing visitors to "try on" virtual costume in museums through AR technology. More importantly, the "non-destructive" characteristics of digital restoration make it the preferred choice for fragile cultural relic research - obtaining cultural relic data through laser scanning and photogrammetry, which not only avoids damage caused by direct contact, but also permanently preserves the original form of costume, providing a digital twin foundation for subsequent research.

6.3.2 The value of constructing a three-dimensional digital resource library for ancient Chinese costume

From the perspective of cultural heritage protection and inheritance, three-dimensional databases provide a revolutionary solution for the sustainable preservation of ancient costume. The ancient Chinese costumes are mostly made of organic materials such as silk, hemp and cotton, which are prone to fade, mildew, fiber breakage and

other problems after years of erosion. For example, the banner costumes of the Tang Dynasty unearthed in the Mogao Grottoes of Dunhuang, the plain gauze clothes of the Han Tomb at Mawangdui, and other precious cultural relics have entered the stage of being protected, and it is difficult to display or conduct physical contact research for a long time. The 3D database combines artificial intelligence and virtual simulation technology with literature records and archaeological discoveries to transform physical information into permanently preserved digital assets. This digital twin like recording method not only avoids environmental risks in physical preservation, but also enables the dynamic inheritance of cultural heritage, allowing cultural relics that are dormant in museum warehouses to truly come to life.

At the level of academic research innovation, the three-dimensional database has reconstructed the methodological system of ancient costume research, promoting interdisciplinary integration. Traditional costume research relies on physical observation, literature review, and two-dimensional image analysis, which have limitations such as incomplete information acquisition, difficulty in data comparison, and strong subjectivity in research conclusions. For example, when scholars study the cutting structure of costume from different dynasties, they can only speculate through flat drawings or physical disassembly, making it difficult to accurately reproduce their three-dimensional shapes and wearing effects. By constructing high-precision digital models of costume, 3D databases can achieve multi-dimensional data extraction. They can not only accurately measure physical parameters such as length, width, and curvature of costume, but also analyze its cutting logic, fabric drape, and motion state through computer-aided design (CAD) technology, providing quantitative basis for costume history research. At the same time, the compatibility and scalability of the database provide possibilities for interdisciplinary research: archaeologists can analyze the cultural transmission paths of costume unearthed from different sites by comparing their three-dimensional models; Textile engineers can reconstruct the weaving process of ancient fabrics based on digital models; Art historians can combine three-dimensional data of costume patterns to study their association with contemporary painting and sculpture art.

From the perspective of industrial transformation and economic value, three-dimensional databases provide core resource support for traditional cultural and creative industries, empowering the upgrading of the industrial chain. In recent years, with the increasing demand for the application of ancient costume elements in fields

such as film and television, games, costume design, and cultural and creative products, enterprises often face problems such as high copyright risks, low fidelity, and high development costs when obtaining costume materials due to the lack of a systematic digital resource library. By establishing a standardized digital asset library for ancient costume, 3D databases can provide enterprises with authorized resources such as 3D models, texture maps, and process parameters, reducing their research and development costs and infringement risks. For example, when shooting ancient costume dramas, film and television production companies can directly retrieve 3D models of costumes that match the historical background from the database, and generate realistic costume effects through 3D rendering technology to avoid historical disputes caused by inaccurate costume restoration; Game companies can use costume models in the database to develop ancient style game characters with historical authenticity, enhancing the cultural connotation and user experience of the game; Costume brands can innovate their designs based on traditional costume elements in databases, combining ancient costume cutting techniques, pattern designs, and modern fashion to launch costume products that combine cultural heritage and fashion sense, meeting consumers' needs for traditional costume.

6.3.3 Further research directions

In the field of cultural heritage protection, the digital restoration of ancient costumes has always faced the dual challenges of insufficient accuracy and lack of vitality. Traditional restoration work highly relies on the subjective experience and manual drawing of archaeological experts, which not only takes time and effort, but also makes it difficult to accurately restore the historical texture of the details, textures, and colors of costume patterns. For example, the Baoxiang flower pattern of Tang Dynasty sacrificial costume in Dunhuang murals has incomplete lines due to the erosion of time, and it is difficult to fully present its symmetrical aesthetics and religious symbolism solely through manual copying; The plain silk robe unearthed from the Mawangdui Han Tomb, with its thin and light silk fibers and primitive colors, also lacks a dynamic reference system, and has never been able to display the ancient wearing effect of "holding it up like nothing" in restoration. However, with the breakthrough maturity of multimodal large models (such as GPT-4V, Sora) and Neural Radiation Field (NeRF) technology, this dilemma is being completely broken. The multimodal big model injects the core driving force of intelligent analysis into costume restoration with its

cross modal understanding and generation ability. Taking GPT-4V as an example, it can not only accurately identify textual descriptions of costume forms in archaeological reports and ancient literature (such as "Yufu Zhi (《舆服志》)" and "Tiangong Kaiwu (《天工开物》)"), but also combine visual materials such as paintings, pottery figurines, and murals from the same period to automatically extract key information. For example, it can extract the sleeve shape and waist proportion of men's shirts from the Five Dynasties period from "Han Xizai Night Banquet (《韩熙载夜宴图》)", restore the pattern themes and symbolic meanings of Uyghur costume from unearthed documents in Turpan, and ultimately generate high-precision initial design drawings that conform to historical context. The sentence is:. This cross modal transformation of "text image design" not only greatly improves the efficiency of restoration, but also avoids subjective biases that may occur in manual interpretation, making the restoration of ancient costume forms truly based on data-driven scientific foundations.

The introduction of NeRF technology has opened up a new dimension of "three-dimensional dynamics" for the digital restoration of ancient costume, completely changing the presentation limitations of "two-dimensional static" in traditional restoration. Traditional restoration results often exist in the form of drawings, renderings, or solid models, which cannot show the sagging and wrinkling changes of costume in different postures, nor can they allow the audience to observe the structural details of costume from multiple angles. For example, the patch patterns of Ming Dynasty costume can only present the front effect in two-dimensional drawings, and the embroidery techniques on the edges and the lining structure on the back are unknown. NeRF technology can construct a three-dimensional volume field with real physical properties through deep learning of two-dimensional images of costume, such as archaeological excavation site photos and museum collection photos, and transform planar images into interactive three-dimensional models. In this model, the user can not only achieve 360 degree arbitrary perspective switching by dragging the mouse, carefully observe the collar structure, button style, and skirt overlapping mode of the costume, but also simulate the morphological changes of costume in dynamic scenes such as walking and turning with the help of a physical engine: for example, the natural swing of the hem of Juzi in the Song Dynasty with the gait, the wrinkle distribution of horseshoe sleeves in the Qing Dynasty flag costume when lifting the arm, and even restore the color change and gloss texture of costume in different environments (such

as court candles, outdoor daylight) by adjusting the light parameters. More importantly, the 3D models constructed by NeRF technology also support deep integration with Virtual Reality (VR) and Augmented Reality (AR) technologies - viewers wearing VR devices can "travel" back to ancient scenes and personally experience the wearing effect of costume; Museums can use AR technology to "revive" ancient costume fragments in display cabinets into complete 3D models, visually presenting their original wearing forms and decorative details. This "high fidelity rendering+dynamic interaction" presentation method makes ancient costume no longer a cold cultural relic in museums, but a living cultural carrier that can be perceived and experienced.

When multimodal models are deeply integrated with Neural Radiance Fields (NeRF) technology, the digital restoration of ancient costume is no longer a simple technical tool, but a core engine for promoting the creative transformation and innovative development of cultural heritage, leading cultural heritage protection from static preservation to a new stage of dynamic inheritance. At the level of cultural research, the ancient costume database constructed through digital restoration provides rich material support for interdisciplinary research: historians can analyze three-dimensional models of costume from different dynasties to study the relationship between costume form and social hierarchy, etiquette culture; Fashion designers can draw inspiration from restored patterns and colors, integrating traditional elements into modern design - for example, Tang Dynasty scroll patterns extracted based on GPT-4V, combined with NeRF restored Song Dynasty costume silhouettes, to design fashion works that combine traditional charm and modern aesthetics, allowing ancient costume culture to be integrated into contemporary life in a new form. At the level of cultural dissemination, digital restoration achievements have broken the temporal and spatial limitations of cultural dissemination through various carriers such as short videos, virtual exhibitions, and games. Young people can choose ancient costumes restored based on NeRF technology as character costumes in games, and learn about costume culture in entertainment; On short video platforms, creators generate ancient costume science popularization animations through multimodal large models, combined with dynamic displays using NeRF technology, transforming complex costume history knowledge into vivid and interesting visual content, attracting millions of netizens' attention. More noteworthy is that digital restoration provides unlimited possibilities for the revitalization and utilization of cultural heritage, such as developing virtual fitting mini programs based on restored Hanfu 3D models, allowing consumers to

customize traditional costume that fits their body shape online; Collaborate with film and television dramas to provide accurate costume and prop models for historical dramas, avoiding "theatrical" style costume misguidance and enhancing the cultural authenticity of film and television works. This full chain empowerment from "research" to "dissemination" and then to "application" not only brings new vitality to ancient costume culture in contemporary society, but also constructs a virtuous cycle of "protection inheritance innovation", providing a replicable and promotable new path for cultural heritage protection.

6.4 Conclusion

This study successfully verified the feasibility of using artificial intelligence and digital technology to reconstruct ancient Chinese costume and construct a three-dimensional database. By integrating AI technology, a complete technical process from fragmented cultural relic data to high fidelity dynamic models was established, effectively overcoming the limitations of traditional research methods. The constructed 3D database of ancient Chinese costume not only provides innovative visual analysis tools for academic research such as costume history and archaeology, but also provides core digital resources for the non-destructive protection, immersive display, and public education of cultural heritage. Although there is still room for improvement in sample coverage and complex process simulation, and further expansion will be achieved through generative artificial intelligence, virtual try on, and blockchain collaborative mechanisms in the future, this study undoubtedly lays a solid foundation for empowering humanities and inheriting excellent traditional Chinese culture with technology, demonstrating broad application prospects.

Chapter 7 Conclusion and prospect

7.1 Research conclusion

This study focuses on the intelligent restoration of unearthed costume, and systematically constructs a multimodal restoration theory and technical system based on artificial intelligence for damaged, faded, and structurally damaged cultural relics. By applying interdisciplinary methods such as deep learning, computer vision, and materials science, this study has systematically solved the three major problems of inaccurate models and incomplete technical systems in the restoration of costume relics. This research has achieved high-precision and automated restoration of costume relics styles, patterns, colors, and structures, promoting the paradigm shift of cultural relics protection from experience driven to data-driven. The main conclusions are as follows. The main conclusions are as follows:

Firstly, in terms of the restoration of costume relics styles and patterns, this study innovatively proposes an intelligent restoration model based on DCGAN. This model adopts a generator with U-Net architecture and a discriminator based on PatchGAN, and achieves semantic consistency and structural coherence completion of incomplete regions through adversarial training strategy. The generator utilizes a skip connection mechanism to fuse shallow texture features with deep semantic information, ensuring the consistency of the overall pattern style while maintaining the authenticity of local details. The experimental results show that the model is significantly better than traditional image restoration algorithms in multiple objective evaluation indicators such as PSNR, SSIM, and FID. Its restoration results have been highly recognized by archaeologists and cultural relic protection experts in terms of visual naturalness, texture refinement, and historical style consistency. In the repair case, the model successfully restored the topology structure and edge details of complex patterns, verifying its excellent performance and robustness in highly incomplete and multi texture interwoven scenes.

Secondly, in terms of color restoration of costume relics, this study constructed a DCLSTNet model that integrates spatiotemporal features to simulate and predict the chemical degradation process and color evolution of dyes in buried environments. This

model integrates the advantages of CNN in spatial feature extraction with the ability of LSTM in time series modeling, and can simultaneously capture the structural changes of dye molecules and the dynamic effects of environmental parameters such as temperature, humidity, and pH. By combining a multispectral imaging system with a high-precision colorimeter, a nonlinear mapping relationship from the current fading state to the original color was established, achieving high-precision color restoration of multiple traditional dyes. In the accelerated aging experiment simulating the tomb environment, the color prediction error of the model is controlled within 5 in the CIELAB color space, which is significantly better than the methods based on linear regression, polynomial fitting or traditional image processing, reflecting its progressiveness and reliability in the modeling of complex degradation mechanisms.

Thirdly, in terms of restoring the structure of costume relics, this study proposes an interactive reverse intelligent restoration method that integrates X-ray tomography technology, 3D reverse engineering, and generative adversarial networks. This method adopts Pix2Pix generative adversarial network as the basic framework, and introduces BC and AC to achieve non-contact high-precision reconstruction of the internal structure and surface morphology of garment relics. Obtaining three-dimensional data of cultural relics through X-ray CT scanning, combined with deep learning-based feature extraction and segmentation algorithms, accurately identifying suture trajectories, fabric layering, and damaged boundaries; Further utilize geometric processing and physical constraint optimization to generate two-dimensional unfolded samples that conform to historical cutting techniques. Experimental results have shown that this method not only avoids irreversible damage to cultural relics caused by traditional physical unfolding methods, but also achieves high accuracy in the restoration of complex costume structures such as Ming Dynasty robes and Han Dynasty skirts, significantly improving the scientific, reproducible, and practical nature of structural restoration.

Fourthly, in terms of the application of intelligent restoration results for costume relics, based on the intelligent restoration of costume relics styles, patterns, structures, and colors in the early stage, this study constructs a large-scale three-dimensional database covering Chinese costume relics throughout history to support the large-scale application and interdisciplinary research of costume relics restoration technology. It integrates four core data resource libraries, including styles, patterns, colors, and structures. More than 500 sets of costume relics data from pre-Qin to Ming and Qing

dynasties have been collected, covering three major types of materials: silk, cotton, and wool. 30% of the data comes from major archaeological discoveries such as the Niya site in Xinjiang and the underground palace of Famen Temple. In terms of application ecology, the database not only provides a standardized dataset for model training in this study, but also becomes a core data resource platform for costume culture research, cultural and creative product development, and public education, promoting the paradigm shift of cultural heritage protection from "single restoration" to "systematic inheritance".

7.2 Research limitations

Although significant progress has been made in the intelligent restoration of costume relics in this study, there are still limitations in the following aspects:

Firstly, the dual constraints of data quality and quantity

The model training heavily relies on unearthed and relatively well-preserved costume relics data. For rare categories or extremely damaged samples from certain dynasties, high-quality data is extremely scarce, which may result in bias in the trained model. The generalization ability for specific types of cultural relics needs further improvement. Ideally, scientific testing data such as mechanical properties, chemical composition, and hyperspectral analysis should be combined with image data. However, obtaining multimodal accurate registration data for the same cultural relic is costly and difficult to operate. Currently, models mainly rely on images and basic metadata for inference, which to some extent limits the physical and chemical accuracy of the restoration results.

Second, the model generalization ability and explanatory ability are insufficient

Despite the excellent performance of deep learning models, their decision-making process still has a "black box" characteristic, and the semantic and cultural implications of the repaired patterns lack clear explanations. For example, the mechanisms behind why DCGAN generates a specific pattern and how DCLSTNet balances influencing factors at different time points are not fully understood, making it difficult for archaeologists to fully trust or intervene in correcting the model's output results. The current model is mainly data-driven, and although physical constraints such as BC-AC are introduced, the embedding of deep physical and chemical processes such as fiber aging mechanics and dye chemical degradation kinetics is still in the preliminary stage.

Models are more about learning correlations rather than establishing causal relationships, and there may be uncertainty in predicting extreme or unseen environmental conditions.

Thirdly, the complexity and automation level of the technical process are not high

The technical implementation threshold is high and the interaction dependence is strong, especially in the process of structural restoration, which still requires a considerable degree of manual intervention, such as the correction of contour line extraction and the definition of 3D stitching relationships. The entire process has not yet been fully automated, and there are still requirements for the professional competence of operators, which to some extent affects efficiency. This limitation not only increases the manpower and time costs of project implementation, but also to some extent limits the scale and speed of technology promotion, especially when facing diverse and highly complex tasks, highlighting the efficiency bottleneck in the current human-machine collaboration mode.

Fourthly, the coverage of application scenarios will be further expanded

The research mainly focuses on common fabrics such as silk, linen, and cotton, and there is relatively insufficient research on the degradation mechanism and restoration methods of special materials such as leather, metal ornaments, and composite materials. The current 3D database mainly focuses on static model display, and there is still room for improvement in more expressive interactive experiences such as dynamic wearing effects of costume and physical simulation when swaying with the wind.

7.3 Future work prospects

In response to the above limitations, future research work will be carried out from the following aspects:

Firstly, expand data sources and enhance the model's generalization ability. We plan to integrate more archaeological excavation reports, museum collection databases, and folk collection resources through cross institutional cooperation to build a more comprehensive and representative dataset of costume relics. Especially strengthen the collection and annotation of costume data for early dynasties and ethnic minorities. At the same time, transfer learning, meta learning and other algorithms are introduced to

enhance the model's adaptability to small sample and low-quality data, and to improve its cross-cultural and cross era generalization performance.

Secondly, develop 3D intelligent restoration and dynamic modeling technology. We plan to extend the existing 2D restoration model to the 3D field, combining 3D scanning, point cloud reconstruction, physical simulation and other technologies to construct an integrated intelligent restoration framework of "image geometry mechanics". For example, the introduction of neural radiation field (NeRF) technology enables high-precision 3D reconstruction of garment relics, and combines finite element analysis (FEA) to simulate the deformation and aging process of cultural relics under different environmental conditions.

Thirdly, enhance the interpretability and cultural consistency of the model. We plan to introduce interpretable AI technologies such as attention mechanisms and semantic segmentation networks to visualize the decision-making process of the model and ensure that the repair results conform to historical semantics. At the same time, cultural constraints are imposed on the generation process by combining archaeological knowledge maps, historical documents (such as "Yufu Zhi"), craft records, and other prior knowledge to avoid temporal displacement or style mixing.

Fourth, promote the implementation of technology and standardization construction. We will develop a lightweight and low-cost portable restoration system to support grassroots cultural and museum units in rapid and preliminary digitization and restoration of cultural relics. At the same time, joint cultural relics protection agencies will develop technical standards and ethical norms for intelligent restoration, establish expert review and public supervision mechanisms for restoration results, and ensure the rationality and transparency of technology application.

Fifth, explore multimodal fusion and interdisciplinary collaborative research. In the future, we will further strengthen cooperation with materials science, chemistry, archaeology and other fields, integrate research results such as fiber degradation models, dye chemical analysis, and burial environment simulation into AI models, and build a more scientific and comprehensive theoretical system for cultural relic protection. In addition, exploring the application of emerging technologies such as blockchain and digital twins in cultural relic tracing, virtual display, copyright protection, etc., to promote the digital inheritance and innovative utilization of cultural heritage.

Appendix 1: Data on costume textitle patterns throughout Chinese history

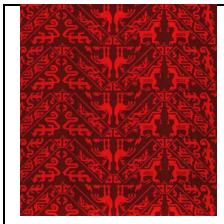	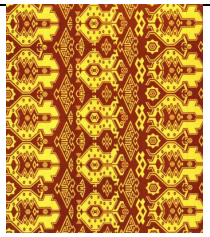			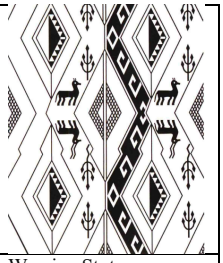
Warring States period(475BC-221BC)	Warring States period(475BC-221BC)	Warring States period(475BC-221BC)	Warring States period(475BC-221BC)	Warring States period(475BC-221BC)
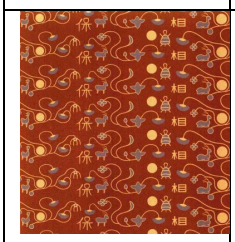	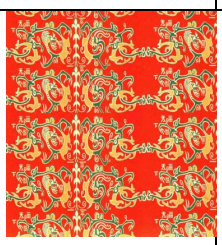			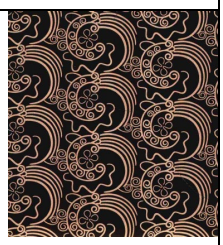
Han dynasty(202 BC - 220AD)	Han dynasty(202 BC - 220AD)	Han dynasty(202 BC - 220AD)	Han dynasty(202 BC - 220AD)	Han dynasty(202 BC - 220AD)
			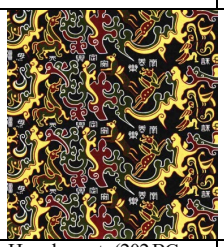	
Han dynasty(202 BC - 220AD)	Han dynasty(202 BC - 220AD)	Han dynasty(202 BC - 220AD)	Han dynasty(202 BC - 220AD)	Han-Jin dynasty(202BC-220AD)
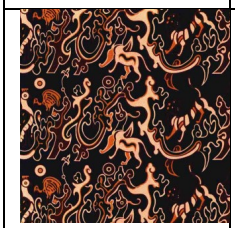		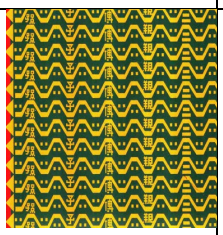	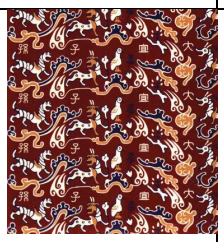	
Han-Jin dynasty(202BC-220AD)	Han-Jin dynasty(202BC-220AD)	Han-Jin dynasty(202BC-220AD)	Han-Jin dynasty(202BC-220AD)	Han-Jin dynasty(202BC-220AD)
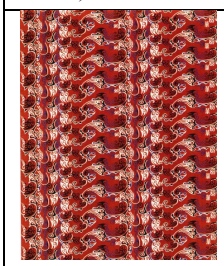		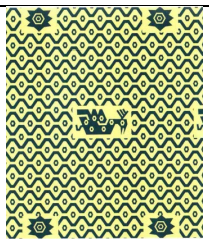		
Han-Jin dynasty(202BC-220AD)	Han-Jin dynasty(202BC-220AD)	Western Han Dynasty(202BC-8AD)	Eastern Han Dynasty(25-220AD)	Eastern Han Dynasty(25-220AD)

	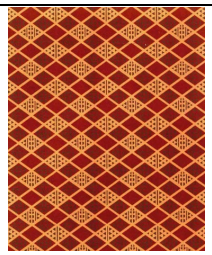	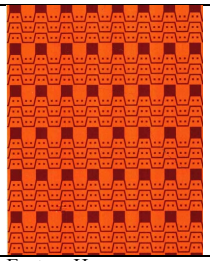	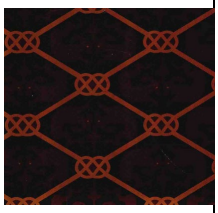	
Eastern Han Dynasty(25-220AD)	Eastern Han Dynasty(25-220AD)	Eastern Han Dynasty(25-220AD)	Eastern Han Dynasty(25-220AD)	Eastern Han Dynasty(25-220AD)
	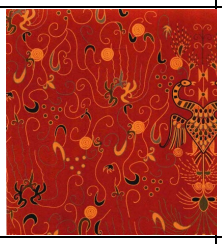	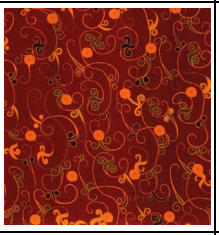		
Eastern Han Dynasty(25-220AD)	Qin Dynasty(351-394AD)	Qin Dynasty(351-394AD)	Eastern Jin (265-439AD	Sixteen Kingdoms period (304-439AD)
		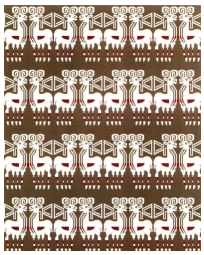	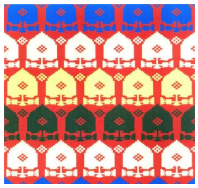	
Northern Dynasties (439-581AD)	Northern Dynasties (439-581AD)	Northern Dynasties (439-581AD)	Northern Dynasties (439-581AD)	Northern Dynasties (439-581AD)
			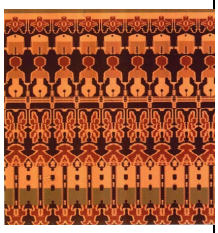	
Northern Dynasties(439-581AD)	Northern Dynasties(439-581AD)	Northern Dynasties(439-581AD)	Northern Dynasties(439-581AD)	Northern Dynasties(439-581AD)
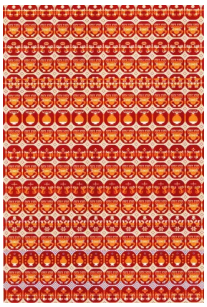	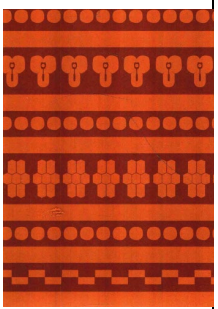		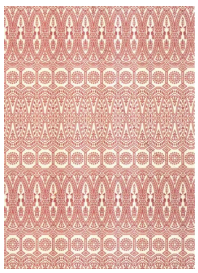	
Northern Dynasties(439-581AD)	Northern Dynasties(439-581AD)	Northern Dynasties(439-581AD)	Northern Dynasties(439-581AD)	Northern Dynasties(439-581AD)
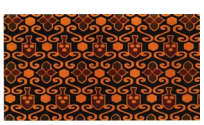	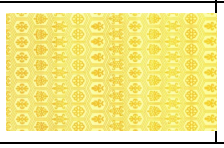			

Northern Dynasties(439-581AD)	Northern Dynasties(439-581AD)	Northern Dynasties(439-581AD)	Northern Dynasties(439-581AD)	Northern Dynasties(439-581AD)
	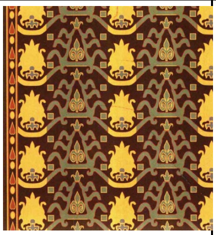			
Northern Dynasties(439-581AD)	Northern Dynasties(439-581AD)	Northern-Sui Dynasties (439-618AD)	Tang dynasty(618-907AD)	Tang dynasty(618-907AD)
		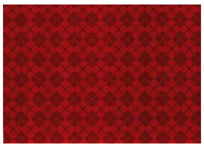	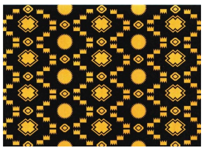	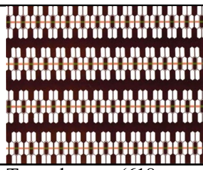
Tang dynasty(618-907AD)	Tang dynasty(618-907AD)	Tang dynasty(618-907AD)	Tang dynasty(618-907AD)	Tang dynasty(618-907AD)
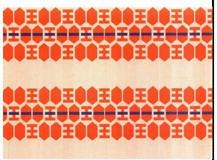			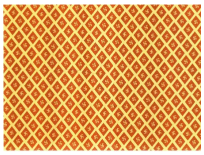	
Tang dynasty(618-907AD)	Tang dynasty(618-907AD)	Tang dynasty(618-907AD)	Tang dynasty(618-907AD)	Tang dynasty(618-907AD)
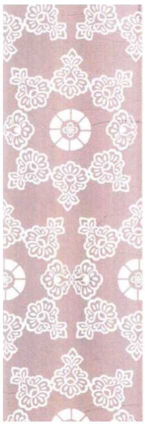				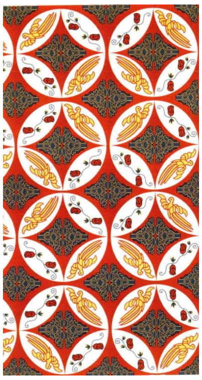
Tang dynasty(618-907AD)	Tang dynasty(618-907AD)	Tang dynasty(618-907AD)	Tang dynasty(618-907AD)	Tang dynasty(618-907AD)
		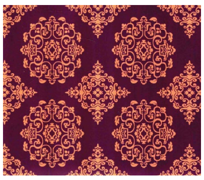	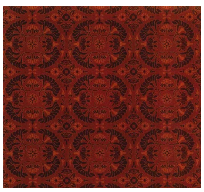	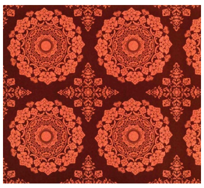
Tang dynasty(618-907AD)	Tang dynasty(618-907AD)	Tang dynasty(618-907AD)	Tang dynasty(618-907AD)	Tang dynasty(618-907AD)

				
Tang dynasty(618-907AD)	Tang dynasty(618-907AD)	Tang dynasty(618-907AD)	Tang dynasty(618-907AD)	Tang dynasty(618-907AD)
				
Tang dynasty(618-907AD)	Tang dynasty(618-907AD)	Tang dynasty(618-907AD)	Tang dynasty(618-907AD)	Tang dynasty(618-907AD)
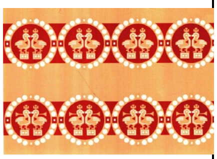				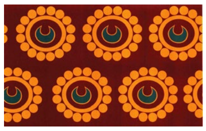
Tang dynasty(618-907AD)	Tang dynasty(618-907AD)	Tang dynasty(618-907AD)	Tang dynasty(618-907AD)	Tang dynasty(618-907AD)
	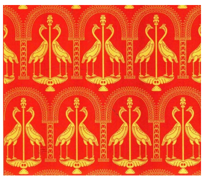			
Tang dynasty(618-907AD)	Tang dynasty(618-907AD)	Tang dynasty(618-907AD)	Tang dynasty(618-907AD)	Tang dynasty(618-907AD)
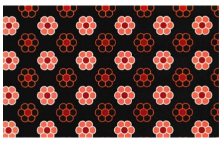		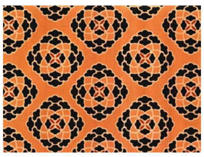	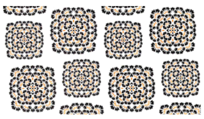	
Tang dynasty(618-907AD)	Tang dynasty(618-907AD)	Tang dynasty(618-907AD)	Tang dynasty(618-907AD)	Tang dynasty(618-907AD)
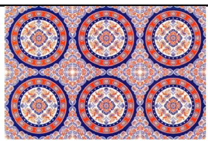				
Tang dynasty(618-907AD)	Tang dynasty(618-907AD)	Tang dynasty(618-907AD)	Tang dynasty(618-907AD)	Tang dynasty(618-907AD)

		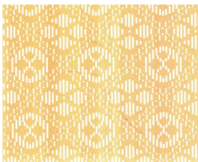		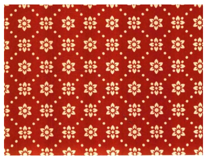
Tang dynasty(618-907AD)	Tang dynasty(618-907AD)	Tang dynasty(618-907AD)	Tang dynasty(618-907AD)	Tang dynasty(618-907AD)
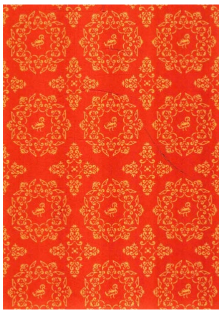	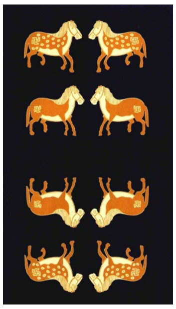			
Tang dynasty(618-907AD)	Tang dynasty(618-907AD)	Tang dynasty(618-907AD)	Tang dynasty(618-907AD)	Tang dynasty(618-907AD)
				
Tang dynasty(618-907AD)	Tang dynasty(618-907AD)	Tang dynasty(618-907AD)	Tang dynasty(618-907AD)	Tang dynasty(618-907AD)

				
Tang dynasty(618-907AD)	Tang dynasty(618-907AD)	Tang dynasty(618-907AD)	Tang dynasty(618-907AD)	Tang dynasty(618-907AD)
	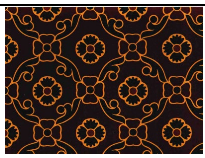	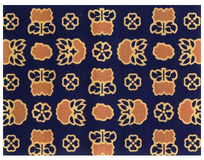		
Tang dynasty(618-907AD)	Tang dynasty(618-907AD)	Tang dynasty(618-907AD)	Tang dynasty(618-907AD)	Tang dynasty(618-907AD)

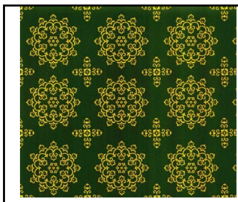			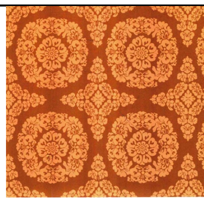	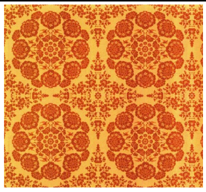
Tang dynasty(618-907AD)	Tang dynasty(618-907AD)	Tang dynasty(618-907AD)	Tang dynasty(618-907AD)	Tang dynasty(618-907AD)
				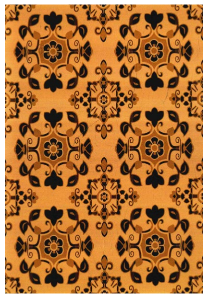
Tang dynasty(618-907AD)	Tang dynasty(618-907AD)	Tang dynasty(618-907AD)	Tang dynasty(618-907AD)	Tang dynasty(618-907AD)
		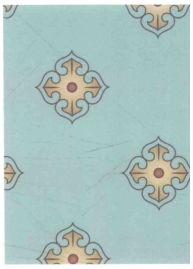	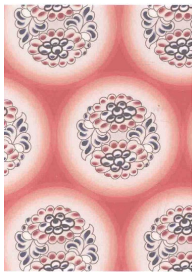	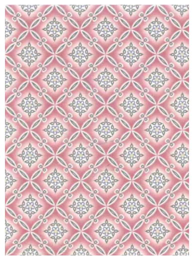
Tang dynasty(618-907AD)	Tang dynasty(618-907AD)	Tang dynasty(618-907AD)	Tang dynasty(618-907AD)	Tang dynasty(618-907AD)
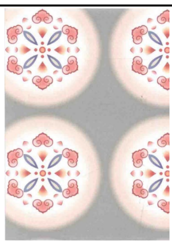				
Tang dynasty(618-907AD)	Tang dynasty(618-907AD)	Tang dynasty(618-907AD)	Tang dynasty(618-907AD)	Tang dynasty(618-907AD)
				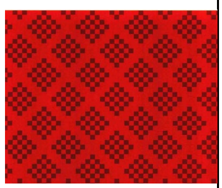
Tang dynasty(618-907AD)	Tang dynasty(618-907AD)	Tang-Song dynasty(618-907AD)	Tang-Song dynasty(618-907AD	Tang-Song dynasty(618-907AD

				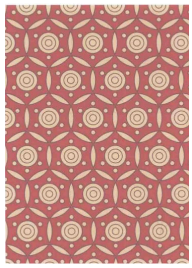
Tang-Five dynasty(618-907AD	Tang-Song dynasty(618-907AD	Tang-Song dynasty(618-907AD	Tang-Song dynasty(618-907AD	Five dynasty(907-960AD)
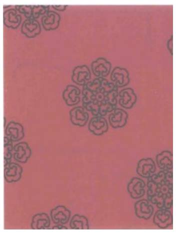			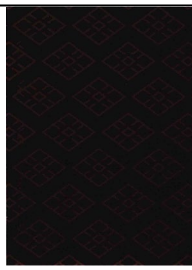	
Five dynasty(907-960AD)	Five dynasty(907-960AD)	Liao dynasty916-1125AD)	Liao dynasty916-1125AD)	Liao dynasty916-1125AD)
			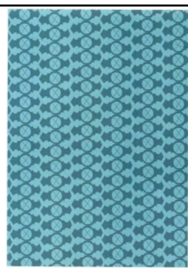	
Liao dynasty916-1125AD)	Liao dynasty916-1125AD)	Liao dynasty916-1125AD)	Liao dynasty916-1125AD)	Liao dynasty916-1125AD)
				
Liao dynasty916-1125AD)	Liao dynasty916-1125AD)	Liao dynasty916-1125AD)	Liao dynasty916-1125AD)	Liao dynasty916-1125AD)
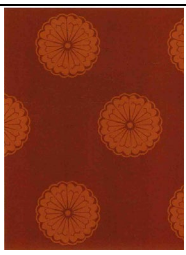	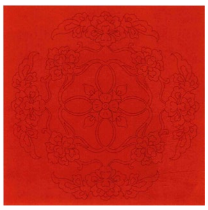			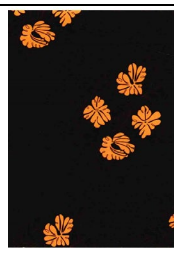
Liao dynasty916-1125AD)	Liao dynasty916-1125AD)	Liao dynasty916-1125AD)	Liao dynasty916-1125AD)	Liao dynasty916-1125AD)

				
Liao dynasty916- 1125AD)	Liao dynasty916- 1125AD)	Liao dynasty916- 1125AD)	Liao dynasty916- 1125AD)	Liao dynasty916- 1125AD)
				
Liao dynasty916- 1125AD)	Liao dynasty916- 1125AD)	Liao dynasty916- 1125AD)	Liao dynasty916- 1125AD)	Liao dynasty916- 1125AD)
				
Liao dynasty916- 1125AD)	Liao dynasty916- 1125AD)	Liao dynasty916- 1125AD)	Liao dynasty916- 1125AD)	Liao dynasty916- 1125AD)
				
Liao dynasty916- 1125AD)	Liao dynasty916- 1125AD)	Liao dynasty916- 1125AD)	Liao dynasty916- 1125AD)	Liao dynasty916- 1125AD)
				
Liao dynasty916- 1125AD)	Liao dynasty916- 1125AD)	Liao dynasty916- 1125AD)	Liao dynasty916- 1125AD)	Liao dynasty916- 1125AD)

				
Liao dynasty916-1125AD)	Liao dynasty916-1125AD)	Liao dynasty916-1125AD)	Liao dynasty916-1125AD)	Liao dynasty916-1125AD)
				
Liao dynasty916-1125AD)	Liao dynasty916-1125AD)	Liao dynasty916-1125AD)	Liao dynasty916-1125AD)	Liao dynasty916-1125AD)
				
Liao dynasty916-1125AD)	Liao dynasty916-1125AD)	Liao dynasty916-1125AD)	Liao dynasty916-1125AD)	Liao dynasty916-1125AD)
				
Liao dynasty916-1125AD)	Liao dynasty916-1125AD)	Liao dynasty916-1125AD)	Liao dynasty916-1125AD)	Liao dynasty916-1125AD)
				
Liao dynasty916-1125AD)	Liao dynasty916-1125AD)	Liao dynasty916-1125AD)	Liao dynasty916-1125AD)	Liao dynasty916-1125AD)

				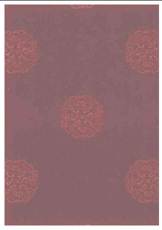
Liao dynasty916-1125AD)	Liao dynasty916-1125AD)	Liao dynasty916-1125AD)	Song dynasty(960-1279AD)	Song dynasty(960-1279AD)
				
Song dynasty(960-1279AD)	Song dynasty(960-1279AD)	Song dynasty(960-1279AD)	Song dynasty(960-1279AD)	Song dynasty(960-1279AD)
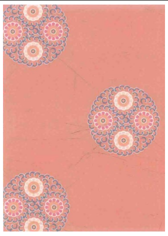				
Song dynasty(960-1279AD)	Song dynasty(960-1279AD)	Song dynasty(960-1279AD)	Song dynasty(960-1279AD)	Song dynasty(960-1279AD)
				
Song dynasty(960-1279AD)	Song dynasty(960-1279AD)	Song dynasty(960-1279AD)	Song dynasty(960-1279AD)	Song dynasty(960-1279AD)
			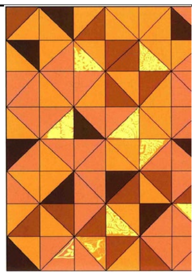	
Northern Song Dynasty(960-1127AD)	Song dynasty(960-1279AD)	Northern Song Dynasty(960-1127AD)	Northern Song Dynasty(960-1127AD)	Northern Song Dynasty(960-1127AD)

				
Northern Song Dynasty(960-1127AD)	Northern Song Dynasty(960-1127AD)	Northern Song Dynasty(960-1127AD)	Northern Song Dynasty(960-1127AD)	Northern Song Dynasty(960-1127AD)
				
Northern Song Dynasty(960-1127AD)	Northern Song Dynasty(960-1127AD)	Southern Song Dynasty(960-1127AD)	Southern Song Dynasty(960-1127AD)	Southern Song Dynasty(960-1127AD)
				
Southern Song Dynasty(960-1127AD)	Southern Song Dynasty(960-1127AD)	Southern Song Dynasty(960-1127AD)	Southern Song Dynasty(960-1127AD)	Southern Song Dynasty(960-1127AD)
				
Southern Song Dynasty(960-1127AD)	Southern Song Dynasty(960-1127AD)	Southern Song Dynasty(960-1127AD)	Southern Song Dynasty(960-1127AD)	Southern Song Dynasty(960-1127AD)
				
Yuan Dynasty(1271-	Yuan Dynasty(1271-	Yuan Dynasty(1271-	Yuan Dynasty(1271-	Yuan Dynasty(1271-

1368AD)	1368AD)	1368AD)	1368AD)	1368AD)
			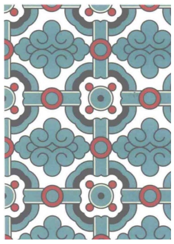	
Yuan Dynasty(1271-1368AD)	Yuan Dynasty(1271-1368AD)	Yuan Dynasty(1271-1368AD)	Yuan Dynasty(1271-1368AD)	Yuan Dynasty(1271-1368AD)
		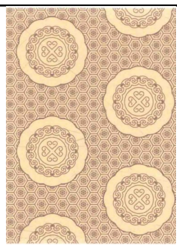		
Yuan Dynasty(1271-1368AD)	Yuan Dynasty(1271-1368AD)	Yuan Dynasty(1271-1368AD)	Yuan Dynasty(1271-1368AD)	Yuan Dynasty(1271-1368AD)
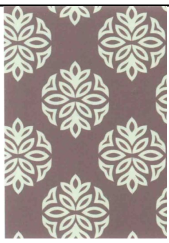			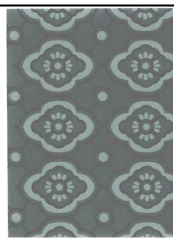	
Yuan Dynasty(1271-1368AD)	Yuan Dynasty(1271-1368AD)	Yuan Dynasty(1271-1368AD)	Yuan Dynasty(1271-1368AD)	Yuan Dynasty(1271-1368AD)
				
Yuan Dynasty(1271-1368AD)	Yuan-Ming Dynasty (1271-1644AD)	17th century	17th century	17th century
				
17th century	17th century	17th century	17th century	17th century

				
17th century	17th century	17th century	17th century	17th century
				
17th century	17th century	17th century	17th century	17th century
				
17th century	Ming Dynasty (1368-1644AD)	Ming Dynasty (1368-1644AD)	Ming Dynasty (1368-1644AD)	Ming Dynasty (1368-1644AD)
	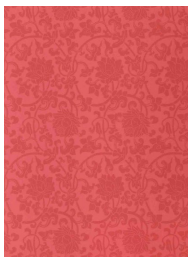			
Ming Dynasty (1368-1644AD)	Ming Dynasty (1368-1644AD)	Ming Dynasty (1368-1644AD)	Ming Dynasty (1368-1644AD)	Ming Dynasty (1368-1644AD)
				
Ming Dynasty (1368-1644AD)	Ming Dynasty (1368-1644AD)	Ming Dynasty (1368-1644AD)	Ming Dynasty (1368-1644AD)	Ming Dynasty (1368-1644AD)

				
Ming Dynasty (1368-1644AD)	Ming Dynasty (1368-1644AD)	Ming Dynasty (1368-1644AD)	Ming Dynasty (1368-1644AD)	Ming Dynasty (1368-1644AD)
			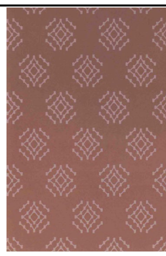	
Ming Dynasty (1368-1644AD)	Ming Dynasty (1368-1644AD)	Ming Dynasty (1368-1644AD)	Ming Dynasty (1368-1644AD)	Ming Dynasty (1368-1644AD)
		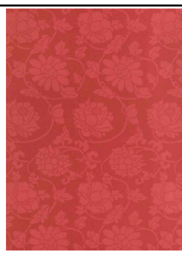		
Ming Dynasty (1368-1644AD)	Ming Dynasty (1368-1644AD)	Ming Dynasty (1368-1644AD)	Ming Dynasty (1368-1644AD)	Ming Dynasty (1368-1644AD)
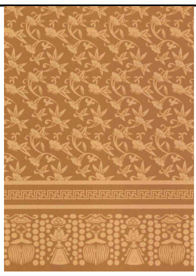				
Ming Dynasty (1368-1644AD)	Ming Dynasty (1368-1644AD)	Ming Dynasty (1368-1644AD)	Ming Dynasty (1368-1644AD)	Ming Dynasty (1368-1644AD)
				
Ming Dynasty (1368-1644AD)	Ming Dynasty (1368-1644AD)	Ming Dynasty (1368-1644AD)	Ming Dynasty (1368-1644AD)	Ming Dynasty (1368-1644AD)

	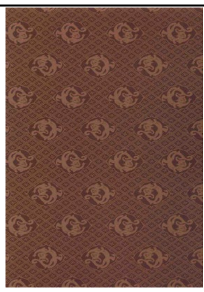			
Ming Dynasty (1368-1644AD)	Ming Dynasty (1368-1644AD)	Ming Dynasty (1368-1644AD)	Ming Dynasty (1368-1644AD)	Ming Dynasty (1368-1644AD)
		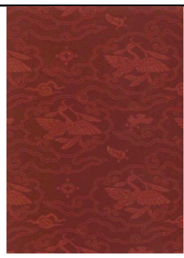		
Ming Dynasty (1368-1644AD)	Ming Dynasty (1368-1644AD)	Ming Dynasty (1368-1644AD)	Ming Dynasty (1368-1644AD)	Ming Dynasty (1368-1644AD)
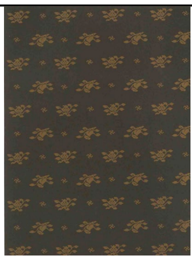		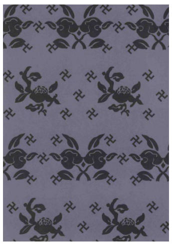		
Ming Dynasty (1368-1644AD)	Ming Dynasty (1368-1644AD)	Ming Dynasty (1368-1644AD)	Ming Dynasty (1368-1644AD)	Ming Dynasty (1368-1644AD)
			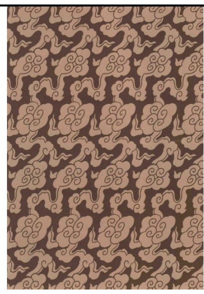	
Ming Dynasty (1368-1644AD)	Ming Dynasty (1368-1644AD)	Ming Dynasty (1368-1644AD)	Ming Dynasty (1368-1644AD)	Ming Dynasty (1368-1644AD)
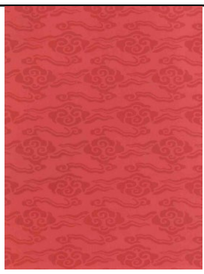		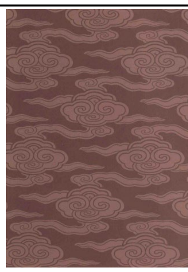	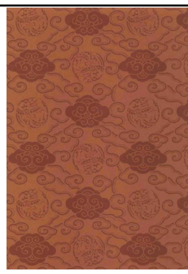	
Ming Dynasty (1368-1644AD)	Ming Dynasty (1368-1644AD)	Ming Dynasty (1368-1644AD)	Ming Dynasty (1368-1644AD)	Ming Dynasty (1368-1644AD)

Appendix 1

	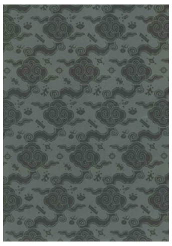			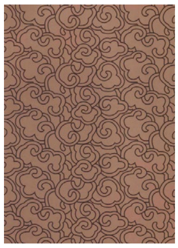
Ming Dynasty (1368-1644AD)	Ming Dynasty (1368-1644AD)	Ming Dynasty (1368-1644AD)	Ming Dynasty (1368-1644AD)	Ming Dynasty (1368-1644AD)
				
Ming Dynasty (1368-1644AD)	Ming Dynasty (1368-1644AD)	Ming Dynasty (1368-1644AD)	Ming Dynasty (1368-1644AD)	Ming Dynasty (1368-1644AD)
		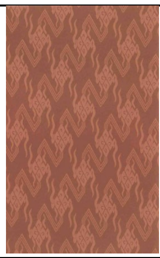		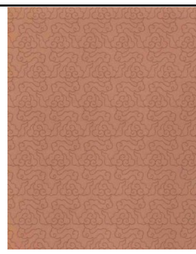
Ming Dynasty (1368-1644AD)	Ming Dynasty (1368-1644AD)	Ming Dynasty (1368-1644AD)	Ming Dynasty (1368-1644AD)	Ming Dynasty (1368-1644AD)
	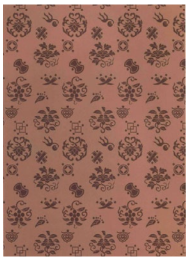	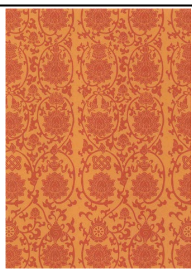	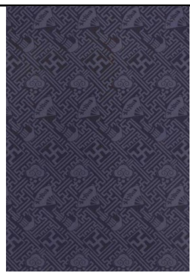	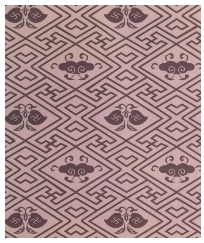
Ming Dynasty (1368-1644AD)	Ming Dynasty (1368-1644AD)	Ming Dynasty (1368-1644AD)	Ming Dynasty (1368-1644AD)	Ming Dynasty (1368-1644AD)
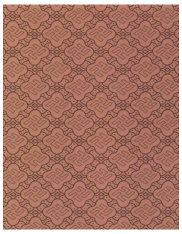	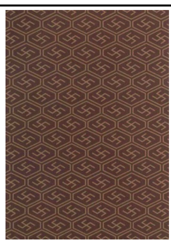	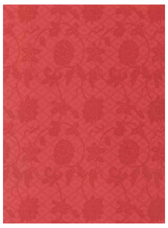		
Ming Dynasty (1368-1644AD)	Ming Dynasty (1368-1644AD)	Ming Dynasty (1368-1644AD)	Ming Dynasty (1368-1644AD)	Ming Dynasty (1368-1644AD)

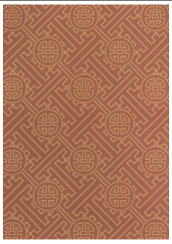			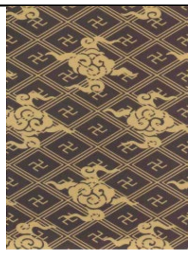	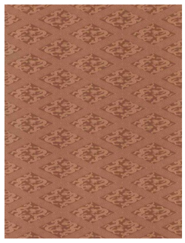
Ming Dynasty (1368-1644AD)	Ming Dynasty (1368-1644AD)	Ming Dynasty (1368-1644AD)	Ming Dynasty (1368-1644AD)	Ming Dynasty (1368-1644AD)
		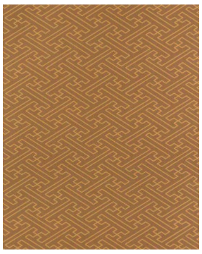		
Ming Dynasty (1368-1644AD)	Ming Dynasty (1368-1644AD)	Ming Dynasty (1368-1644AD)	Ming Dynasty (1368-1644AD)	Ming Dynasty (1368-1644AD)
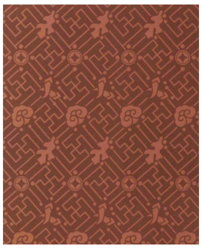	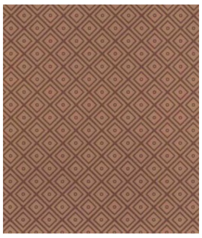	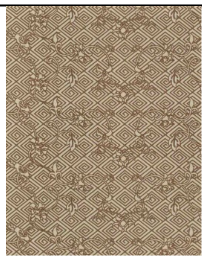		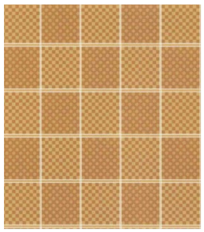
Ming Dynasty (1368-1644AD)	Ming Dynasty (1368-1644AD)	Ming Dynasty (1368-1644AD)	Ming Dynasty (1368-1644AD)	Ming Dynasty (1368-1644AD)
				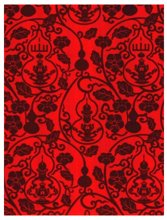
Ming Dynasty (1368-1644AD)	Ming Dynasty (1368-1644AD)	Ming Dynasty (1368-1644AD)	Ming Dynasty (1368-1644AD)	Ming Dynasty (1368-1644AD)
				
Ming Dynasty (1368-1644AD)	Ming Dynasty (1368-1644AD)	Ming Dynasty (1368-1644AD)	Ming Dynasty (1368-1644AD)	Ming Dynasty (1368-1644AD)

				
Ming Dynasty (1368-1644AD)	Ming Dynasty (1368-1644AD)	Ming Dynasty (1368-1644AD)	Ming Dynasty (1368-1644AD)	Ming Dynasty (1368-1644AD)
				
Ming Dynasty (1368-1644AD)	Ming Dynasty (1368-1644AD)	Ming Dynasty (1368-1644AD)	Ming Dynasty (1368-1644AD)	Ming Dynasty (1368-1644AD)
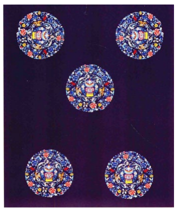	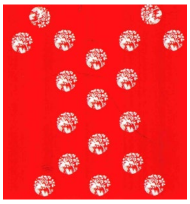		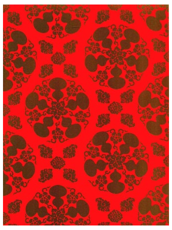	
Ming Dynasty (1368-1644AD)	Ming Dynasty (1368-1644AD)	Ming Dynasty (1368-1644AD)	Ming Dynasty (1368-1644AD)	Ming Dynasty (1368-1644AD)
				
Ming Dynasty (1368-1644AD)	Ming Dynasty (1368-1644AD)	Ming Dynasty (1368-1644AD)	Ming Dynasty (1368-1644AD)	Ming Dynasty (1368-1644AD)
				
Ming Dynasty (1368-1644AD)	Ming Dynasty (1368-1644AD)	Ming Dynasty (1368-1644AD)	Ming Dynasty (1368-1644AD)	Ming Dynasty (1368-1644AD)

				
Ming Dynasty (1368-1644AD)	Ming Dynasty (1368-1644AD)	Ming Dynasty (1368-1644AD)	Ming Dynasty (1368-1644AD)	Ming Dynasty (1368-1644AD)
				
Ming Dynasty (1368-1644AD)	Ming Dynasty (1368-1644AD)	Ming Dynasty (1368-1644AD)	Ming Dynasty (1368-1644AD)	Ming Dynasty (1368-1644AD)
			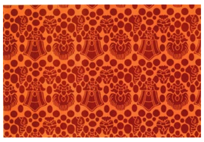	
Ming Dynasty (1368-1644AD)	Ming Dynasty (1368-1644AD)	Ming Dynasty (1368-1644AD)	Ming Dynasty (1368-1644AD)	Ming Dynasty (1368-1644AD)
	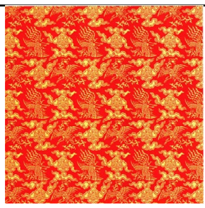	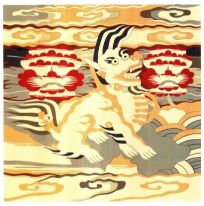		
Ming Dynasty (1368-1644AD)	Ming Dynasty (1368-1644AD)	Ming Dynasty (1368-1644AD)	Ming Dynasty (1368-1644AD)	Ming Dynasty (1368-1644AD)
				
Ming Dynasty (1368-1644AD)	Ming Dynasty (1368-1644AD)	Ming Dynasty (1368-1644AD)	Ming Dynasty (1368-1644AD)	Ming Dynasty (1368-1644AD)

				
Ming Dynasty (1368-1644AD)	Ming Dynasty (1368-1644AD)	Ming Dynasty (1368-1644AD)	Ming Dynasty (1368-1644AD)	Ming Dynasty (1368-1644AD)
				
Ming Dynasty (1368-1644AD)	Ming Dynasty (1368-1644AD)	Ming Dynasty (1368-1644AD)	Ming Dynasty (1368-1644AD)	Ming Dynasty (1368-1644AD)
				
Ming Dynasty (1368-1644AD)	Ming Dynasty (1368-1644AD)	Ming Dynasty (1368-1644AD)	Ming Dynasty (1368-1644AD)	Ming Dynasty (1368-1644AD)
				
Ming Dynasty (1368-1644AD)	Ming Dynasty (1368-1644AD)	Ming Dynasty (1368-1644AD)	Ming Dynasty (1368-1644AD)	Ming Dynasty (1368-1644AD)
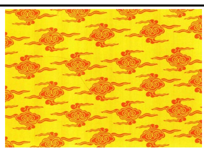	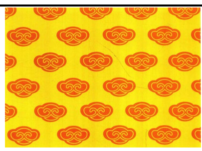			
Ming Dynasty (1368-1644AD)	Ming Dynasty (1368-1644AD)	Ming Dynasty (1368-1644AD)	Ming Dynasty (1368-1644AD)	Ming Dynasty (1368-1644AD)

				
Ming Dynasty (1368-1644AD)	Ming Dynasty (1368-1644AD)	Ming Dynasty (1368-1644AD)	Ming Dynasty (1368-1644AD)	Ming Dynasty (1368-1644AD)
				
Ming Dynasty (1368-1644AD)	Ming Dynasty (1368-1644AD)	Ming Dynasty (1368-1644AD)	Ming Dynasty (1368-1644AD)	Ming Dynasty (1368-1644AD)
		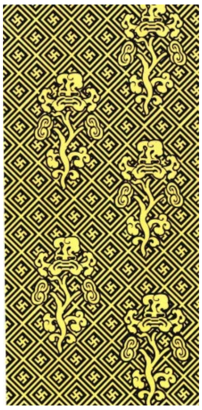		
Ming Dynasty (1368-1644AD)	Ming Dynasty (1368-1644AD)	Ming Dynasty (1368-1644AD)	Ming Dynasty (1368-1644AD)	Ming Dynasty (1368-1644AD)

				
Ming Dynasty (1368-1644AD)	Ming Dynasty (1368-1644AD)	Ming Dynasty (1368-1644AD)	Ming Dynasty (1368-1644AD)	Ming Dynasty (1368-1644AD)
		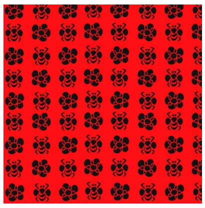		
Ming Dynasty (1368-1644AD)	Ming Dynasty (1368-1644AD)	Ming Dynasty (1368-1644AD)	Ming Dynasty (1368-1644AD)	Ming Dynasty (1368-1644AD)
				
Ming Dynasty (1368-1644AD)	Ming Dynasty (1368-1644AD)	Ming Dynasty (1368-1644AD)	Ming Dynasty (1368-1644AD)	Ming Dynasty (1368-1644AD)
				
Ming Dynasty (1368-1644AD)	Ming Dynasty (1368-1644AD)	Ming Dynasty (1368-1644AD)	Ming Dynasty (1368-1644AD)	Ming Dynasty (1368-1644AD)
				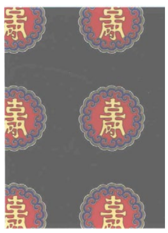

Ming Dynasty (1368-1644AD)	Ming Dynasty (1368-1644AD)	Ming Dynasty (1368-1644AD)	Ming Dynasty (1368-1644AD)	Ming Dynasty (1368-1644AD)
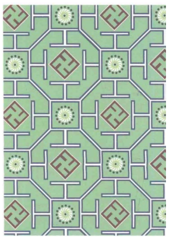				
Ming Dynasty (1368-1644AD)	Ming Dynasty (1368-1644AD)	Ming Dynasty (1368-1644AD)	Ming Dynasty (1368-1644AD)	Ming Dynasty (1368-1644AD)
	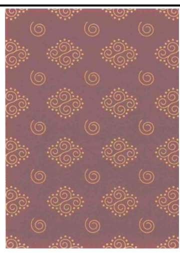	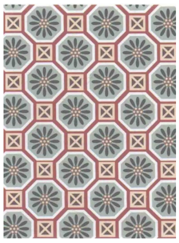		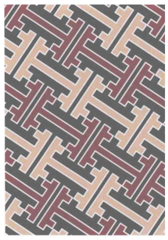
Ming Dynasty (1368-1644AD)	Ming Dynasty (1368-1644AD)	Ming Dynasty (1368-1644AD)	Ming Dynasty (1368-1644AD)	Ming Dynasty (1368-1644AD)
			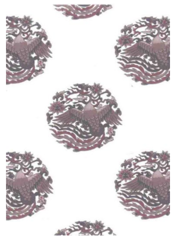	
Ming Dynasty (1368-1644AD)	Ming Dynasty (1368-1644AD)	Ming Dynasty (1368-1644AD)	Ming Dynasty (1368-1644AD)	Ming Dynasty (1368-1644AD)
	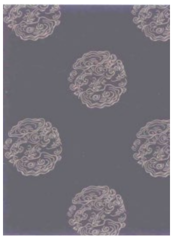	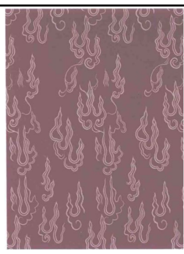	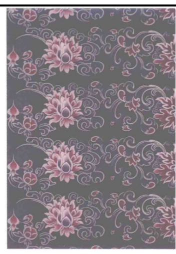	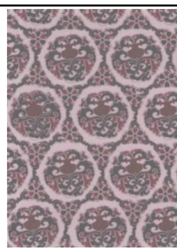
Ming Dynasty (1368-1644AD)	Ming Dynasty (1368-1644AD)	Ming Dynasty (1368-1644AD)	Ming Dynasty (1368-1644AD)	Ming Dynasty (1368-1644AD)
		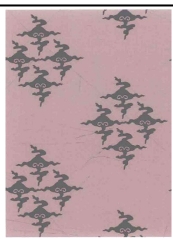		
Ming Dynasty (1368-1644AD)	Ming Dynasty (1368-1644AD)	Ming Dynasty (1368-1644AD)	Ming Dynasty (1368-1644AD)	Ming Dynasty (1368-1644AD)

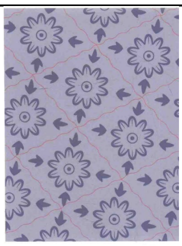			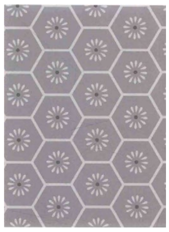	
Ming Dynasty (1368-1644AD)	Ming Dynasty (1368-1644AD)	Ming Dynasty (1368-1644AD)	Ming Dynasty (1368-1644AD)	Ming Dynasty (1368-1644AD)
	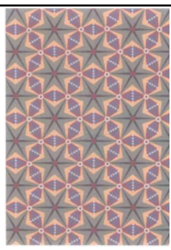	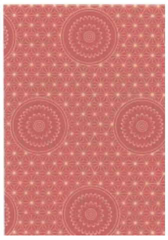	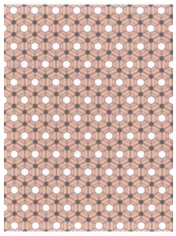	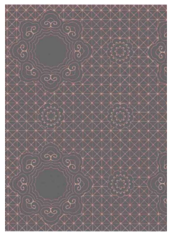
Ming Dynasty (1368-1644AD)	Ming Dynasty (1368-1644AD)	Ming Dynasty (1368-1644AD)	Ming Dynasty (1368-1644AD)	Ming Dynasty (1368-1644AD)
			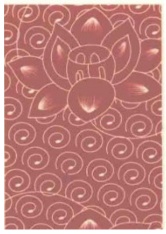	
Ming Dynasty (1368-1644AD)	Ming Dynasty (1368-1644AD)	Ming Dynasty (1368-1644AD)	Ming Dynasty (1368-1644AD)	Ming Dynasty (1368-1644AD)
			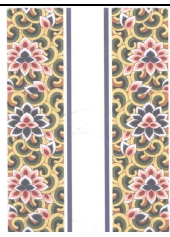	
Ming Dynasty (1368-1644AD)	Ming Dynasty (1368-1644AD)	Ming Dynasty (1368-1644AD)	Ming Dynasty (1368-1644AD)	Ming Dynasty (1368-1644AD)
			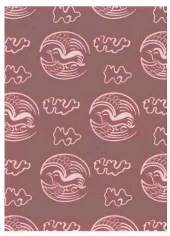	
Ming Dynasty (1368-1644AD)	Ming Dynasty (1368-1644AD)	Ming Dynasty (1368-1644AD)	Ming Dynasty (1368-1644AD)	Ming and Qing Dynasties (1368-1912AD)

		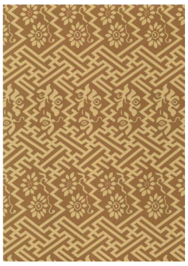	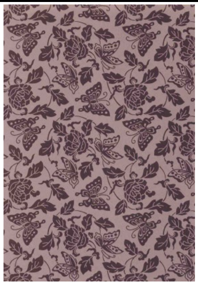	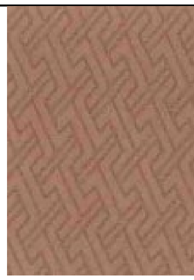
Ming and Qing Dynasties (1368-1912AD)	Ming and Qing Dynasties (1368-1912AD)	Ming and Qing Dynasties (1368-1912AD)	Ming and Qing Dynasties (1368-1912AD)	Ming and Qing Dynasties (1368-1912AD)
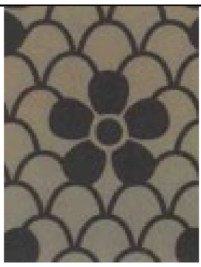		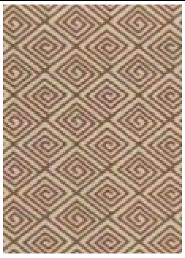	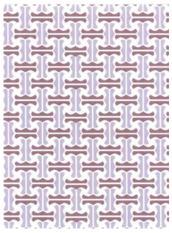	
Ming and Qing Dynasties (1368-1912AD)	Ming and Qing Dynasties (1368-1912AD)	Ming and Qing Dynasties (1368-1912AD)	Qing Dynasties (1636-1912AD)	Qing Dynasties (1636-1912AD)
				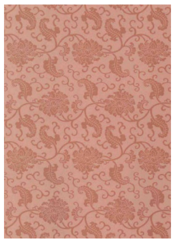
Qing Dynasties (1636-1912AD)	Qing Dynasties (1636-1912AD)	Qing Dynasties (1636-1912AD)	Qing Dynasties (1636-1912AD)	Qing Dynasties (1636-1912AD)
			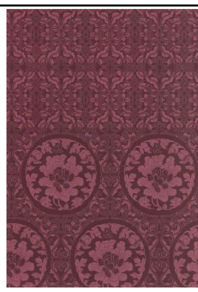	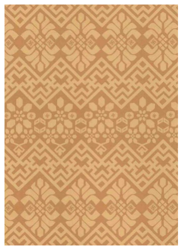
Qing Dynasties (1636-1912AD)	Qing Dynasties (1636-1912AD)	Qing Dynasties (1636-1912AD)	Qing Dynasties (1636-1912AD)	Qing Dynasties (1636-1912AD)
	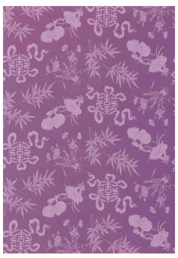			
Qing Dynasties (1636-1912AD)	Qing Dynasties (1636-1912AD)	Qing Dynasties (1636-1912AD)	Qing Dynasties (1636-1912AD)	Qing Dynasties (1636-1912AD)

			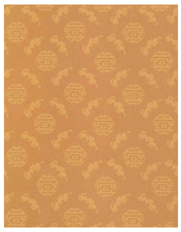	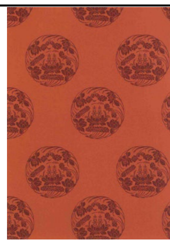
Qing Dynasties (1636-1912AD)	Qing Dynasties (1636-1912AD)	Qing Dynasties (1636-1912AD)	Qing Dynasties (1636-1912AD)	Qing Dynasties (1636-1912AD)
				
Qing Dynasties (1636-1912AD)	Qing Dynasties (1636-1912AD)	Qing Dynasties (1636-1912AD)	Qing Dynasties (1636-1912AD)	Qing Dynasties (1636-1912AD)
				
Qing Dynasties (1636-1912AD)	Qing Dynasties (1636-1912AD)	Qing Dynasties (1636-1912AD)	Qing Dynasties (1636-1912AD)	Qing Dynasties (1636-1912AD)
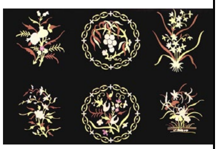			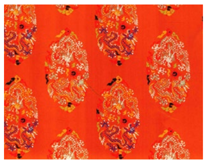	
Qing Dynasties (1636-1912AD)	Qing Dynasties (1636-1912AD)	Qing Dynasties (1636-1912AD)	Qing Dynasties (1636-1912AD)	Qing Dynasties (1636-1912AD)
				
Qing Dynasties (1636-1912AD)	Qing Dynasties (1636-1912AD)	Qing Dynasties (1636-1912AD)	Qing Dynasties (1636-1912AD)	Qing Dynasties (1636-1912AD)
	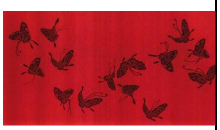			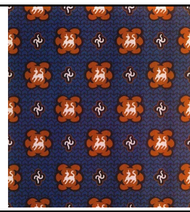
Qing Dynasties (1636-1912AD)	Qing Dynasties (1636-1912AD)	Qing Dynasties (1636-1912AD)	Qing Dynasties (1636-1912AD)	Qing Dynasties (1636-1912AD)

				
Qing Dynasties (1636-1912AD)	Qing Dynasties (1636-1912AD)	Qing Dynasties (1636-1912AD)	Qing Dynasties (1636-1912AD)	Qing Dynasties (1636-1912AD)
				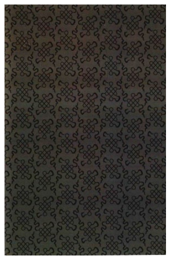
Qing Dynasties (1636-1912AD)	Qing Dynasties (1636-1912AD)	Qing Dynasties (1636-1912AD)	Qing Dynasties (1636-1912AD)	Qing Dynasties (1636-1912AD)
			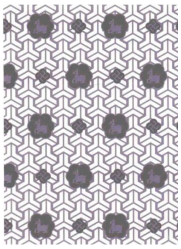	
Qing Dynasties (1636-1912AD)	Qing Dynasties (1636-1912AD)	Qing Dynasties (1636-1912AD)	Qing Dynasties (1636-1912AD)	Qing Dynasties (1636-1912AD)
	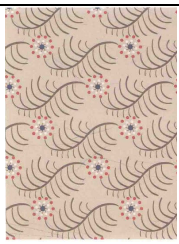		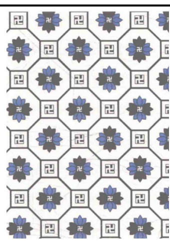	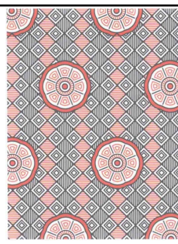
Qing Dynasties (1636-1912AD)	Qing Dynasties (1636-1912AD)	Qing Dynasties (1636-1912AD)	Qing Dynasties (1636-1912AD)	Qing Dynasties (1636-1912AD)
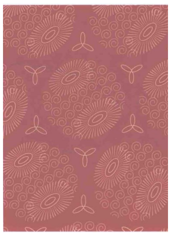	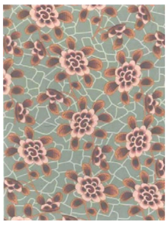			
Qing Dynasties (1636-1912AD)	Qing Dynasties (1636-1912AD)	Qing Dynasties (1636-1912AD)	Qing Dynasties (1636-1912AD)	Qing Dynasties (1636-1912AD)

		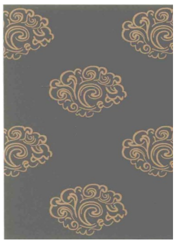	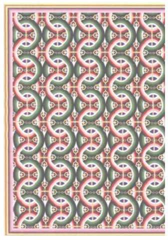	
Qing Dynasties (1636-1912AD)	Qing Dynasties (1636-1912AD)	Qing Dynasties (1636-1912AD)	Qing Dynasties (1636-1912AD)	Qing Dynasties (1636-1912AD)
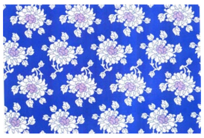				
Qing Dynasties (1636-1912AD)	Qing Dynasties (1636-1912AD)	Qing Dynasties (1636-1912AD)	Qing Dynasties (1636-1912AD)	Qing Dynasties (1636-1912AD)
		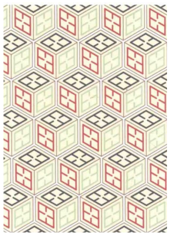	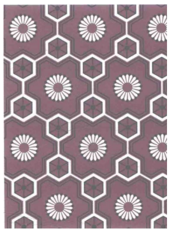	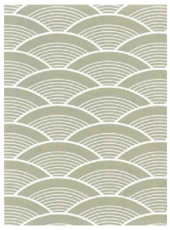
Qing Dynasties (1636-1912AD)	Qing Dynasties (1636-1912AD)	Qing Dynasties (1636-1912AD)	Qing Dynasties (1636-1912AD)	Qing Dynasties (1636-1912AD)
				
Qing Dynasties (1636-1912AD)	Qing Dynasties (1636-1912AD)	Qing Dynasties (1636-1912AD)	Qing Dynasties (1636-1912AD)	Qing Dynasties (1636-1912AD)
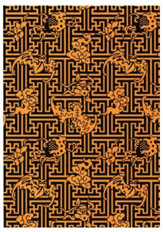				
Qing Dynasties (1636-1912AD)	Qing Dynasties (1636-1912AD)	Qing Dynasties (1636-1912AD)	Qing Dynasties (1636-1912AD)	Qing Dynasties (1636-1912AD)

				
Qing Dynasties (1636-1912AD)	Qing Dynasties (1636-1912AD)	Qing Dynasties (1636-1912AD)	Qing Dynasties (1636-1912AD)	Qing Dynasties (1636-1912AD)
				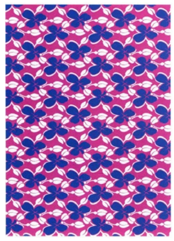
Qing Dynasties (1636-1912AD)	Qing Dynasties (1636-1912AD)	Qing Dynasties (1636-1912AD)	Qing Dynasties (1636-1912AD)	Qing Dynasties (1636-1912AD)
				
Qing Dynasties (1636-1912AD)	Qing Dynasties (1636-1912AD)	Qing Dynasties (1636-1912AD)	Qing Dynasties (1636-1912AD)	Qing Dynasties (1636-1912AD)
				
Qing Dynasties (1636-1912AD)	Qing Dynasties (1636-1912AD)	Qing Dynasties (1636-1912AD)	Qing Dynasties (1636-1912AD)	Qing Dynasties (1636-1912AD)
				
Qing Dynasties (1636-1912AD)	Qing Dynasties (1636-1912AD)	Qing Dynasties (1636-1912AD)	Qing Dynasties (1636-1912AD)	Qing Dynasties (1636-1912AD)

				
Qing Dynasties (1636-1912AD)	Qing Dynasties (1636-1912AD)	Qing Dynasties (1636-1912AD)	Qing Dynasties (1636-1912AD)	Qing Dynasties (1636-1912AD)
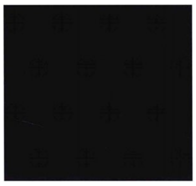				
Qing Dynasties (1636-1912AD)	Qing Dynasties (1636-1912AD)	Qing Dynasties (1636-1912AD)	Qing Dynasties (1636-1912AD)	Qing Dynasties (1636-1912AD)
			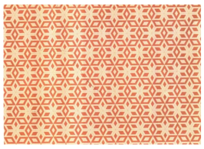	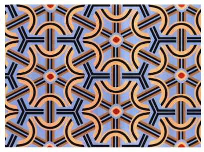
Qing Dynasties (1636-1912AD)	Qing Dynasties (1636-1912AD)	Qing Dynasties (1636-1912AD)	Qing Dynasties (1636-1912AD)	Qing Dynasties (1636-1912AD)
	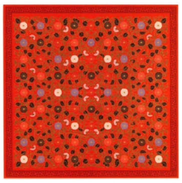			
Qing Dynasties (1636-1912AD)	Qing Dynasties (1636-1912AD)	Qing Dynasties (1636-1912AD)	Qing Dynasties (1636-1912AD)	Qing Dynasties (1636-1912AD)
		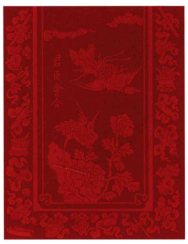		
Qing Dynasties (1636-1912AD)	Qing Dynasties (1636-1912AD)	Qing Dynasties (1636-1912AD)	Qing Dynasties (1636-1912AD)	Qing Dynasties (1636-1912AD)

				
Qing Dynasties (1636-1912AD)	Qing Dynasties (1636-1912AD)	Qing Dynasties (1636-1912AD)	Qing Dynasties (1636-1912AD)	the Republic of China era (1912-1949AD)
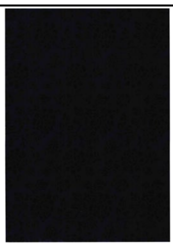				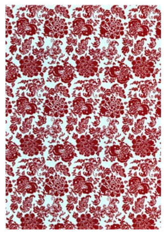
Qing Dynasties (1636-1912AD)	Qing Dynasties (1636-1912AD)	Qing Dynasties (1636-1912AD)	Qing Dynasties (1636-1912AD)	Qing Dynasties (1636-1912AD)
			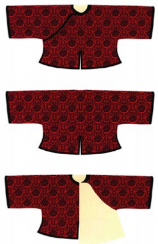	
Qing Dynasties (1636-1912AD)	Qing Dynasties (1636-1912AD)	Qing Dynasties (1636-1912AD)	Qing Dynasties (1636-1912AD)	Qing Dynasties (1636-1912AD)
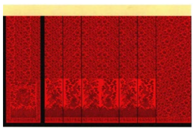				
Qing Dynasties (1636-1912AD)	Qing Dynasties (1636-1912AD)	Qing Dynasties (1636-1912AD)	Qing Dynasties (1636-1912AD)	Qing Dynasties (1636-1912AD)
				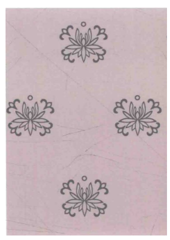
Qing Dynasties (1636-1912AD)	Qing Dynasties (1636-1912AD)	Qing Dynasties (1636-1912AD)	Qing Dynasties (1636-1912AD)	Qing Dynasties (1636-1912AD)

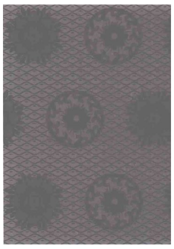		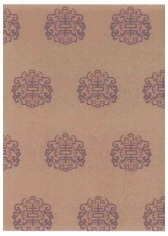	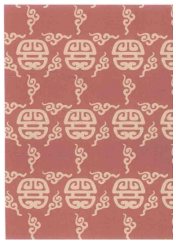	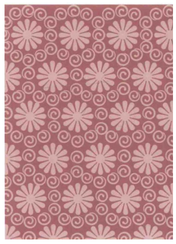
Qing Dynasties (1636-1912AD)	Qing Dynasties (1636-1912AD)	Qing Dynasties (1636-1912AD)	Qing Dynasties (1636-1912AD)	Qing Dynasties (1636-1912AD)
		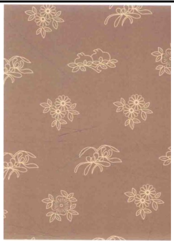		
Qing Dynasties (1636-1912AD)	Qing Dynasties (1636-1912AD)	Qing Dynasties (1636-1912AD)	Qing Dynasties (1636-1912AD)	Qing Dynasties (1636-1912AD)
				
Qing Dynasties (1636-1912AD)	Qing Dynasties (1636-1912AD)	Qing Dynasties (1636-1912AD)	Qing Dynasties (1636-1912AD)	Qing Dynasties (1636-1912AD)
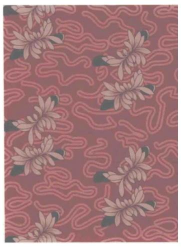	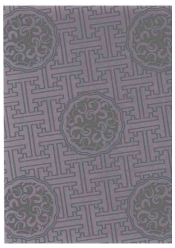			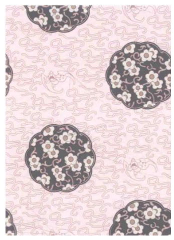
Qing Dynasties (1636-1912AD)	Qing Dynasties (1636-1912AD)	Qing Dynasties (1636-1912AD)	Qing Dynasties (1636-1912AD)	Qing Dynasties (1636-1912AD)
		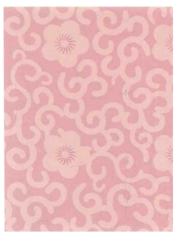		
Qing Dynasties (1636-1912AD)	Qing Dynasties (1636-1912AD)	Qing Dynasties (1636-1912AD)	Qing Dynasties (1636-1912AD)	Qing Dynasties (1636-1912AD)

	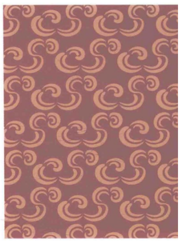	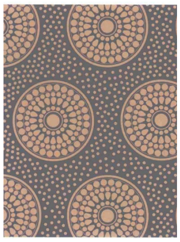	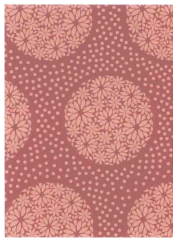	
Qing Dynasties (1636-1912AD)	Qing Dynasties (1636-1912AD)	Qing Dynasties (1636-1912AD)	Qing Dynasties (1636-1912AD)	Qing Dynasties (1636-1912AD)
			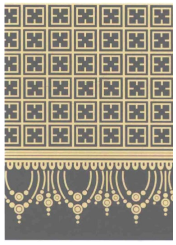	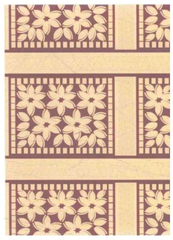
Qing Dynasties (1636-1912AD)	Qing Dynasties (1636-1912AD)	Qing Dynasties (1636-1912AD)	Qing Dynasties (1636-1912AD)	Qing Dynasties (1636-1912AD)
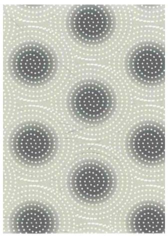				
Qing Dynasties (1636-1912AD)	Qing Dynasties (1636-1912AD)	Qing Dynasties (1636-1912AD)	Qing Dynasties (1636-1912AD)	Qing Dynasties (1636-1912AD)
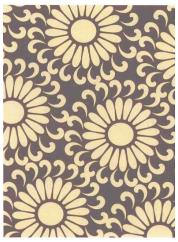				
Qing Dynasties (1636-1912AD)	Qing Dynasties (1636-1912AD)	Qing Dynasties (1636-1912AD)	Qing Dynasties (1636-1912AD)	Qing Dynasties (1636-1912AD)
				
Qing Dynasties (1636-1912AD)	Qing Dynasties (1636-1912AD)	Qing Dynasties (1636-1912AD)	藏传 :菱格花卉纹	藏传 ：寿字纹

	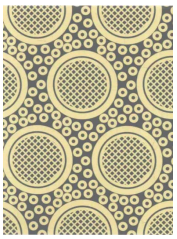			
藏传：如意棋格纹	藏传：珠地团窠纹	藏传：卍字纹		

Appendix 2: Python code for costume style and textile pattern restoration based on DCGAN

```
import torch
import torch.nn as nn
from torch.utils.data import Dataset, DataLoader
from torchvision import transforms, models

# 1. Definition generator and discriminator
class Generator(nn.Module):
    def __init__(self):
        super().__init__()
        self.main = nn.Sequential(
            nn.Linear(100, 4*4*1024),
            nn.BatchNorm1d(4*4*1024),
            nn.ReLU(),
            # Transposed convolution...
        )

    def forward(self, noise, mask):
            # Realize noise to image generation and mask fusion
            return generated_img

class Discriminator(nn.Module):
    def __init__(self):
        super().__init__()
        self.main = nn.Sequential(
            nn.Conv2d(3, 64, 4, stride=2, padding=1),
            nn.LeakyReLU(0.2),
            # Convolution layer...
        )

def forward(self, img):
    return prob_real

# 2. Data loading and pre-processing
class CostumeDataset(Dataset):
```

```
    def __init__(self, img_paths, mask_paths):
        self.transform = transforms.Compose([
            transforms.Resize(128),
            transforms.ToTensor(),
            transforms.Normalize([0.5]*3, [0.5]*3)
        ])

    def __getitem__(self, idx):
        img = Image.open(img_paths[idx])
        mask = Image.open(mask_paths[idx])
        return self.transform(img), self.transform(mask)

# 3. Training cycle
device = torch.device("cuda" if torch.cuda.is_available() else "cpu")
G = Generator().to(device)
D = Discriminator().to(device)

for epoch in range(num_epochs):
    for real_imgs, masks in dataloader:
        # Training discriminator
        D.zero_grad()
        noise = torch.randn(real_imgs.size(0), 100, device=device)
        fake_imgs = G(noise, masks)
        d_loss_real = torch.mean(D(real_imgs))
        d_loss_fake = torch.mean(D(fake_imgs.detach()))
        d_loss = -torch.mean(torch.log(d_loss_real) + torch.log(1 - d_loss_fake))
        d_loss.backward()
        D_optimizer.step()

        # Training Builder
        G.zero_grad()
        g_loss = -torch.mean(torch.log(D(fake_imgs)))
        g_loss.backward()
        G_optimizer.step()
```

Appendix 3: The dataset for color simulation and restoration of costume relics

序号	Time (hours)	L*	a*	b*
1	0	52.39737132	62.09628	40.6951
2	0.5	51.87119174	62.53298	41.52889
3	1	52.48176357	61.22639	39.91043
4	1.5	53.16385254	63.22635	40.01604
5	2	51.73992824	60.18891	40.67524
6	2.5	51.72177001	62.94771	39.80003
7	3	53.15428483	61.704	39.35068
8	3.5	52.48670372	62.49901	39.65482
9	4	51.47902414	61.94484	40.63399
10	4.5	52.27050575	61.88746	41.31116
11	5	51.44758397	62.01092	41.30641
12	5.5	51.42760109	62.17168	42.03424
13	6	51.97562782	61.21832	40.82384
14	6.5	50.23331325	62.2662	40.91009
15	7	50.36588898	60.52779	40.49943
16	7.5	51.27788535	61.34814	40.51693
17	8	50.89934894	61.97825	42.32148
18	8.5	51.94291651	62.06259	40.84478
19	9	50.94701052	61.59233	40.89299
20	9.5	50.52550428	60.86615	39.67697
21	10	52.80979005	61.85541	40.90009
22	10.5	51.43858011	60.55977	41.07712
23	11	51.65516015	62.45364	41.41742
24	11.5	50.4432818	60.94206	41.01197

25	12	51.12952325	59.7354	40.38525
26	12.5	51.6357229	59.96869	40.32985
27	13	50.60815168	60.91672	40.38649
28	13.5	51.81147298	60.95106	40.50867
29	14	51.01237795	62.37236	41.41583
30	14.5	51.24151455	59.92329	41.23861
31	15	50.9754912	60.74315	40.96164
32	15.5	52.92067229	59.82156	41.96149
33	16	51.41005152	60.23252	38.19196
34	16.5	50.55668641	61.93139	39.92775
35	17	52.04290323	59.63275	40.26562
36	17.5	50.39021082	60.96909	39.71572
37	18	51.51600135	60.77145	39.48858
38	18.5	49.7632054	60.39548	38.83753
39	19	50.25042998	60.78809	39.94109
40	19.5	51.45251141	59.40228	40.88428
41	20	51.86784557	61.61314	40.76713
42	20.5	51.39622309	61.78577	39.5252
43	21	51.14867229	60.24142	40.28204
44	21.5	50.98237668	62.10009	41.17087
45	22	50.02251704	59.80029	38.8477
46	22.5	50.61154053	60.39778	39.91566
47	23	50.80099242	61.18091	40.25091
48	23.5	51.99729503	59.62619	40.00872
49	24	51.40859195	58.84617	40.66022
50	24.5	49.70537153	58.62008	38.76046
51	25	51.35718343	61.5162	39.1331
52	25.5	50.77196929	59.40242	40.46242

53	26	50.52062263	59.63519	38.53406
54	26.5	51.53363263	58.85173	40.52431
55	27	51.85122884	60.45881	40.21383
56	27.5	51.75359719	59.03312	40.42659
57	28	50.3193492	59.22361	39.43672
58	28.5	50.72550969	59.81452	40.19912
59	29	51.22005295	58.68198	38.83254
60	29.5	51.71764716	59.34869	39.41789
61	30	50.53604677	60.57169	39.7577
62	30.5	50.75304031	59.75093	38.98878
63	31	49.99868708	59.47119	39.86142
64	31.5	49.90898356	59.4971	38.75074
65	32	51.49816955	58.97239	39.86021
66	32.5	51.91534718	60.83914	41.01796
67	33	50.75495955	58.55103	38.59835
68	33.5	51.59761268	59.32808	39.56485
69	34	51.06632011	59.20996	38.26775
70	34.5	50.24314665	59.88358	38.87499
71	35	51.03059631	59.91777	40.08216
72	35.5	51.95415267	58.9683	39.15535
73	36	50.67731239	59.18517	40.07305
74	36.5	51.93994416	59.17421	39.74311
75	37	48.57469537	57.05245	39.38608
76	37.5	51.31028189	57.55778	38.59346
77	38	50.70467218	58.30375	39.9447
78	38.5	50.37810948	58.29739	39.61894
79	39	50.67301102	57.74613	38.13253
80	39.5	48.99184051	59.26414	38.56269

81	40	50.38845756	58.62512	37.09844
82	40.5	50.83219076	58.41065	38.20053
83	41	51.71112776	57.53649	39.0217
84	41.5	50.09651436	58.46481	38.40711
85	42	49.84665985	56.35816	38.56586
86	42.5	50.07437948	58.28824	40.32305
87	43	51.19044337	58.42827	40.01307
88	43.5	50.70346532	58.53041	38.61371
89	44	49.99900519	57.04477	39.78372
90	44.5	50.8157824	58.43511	40.10024
91	45	50.46519178	57.38135	39.60264
92	45.5	51.14481318	57.52378	39.32642
93	46	49.79062833	58.7074	39.94542
94	46.5	50.07252088	59.70366	39.66187
95	47	50.00335003	58.09281	38.05529
96	47.5	49.12861671	57.35742	38.85414
97	48	50.51872317	58.12144	38.54315
98	48.5	50.47307561	58.68117	39.88633
99	49	50.25073275	58.3862	38.47956
100	49.5	50.04138903	60.04339	38.32171
101	50	49.07918505	57.23615	39.72437
102	50.5	49.85739444	57.96975	39.09035
103	51	49.90217429	58.96668	40.55163
104	51.5	49.51696544	58.87607	38.15201
105	52	50.01220619	56.08672	38.40635
106	52.5	50.44692908	57.60375	39.69861
107	53	51.61509689	58.75375	37.7574
108	53.5	50.22827634	59.83836	39.81607

109	54	50.27712645	58.04863	37.77401
110	54.5	49.9940076	57.15108	39.20782
111	55	48.50103167	56.59781	37.22488
112	55.5	49.99732799	59.14	38.71511
113	56	50.04921984	57.90785	37.56308
114	56.5	51.95413206	56.60629	40.17944
115	57	49.81215842	57.08214	37.76083
116	57.5	50.18980001	57.45275	37.93478
117	58	49.90331378	57.59962	39.00595
118	58.5	48.97866795	56.40488	38.0766
119	59	50.81040192	56.59325	39.09709
120	59.5	50.4802295	55.72231	37.94819
121	60	50.49405415	57.83655	37.86632
122	60.5	49.11627025	56.69155	38.45443
123	61	50.94857339	57.29804	37.48274
124	61.5	48.68742093	58.02296	38.75319
125	62	50.26095739	57.02124	39.11776
126	62.5	51.52641225	56.71519	38.83816
127	63	48.96420082	56.92096	38.89023
128	63.5	49.28617992	56.77665	36.81558
129	64	49.80153352	57.68334	37.96602
130	64.5	49.30163231	56.89541	38.13356
131	65	48.44648859	56.17158	39.45867
132	65.5	49.7244823	57.40577	37.80996
133	66	48.80240762	57.51229	36.41353
134	66.5	50.01374929	55.41768	37.43166
135	67	48.88196679	57.67505	37.68581
136	67.5	50.84009061	56.70109	36.46953

137	68	48.95618344	56.59646	38.94963
138	68.5	49.30778592	57.1357	36.89896
139	69	50.19890404	55.8374	38.49142
140	69.5	48.54606002	57.01493	37.24067
141	70	49.69538669	55.91081	39.30017
142	70.5	50.54180628	54.99294	37.85366
143	71	48.19278489	55.33538	37.67131
144	71.5	49.60916403	56.54793	38.45723
145	72	49.65205469	55.29868	37.20883
146	72.5	50.05230433	57.30389	38.45515
147	73	48.4199891	56.92806	37.58944
148	73.5	48.33589406	57.00422	37.47916
149	74	49.79252834	55.99815	37.86487
150	74.5	49.5952846	56.0655	37.04327
151	75	49.54081898	54.86515	37.7424
152	75.5	49.60031714	56.57769	38.14681
153	76	48.76187871	56.04589	36.00835
154	76.5	49.4744474	56.15687	38.70852
155	77	49.50585441	57.01469	38.4684
156	77.5	48.68267333	55.14032	36.3121
157	78	50.72953813	55.48525	36.16758
158	78.5	49.59875495	55.80861	38.42963
159	79	48.24942194	54.76005	38.3479
160	79.5	49.71048978	55.31948	38.21491
161	80	48.38828973	55.8251	36.55514
162	80.5	49.78049695	55.13162	39.13981
163	81	50.06050595	56.40039	37.05312
164	81.5	48.45988987	54.10572	37.82894

165	82	49.86994888	56.17397	37.81902
166	82.5	49.41229099	55.76602	38.8722
167	83	49.72253866	54.74336	37.67826
168	83.5	50.56515521	54.42027	37.89107
169	84	48.83424663	53.45697	37.47699
170	84.5	48.4104105	54.44649	36.56171
171	85	48.2846362	55.88182	35.64436
172	85.5	48.32645383	54.9607	37.50567
173	86	48.90028101	55.89746	36.33005
174	86.5	49.21775027	54.43272	37.72042
175	87	49.14905363	55.45586	37.53963
176	87.5	49.57232589	54.27777	37.50053
177	88	48.9038651	54.04092	36.53902
178	88.5	50.03918113	54.68933	38.19097
179	89	48.64752467	54.20473	37.72194
180	89.5	51.01828773	53.46414	36.37717
181	90	49.32559451	54.51427	38.95778
182	90.5	48.12224881	54.70702	37.11473
183	91	47.93418105	55.59834	36.19636
184	91.5	49.15979916	55.2949	36.63755
185	92	48.57798314	55.48324	36.01757
186	92.5	49.31089189	55.04543	38.29269
187	93	49.10122569	54.69712	38.04998
188	93.5	48.64732252	53.40979	37.75768
189	94	48.0111067	54.47478	37.58751
190	94.5	47.45962589	54.79428	38.12577
191	95	48.29725966	55.44479	36.91401
192	95.5	49.32256457	54.78988	37.42626

193	96	48.79170041	55.19521	36.41915
194	96.5	47.60682022	53.33937	36.92645
195	97	48.72494776	53.86593	37.38983
196	97.5	48.87765466	54.43267	34.54542
197	98	47.84531849	54.9801	36.49514
198	98.5	48.65839416	53.89734	37.10348
199	99	48.56499663	53.90977	36.89007
200	99.5	47.58707493	54.48767	36.57077
201	100	48.77070852	52.99951	37.38463
202	100.5	48.91613966	55.14842	36.32776
203	101	49.31699237	53.12149	35.89704
204	101.5	49.27663829	52.25227	37.80223
205	102	47.31451236	53.75755	37.66999
206	102.5	47.64944496	55.07066	36.33722
207	103	48.79479628	54.14347	36.74226
208	103.5	48.77686582	54.23762	37.45469
209	104	48.76095013	53.63232	36.79382
210	104.5	51.41417801	53.4398	37.16347
211	105	48.77179199	52.2883	37.10047
212	105.5	49.20662477	51.67926	36.44541
213	106	49.04447227	53.60636	37.09422
214	106.5	48.78548837	54.46198	35.89027
215	107	47.9952704	53.64988	36.95841
216	107.5	48.83777751	53.8361	36.56448
217	108	47.5954642	54.56687	36.31596
218	108.5	48.00739764	53.52561	35.58793
219	109	47.79169574	53.1272	36.67145
220	109.5	48.22862584	52.53326	36.57775

221	110	49.99799924	54.76864	35.85603
222	110.5	46.63561199	53.53491	35.23107
223	111	48.66158994	52.32162	35.17383
224	111.5	46.80557264	52.10243	36.267
225	112	47.70136927	54.0047	36.69631
226	112.5	48.93325057	52.13521	37.91196
227	113	48.09669532	54.41117	36.37674
228	113.5	47.16626258	50.68589	35.09344
229	114	47.43940841	53.99213	36.20911
230	114.5	48.53852844	53.20658	37.35665
231	115	47.39376168	52.87498	35.79024
232	115.5	48.13443248	52.60281	37.21229
233	116	47.98093957	54.21885	36.43892
234	116.5	47.40642419	53.23503	36.7968
235	117	49.62608798	51.90997	37.74733
236	117.5	48.40130203	51.22057	34.77141
237	118	46.25729272	52.70073	36.9394
238	118.5	48.00981608	52.52126	36.12742
239	119	47.31447516	51.26947	35.42484
240	119.5	48.50910856	52.40432	36.08468
241	120	47.17640873	51.95279	37.49899
242	120.5	47.70190544	52.38269	37.19519
243	121	48.18095955	52.91935	34.5077
244	121.5	48.45285487	53.49608	35.47345
245	122	46.78330043	52.9925	36.8247
246	122.5	47.45922925	51.65166	36.03405
247	123	47.33017252	52.4874	36.01812
248	123.5	47.17076976	52.20623	34.75895

249	124	49.08910676	51.05355	35.39833
250	124.5	47.9840448	52.40137	34.88926
251	125	46.63467416	53.53167	34.63428
252	125.5	48.36099862	52.03586	34.93188
253	126	49.30776759	50.69818	35.17673
254	126.5	48.41935424	51.96137	35.29146
255	127	46.36123129	50.92984	35.2078
256	127.5	47.17269106	52.55538	36.67904
257	128	48.55696412	52.24809	35.11814
258	128.5	46.96066234	51.6552	36.96599
259	129	47.86522199	51.49076	35.41906
260	129.5	48.11324804	51.54969	36.1388
261	130	46.73537659	51.6899	36.14557
262	130.5	47.41268667	51.02933	35.03161
263	131	44.85068488	50.50077	35.46865
264	131.5	46.60758625	52.48582	35.31001
265	132	47.20844526	51.23045	35.99158
266	132.5	46.39568247	51.63634	35.57181
267	133	48.68325309	51.69489	35.05745
268	133.5	46.21663178	51.68827	35.7327
269	134	46.99213593	50.45561	35.89044
270	134.5	47.43219643	50.01803	37.08009
271	135	48.46406083	50.85181	35.63587
272	135.5	46.14579651	51.60342	35.5707
273	136	48.20846706	50.6686	35.88674
274	136.5	47.26957813	50.93116	34.76585
275	137	46.45964616	52.8811	34.12632
276	137.5	47.59800306	49.66711	35.23841

277	138	47.37104102	50.50363	36.32714
278	138.5	46.71509852	52.58918	36.43769
279	139	47.23459824	51.00048	33.92873
280	139.5	46.85399602	50.43566	35.9465
281	140	47.23655687	51.89977	33.64721
282	140.5	47.65894941	50.97328	35.74382
283	141	48.38156598	50.61481	35.6774
284	141.5	46.10601355	51.01174	33.96017
285	142	48.78621184	50.29577	36.12084
286	142.5	45.50163986	49.9727	36.69733
287	143	46.92541274	50.66028	35.23375
288	143.5	47.50103107	49.90684	35.37801
289	144	47.23871305	50.68871	36.43
290	144.5	46.49930795	50.92822	34.32714
291	145	46.81452353	51.2917	34.32885
292	145.5	46.5701801	51.47618	34.51973
293	146	46.47665431	50.21386	35.20243
294	146.5	47.61139882	50.90261	35.18184
295	147	47.2009063	50.86176	34.69322
296	147.5	46.34454876	50.69468	34.87703
297	148	47.6021446	50.01357	34.66733
298	148.5	47.11189833	49.53942	34.68712
299	149	47.49994815	50.72823	34.44733
300	149.5	47.33696702	48.92592	34.43539
301	150	46.15367917	50.04195	33.42459
302	150.5	46.3523473	48.17815	34.82803
303	151	47.38194971	49.11679	33.42413
304	151.5	47.25603947	49.44909	35.57068

305	152	46.73465613	50.99308	34.50394
306	152.5	46.8288792	50.63112	34.838
307	153	47.74079481	49.60244	34.61663
308	153.5	46.22905711	50.59407	34.70158
309	154	47.12364918	50.68567	35.88925
310	154.5	46.50787992	49.81207	33.77905
311	155	46.47915757	48.79816	33.54329
312	155.5	47.51599821	49.70441	34.91916
313	156	47.28098973	49.75753	34.40868
314	156.5	47.25514998	48.815	35.07481
315	157	47.63241665	50.05976	35.34212
316	157.5	46.58853372	49.95514	33.86553
317	158	47.10099577	50.05253	35.21508
318	158.5	46.29092844	49.88486	33.89658
319	159	46.78218908	50.21084	34.75558
320	159.5	46.4024614	49.44878	33.68818
321	160	46.56789816	49.71897	34.76522
322	160.5	46.95015825	49.20467	34.62461
323	161	45.80319302	49.02061	33.74079
324	161.5	48.11542201	50.52418	33.51823
325	162	45.6204466	47.78396	35.18731
326	162.5	45.43766362	50.0858	34.20624
327	163	47.3192629	48.8534	35.36013
328	163.5	47.00986972	48.71527	34.09765
329	164	46.85960647	49.49005	35.55599
330	164.5	46.84676376	48.05462	33.73742
331	165	46.31807234	48.55903	35.65622
332	165.5	45.59385434	48.4981	34.59942

333	166	46.35609524	48.96588	34.76168
334	166.5	45.73752165	48.4653	33.62054
335	167	47.04315191	50.35514	34.98907
336	167.5	46.12922098	50.47752	34.99878
337	168	45.57028555	47.388	34.11004
338	168.5	45.95739673	49.40676	32.64435
339	169	46.52867832	49.62396	33.44285
340	169.5	45.73118693	49.33717	33.42471
341	170	45.50822932	48.34208	34.65697
342	170.5	46.34480013	48.63909	33.90746
343	171	46.329674	48.20158	33.90501
344	171.5	45.71200223	48.42984	33.79046
345	172	45.72458781	47.76395	35.40097
346	172.5	46.27092573	48.60599	34.24386
347	173	44.91069128	47.46151	34.34781
348	173.5	44.92706635	48.46959	33.67616
349	174	45.46216625	47.5968	34.13003
350	174.5	45.8500538	48.72712	33.35526
351	175	46.25343311	47.98415	34.39288
352	175.5	47.1688932	48.72619	33.18275
353	176	46.65864273	49.32505	34.67747
354	176.5	45.82847664	49.69744	33.47624
355	177	45.92513256	46.36959	34.80504
356	177.5	45.12224573	47.69078	35.55429
357	178	45.89338803	48.08182	34.01147
358	178.5	45.66120657	48.65874	35.04204
359	179	46.1342489	46.9364	34.57606
360	179.5	45.19823548	47.43724	32.81084

361	180	46.25944924	48.29346	34.02799
362	180.5	47.05412058	48.22336	34.32239
363	181	45.72488436	48.42385	34.3818
364	181.5	46.1172305	48.44302	34.0284
365	182	46.33195057	48.32531	34.0003
366	182.5	45.44283886	48.17573	33.85434
367	183	45.92707469	48.0318	33.93905
368	183.5	45.7418657	48.48543	32.83581
369	184	45.79392933	46.12861	33.60803
370	184.5	45.0813829	49.122	32.61688
371	185	45.70340674	46.08944	33.36343
372	185.5	46.0662107	46.95621	33.27117
373	186	46.81274601	47.60467	33.20237
374	186.5	46.40327244	48.29073	32.86679
375	187	47.34243199	45.32301	33.90613
376	187.5	44.99004381	47.66334	33.41857
377	188	46.28581979	48.28638	33.31901
378	188.5	45.71868389	48.41474	32.51163
379	189	47.30790522	47.02794	33.38174
380	189.5	44.89348241	47.31183	34.51881
381	190	44.85240732	47.02631	34.51339
382	190.5	45.02874	47.17183	33.86593
383	191	43.79321243	46.62728	33.31338
384	191.5	45.05580546	46.70814	33.97908
385	192	44.85318939	47.73386	32.98041
386	192.5	45.56490216	47.45849	33.2573
387	193	45.70208909	47.71333	32.88511
388	193.5	46.91372373	47.45816	34.18824

389	194	46.15723443	47.81733	34.06799
390	194.5	44.9194863	47.92337	33.39869
391	195	44.64639692	45.79438	34.79389
392	195.5	45.74278897	46.47129	33.72137
393	196	44.27719761	46.93664	33.65881
394	196.5	46.78268728	47.07062	33.55561
395	197	46.24521401	46.51974	32.32898
396	197.5	44.91046858	47.7525	32.60588
397	198	43.89945422	48.57394	33.26011
398	198.5	46.33721803	47.10603	33.24923
399	199	45.14665208	46.99171	33.74068
400	199.5	46.21270638	47.57097	32.71711
401	200	43.93108611	45.36592	33.2905
402	200.5	44.71130867	46.84858	33.28736
403	201	45.17918963	47.57626	33.30163
404	201.5	45.19677067	46.24577	33.19478
405	202	44.78333087	45.74632	32.04116
406	202.5	45.62586577	46.54623	31.33785
407	203	44.25769759	46.61365	32.37602
408	203.5	44.98210398	45.90262	32.68715
409	204	45.17646323	48.27385	32.1519
410	204.5	45.47600248	46.18135	33.03275
411	205	45.61797351	45.6088	33.93202
412	205.5	44.13320366	46.42427	33.62341
413	206	43.78986723	47.19292	33.3983
414	206.5	46.02354678	46.44804	33.79615
415	207	45.25150879	46.7901	32.25088
416	207.5	44.37112613	45.67194	32.60783

417	208	46.19510022	47.52685	33.44784
418	208.5	45.03098714	46.75365	32.55904
419	209	45.86615947	47.11004	32.58551
420	209.5	44.96101631	46.53163	34.39403
421	210	46.53988517	46.86705	32.96318
422	210.5	46.2798503	45.47637	34.28046
423	211	44.6607026	45.74937	31.39367
424	211.5	45.62143247	47.18739	32.33037
425	212	45.34478376	47.32574	33.14489
426	212.5	45.90770102	45.12805	32.87559
427	213	44.02517527	46.21327	31.13896
428	213.5	45.33027896	45.63653	32.58252
429	214	45.61250662	45.39148	34.7274
430	214.5	43.34311017	46.14482	32.92933
431	215	43.78783515	46.79759	33.19817
432	215.5	43.0874019	46.21404	32.18229
433	216	44.48761334	45.56502	32.87491
434	216.5	45.26152925	46.20045	32.65327
435	217	45.8737432	45.46854	33.54104
436	217.5	44.71550097	46.0542	33.49846
437	218	45.94349064	46.80968	32.93774
438	218.5	43.52089556	43.99881	32.65139
439	219	43.24665477	46.26639	31.23422
440	219.5	44.54931201	44.36541	31.18924
441	220	44.88539745	46.54741	32.60885
442	220.5	44.53638967	45.02325	33.22594
443	221	42.89299763	44.52687	33.57456
444	221.5	44.46006657	46.02538	31.78031

445	222	43.47220376	45.72868	31.26766
446	222.5	45.0359396	44.6062	33.20437
447	223	44.77790781	44.37138	31.78921
448	223.5	43.71715849	45.19204	31.16229
449	224	44.04240734	44.34703	32.01198
450	224.5	43.59057405	44.42942	31.98103
451	225	44.37225103	45.33941	33.42905
452	225.5	45.17096305	44.44255	33.04843
453	226	43.60272868	45.52484	31.74903
454	226.5	44.77901249	46.34411	33.44033
455	227	43.93604037	45.00155	32.40502
456	227.5	43.71042483	45.19294	33.13671
457	228	44.24358087	46.67175	33.33284
458	228.5	43.4854988	44.07566	32.04409
459	229	43.85526613	45.94722	32.69429
460	229.5	43.32438161	45.81944	31.89491
461	230	45.8389678	45.61474	32.94748
462	230.5	44.27990773	45.93325	32.25872
463	231	43.6764311	45.09289	32.93786
464	231.5	44.39191547	44.37069	33.37253
465	232	44.11539456	45.68131	32.57363
466	232.5	44.01301218	45.68058	32.04421
467	233	44.6656575	45.62722	32.04066
468	233.5	44.764872	44.74726	29.71965
469	234	43.71901202	44.10742	31.49819
470	234.5	43.66731085	44.8022	32.79766
471	235	43.892482	45.37165	32.81068
472	235.5	42.25554975	45.40613	31.43031

473	236	42.86950255	44.2117	32.13282
474	236.5	45.15972893	44.77657	31.83295
475	237	45.36678321	43.44609	32.51926
476	237.5	43.83616512	45.24994	33.71769
477	238	44.48122983	43.80422	32.5008
478	238.5	44.25358009	45.02798	31.38112
479	239	46.4522857	43.44926	31.83778
480	239.5	44.86944747	45.16279	33.00531
481	240	43.85606533	44.5641	30.74009
482	240.5	43.1785843	43.65054	31.35826
483	241	42.64248224	44.79773	32.40156
484	241.5	44.07503822	43.7414	32.85235
485	242	43.29182011	44.78239	32.28736
486	242.5	42.74373651	43.93254	31.29814
487	243	43.34892532	42.7441	32.19604
488	243.5	42.98559474	43.30413	32.08157
489	244	45.18520135	43.71488	32.01413
490	244.5	44.52546011	45.12293	31.63916
491	245	43.79843582	44.71848	31.74257
492	245.5	44.97344025	45.26587	30.95753
493	246	43.83605594	45.25892	33.65107
494	246.5	43.06981566	43.47747	31.77588
495	247	44.96202937	43.72376	32.07248
496	247.5	44.15935058	43.51482	31.44274
497	248	42.88312343	43.27596	32.27672
498	248.5	43.54535256	42.30931	30.54514
499	249	42.98183741	43.74007	30.17082
500	249.5	42.56080609	42.6928	31.52636

501	250	44.39270712	43.66332	33.17743
502	250.5	45.16402295	45.35271	32.48429
503	251	42.50236548	43.22206	30.85433
504	251.5	44.05633017	43.75483	31.89742
505	252	43.07018131	44.29382	30.95924
506	252.5	43.18574099	43.76224	31.79265
507	253	43.08627742	43.74153	31.83852
508	253.5	42.85375654	43.18718	32.15969
509	254	43.5685284	43.26118	30.14948
510	254.5	42.84971827	42.64827	30.37306
511	255	43.71561642	44.06273	31.3086
512	255.5	43.4438384	41.96234	30.52666
513	256	43.2776537	44.10207	30.44836
514	256.5	42.72754979	42.17192	31.53718
515	257	42.97697755	44.03467	30.57043
516	257.5	44.02750682	42.95126	33.09295
517	258	43.80873213	42.21856	30.84387
518	258.5	42.61076404	43.63726	31.0378
519	259	43.45708926	43.88663	31.47562
520	259.5	43.9635536	42.76296	30.01483
521	260	42.01174548	43.65974	31.61161
522	260.5	43.76678897	41.22504	31.4616
523	261	42.78683822	41.9665	30.89261
524	261.5	43.75825789	44.0268	31.37484
525	262	42.67601866	42.78385	31.48197
526	262.5	41.82757264	41.44296	32.27115
527	263	41.954302	42.34359	33.10687
528	263.5	43.27966684	42.13394	30.24114

529	264	43.43384511	42.70989	30.03614
530	264.5	42.48748733	42.51608	31.13991
531	265	43.70669342	42.92587	29.37827
532	265.5	41.85148751	42.69721	31.54465
533	266	43.11272912	43.81066	31.0993
534	266.5	42.18167468	43.03261	31.28639
535	267	42.61391873	43.02924	30.73343
536	267.5	43.15821181	43.56537	31.16404
537	268	42.41687272	42.2924	31.32157
538	268.5	42.78247479	41.5641	31.08756
539	269	43.88007457	43.50939	29.83523
540	269.5	42.5984532	42.62271	31.03269
541	270	43.71345204	42.59577	32.36204
542	270.5	42.12606979	41.9479	31.05537
543	271	43.43862081	41.93137	30.95611
544	271.5	44.15297982	43.07255	32.0783
545	272	41.00736205	43.15323	30.2176
546	272.5	42.33211945	42.96291	31.50966
547	273	43.41625661	42.9406	30.35763
548	273.5	42.77713112	42.73185	31.63486
549	274	43.22145791	42.35226	31.38789
550	274.5	42.4263321	42.07718	30.40349
551	275	42.96377638	43.1562	30.50441
552	275.5	42.75495231	41.85944	31.48331
553	276	43.79871455	42.4249	29.20058
554	276.5	43.05302563	41.45623	30.31529
555	277	43.10457639	41.54254	31.14907
556	277.5	42.49000323	41.85162	30.39017

557	278	42.41443562	41.36797	30.72846
558	278.5	42.44349509	42.62001	28.97158
559	279	43.09012964	40.87392	29.90485
560	279.5	42.42281186	42.00237	31.11594
561	280	42.97645609	41.99966	29.95553
562	280.5	44.38999884	40.4157	29.49833
563	281	43.41162519	41.48223	31.37356
564	281.5	42.43895906	42.01033	30.9208
565	282	43.64580672	42.1195	29.62141
566	282.5	42.34343821	41.58384	30.58703
567	283	41.02446703	42.25958	29.61548
568	283.5	41.83357098	41.60143	30.32228
569	284	41.12848509	41.67063	30.56906
570	284.5	42.32899166	41.83188	29.7655
571	285	42.61002619	42.34302	30.9902
572	285.5	43.92153559	41.03174	31.09826
573	286	42.82702711	41.15376	30.57529
574	286.5	42.37530948	40.97903	30.67968
575	287	43.19922426	41.21934	29.17031
576	287.5	40.75190666	42.59706	31.4064
577	288	42.69442687	41.88524	30.22768
578	288.5	43.10775291	40.4932	29.53663
579	289	41.29332249	40.88875	30.38561
580	289.5	43.37633065	41.63837	30.84943
581	290	42.71726568	40.58602	30.64705
582	290.5	42.09938456	40.70205	29.35355
583	291	42.92299192	42.3294	30.81155
584	291.5	44.21847744	40.73387	30.14106

585	292	42.53257808	41.95945	30.57471
586	292.5	42.57082866	42.17115	29.51666
587	293	41.98993578	40.55132	30.97881
588	293.5	41.6627265	40.39733	30.27243
589	294	42.99205333	40.85963	31.0615
590	294.5	41.62810548	40.18089	28.86675
591	295	42.35541859	41.11989	28.95771
592	295.5	41.90123787	40.82983	29.87103
593	296	42.6517511	41.25413	31.22138
594	296.5	42.52070551	42.05456	31.60176
595	297	43.06902155	41.56235	29.305
596	297.5	41.81619542	41.27112	30.04243
597	298	41.9935327	39.27829	30.10837
598	298.5	41.41165096	41.17724	30.54303
599	299	41.82446178	42.17208	30.66075
600	299.5	42.4669764	38.35701	29.04554
601	300	42.75597168	41.28841	29.97302
602	300.5	41.39789848	40.58091	28.29882
603	301	42.81657058	40.00008	30.53858
604	301.5	43.1906564	41.29235	29.60336
605	302	42.42215947	41.99076	28.89427
606	302.5	43.57811878	41.21476	30.10894
607	303	41.44292651	40.26921	29.53134
608	303.5	41.051515	39.783	30.82075
609	304	40.6095486	40.62512	29.08187
610	304.5	43.21465144	41.1796	31.55866
611	305	42.52660485	40.1431	30.44831
612	305.5	41.94394607	40.19213	30.7792

613	306	42.19769534	42.65375	28.91036
614	306.5	41.05864097	41.2308	31.14859
615	307	43.9009507	41.25973	28.73219
616	307.5	42.03304811	39.14317	29.51879
617	308	42.00251418	39.71744	30.71478
618	308.5	42.48094396	40.31475	30.0609
619	309	42.2704755	39.42593	28.64859
620	309.5	42.05011791	41.47901	30.53269
621	310	41.22397884	41.29881	29.88078
622	310.5	42.21888593	39.71561	29.26031
623	311	43.3326888	41.5415	28.34413
624	311.5	42.88876833	40.08289	29.91002
625	312	43.0723498	42.12975	29.41596
626	312.5	41.37420129	40.14596	29.65624
627	313	40.97686842	40.46315	28.24753
628	313.5	41.65330631	41.09413	29.16528
629	314	41.78390445	40.96834	29.86896
630	314.5	42.60007153	40.32687	30.97041
631	315	40.35614552	39.77744	29.28955
632	315.5	42.91916149	40.27374	30.59295
633	316	41.55452404	39.18159	30.05274
634	316.5	41.32483973	39.92837	29.59445
635	317	40.84208041	38.89137	28.58211
636	317.5	40.31330301	38.32627	28.60018
637	318	42.28115435	39.7635	29.85517
638	318.5	41.66670689	40.70519	28.92453
639	319	40.56152352	40.40823	28.83804
640	319.5	40.54287405	39.5743	29.17045

641	320	41.29575923	41.00968	29.16848
642	320.5	42.88505922	39.12912	30.00478
643	321	41.32762902	38.02241	28.8644
644	321.5	40.31825292	37.78331	29.89443
645	322	41.30964311	38.55638	29.58985
646	322.5	41.27353406	40.12699	27.88354
647	323	39.31968405	38.93823	29.44301
648	323.5	41.41924299	39.78723	27.05786
649	324	41.26342186	40.70791	28.46057
650	324.5	41.99063026	38.48324	29.5319
651	325	42.89833079	39.71857	29.13761
652	325.5	42.30592377	39.73942	27.71652
653	326	41.17507169	38.59215	28.22021
654	326.5	40.49047789	40.33662	27.01313
655	327	43.4199075	38.99562	28.01093
656	327.5	41.39412051	38.89134	29.53297
657	328	41.34342037	40.8602	28.60852
658	328.5	41.2985131	39.56171	29.17517
659	329	41.46182227	39.85634	29.03489
660	329.5	41.17341249	40.17265	29.0348
661	330	40.81552263	38.54101	29.81202
662	330.5	40.82252155	40.03391	28.81597
663	331	41.21936761	38.60522	29.69162
664	331.5	40.79639699	38.54374	26.96601
665	332	40.6464318	38.73457	29.82183
666	332.5	41.28742929	38.42726	27.88544
667	333	40.98388506	39.5554	28.04397
668	333.5	42.37664799	39.08422	28.32346

669	334	39.03826957	38.45027	29.73908
670	334.5	42.01784775	39.35568	28.1454
671	335	42.12711232	38.56876	28.31698
672	335.5	39.45713891	38.49931	28.05721
673	336	40.82731299	38.77359	29.01574
674	336.5	40.78992738	39.07831	29.39119
675	337	39.94669275	38.99233	30.14465
676	337.5	40.43607583	38.36279	30.68594
677	338	40.1555006	39.30403	29.27113
678	338.5	42.43141476	38.42139	29.02842
679	339	41.76378327	38.04831	27.74694
680	339.5	42.01813181	37.37089	30.23318
681	340	41.56387759	39.30488	28.86299
682	340.5	40.06895574	38.50129	28.44436
683	341	40.53824319	38.63315	28.97059
684	341.5	41.3350263	39.27417	28.13644
685	342	39.95149668	38.02871	26.76035
686	342.5	41.48527496	37.28424	29.0729
687	343	40.7082982	38.41272	29.67442
688	343.5	40.58638918	38.57643	29.03097
689	344	41.44070612	38.09296	28.56476
690	344.5	41.21304612	39.45542	28.56605
691	345	40.55456486	36.26072	28.67826
692	345.5	41.75650897	39.11893	28.63878
693	346	39.9499068	38.82906	28.46193
694	346.5	41.29322328	38.53483	28.5158
695	347	41.26067814	35.47398	29.72458
696	347.5	40.52428731	39.14312	28.84344

697	348	41.0185632	37.26819	28.5348
698	348.5	39.74250324	37.65653	28.96313
699	349	41.46835802	37.89958	28.94826
700	349.5	40.566962	38.33537	29.1627
701	350	40.28245757	38.49438	27.78547
702	350.5	41.52560064	38.67053	27.99167
703	351	40.10868056	38.58238	27.71036
704	351.5	39.53115371	38.1055	28.95969
705	352	39.39839163	38.20937	28.90573
706	352.5	41.11428012	36.97753	27.29797
707	353	39.59091085	37.22282	28.61438
708	353.5	42.00487683	38.51354	29.38464
709	354	38.92129008	38.44049	28.08374
710	354.5	41.92979579	38.32334	28.50834
711	355	40.72724674	37.30635	28.82672
712	355.5	40.46686931	38.41989	27.17106
713	356	40.09411653	36.73612	28.33429
714	356.5	40.83517765	38.50065	29.21558
715	357	40.47158292	37.40373	27.70852
716	357.5	41.37015908	38.93344	28.83427
717	358	40.56473154	36.34265	28.17524
718	358.5	40.57942764	38.94424	27.59913
719	359	40.15413822	37.21808	28.04676
720	359.5	40.38531821	37.17743	27.6883
721	360	40.66296779	37.61065	27.3838
722	360.5	39.03444829	36.87091	27.87623
723	361	39.30989623	37.34452	28.11971
724	361.5	40.96892236	36.78611	27.91739

725	362	40.4968749	36.7892	27.82322
726	362.5	40.19887229	37.71343	28.2016
727	363	40.34668746	36.57655	28.43122
728	363.5	40.59589197	36.65715	27.07612
729	364	39.87191009	36.14739	27.77478
730	364.5	39.66697022	36.81641	26.38318
731	365	40.43219131	38.2428	27.81759
732	365.5	39.47872292	36.49074	28.0531
733	366	40.57393431	36.55617	28.37384
734	366.5	38.87118112	37.27063	28.02664
735	367	41.04249334	36.79288	28.32725
736	367.5	40.58317257	38.84609	27.92626
737	368	40.39584905	36.90761	27.31903
738	368.5	40.96311365	37.27989	26.95208
739	369	41.49528095	37.74083	27.61981
740	369.5	40.96034289	37.69959	27.20258
741	370	38.66209781	37.1207	27.70523
742	370.5	39.0970909	36.77932	27.39291
743	371	39.60685781	38.50162	28.10709
744	371.5	40.11355062	36.77678	27.79641
745	372	40.49277501	36.47745	28.10068
746	372.5	39.48402767	36.28835	28.08203
747	373	40.20001597	35.39783	27.56983
748	373.5	39.43228096	37.41083	27.60435
749	374	39.53336271	34.84936	28.08577
750	374.5	38.88324262	36.69754	29.6267
751	375	39.25598435	36.51254	26.86412
752	375.5	38.89922761	38.44274	27.67432

753	376	39.18588594	35.1598	26.66984
754	376.5	40.79551212	35.87861	27.59518
755	377	39.17909861	36.46501	27.05817
756	377.5	42.03054731	36.39027	27.487
757	378	40.3053248	36.08308	27.6927
758	378.5	40.04457308	36.43237	27.16247
759	379	39.19605656	35.46397	26.11251
760	379.5	40.42903417	36.73185	28.66549
761	380	39.39432437	34.56341	28.18204
762	380.5	39.93849573	36.37449	27.39173
763	381	41.87501364	35.88936	26.76596
764	381.5	39.7361611	37.15722	27.53534
765	382	40.71849556	37.72301	27.7417
766	382.5	39.22260852	36.0285	28.05451
767	383	39.7432365	37.38053	28.11387
768	383.5	41.17395031	35.98968	28.25024
769	384	39.24182353	35.44431	26.00263
770	384.5	41.17944827	37.58859	27.13722
771	385	40.28178808	36.58316	28.16105
772	385.5	39.25171509	36.14478	26.6133
773	386	40.19372154	36.66568	28.31326
774	386.5	40.45195061	36.31004	28.7718
775	387	40.15747159	36.01004	28.26216
776	387.5	38.38996526	34.97903	27.8241
777	388	39.05056157	35.79853	26.92249
778	388.5	39.42038754	36.48836	27.49149
779	389	39.54499169	35.86636	26.17499
780	389.5	40.08721695	36.66127	26.61268

781	390	39.71898576	36.22118	26.65463
782	390.5	38.4947	35.18662	27.25856
783	391	39.85328915	34.80868	26.88096
784	391.5	40.0237597	35.71317	27.38971
785	392	39.96928853	35.39446	27.86842
786	392.5	40.37225066	36.05784	26.58412
787	393	40.16093855	35.18922	27.25653
788	393.5	39.84732448	35.2464	26.79063
789	394	39.41003227	36.55616	27.2613
790	394.5	38.12358536	35.80727	27.64388
791	395	39.78224277	35.10155	27.81771
792	395.5	39.59089727	35.65289	27.60275
793	396	39.62821394	36.71697	27.38349
794	396.5	38.37576059	35.82395	25.90193
795	397	38.51852763	36.03838	26.1589
796	397.5	40.21211337	34.93734	26.35038
797	398	39.32417002	36.3354	27.28245
798	398.5	39.88724258	37.34389	25.94858
799	399	39.35092942	34.8314	27.23724
800	399.5	39.33831714	34.49425	27.16464
801	400	40.0513816	35.5554	25.39037
802	400.5	38.87416592	36.09058	26.0547
803	401	39.35015028	35.2923	27.74575
804	401.5	38.88969019	34.4981	27.45445
805	402	38.89817501	35.22907	26.20209
806	402.5	38.98470068	35.7697	26.04041
807	403	39.39601659	34.94091	24.89392
808	403.5	38.82158666	35.72766	28.01714

809	404	40.19547126	36.14896	26.85886
810	404.5	38.46146611	35.38473	28.31891
811	405	39.01394504	35.14556	26.64452
812	405.5	38.7979527	35.80679	27.00987
813	406	40.29361984	34.43384	27.48278
814	406.5	39.27958614	34.33038	28.06676
815	407	39.93412753	34.85633	27.14246
816	407.5	37.90651796	34.65155	26.72953
817	408	39.29492563	34.37785	26.73595
818	408.5	39.779314	36.4604	25.86289
819	409	39.11976528	36.70913	26.38004
820	409.5	39.8926559	34.6641	26.71252
821	410	38.61277914	34.99598	27.76306
822	410.5	40.14043093	34.7479	26.29951
823	411	40.83841933	35.75975	27.47969
824	411.5	38.69538262	35.89386	26.55012
825	412	38.61560886	33.40315	27.59647
826	412.5	40.12108064	35.1814	27.12903
827	413	40.20839773	33.73078	27.06106
828	413.5	38.51282372	36.15852	27.34282
829	414	38.58133878	35.07979	27.21234
830	414.5	38.67844181	34.04461	27.38293
831	415	37.81469512	34.48595	28.22337
832	415.5	38.14172476	34.42355	27.79755
833	416	38.05972926	35.05058	26.86327
834	416.5	38.23520413	35.43978	26.12283
835	417	38.80809935	33.66347	26.75546
836	417.5	39.00962888	36.02884	24.90748

837	418	40.04907207	35.81821	27.09774
838	418.5	37.99640779	33.80923	25.57265
839	419	39.56897304	34.54358	27.3048
840	419.5	38.59675289	35.82986	27.97718
841	420	38.71480659	35.42343	25.21835
842	420.5	39.28067149	34.14361	26.32501
843	421	37.82908137	35.04039	25.49989
844	421.5	39.01963461	36.76261	24.95494
845	422	38.83332115	34.42494	26.23871
846	422.5	39.08057771	33.81066	26.81808
847	423	38.90441367	34.4307	26.89966
848	423.5	40.62378566	34.46601	26.40548
849	424	38.13582509	33.82516	24.93716
850	424.5	38.20769577	34.57413	26.35346
851	425	38.12046191	33.19336	25.04694
852	425.5	38.16107836	33.64052	25.08561
853	426	38.0820408	34.75563	25.41598
854	426.5	39.52965891	32.72124	27.03953
855	427	39.70134899	34.8238	26.62213
856	427.5	38.09485319	32.46781	26.43025
857	428	37.87207512	32.66849	25.46835
858	428.5	38.9016061	33.63054	25.83449
859	429	38.06921401	34.2354	25.03489
860	429.5	39.00386141	35.04233	27.20872
861	430	38.6463826	34.00444	27.86138
862	430.5	37.25798183	33.73733	26.53515
863	431	39.69511894	34.37449	26.66158
864	431.5	39.88035928	33.19038	25.93532

865	432	37.93997327	33.97492	24.75325
866	432.5	38.10659475	32.88013	25.35997
867	433	38.6320048	33.88208	25.64916
868	433.5	38.65743911	33.68848	25.69961
869	434	38.90327499	33.12529	25.50185
870	434.5	39.9711738	33.8771	26.01872
871	435	38.20802769	33.8483	25.28675
872	435.5	37.69752767	34.63822	27.68744
873	436	37.21929477	32.38977	24.84733
874	436.5	37.7245955	33.58988	26.63587
875	437	38.26943204	33.01896	25.70293
876	437.5	39.71817867	34.29945	26.26905
877	438	37.8550468	34.18326	26.29171
878	438.5	38.43477435	33.96293	25.99727
879	439	38.2292185	32.97008	24.95136
880	439.5	39.17968895	34.21806	25.57885
881	440	40.23714248	32.26213	25.96619
882	440.5	37.7775284	32.07455	25.90251
883	441	37.79730343	32.41869	24.9853
884	441.5	39.01081992	33.38921	26.82323
885	442	38.70764533	33.93273	23.78187
886	442.5	39.62614359	30.98841	25.5631
887	443	38.60257054	34.40408	25.01262
888	443.5	37.83464925	33.42744	25.88189
889	444	38.5812664	32.04502	26.53603
890	444.5	38.98236967	33.35669	24.58358
891	445	38.73846149	34.12667	27.57854
892	445.5	38.47456858	33.70893	25.84365

893	446	38.90876737	34.08538	25.97407
894	446.5	38.97754702	32.08989	24.50342
895	447	39.13452534	32.82847	25.6045
896	447.5	38.5344583	32.39671	26.40564
897	448	37.86849284	34.48734	25.78278
898	448.5	38.10625981	33.6016	25.71356
899	449	38.94080225	35.34456	25.54648
900	449.5	37.30875741	32.66973	24.47213
901	450	38.24396011	32.44095	24.45414
902	450.5	37.62107058	32.88332	26.48316
903	451	37.9454623	34.07718	26.24011
904	451.5	38.93195739	32.65853	26.3451
905	452	38.04880926	33.02791	24.84923
906	452.5	37.91981799	32.98267	25.36805
907	453	36.78152722	32.91389	26.46616
908	453.5	38.45316301	32.33737	24.48442
909	454	38.35930017	32.72646	26.35788
910	454.5	39.5602739	32.66923	24.9714
911	455	37.57020947	32.7843	24.74308
912	455.5	37.97851888	33.52222	25.38839
913	456	37.98947676	34.15298	24.50698
914	456.5	39.03870826	32.04922	23.86973
915	457	37.68728967	32.38507	25.43475
916	457.5	37.97352839	32.01578	25.78802
917	458	38.22341808	32.8026	26.31953
918	458.5	37.8731825	32.19939	25.81957
919	459	37.35354725	32.79908	26.89301
920	459.5	37.85276971	33.46733	26.39627

921	460	38.5432113	30.54096	25.88459
922	460.5	36.84990646	32.93226	25.65574
923	461	37.76431185	32.14792	26.25166
924	461.5	37.08466149	32.86165	23.4839
925	462	38.58762209	31.7534	24.85702
926	462.5	36.39986651	33.40487	23.74103
927	463	37.15811441	33.15578	25.74505
928	463.5	37.89386186	32.85714	24.60713
929	464	38.83135665	33.01437	27.60383
930	464.5	37.51318689	31.76063	24.76055
931	465	37.10848175	31.83879	25.24677
932	465.5	39.0444259	32.91381	24.82666
933	466	36.3679526	31.67507	24.74421
934	466.5	35.75418703	33.42316	24.12486
935	467	37.85211602	31.9852	24.08477
936	467.5	37.08533834	32.62303	23.35212
937	468	36.65687732	33.87837	25.51891
938	468.5	38.02743517	31.61146	24.72966
939	469	37.64268162	32.20893	26.60312
940	469.5	36.98327376	32.97477	24.04776
941	470	36.39719335	32.86996	26.21098
942	470.5	38.10630752	31.82422	26.27459
943	471	37.91541197	31.65063	26.02529
944	471.5	37.30282429	31.85507	25.17837
945	472	38.84639311	33.17744	24.70685
946	472.5	36.49993881	31.77347	25.98516
947	473	36.12251417	32.03685	24.31803
948	473.5	36.77634011	31.61056	25.15467

949	474	37.28033459	32.49407	24.89002
950	474.5	37.49841637	32.03171	24.1988
951	475	37.09770193	31.08221	25.1213
952	475.5	37.55928564	31.08759	25.47926
953	476	36.26336489	30.24147	24.12807
954	476.5	38.40656779	31.15301	25.22777
955	477	37.1727994	32.43096	23.06341
956	477.5	38.11932581	32.83256	23.99426
957	478	37.48664278	32.29977	24.45468
958	478.5	37.56484299	32.17281	25.0934
959	479	37.64223671	31.60568	25.48996
960	479.5	37.53157677	32.30465	24.84775
961	480	37.67457971	31.89157	25.22176
962	480.5	38.21071966	33.08395	24.62702
963	481	37.29161526	31.53949	25.06629
964	481.5	37.68860656	32.67053	25.01103
965	482	37.03662479	32.2733	24.30931
966	482.5	38.24752144	32.14027	24.41925
967	483	36.5413327	29.92065	25.17069
968	483.5	38.5102223	32.25113	26.1273
969	484	37.02437155	31.38372	25.63013
970	484.5	35.89891032	31.10856	23.74844
971	485	37.13305097	30.25535	23.73833
972	485.5	36.47276768	31.41521	24.19735
973	486	37.67716995	31.42453	24.69207
974	486.5	36.46960657	30.33332	24.63862
975	487	36.62181417	30.17514	25.57933
976	487.5	35.45418803	31.72112	25.61029

977	488	36.59103979	32.00727	24.56583
978	488.5	35.00085014	31.44022	24.36625
979	489	35.65990462	32.18677	24.94892
980	489.5	37.5224364	31.17511	25.37321
981	490	37.52982713	31.17888	24.95173
982	490.5	37.2286399	30.46689	24.15168
983	491	36.10178429	29.93048	23.99425
984	491.5	36.824292	32.64059	23.58272
985	492	36.84667945	32.0401	24.61315
986	492.5	35.90997464	29.99926	24.94402
987	493	38.02649446	31.2161	25.02057
988	493.5	37.51277958	30.9897	25.34128
989	494	36.62123686	30.82881	25.5913
990	494.5	36.80663982	30.69906	23.29427
991	495	36.93896485	31.30958	24.70525
992	495.5	35.12600267	31.63741	24.72005
993	496	36.54878512	31.2831	24.29669
994	496.5	36.1880806	30.84311	23.68039
995	497	35.91951745	30.79209	25.48599
996	497.5	36.48308319	31.64569	23.84664
997	498	38.13326711	31.24537	22.5507
998	498.5	37.19495113	30.91116	24.30806
999	499	36.2124971	30.8027	24.08896
1000	499.5	37.11467446	31.08606	25.75266

This doctoral thesis only provides 1000 sample data, with a total of 8760 samples. If you need all the sample data, please download it from the following link : https://pan.baidu.com/s/1huOl4P16l_fmX8cVdLqd_Q?pwd=u23u

Appendix 4: Python code for costume color restoration based on DCLSTNet

```
# Read data
df = pd.read_csv('cotton_madder_tomb_environment_1year.csv')
time = df['Time (hours)'].values.reshape(-1, 1)
lab = df[['L*', 'a*', 'b*']].values

# Standardized time series and LAB values
scaler_time = StandardScaler()
scaler_lab = StandardScaler()
time_scaled = scaler_time.fit_transform(time)
lab_scaled = scaler_lab.fit_transform(lab)
# Building time series samples
def create_sequences(time_data, lab_data, seq_length):
        X, y = [], []
        for i in range(len(time_data) - seq_length):
            X.append(time_data[i:i+seq_length])
            y.append(lab_data[i+seq_length])
        return np.array(X), np.array(y)

seq_length = 10
X, y = create_sequences(time_scaled, lab_scaled, seq_length)

# Divide training set and test set
X_train, X_test, y_train, y_test = train_test_split(X, y, test_size=0.2, shuffle=False)

# Convert to PyTorch Tensor
X_train = torch.FloatTensor(X_train)
y_train = torch.FloatTensor(y_train)
X_test = torch.FloatTensor(X_test)
y_test = torch.FloatTensor(y_test)

# Define DCLSTNet model
class DCLSTNet(nn.Module):
        def __init__(self, input_size, output_size, hidden_size, num_layers,
```

```
            kernel_size=3):
34                  super(DCLSTNet, self).__init__()
35                  self.conv = nn.Conv1d(in_channels=input_size, out_channels=hidden_size,
                    kernel_size=kernel_size, padding=1)
36                  self.relu = nn.ReLU()
37                  self.lstm = nn.LSTM(hidden_size, hidden_size, num_layers,
                    batch_first=True)
38                  self.fc = nn.Linear(hidden_size, output_size)
39
40          def forward(self, x):
41                  # x shape: (batch, seq_len, input_size)
42                  x = x.transpose(1, 2)  # (batch, input_size, seq_len)
43                  x = self.conv(x)
44                  x = self.relu(x)
45                  x = x.transpose(1, 2)  # (batch, seq_len, hidden_size)
46                  _, (h_n, _) = self.lstm(x)
47                  out = self.fc(h_n[-1])
48                  return out
49
50  # Hyperparameter
51  input_size = 1   # Time as input
52  output_size = 3   # Output L *, a *, b*
53  hidden_size = 64
54  num_layers = 2
55  learning_rate = 0.001
56  num_epochs = 100
57
58  # nitialize model
59  model = DCLSTNet(input_size, output_size, hidden_size, num_layers)
60  criterion = nn.MSELoss()
61  optimizer = optim.Adam(model.parameters(), lr=learning_rate)
62
63  # Training model
64  train_losses = []
65  test_losses = []
66
67  for epoch in range(num_epochs):
68          model.train()
```

```
69                optimizer.zero_grad()
70                outputs = model(X_train)
71                loss = criterion(outputs, y_train)
72                loss.backward()
73                optimizer.step()
74                train_losses.append(loss.item())
75
76                # Test set loss
77                model.eval()
78                with torch.no_grad():
79                    test_outputs = model(X_test)
80                    test_loss = criterion(test_outputs, y_test)
81                    test_losses.append(test_loss.item())
82
83                if (epoch+1) % 10 == 0:
84                    print(f'Epoch [{epoch+1}/{num_epochs}], Train Loss: {loss.item():.4f},
                      Test Loss: {test_loss.item():.4f}')
85
86    # Draw loss curve
87    plt.plot(train_losses, label='Train Loss')
88    plt.plot(test_losses, label='Test Loss')
89    plt.legend()
90    plt.xlabel('Epoch')
91    plt.ylabel('Loss')
92    plt.title('Training and Test Loss')
93    plt.show()
94
95    # Forecast all data
96    model.eval()
97    with torch.no_grad():
98                all_X = torch.FloatTensor(X)
99                predictions_scaled = model(all_X).numpy()
100               predictions = scaler_lab.inverse_transform(predictions_scaled)
101
102   # Draw forecast results
103   plt.figure(figsize=(12, 8))
104   colors = ['r', 'g', 'b']
105   labels = ['L*', 'a*', 'b*']
```

```
106 for i in range(3):
107         plt.subplot(3, 1, i+1)
108         plt.plot(lab[seq_length:, i], label='True', color=colors[i])
109         plt.plot(predictions[:, i], label='Predicted', linestyle='--', color=colors[i])
110         plt.legend()
111         plt.ylabel(labels[i])
112 plt.xlabel('Time (hours)')
113 plt.suptitle('True vs Predicted LAB Values')
114 plt.show()
```

Appendix 5: Restoration data of Chinese excavated costumes


Unearthed Costume
(475BC-221BC)
Flat
Unearthed Costume
(475BC-221BC)
Flat
Pattern
Virtual restoration
drawing
Pattern
Virtual restoration
drawing
Unearthed Costume
(475BC-221BC)
Flat
Unearthed Costume
(475BC-221BC)
Flat
Pattern
Virtual restoration
drawing
Pattern
Virtual restoration
drawing
Unearthed Costume
(475BC-221BC)
Flat
Unearthed Costume
(1046BC-771BC)
Flat
Pattern
Virtual restoration
drawing
Pattern
Virtual restoration
drawing


Unearthed Costume (202BC—8AD)
Flat
Pattern
Virtual restoration drawing
Unearthed Costume (202BC—8AD)
Flat
Pattern
Virtual restoration drawing
Unearthed Costume (202BC—8AD)
Flat
Pattern
Virtual restoration drawing
Unearthed Costume (202BC—8AD)
Flat
Pattern
Virtual restoration drawing
Unearthed Costume (202BC—8AD)
Flat
Pattern
Virtual restoration drawing
Unearthed Costume (33AD—184AD)
Flat
Pattern
Virtual restoration drawing


Unearthed Costume (202BC—8AD)
Flat
Unearthed Costume (202BC—8AD)
Flat
Pattern
Virtual restoration drawing
Pattern
Virtual restoration drawing
Unearthed Costume (202BC—8AD)
Flat
Unearthed Costume (202BC—8AD)
Flat
Pattern
Virtual restoration drawing
Pattern
Virtual restoration drawing
Unearthed Costume (202BC—8AD)
Flat
Unearthed Costume (202BC—8AD)
Flat
Pattern
Virtual restoration drawing
Pattern
Virtual restoration drawing


Unearthed Costume (202BC—8AD)
Flat
Unearthed Costume (202BC—8AD)
Flat
Pattern
Virtual restoration drawing
Pattern
Virtual restoration drawing
Unearthed Costume (202BC—8AD)
Flat
Unearthed Costume (202BC—8AD)
Flat
Pattern
Virtual restoration drawing
Pattern
Virtual restoration drawing
Unearthed Costume (202BC—8AD)
Flat
Unearthed Costume (202BC—8AD)
Flat
Pattern
Virtual restoration drawing
Pattern
Virtual restoration drawing

Unearthed Costume
(386AD-581AD)

Flat

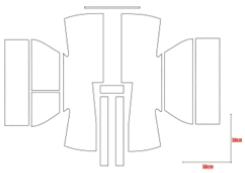

Pattern

Virtual restoration drawing

Unearthed Costume
(386AD-581AD)

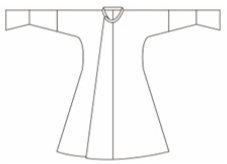

Flat

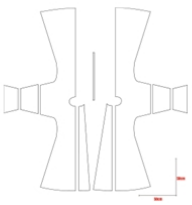

Pattern

Virtual restoration drawing

Unearthed Costume
(386AD-581AD)

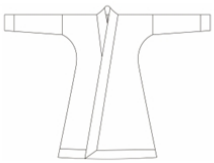

Flat

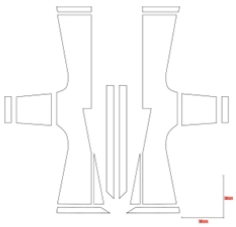

Pattern

Virtual restoration drawing

Unearthed Costume
(220AD-420AD)

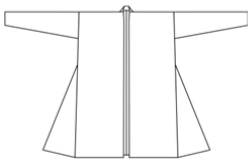

Flat

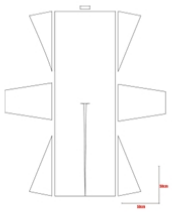

Pattern

Virtual restoration drawing

Unearthed Costume
(386AD-534AD)

Flat

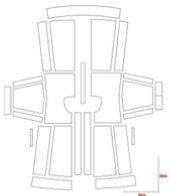

Pattern

Virtual restoration drawing

Unearthed Costume
(220AD-317AD)

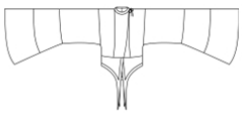

Flat

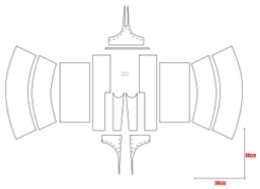

Pattern

Virtual restoration drawing

Unearthed Costume
(220AD-589AD)

Flat

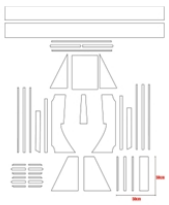

Pattern

Virtual restoration drawing

Unearthed Costume
(220AD-589AD)

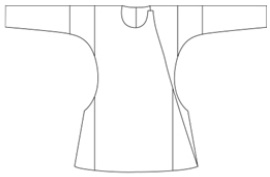

Flat

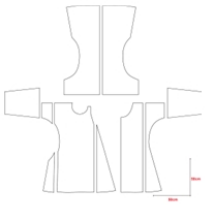

Pattern

Virtual restoration drawing

Unearthed Costume
(220AD-589AD)

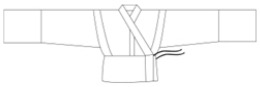

Flat

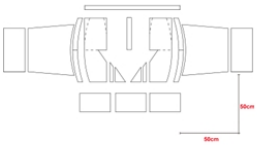

Pattern

Virtual restoration drawing

Unearthed Costume
(220AD-317AD)

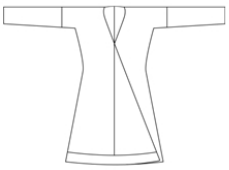

Flat

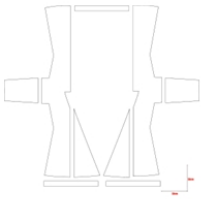

Pattern

Virtual restoration drawing

Unearthed Costume
(220AD-317AD)

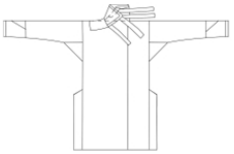

Flat

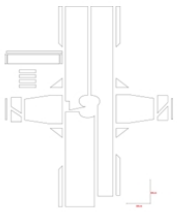

Pattern

Virtual restoration drawing

Unearthed Costume
(220AD-317AD)

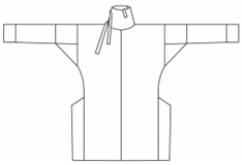

Flat

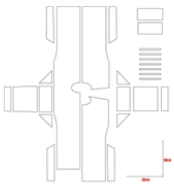

Pattern

Virtual restoration drawing

Unearthed Costume
(220AD-589AD)

Flat

Unearthed Costume
(220AD-589AD)

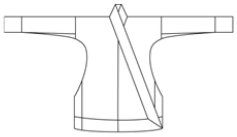

Flat

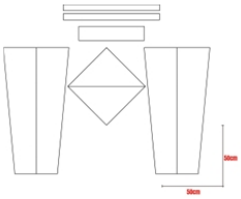

Pattern

Virtual restoration drawing

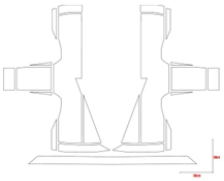

Pattern

Virtual restoration drawing

Unearthed Costume
(220AD-317AD)

Flat

Unearthed Costume
(220AD-317AD)

Flat

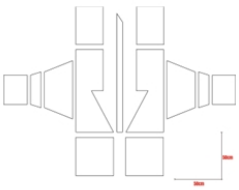

Pattern

Virtual restoration drawing

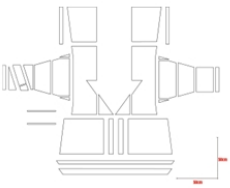

Pattern

Virtual restoration drawing

Unearthed Costume
(220AD-589AD)

Flat

Unearthed Costume
(220AD-589AD)

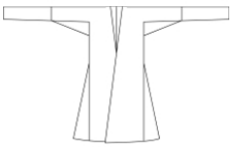

Flat

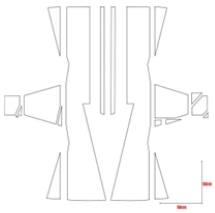

Pattern

Virtual restoration drawing

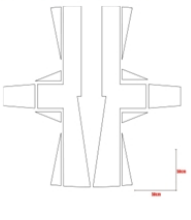

Pattern

Virtual restoration drawing

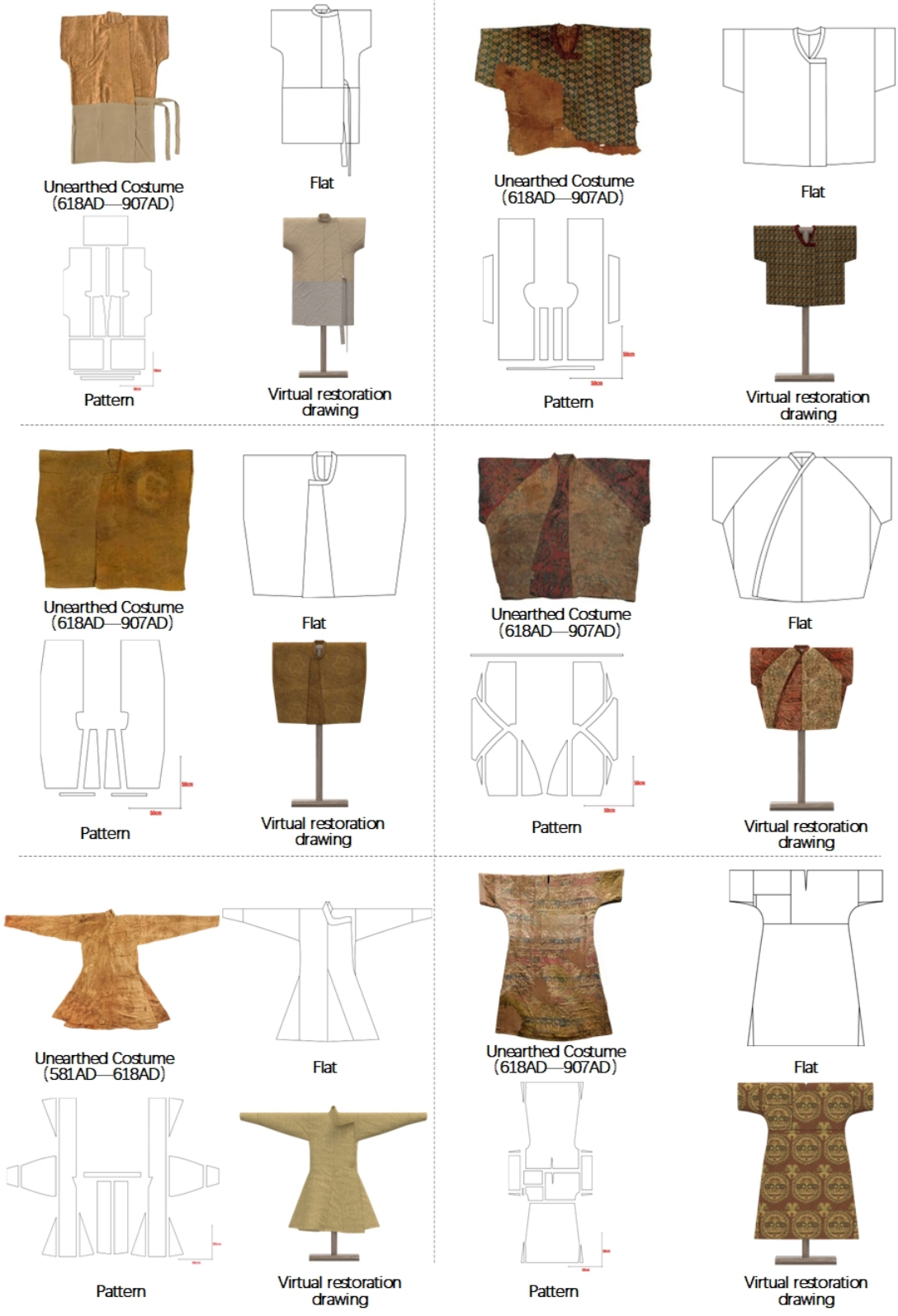
Unearthed Costume
(618AD—907AD)
Flat
Pattern
Virtual restoration drawing
Unearthed Costume
(618AD—907AD)
Flat
Pattern
Virtual restoration drawing
Unearthed Costume
(618AD—907AD)
Flat
Pattern
Virtual restoration drawing
Unearthed Costume
(618AD—907AD)
Flat
Pattern
Virtual restoration drawing
Unearthed Costume
(581AD—618AD)
Flat
Pattern
Virtual restoration drawing
Unearthed Costume
(618AD—907AD)
Flat
Pattern
Virtual restoration drawing


Unearthed Costume
(618AD—907AD)
Flat
Unearthed Costume
(581AD—618AD)
Flat
Pattern
Virtual restoration
drawing
Pattern
Virtual restoration
drawing
Unearthed Costume
(581AD—618AD)
Flat
Unearthed Costume
(618AD—907AD)
Flat
Pattern
Virtual restoration
drawing
Pattern
Virtual restoration
drawing
Unearthed Costume
(618AD—907AD)
Flat
Unearthed Costume
(618AD—907AD)
Flat
Pattern
Virtual restoration
drawing
Pattern
Virtual restoration
drawing


Unearthed Costume
(618AD—907AD)
Flat
Pattern
Virtual restoration drawing
Unearthed Costume
(618AD—907AD)
Flat
Pattern
Virtual restoration drawing
Unearthed Costume
(581AD—618AD)
Flat
Pattern
Virtual restoration drawing
Unearthed Costume
(618AD—907AD)
Flat
Pattern
Virtual restoration drawing
Unearthed Costume
(618AD—907AD)
Flat
Pattern
Virtual restoration drawing
Unearthed Costume
(618AD—907AD)
Flat
Pattern
Virtual restoration drawing


Unearthed Costume (618AD—907AD)
Flat
Unearthed Costume (618AD—907AD)
Flat
Pattern
Virtual restoration drawing
Pattern
Virtual restoration drawing
Unearthed Costume (618AD—907AD)
Flat
Unearthed Costume (618AD—907AD)
Flat
Pattern
Virtual restoration drawing
Pattern
Virtual restoration drawing
Unearthed Costume (618AD—907AD)
Flat
Unearthed Costume (618AD—907AD)
Flat
Pattern
Virtual restoration drawing
Pattern
Virtual restoration drawing


Unearthed Costume (618AD—907AD)
Flat
Unearthed Costume (618AD—907AD)
Flat
Pattern
Virtual restoration drawing
Pattern
Virtual restoration drawing
Unearthed Costume (618AD—907AD)
Flat
Unearthed Costume (618AD—907AD)
Flat
Pattern
Virtual restoration drawing
Pattern
Virtual restoration drawing
Unearthed Costume (618AD—907AD)
Flat
Unearthed Costume (618AD—907AD)
Flat
Pattern
Virtual restoration drawing
Pattern
Virtual restoration drawing

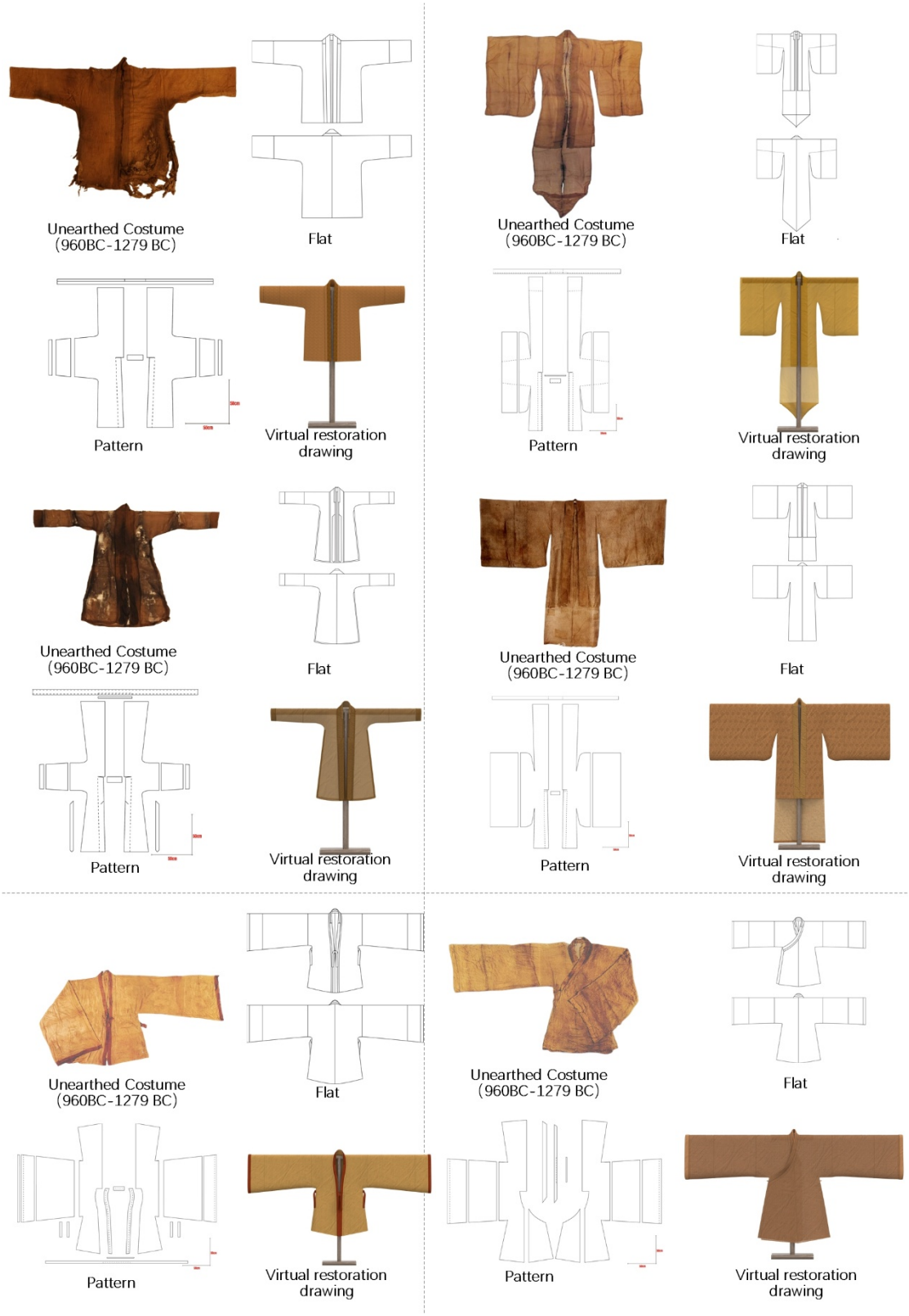
Unearthed Costume
(960BC-1279 BC)
Flat
Pattern
Virtual restoration
drawing
Unearthed Costume
(960BC-1279 BC)
Flat
Pattern
Virtual restoration
drawing
Unearthed Costume
(960BC-1279 BC)
Flat
Pattern
Virtual restoration
drawing
Unearthed Costume
(960BC-1279 BC)
Flat
Pattern
Virtual restoration
drawing
Unearthed Costume
(960BC-1279 BC)
Flat
Pattern
Virtual restoration
drawing
Unearthed Costume
(960BC-1279 BC)
Flat
Pattern
Virtual restoration
drawing

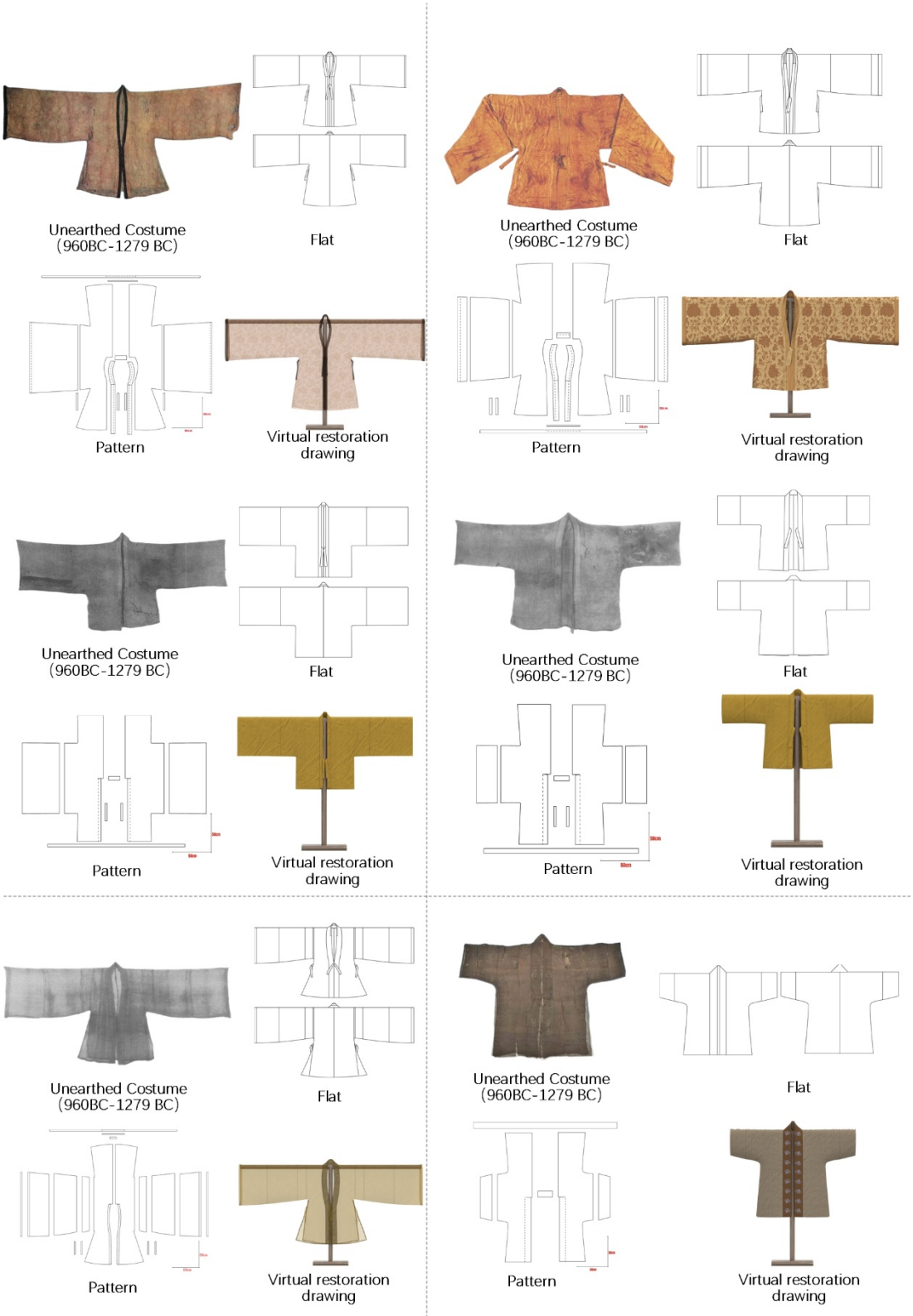
Unearthed Costume
(960BC-1279 BC)
Flat
Pattern
Virtual restoration
drawing
Unearthed Costume
(960BC-1279 BC)
Flat
Pattern
Virtual restoration
drawing
Unearthed Costume
(960BC-1279 BC)
Flat
Pattern
Virtual restoration
drawing
Unearthed Costume
(960BC-1279 BC)
Flat
Pattern
Virtual restoration
drawing
Unearthed Costume
(960BC-1279 BC)
Flat
Pattern
Virtual restoration
drawing
Unearthed Costume
(960BC-1279 BC)
Flat
Pattern
Virtual restoration
drawing

Unearthed Costume
(960BC-1279 BC)

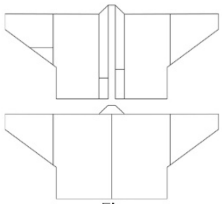

Flat

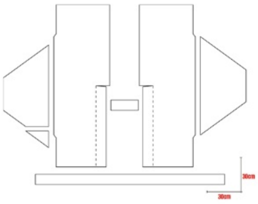

Pattern

Virtual restoration drawing

Unearthed Costume
(960BC-1279 BC)

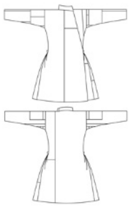

Flat

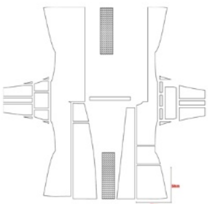

Pattern

Virtual restoration drawing

Unearthed Costume
(960BC-1279 BC)

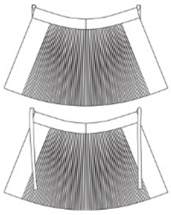

Flat

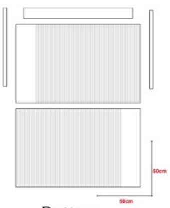

Pattern

Virtual restoration drawing

Unearthed Costume
(960BC-1279 BC)

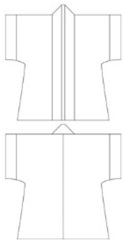

Flat

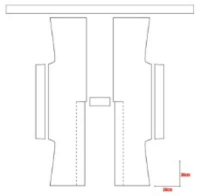

Pattern

Virtual restoration drawing

Unearthed Costume
(960BC-1279 BC)

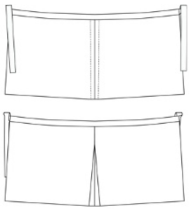

Flat

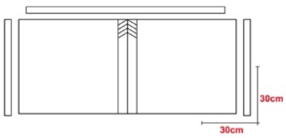

Pattern

Virtual restoration drawing

Unearthed Costume
(960BC-1279 BC)

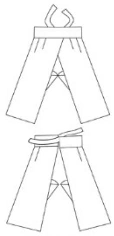

Flat

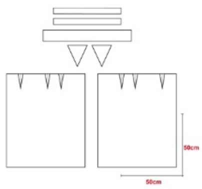

Pattern

Virtual restoration drawing


Unearthed Costume (960BC-1279 BC)
Flat
Pattern
Virtual restoration drawing
Unearthed Costume (960BC-1279 BC)
Flat
Pattern
Virtual restoration drawing
Unearthed Costume (960BC-1279 BC)
Flat
Pattern
Virtual restoration drawing
Unearthed Costume (960BC-1279 BC)
Flat
Pattern
Virtual restoration drawing
Unearthed Costume (960BC-1279 BC)
Flat
Pattern
Virtual restoration drawing
Unearthed Costume (960BC-1279 BC)
Flat
Pattern
Virtual restoration drawing

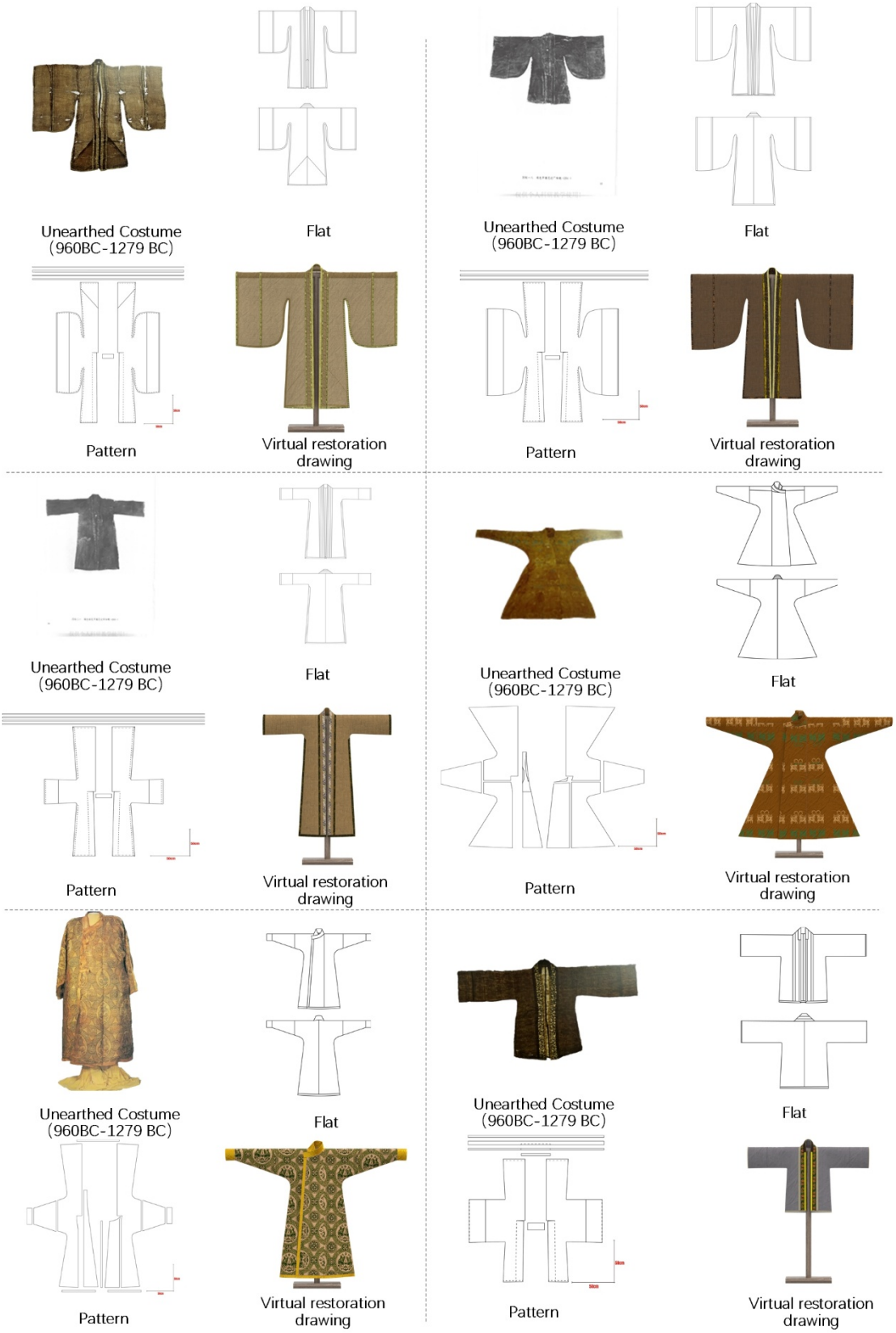
Unearthed Costume
(960BC-1279 BC)
Flat
Pattern
Virtual restoration drawing
Unearthed Costume
(960BC-1279 BC)
Flat
Pattern
Virtual restoration drawing
Unearthed Costume
(960BC-1279 BC)
Flat
Pattern
Virtual restoration drawing
Unearthed Costume
(960BC-1279 BC)
Flat
Pattern
Virtual restoration drawing
Unearthed Costume
(960BC-1279 BC)
Flat
Pattern
Virtual restoration drawing
Unearthed Costume
(960BC-1279 BC)
Flat
Pattern
Virtual restoration drawing

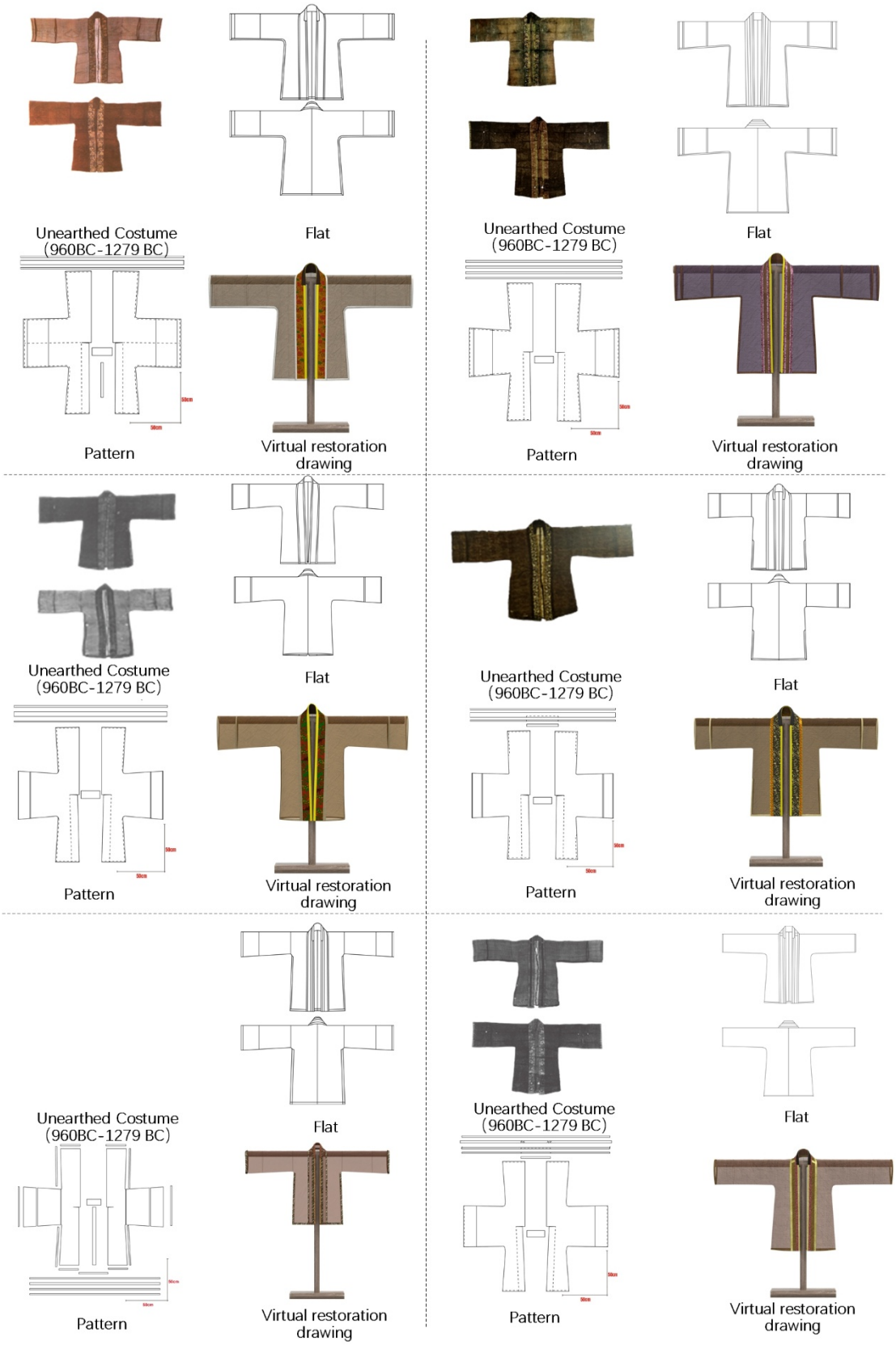
Unearthed Costume (960BC-1279 BC)
Flat
Pattern
Virtual restoration drawing
Unearthed Costume (960BC-1279 BC)
Flat
Pattern
Virtual restoration drawing
Unearthed Costume (960BC-1279 BC)
Flat
Pattern
Virtual restoration drawing
Unearthed Costume (960BC-1279 BC)
Flat
Pattern
Virtual restoration drawing
Unearthed Costume (960BC-1279 BC)
Flat
Pattern
Virtual restoration drawing

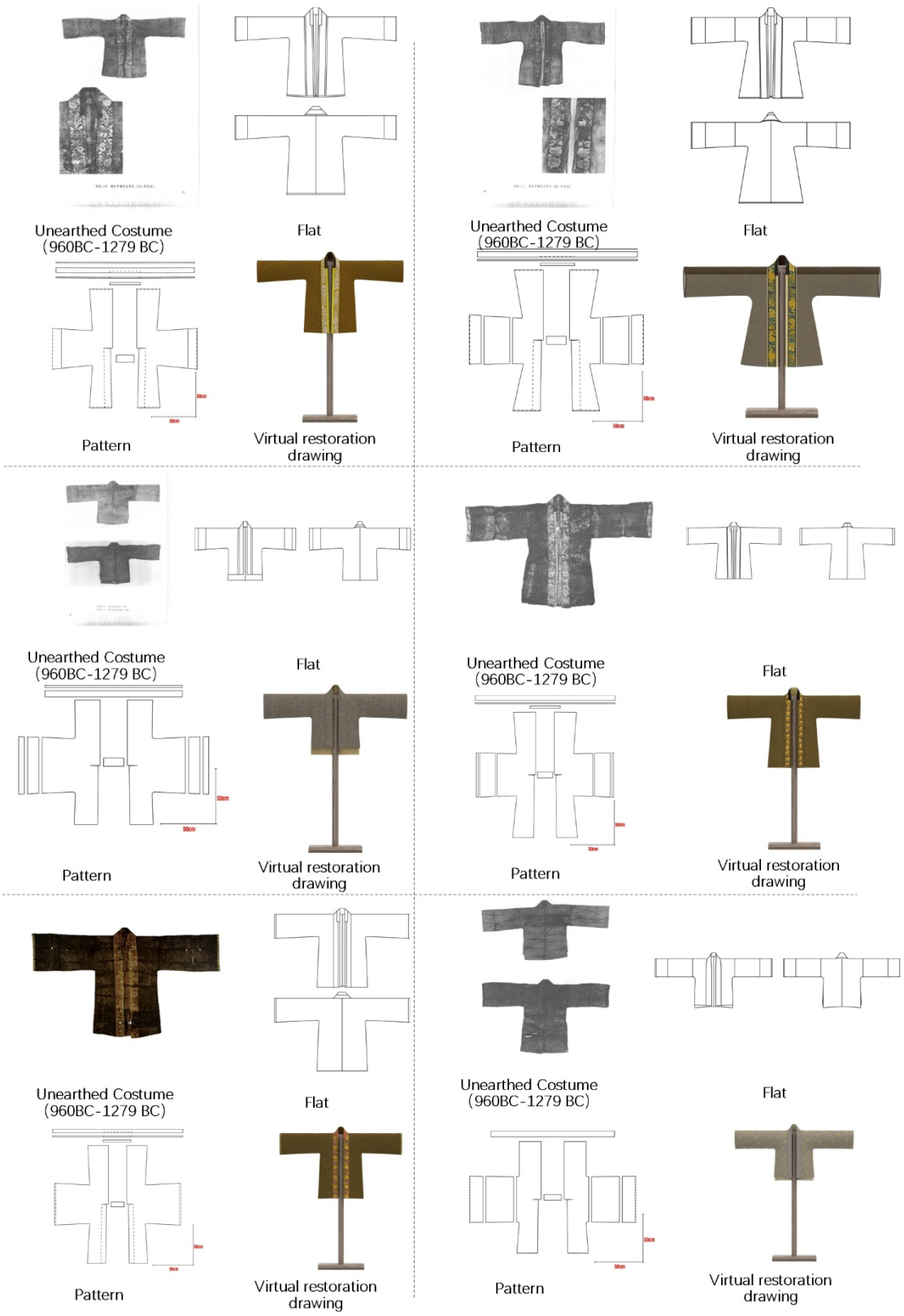
Unearthed Costume
(960BC-1279 BC)
Flat
Pattern
Virtual restoration
drawing
Unearthed Costume
(960BC-1279 BC)
Flat
Pattern
Virtual restoration
drawing
Unearthed Costume
(960BC-1279 BC)
Flat
Pattern
Virtual restoration
drawing
Unearthed Costume
(960BC-1279 BC)
Flat
Pattern
Virtual restoration
drawing
Unearthed Costume
(960BC-1279 BC)
Flat
Pattern
Virtual restoration
drawing
Unearthed Costume
(960BC-1279 BC)
Flat
Pattern
Virtual restoration
drawing

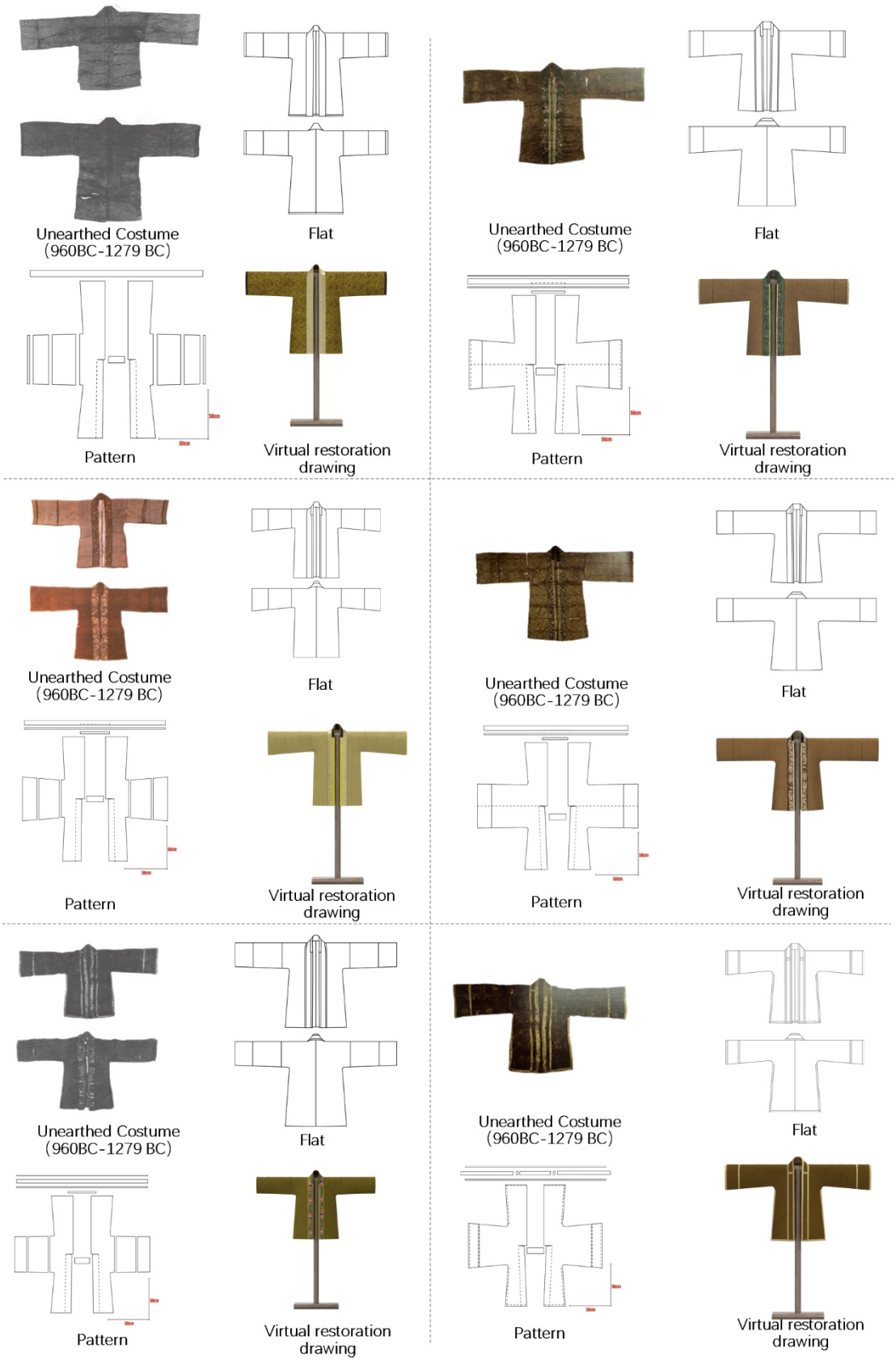
Unearthed Costume
(960BC-1279 BC)
Flat
Pattern
Virtual restoration
drawing
Unearthed Costume
(960BC-1279 BC)
Flat
Pattern
Virtual restoration
drawing
Unearthed Costume
(960BC-1279 BC)
Flat
Pattern
Virtual restoration
drawing
Unearthed Costume
(960BC-1279 BC)
Flat
Pattern
Virtual restoration
drawing
Unearthed Costume
(960BC-1279 BC)
Flat
Pattern
Virtual restoration
drawing
Unearthed Costume
(960BC-1279 BC)
Flat
Pattern
Virtual restoration
drawing

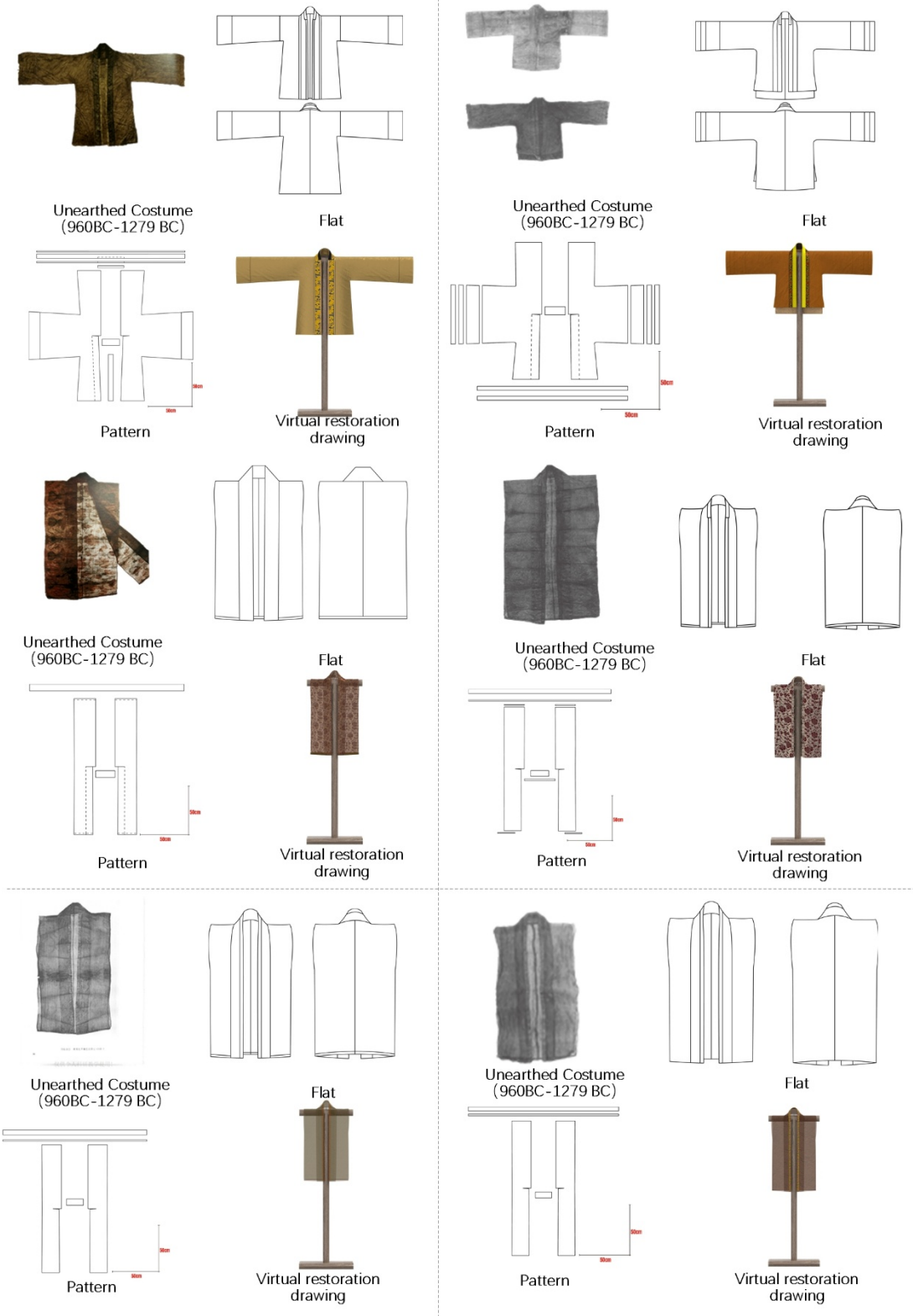
Unearthed Costume
(960BC-1279 BC)
Flat
Pattern
Virtual restoration
drawing
Unearthed Costume
(960BC-1279 BC)
Flat
Pattern
Virtual restoration
drawing
Unearthed Costume
(960BC-1279 BC)
Flat
Pattern
Virtual restoration
drawing
Unearthed Costume
(960BC-1279 BC)
Flat
Pattern
Virtual restoration
drawing
Unearthed Costume
(960BC-1279 BC)
Flat
Pattern
Virtual restoration
drawing
Unearthed Costume
(960BC-1279 BC)
Flat
Pattern
Virtual restoration
drawing


Unearthed Costume
(960BC-1279 BC)
Flat
Pattern
Virtual restoration
drawing
Unearthed Costume
(960BC-1279 BC)
Flat
Pattern
Virtual restoration
drawing
Unearthed Costume
(960BC-1279 BC)
Flat
Pattern
Virtual restoration
drawing
Unearthed Costume
(960BC-1279 BC)
Flat
Pattern
Virtual restoration
drawing
Unearthed Costume
(960BC-1279 BC)
Flat
Pattern
Virtual restoration
drawing
Unearthed Costume
(960BC-1279 BC)
Flat
Pattern
Virtual restoration
drawing

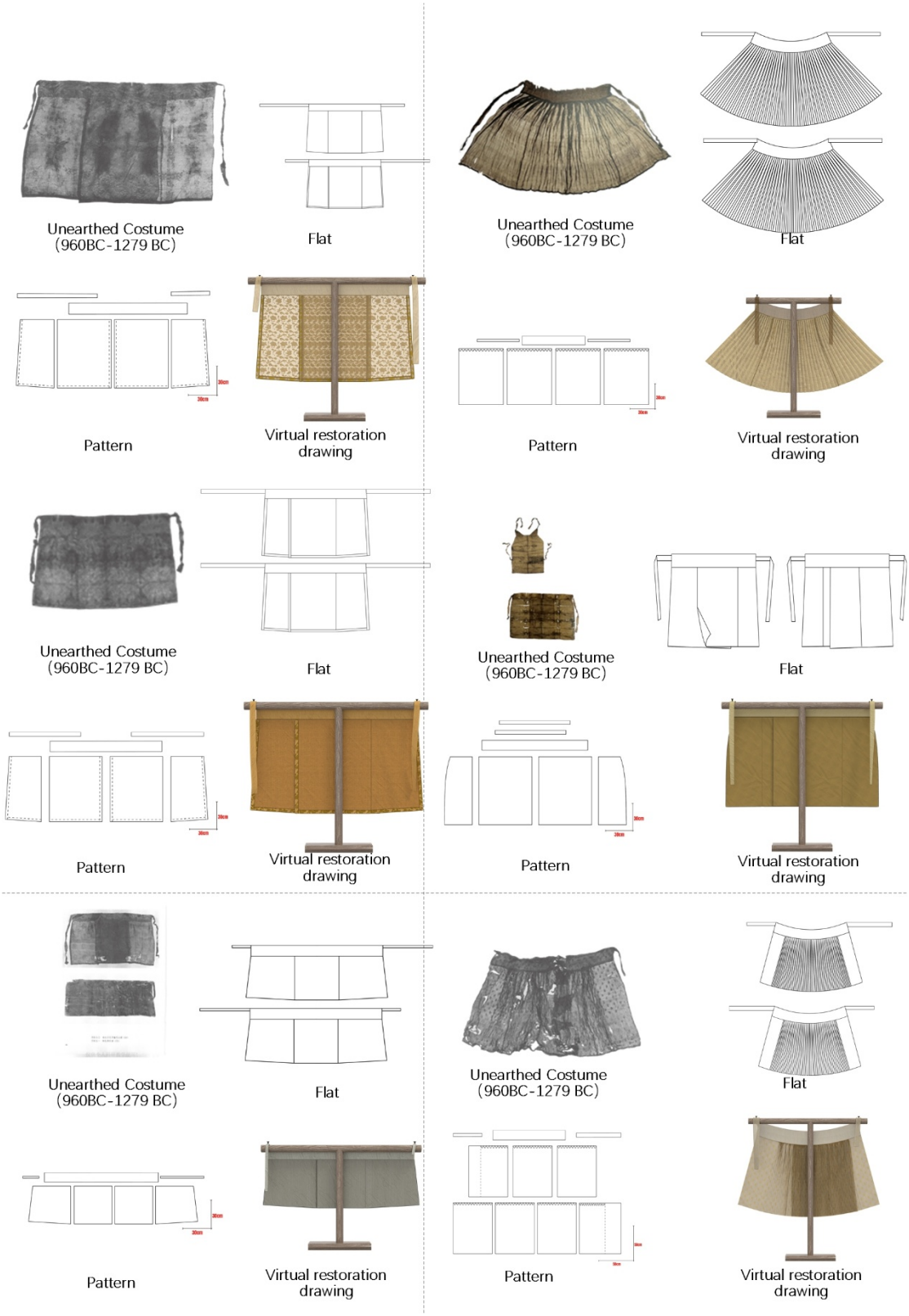
Unearthed Costume
(960BC-1279 BC)
Flat
Unearthed Costume
(960BC-1279 BC)
Flat
Pattern
Virtual restoration
drawing
Pattern
Virtual restoration
drawing
Unearthed Costume
(960BC-1279 BC)
Flat
Unearthed Costume
(960BC-1279 BC)
Flat
Pattern
Virtual restoration
drawing
Pattern
Virtual restoration
drawing
Unearthed Costume
(960BC-1279 BC)
Flat
Unearthed Costume
(960BC-1279 BC)
Flat
Pattern
Virtual restoration
drawing
Pattern
Virtual restoration
drawing

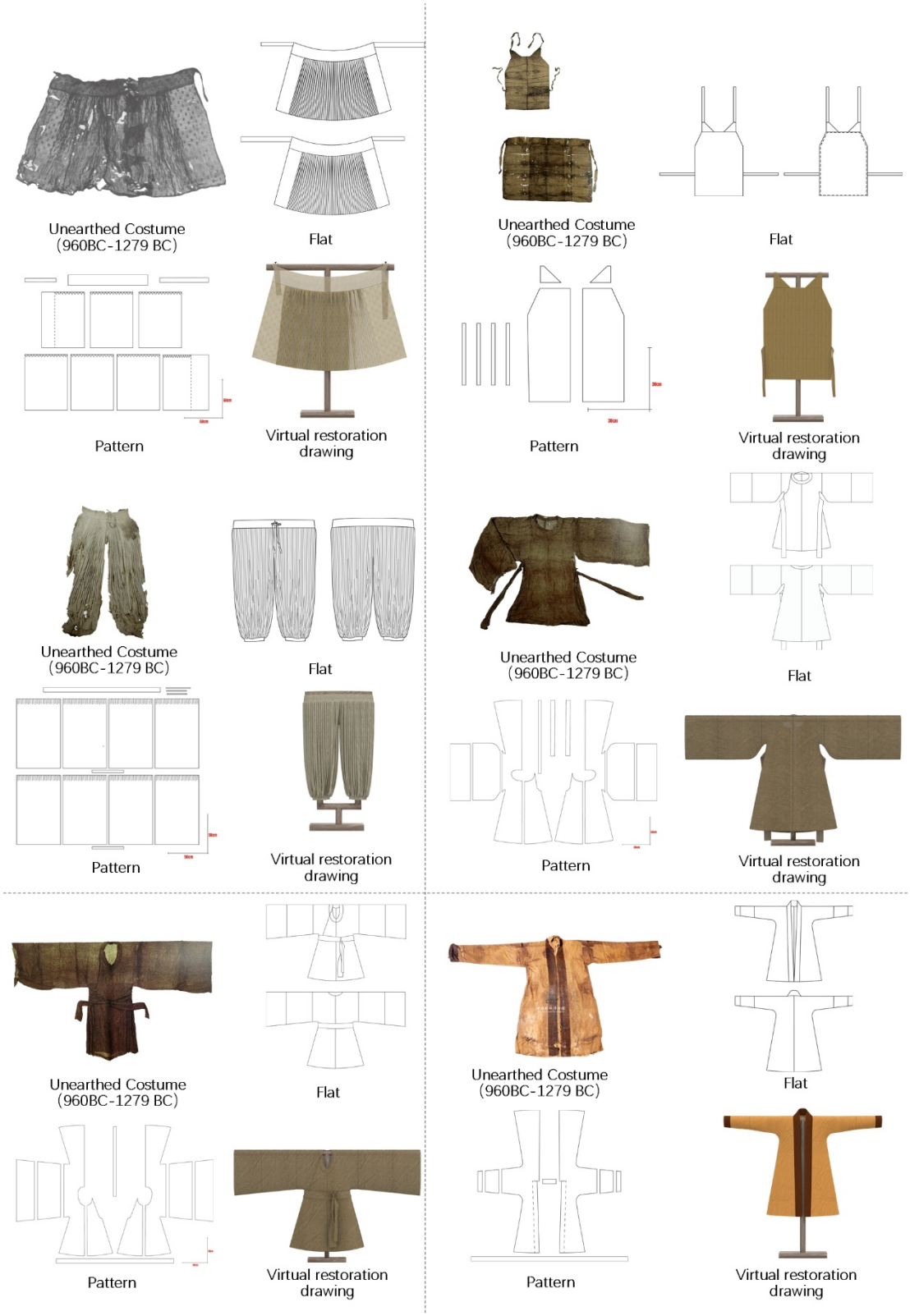
Unearthed Costume
(960BC-1279 BC)
Flat
Pattern
Virtual restoration
drawing
Unearthed Costume
(960BC-1279 BC)
Flat
Pattern
Virtual restoration
drawing
Unearthed Costume
(960BC-1279 BC)
Flat
Pattern
Virtual restoration
drawing
Unearthed Costume
(960BC-1279 BC)
Flat
Pattern
Virtual restoration
drawing
Unearthed Costume
(960BC-1279 BC)
Flat
Pattern
Virtual restoration
drawing
Unearthed Costume
(960BC-1279 BC)
Flat
Pattern
Virtual restoration
drawing


Unearthed Costume
(960BC-1279 BC)
Flat
Pattern
Virtual restoration
drawing
Unearthed Costume
(960BC-1279 BC)
Flat
Pattern
Virtual restoration
drawing
Unearthed Costume
(960BC-1279 BC)
Flat
Pattern
Virtual restoration
drawing
Unearthed Costume
(960BC-1279 BC)
Flat
Pattern
Virtual restoration
drawing
Unearthed Costume
(960BC-1279 BC)
Flat
Pattern
Virtual restoration
drawing
Unearthed Costume
(960BC-1279 BC)
Flat
Pattern
Virtual restoration
drawing

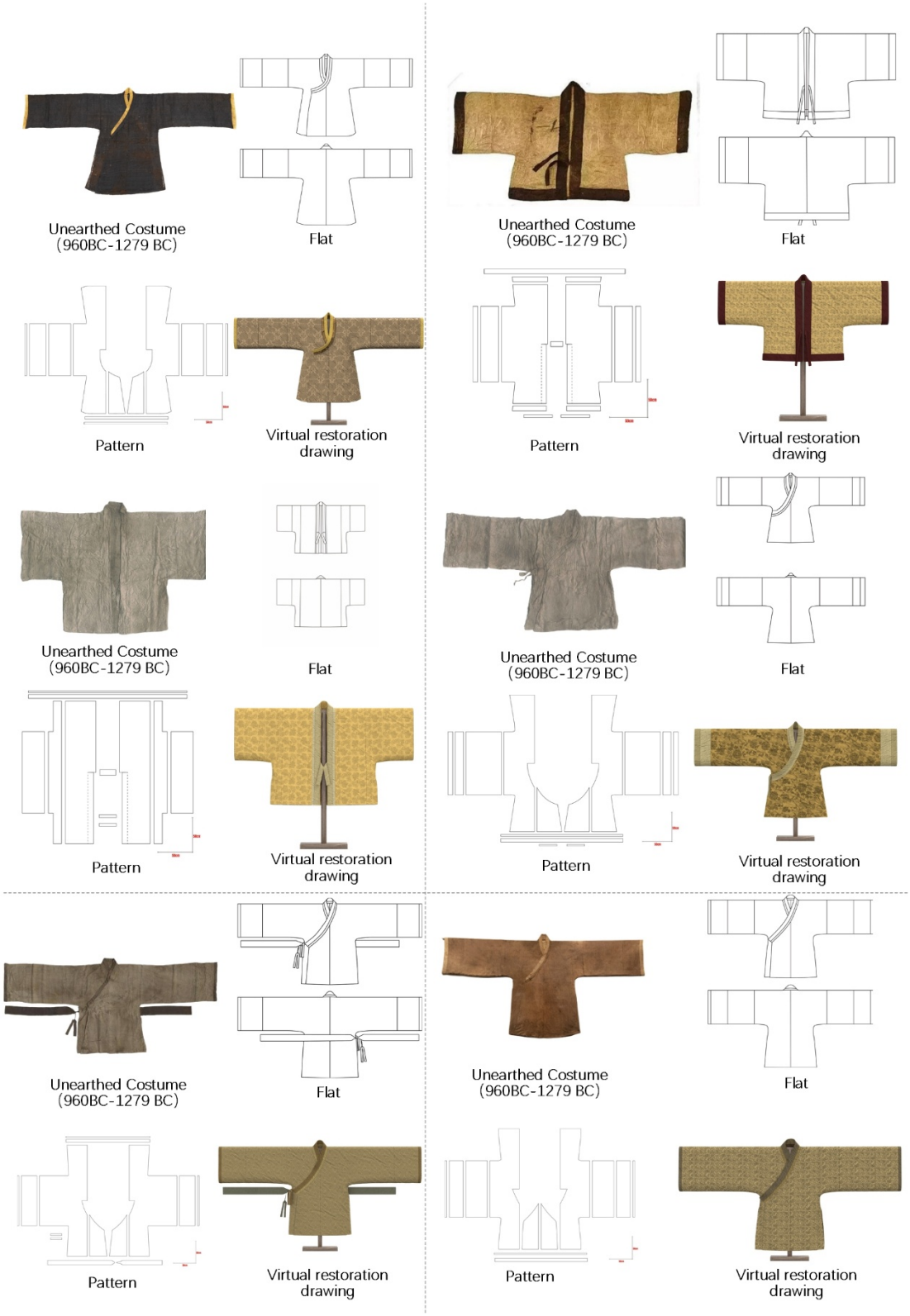
Unearthed Costume
(960BC-1279 BC)
Flat
Pattern
Virtual restoration
drawing
Unearthed Costume
(960BC-1279 BC)
Flat
Pattern
Virtual restoration
drawing
Unearthed Costume
(960BC-1279 BC)
Flat
Pattern
Virtual restoration
drawing
Unearthed Costume
(960BC-1279 BC)
Flat
Pattern
Virtual restoration
drawing
Unearthed Costume
(960BC-1279 BC)
Flat
Pattern
Virtual restoration
drawing
Unearthed Costume
(960BC-1279 BC)
Flat
Pattern
Virtual restoration
drawing

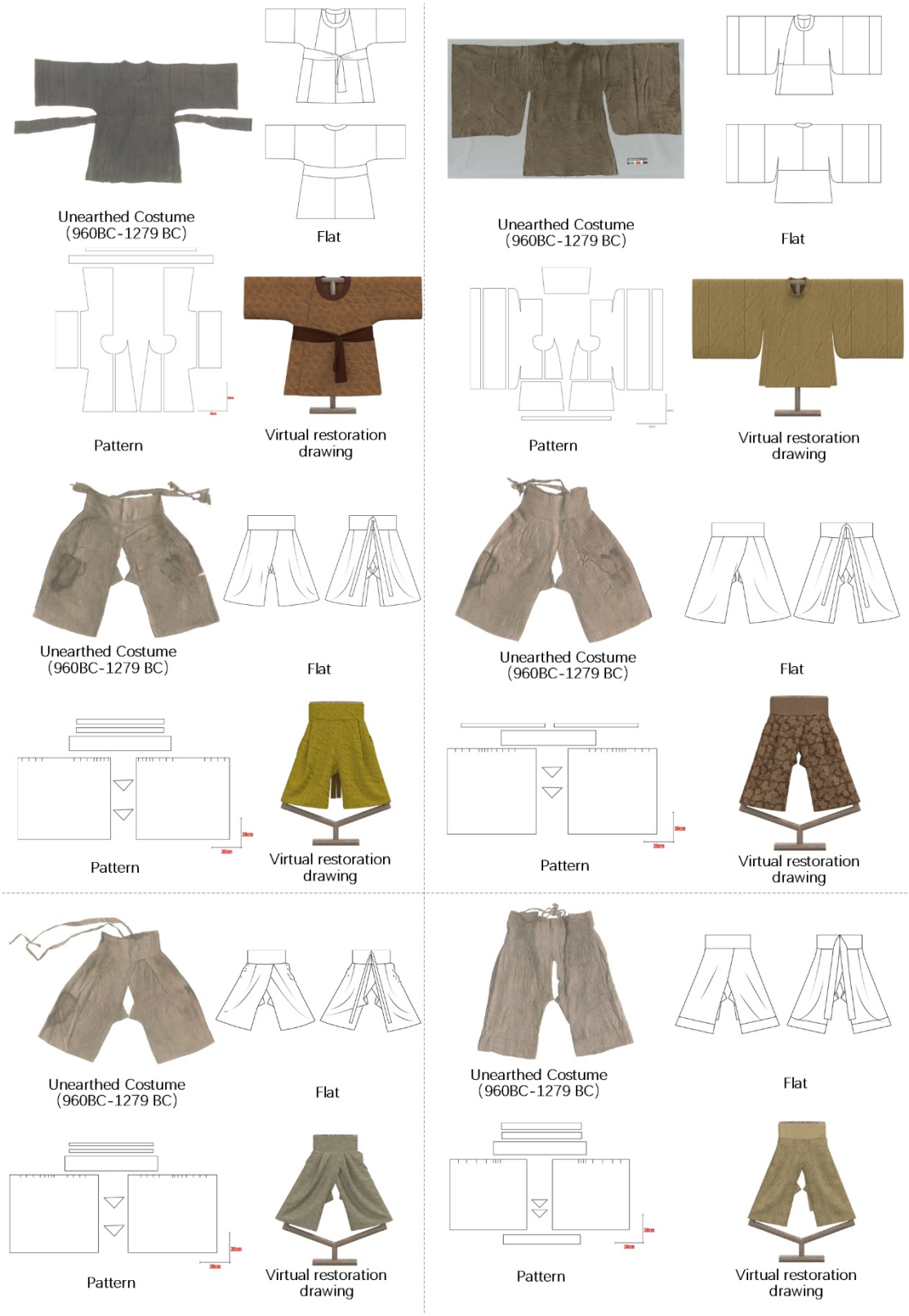
Unearthed Costume
(960BC-1279 BC)
Flat
Unearthed Costume
(960BC-1279 BC)
Flat
Pattern
Virtual restoration
drawing
Pattern
Virtual restoration
drawing
Unearthed Costume
(960BC-1279 BC)
Flat
Unearthed Costume
(960BC-1279 BC)
Flat
Pattern
Virtual restoration
drawing
Pattern
Virtual restoration
drawing
Unearthed Costume
(960BC-1279 BC)
Flat
Unearthed Costume
(960BC-1279 BC)
Flat
Pattern
Virtual restoration
drawing
Pattern
Virtual restoration
drawing

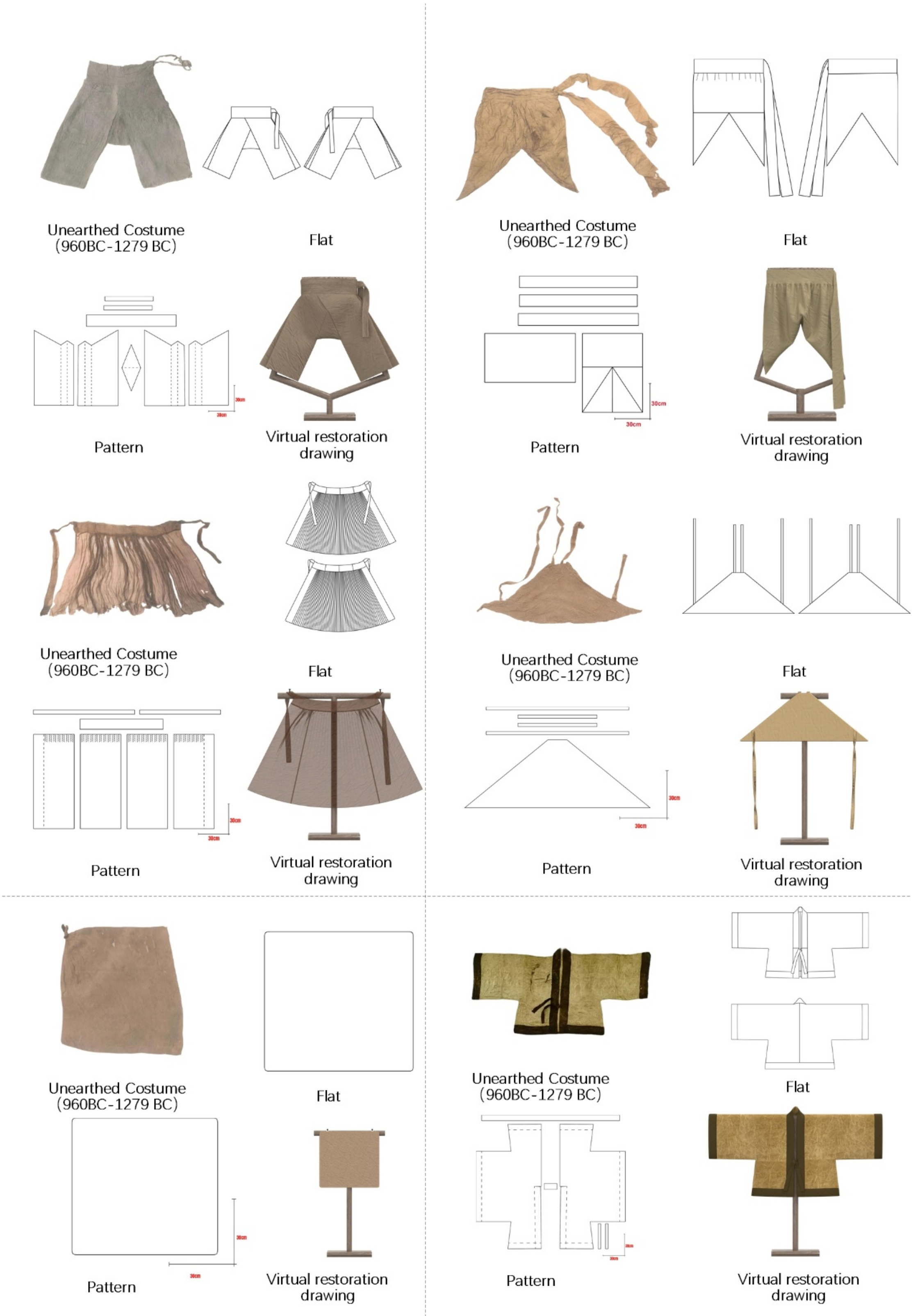

Unearthed Costume (960BC-1279 BC)
Flat
Pattern
Virtual restoration drawing
Unearthed Costume (960BC-1279 BC)
Flat
Pattern
Virtual restoration drawing
Unearthed Costume (960BC-1279 BC)
Flat
Pattern
Virtual restoration drawing
Unearthed Costume (960BC-1279 BC)
Flat
Pattern
Virtual restoration drawing
Unearthed Costume (960BC-1279 BC)
Flat
Pattern
Virtual restoration drawing
Unearthed Costume (960BC-1279 BC)
Flat
Pattern
Virtual restoration drawing


Unearthed Costume (916AD—1125AD)
Flat
Unearthed Costume (916AD—1125AD)
Flat
Pattern
Virtual restoration drawing
Pattern
Virtual restoration drawing
Unearthed Costume (916AD—1125AD)
Flat
Unearthed Costume (916AD—1125AD)
Flat
Pattern
Virtual restoration drawing
Pattern
Virtual restoration drawing
Unearthed Costume (916AD—1125AD)
Flat
Unearthed Costume (916AD—1125AD)
Flat
Pattern
Virtual restoration drawing
Pattern
Virtual restoration drawing


Unearthed Costume
(1271AD—1368AD)
Flat
Unearthed Costume
(1271AD—1368AD)
Flat
Pattern
Virtual restoration
drawing
Pattern
Virtual restoration
drawing
Unearthed Costume
(1271AD—1368AD)
Flat
Unearthed Costume
(1125AD—1234AD)
Flat
Pattern
Virtual restoration
drawing
Pattern
Virtual restoration
drawing
Unearthed Costume
(1271AD—1368AD)
Flat
Unearthed Costume
(916AD—1125AD)
Flat
Pattern
Virtual restoration
drawing
Pattern
Virtual restoration
drawing


Unearthed Costume
(1125AD—1234AD)
Flat
Unearthed Costume
(1125AD—1234AD)
Flat
Pattern
Virtual restoration
drawing
Pattern
Virtual restoration
drawing
Unearthed Costume
(916AD—1125AD)
Flat
Unearthed Costume
(1271AD—1368AD)
Flat
Pattern
Virtual restoration
drawing
Pattern
Virtual restoration
drawing
Unearthed Costume
(1271AD—1368AD)
Flat
Unearthed Costume
(916AD—1125AD)
Flat
Pattern
Virtual restoration
drawing
Pattern
Virtual restoration
drawing


Unearthed Costume
(1125AD—1234AD)
Flat
Unearthed Costume
(1125AD—1234AD)
Flat
Pattern
Virtual restoration
drawing
Pattern
Virtual restoration
drawing
Unearthed Costume
(916AD—1125AD)
Flat
Unearthed Costume
(916AD—1125AD)
Flat
Pattern
Virtual restoration
drawing
Pattern
Virtual restoration
drawing
Unearthed Costume
(916AD—1125AD)
Flat
Unearthed Costume
(1271AD—1368AD)
Flat
Pattern
Virtual restoration
drawing
Pattern
Virtual restoration
drawing


Unearthed Costume
(1271AD—1368AD)
Flat
Pattern
Virtual restoration drawing
Unearthed Costume
(1271AD—1368AD)
Flat
Pattern
Virtual restoration drawing
Unearthed Costume
(1271AD—1368AD)
Flat
Pattern
Virtual restoration drawing
Unearthed Costume
(916AD—1125AD)
Flat
Pattern
Virtual restoration drawing
Unearthed Costume
(916AD—1125AD)
Flat
Pattern
Virtual restoration drawing
Unearthed Costume
(1271AD—1368AD)
Flat
Pattern
Virtual restoration drawing


Unearthed Costume
(1271AD—1368AD)
Flat
Pattern
Virtual restoration drawing
Unearthed Costume
(916AD—1125AD)
Flat
Pattern
Virtual restoration drawing
Unearthed Costume
(1271AD—1368AD)
Flat
Pattern
Virtual restoration drawing
Unearthed Costume
(1271AD—1368AD)
Flat
Pattern
Virtual restoration drawing
Unearthed Costume
(1271AD—1368AD)
Flat
Pattern
Virtual restoration drawing
Unearthed Costume
(1125AD—1234AD)
Flat
Pattern
Virtual restoration drawing


Unearthed Costume (1125AD—1234AD)
Flat
Pattern
Virtual restoration drawing
Unearthed Costume (1125AD—1234AD)
Flat
Pattern
Virtual restoration drawing
Unearthed Costume (916AD—1125AD)
Flat
Pattern
Virtual restoration drawing
Unearthed Costume (1271AD—1368AD)
Flat
Pattern
Virtual restoration drawing
Unearthed Costume (1271AD—1368AD)
Flat
Pattern
Virtual restoration drawing
Unearthed Costume (1271AD—1368AD)
Flat
Pattern
Virtual restoration drawing

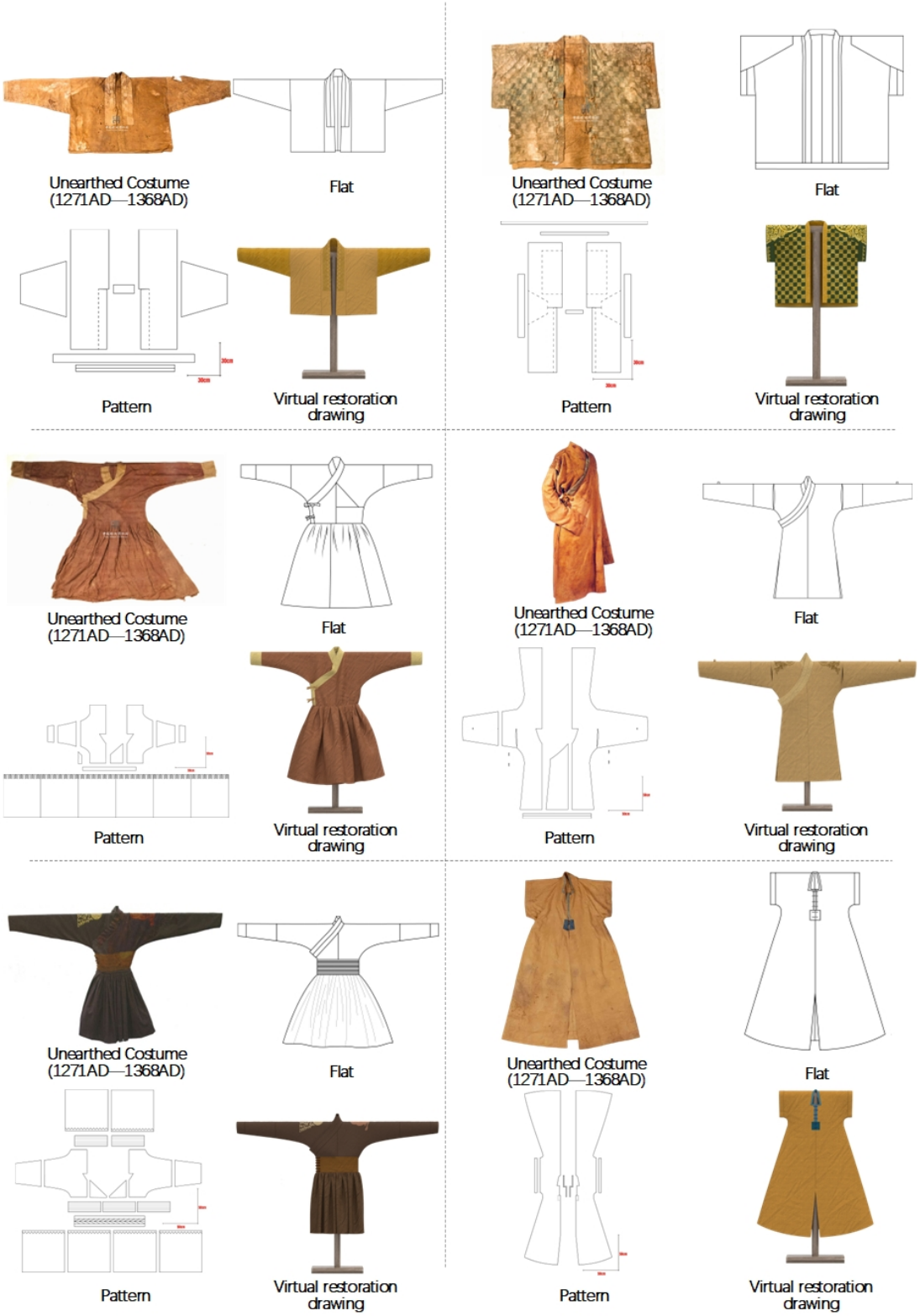
Unearthed Costume
(1271AD—1368AD)
Flat
Pattern
Virtual restoration
drawing
Unearthed Costume
(1271AD—1368AD)
Flat
Pattern
Virtual restoration
drawing
Unearthed Costume
(1271AD—1368AD)
Flat
Pattern
Virtual restoration
drawing
Unearthed Costume
(1271AD—1368AD)
Flat
Pattern
Virtual restoration
drawing
Unearthed Costume
(1271AD—1368AD)
Flat
Pattern
Virtual restoration
drawing
Unearthed Costume
(1271AD—1368AD)
Flat
Pattern
Virtual restoration
drawing


Unearthed Costume
(1271AD—1368AD)
Flat
Pattern
Virtual restoration drawing
Unearthed Costume
(1271AD—1368AD)
Flat
Pattern
Virtual restoration drawing
Unearthed Costume
(1271AD—1368AD)
Flat
Pattern
Virtual restoration drawing
Unearthed Costume
(618AD—907AD)
Flat
Pattern
Virtual restoration drawing
Unearthed Costume
(1271AD—1368AD)
Flat
Pattern
Virtual restoration drawing
Unearthed Costume
(916AD—1125AD)
Flat
Pattern
Virtual restoration drawing


Unearthed Costume(1368AD - 1644AD)


Flat


Pattern


Virtual restoration drawing


Unearthed Costume(1368AD - 1644AD)

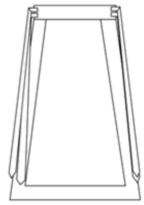
Flat

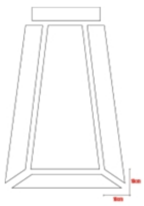
Pattern


Virtual restoration drawing

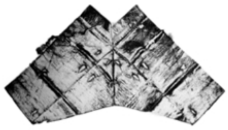
Unearthed Costume(1368AD - 1644AD)

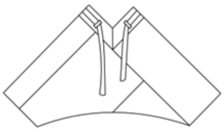
Flat

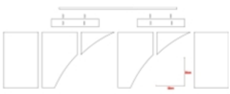
Pattern


Virtual restoration drawing


Unearthed Costume(1368AD - 1644AD)

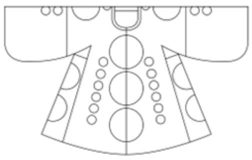
Flat

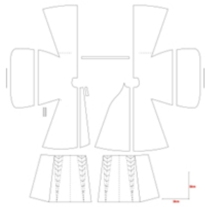
Pattern


Virtual restoration drawing


Unearthed Costume(1368AD - 1644AD)

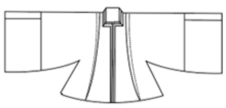
Flat

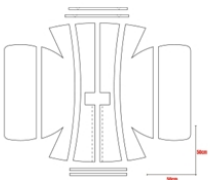
Pattern


Virtual restoration drawing


Unearthed Costume(1368AD - 1644AD)

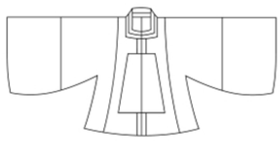
Flat

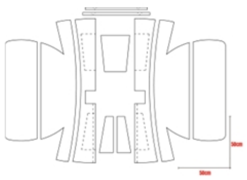
Pattern


Virtual restoration drawing


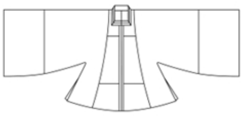

Unearthed Costume(1368AD - 1644AD)

Flat

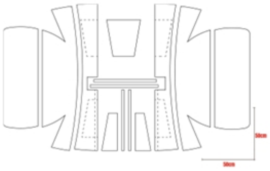


Pattern

Virtual restoration drawing


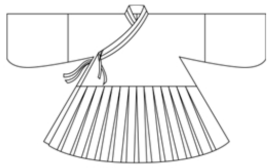

Unearthed Costume(1368AD - 1644AD)

Flat

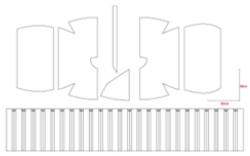


Pattern

Virtual restoration drawing


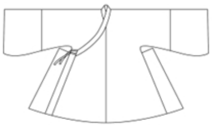

Unearthed Costume(1368AD - 1644AD)

Flat


Pattern

Virtual restoration drawing


Unearthed Costume(1368AD - 1644AD)

Flat

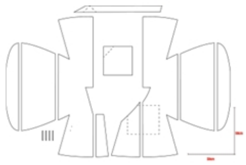


Pattern

Virtual restoration drawing


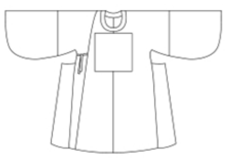

Unearthed Costume(1368AD - 1644AD)

Flat

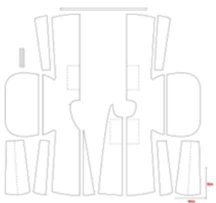


Pattern

Virtual restoration drawing


Unearthed Costume(1368AD - 1644AD)

Flat

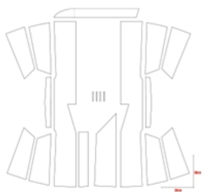


Pattern

Virtual restoration drawing


Unearthed Costume(1368AD - 1644AD)

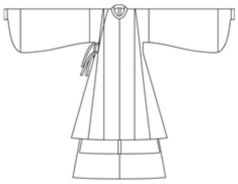
Flat

Pattern


Virtual restoration drawing


Unearthed Costume(1368AD - 1644AD)

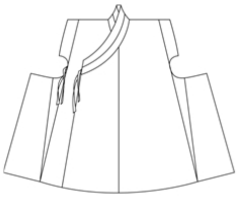
Flat

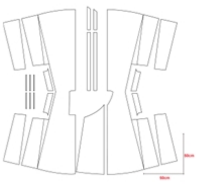
Pattern


Virtual restoration drawing


Unearthed Costume(1368AD - 1644AD)


Flat

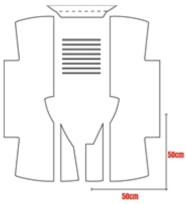
Pattern


Virtual restoration drawing


Unearthed Costume(1368AD - 1644AD)

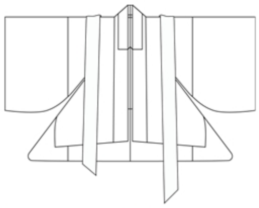
Flat

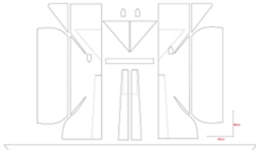
Pattern


Virtual restoration drawing


Unearthed Costume(1368AD - 1644AD)

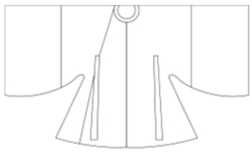
Flat

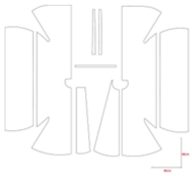
Pattern


Virtual restoration drawing


Unearthed Costume(1368AD - 1644AD)

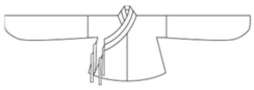
Flat

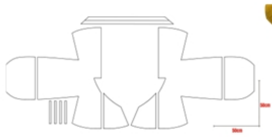
Pattern


Virtual restoration drawing

Appendix 5


Unearthed Costume(1368AD－1644AD)

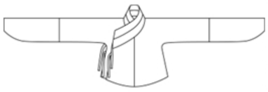
Flat

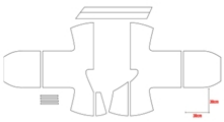
Pattern


Virtual restoration drawing


Unearthed Costume(1368AD－1644AD)


Flat

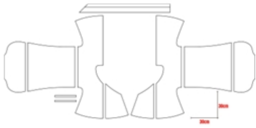
Pattern


Virtual restoration drawing


Unearthed Costume(1368AD－1644AD)

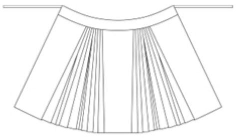
Flat

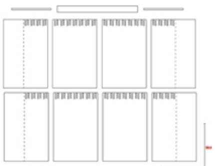
Pattern


Virtual restoration drawing


Unearthed Costume(1368AD－1644AD)

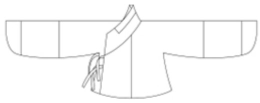
Flat

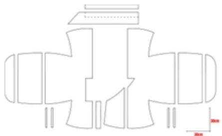
Pattern


Virtual restoration drawing


Unearthed Costume(1368AD－1644AD)

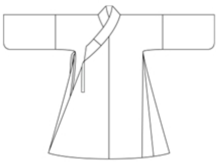
Flat

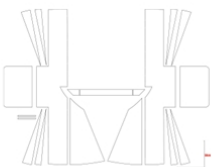
Pattern


Virtual restoration drawing


Unearthed Costume(1368AD－1644AD)

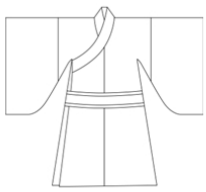
Flat

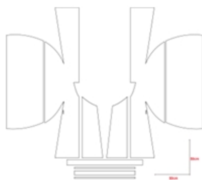
Pattern


Virtual restoration drawing


Unearthed Costume(1368AD - 1644AD)
Flat
Pattern
Virtual restoration drawing
Unearthed Costume(1368AD - 1644AD)
Flat
Pattern
Virtual restoration drawing
Unearthed Costume(1368AD - 1644AD)
Flat
Pattern
Virtual restoration drawing
Unearthed Costume(1368AD - 1644AD)
Flat
Pattern
Virtual restoration drawing
Unearthed Costume(1368AD - 1644AD)
Flat
Pattern
Virtual restoration drawing
Unearthed Costume(1368AD - 1644AD)
Flat
Pattern
Virtual restoration drawing

Unearthed Costume(1368AD – 1644AD)

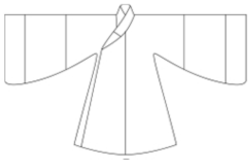

Flat

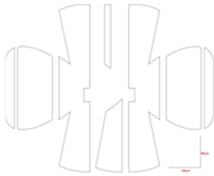

Pattern

Virtual restoration drawing

Unearthed Costume(1368AD – 1644AD)

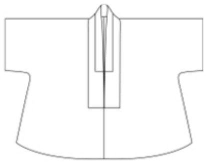

Flat

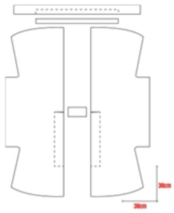

Pattern

Virtual restoration drawing

Unearthed Costume(1368AD – 1644AD)

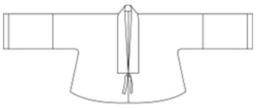

Flat

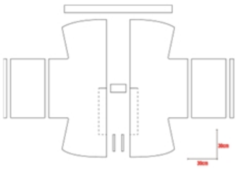

Pattern

Virtual restoration drawing

Unearthed Costume(1368AD – 1644AD)

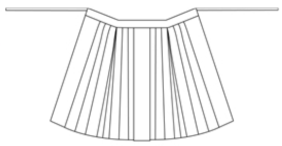

Flat

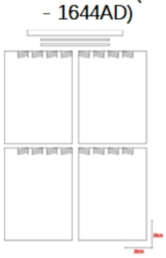

Pattern

Virtual restoration drawing

Unearthed Costume(1368AD – 1644AD)

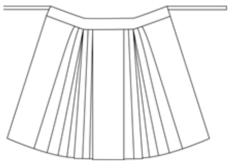

Flat

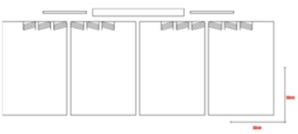

Pattern

Virtual restoration drawing

Unearthed Costume(1368AD – 1644AD)

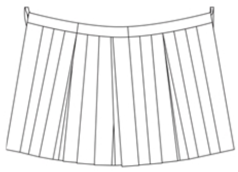

Flat

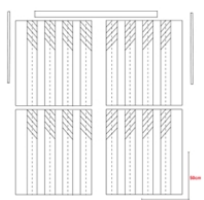

Pattern

Virtual restoration drawing

Appendix 5


Unearthed Costume(1368AD - 1644AD)

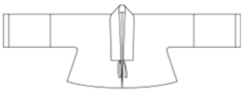
Flat

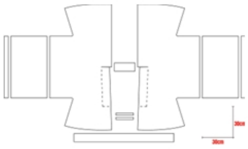
Pattern


Virtual restoration drawing


Unearthed Costume(1368AD - 1644AD)

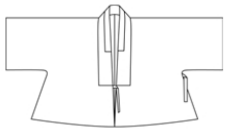
Flat

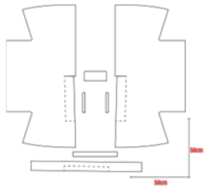
Pattern


Virtual restoration drawing


Unearthed Costume(1368AD - 1644AD)


Flat

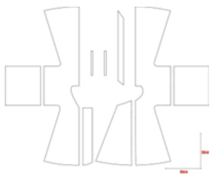
Pattern


Virtual restoration drawing


Unearthed Costume(1368AD - 1644AD)


Flat

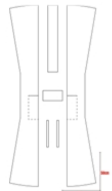
Pattern


Virtual restoration drawing


Unearthed Costume(1368AD - 1644AD)

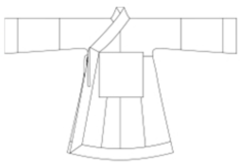
Flat

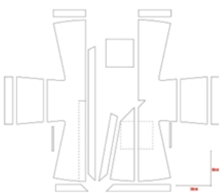
Pattern


Virtual restoration drawing


Unearthed Costume(1368AD - 1644AD)

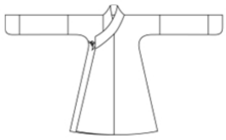
Flat

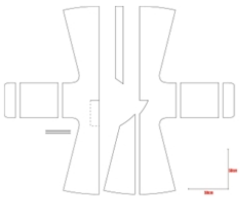
Pattern


Virtual restoration drawing


Unearthed Costume(1368AD - 1644AD)

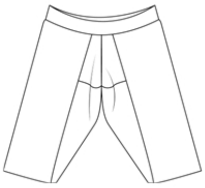
Flat

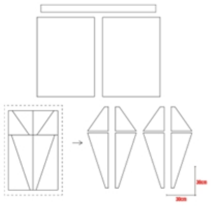
Pattern


Virtual restoration drawing


Unearthed Costume(1368AD - 1644AD)


Flat

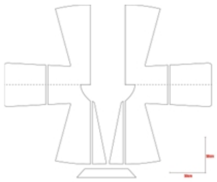
Pattern


Virtual restoration drawing


Unearthed Costume(1368AD - 1644AD)

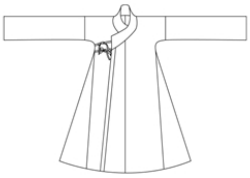
Flat

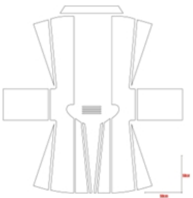
Pattern


Virtual restoration drawing


Unearthed Costume(1368AD - 1644AD)

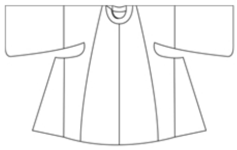
Flat

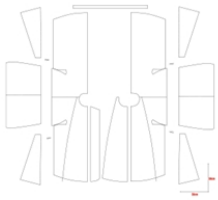
Pattern


Virtual restoration drawing


Unearthed Costume(1368AD - 1644AD)

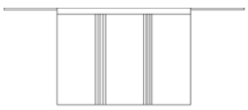
Flat

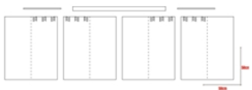
Pattern


Virtual restoration drawing


Unearthed Costume(1368AD - 1644AD)


Flat

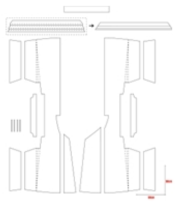
Pattern


Virtual restoration drawing


Unearthed Costume(1368AD - 1644AD)

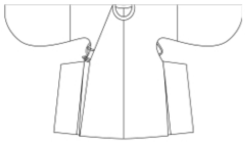
Flat

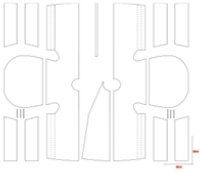
Pattern


Virtual restoration drawing


Unearthed Costume(1368AD - 1644AD)

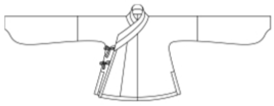
Flat

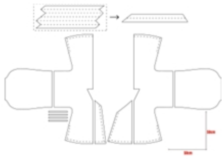
Pattern


Virtual restoration drawing


Unearthed Costume(1368AD - 1644AD)

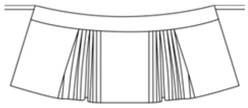
Flat

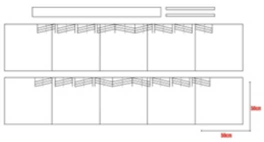
Pattern


Virtual restoration drawing


Unearthed Costume(1368AD - 1644AD)

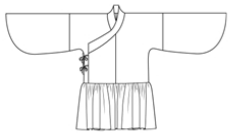
Flat

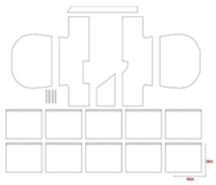
Pattern


Virtual restoration drawing


Unearthed Costume(1368AD - 1644AD)

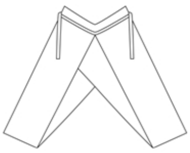
Flat

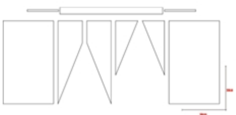
Pattern


Virtual restoration drawing


Unearthed Costume(1368AD - 1644AD)

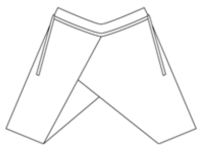
Flat

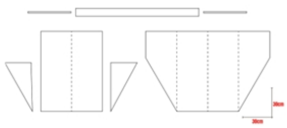
Pattern


Virtual restoration drawing


Unearthed Costume(1368AD - 1644AD)


Flat

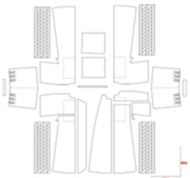
Pattern


Virtual restoration drawing


Unearthed Costume(1368AD - 1644AD)

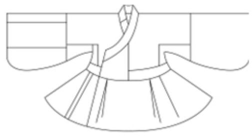
Flat

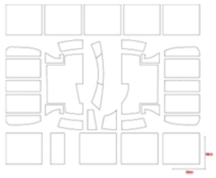
Pattern


Virtual restoration drawing


Unearthed Costume(1368AD - 1644AD)


Flat

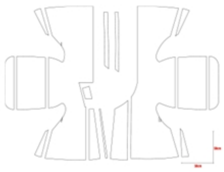
Pattern


Virtual restoration drawing


Unearthed Costume(1368AD - 1644AD)

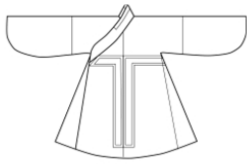
Flat

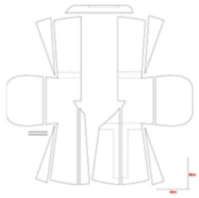
Pattern


Virtual restoration drawing


Unearthed Costume(1368AD - 1644AD)

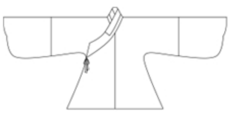
Flat

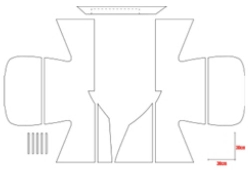
Pattern


Virtual restoration drawing


Unearthed Costume(1368AD - 1644AD)

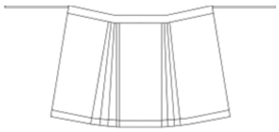
Flat

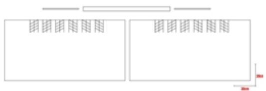
Pattern


Virtual restoration drawing


Unearthed Costume(1368AD - 1644AD)


Flat

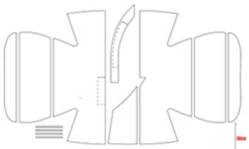
Pattern


Virtual restoration drawing


Unearthed Costume(1368AD - 1644AD)

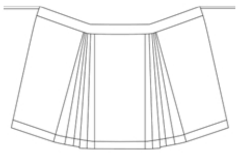
Flat


Pattern


Virtual restoration drawing


Unearthed Costume(1368AD - 1644AD)

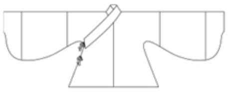
Flat

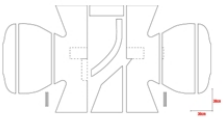
Pattern


Virtual restoration drawing


Unearthed Costume(1368AD - 1644AD)

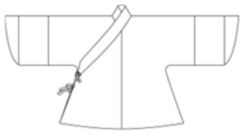
Flat


Pattern


Virtual restoration drawing


Unearthed Costume(1368AD - 1644AD)

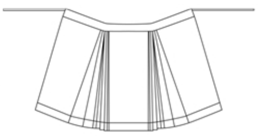
Flat

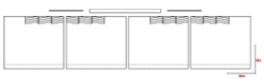
Pattern


Virtual restoration drawing


Unearthed Costume(1368AD - 1644AD)

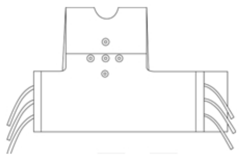
Flat

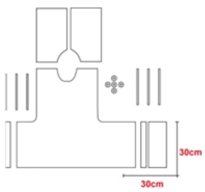

Pattern


Virtual restoration drawing

Unearthed Costume(1368AD - 1644AD)

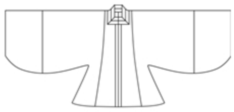

Flat

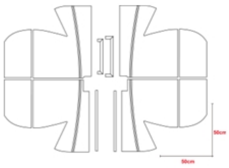

Pattern

Virtual restoration drawing

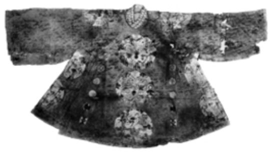

Unearthed Costume(1368AD - 1644AD)

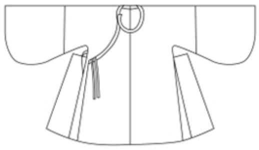

Flat

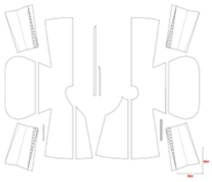

Pattern

Virtual restoration drawing

Unearthed Costume(1368AD - 1644AD)

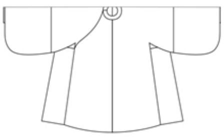

Flat

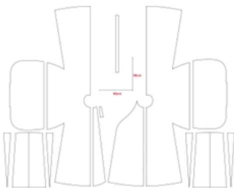

Pattern

Virtual restoration drawing

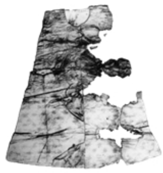

Unearthed Costume(1368AD - 1644AD)

Flat

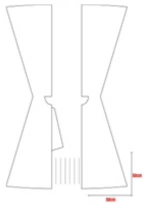

Pattern

Virtual restoration drawing

Unearthed Costume(1368AD - 1644AD)

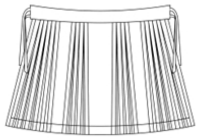

Flat

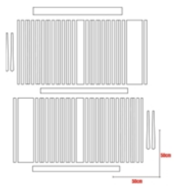

Pattern

Virtual restoration drawing

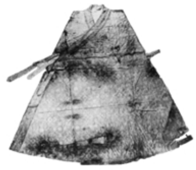

Unearthed Costume(1368AD - 1644AD)

Flat

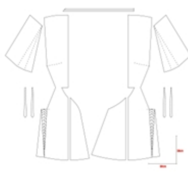

Pattern

Virtual restoration drawing

Unearthed Costume(1368AD – 1644AD)

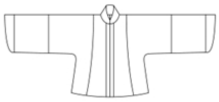

Flat

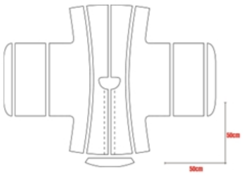

Pattern

Virtual restoration drawing

Unearthed Costume(1368AD – 1644AD)

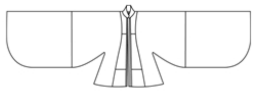

Flat

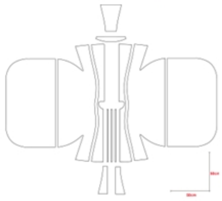

Pattern

Virtual restoration drawing

Unearthed Costume(1368AD – 1644AD)

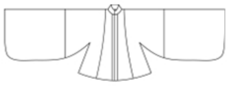

Flat

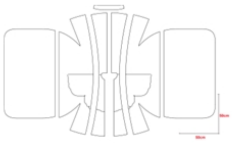

Pattern

Virtual restoration drawing

Unearthed Costume(1368AD – 1644AD)

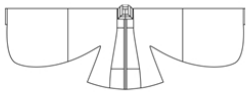

Flat

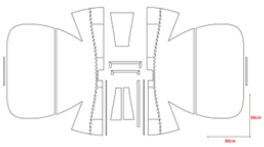

Pattern

Virtual restoration drawing

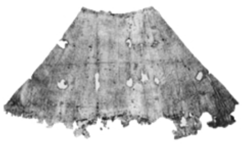

Unearthed Costume(1368AD – 1644AD)

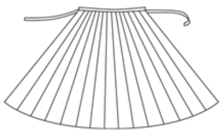

Flat

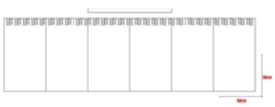

Pattern

Virtual restoration drawing

Unearthed Costume(1368AD – 1644AD)

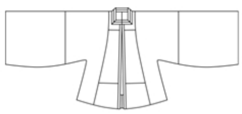

Flat

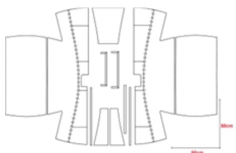

Pattern

Virtual restoration drawing


Unearthed Costume(1368AD - 1644AD)

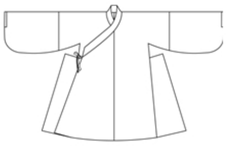
Flat

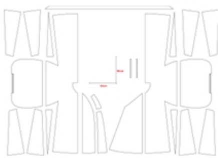
Pattern


Virtual restoration drawing


Unearthed Costume(1368AD - 1644AD)

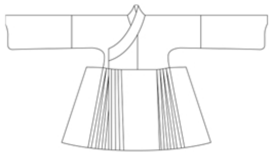
Flat

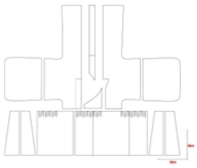
Pattern


Virtual restoration drawing


Unearthed Costume(1368AD - 1644AD)

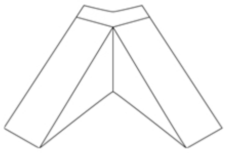
Flat

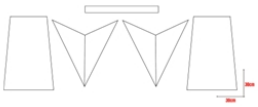
Pattern


Virtual restoration drawing


Unearthed Costume(1368AD - 1644AD)

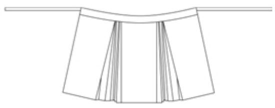
Flat

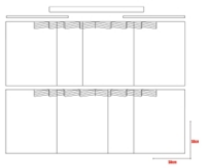
Pattern


Virtual restoration drawing


Unearthed Costume(1368AD - 1644AD)


Flat


Pattern


Virtual restoration drawing


Unearthed Costume(1368AD - 1644AD)

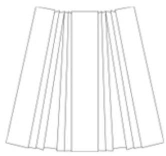
Flat

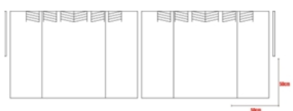
Pattern


Virtual restoration drawing


Unearthed Costume(1368AD - 1644AD)

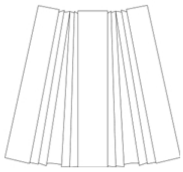
Flat


Pattern


Virtual restoration drawing


Unearthed Costume(1368AD - 1644AD)

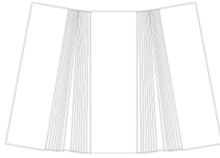
Flat

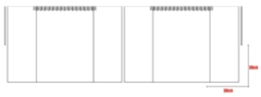
Pattern


Virtual restoration drawing


Unearthed Costume(1368AD - 1644AD)

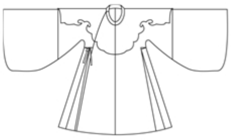
Flat

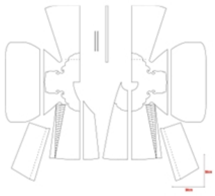
Pattern


Virtual restoration drawing


Unearthed Costume(1368AD - 1644AD)

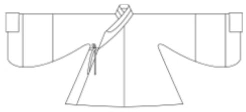
Flat

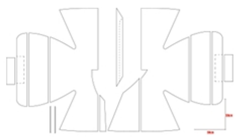
Pattern


Virtual restoration drawing


Unearthed Costume(1368AD - 1644AD)


Flat

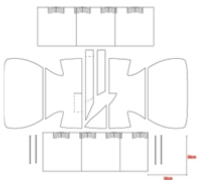
Pattern


Virtual restoration drawing


Unearthed Costume(1368AD - 1644AD)

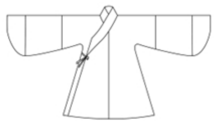
Flat

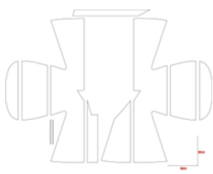
Pattern


Virtual restoration drawing

Unearthed Costume
(1616AD-1911AD)

Flat

Unearthed Costume
(1616AD-1911AD)

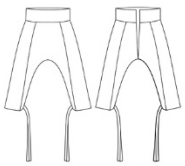

Flat

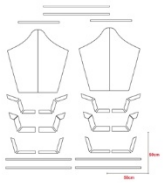

Pattern

Virtual restoration drawing

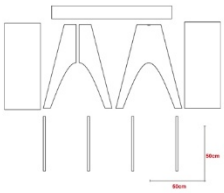

Pattern

Virtual restoration drawing

Unearthed Costume
(1616AD-1911AD)

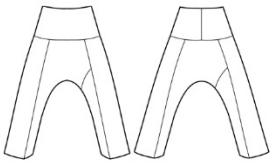

Flat

Unearthed Costume
(1616AD-1911AD)

Flat

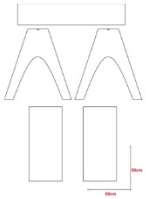

Pattern

Virtual restoration drawing

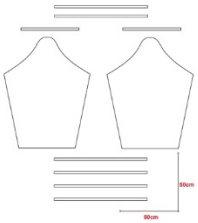

Pattern

Virtual restoration drawing

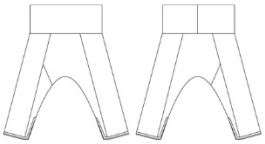

Flat

Unearthed Costume
(1616AD-1911AD)

Flat

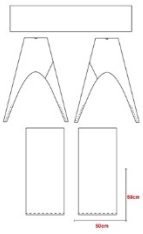

Pattern

Virtual restoration drawing

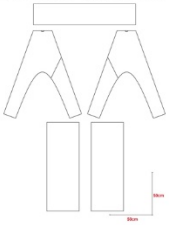

Pattern

Virtual restoration drawing


Unearthed Costume
(1616AD-1911AD)

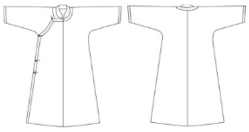
Flat

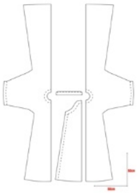
Pattern


Virtual restoration drawing


Unearthed Costume
(1616AD-1911AD)

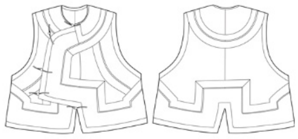
Flat

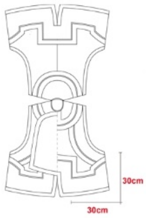
Pattern


Virtual restoration drawing


Unearthed Costume
(1616AD-1911AD)

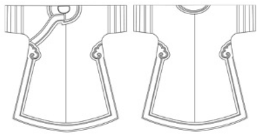
Flat

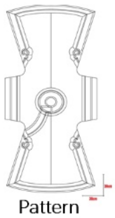
Pattern


Virtual restoration drawing


Unearthed Costume
(1616AD-1911AD)

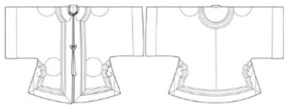
Flat

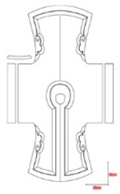
Pattern


Virtual restoration drawing


Unearthed Costume
(1616AD-1911AD)

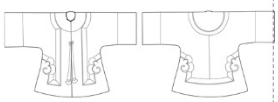
Flat

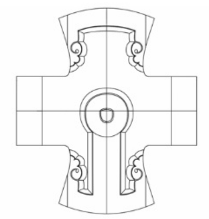
Pattern


Virtual restoration drawing


Unearthed Costume
(1616AD-1911AD)

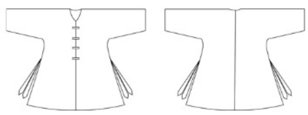
Flat

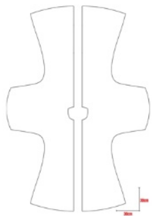
Pattern


Virtual restoration drawing


Unearthed Costume
(1616AD-1911AD)

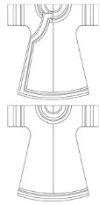
Flat

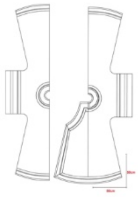
Pattern


Virtual restoration drawing


Unearthed Costume
(1616AD-1911AD)

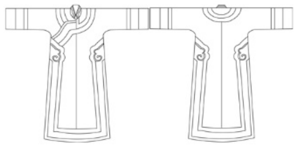
Flat

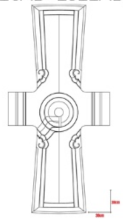
Pattern


Virtual restoration drawing


Unearthed Costume
(1616AD-1911AD)

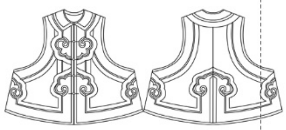
Flat

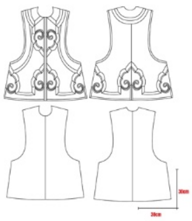
Pattern


Virtual restoration drawing


Unearthed Costume
(1616AD-1911AD)

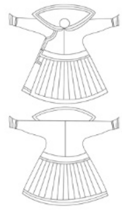
Flat

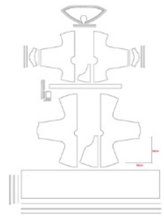
Pattern


Virtual restoration drawing


Unearthed Costume
(1616AD-1911AD)

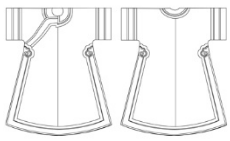
Flat

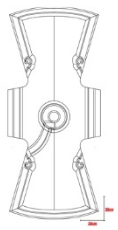
Pattern


Virtual restoration drawing


Unearthed Costume
(1616AD-1911AD)

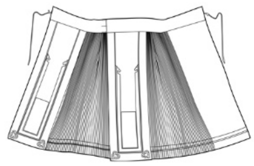
Flat

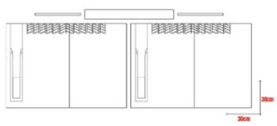
Pattern


Virtual restoration drawing

Unearthed Costume
(1616AD-1911AD)

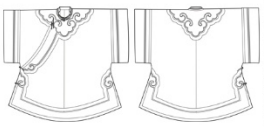

Flat

Unearthed Costume
(1616AD-1911AD)

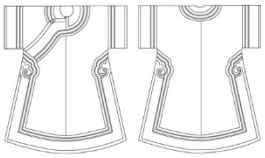

Flat

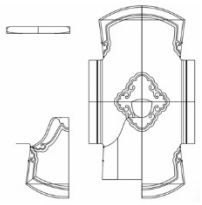

Pattern

Virtual restoration drawing

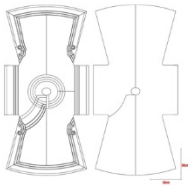

Pattern

Virtual restoration drawing

Unearthed Costume
(1616AD-1911AD)

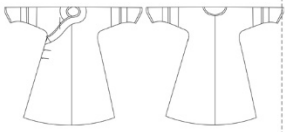

Flat

(1616AD-1911AD)

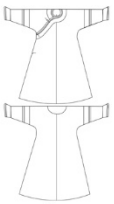

Flat

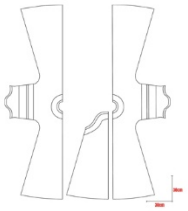

Pattern

Virtual restoration drawing

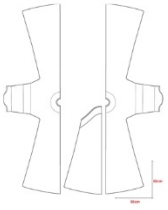

Pattern

Virtual restoration drawing

Unearthed Costume
(1616AD-1911AD)

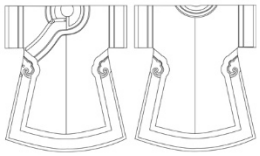

Flat

Unearthed Costume
(1616AD-1911AD)

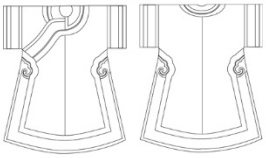

Flat

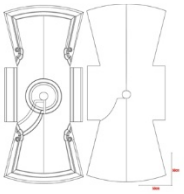

Pattern

Virtual restoration drawing

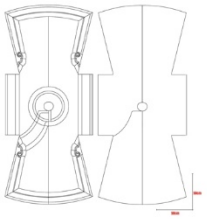

Pattern

Virtual restoration drawing


Unearthed Costume
(1616AD-1911AD)

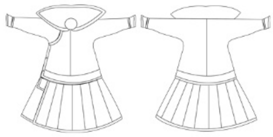
Flat


Unearthed Costume
(1616AD-1911AD)

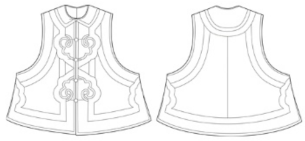
Flat

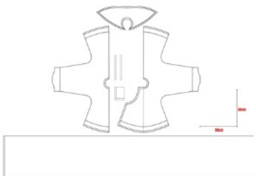
Pattern


Virtual restoration drawing


Pattern


Virtual restoration drawing


Unearthed Costume
(1616AD-1911AD)

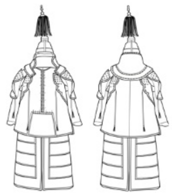
Flat


Unearthed Costume
(1616AD-1911AD)

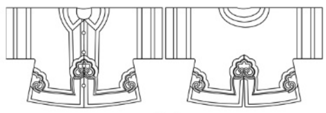
Flat

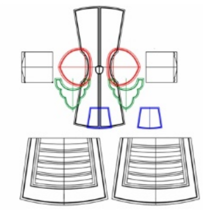
Pattern


Virtual restoration drawing

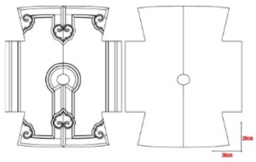
Pattern


Virtual restoration drawing


Unearthed Costume
(1616AD-1911AD)


Flat


Unearthed Costume
(1616AD-1911AD)

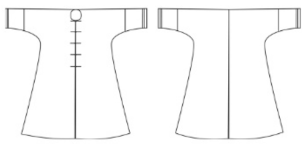
Flat

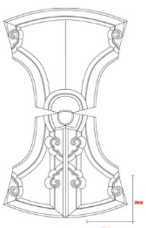
Pattern


Virtual restoration drawing

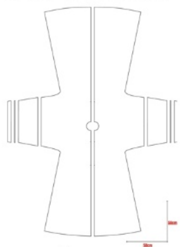
Pattern


Virtual restoration drawing


Unearthed Costume
(1616AD-1911AD)

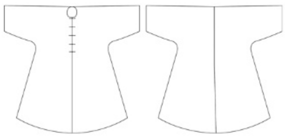
Flat

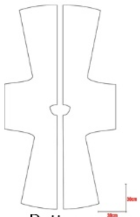
Pattern


Virtual restoration drawing


Unearthed Costume
(1616AD-1911AD)

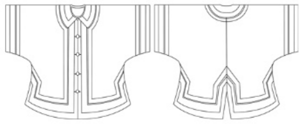
Flat

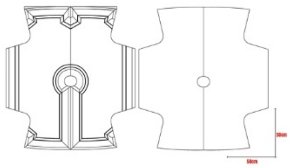
Pattern


Virtual restoration drawing


Unearthed Costume
(1616AD-1911AD)

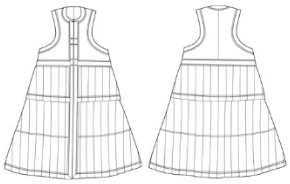
Flat

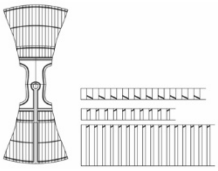
Pattern


Virtual restoration drawing


Unearthed Costume
(1616AD-1911AD)

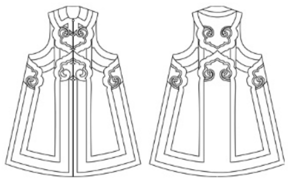
Flat

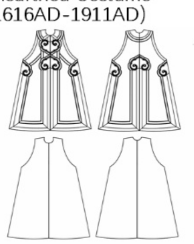
Pattern


Virtual restoration drawing


Unearthed Costume
(1616AD-1911AD)

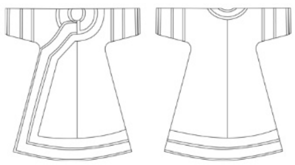
Flat

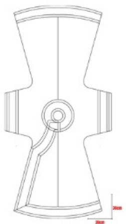
Pattern


Virtual restoration drawing


Unearthed Costume
(1616AD-1911AD)

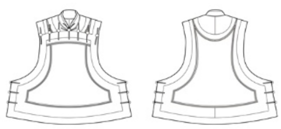
Flat

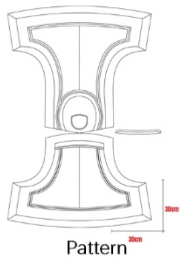
Pattern


Virtual restoration drawing


Unearthed Costume
(1616AD-1911AD)
Flat
Pattern
Virtual restoration drawing

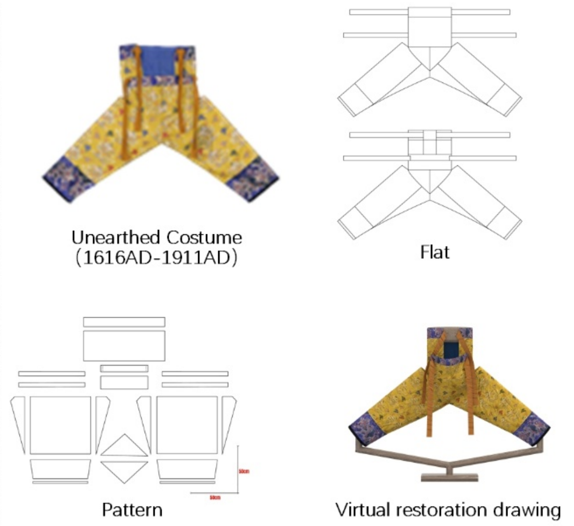
Unearthed Costume
(1616AD-1911AD)
Flat
Pattern
Virtual restoration drawing

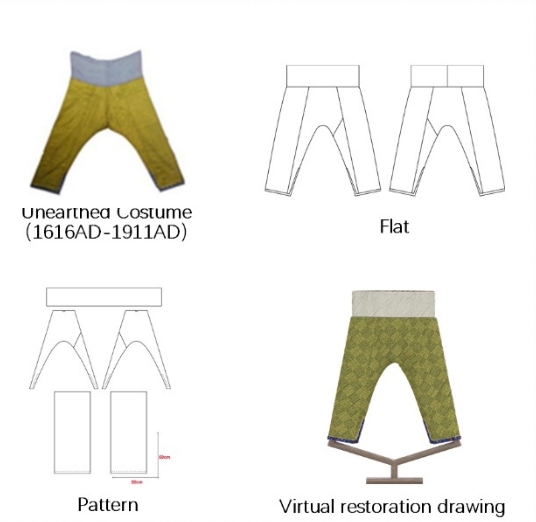
Unearthed Costume
(1616AD-1911AD)
Flat
Pattern
Virtual restoration drawing

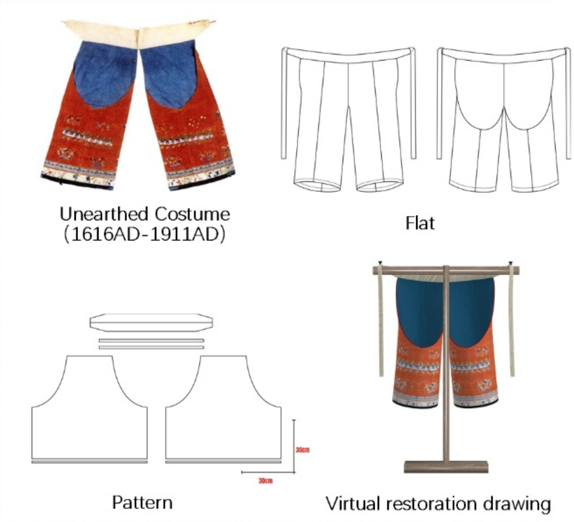
Unearthed Costume
(1616AD-1911AD)
Flat
Pattern
Virtual restoration drawing

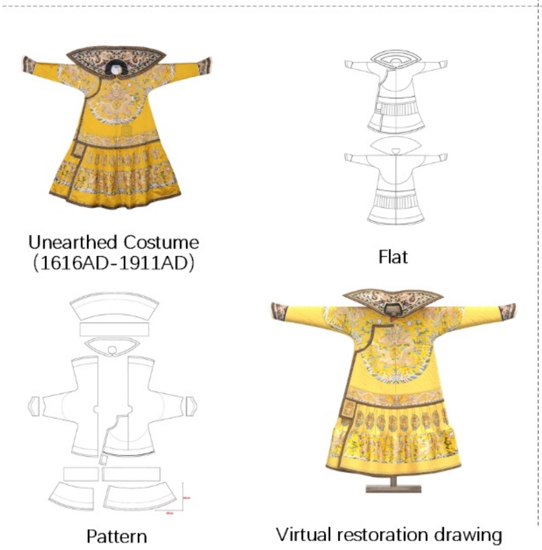
Unearthed Costume
(1616AD-1911AD)
Flat
Pattern
Virtual restoration drawing

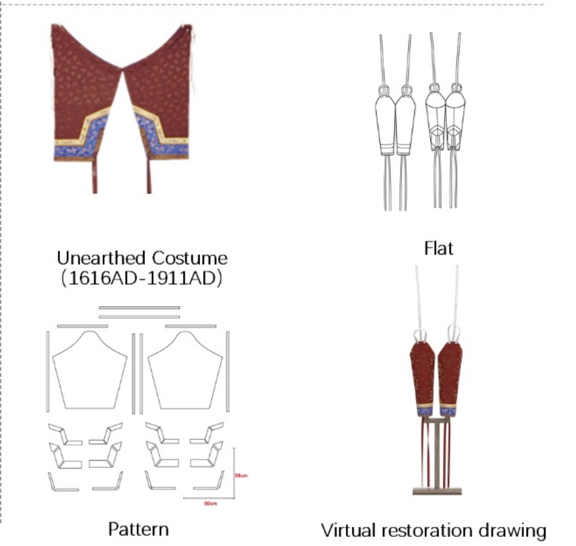
Unearthed Costume
(1616AD-1911AD)
Flat
Pattern
Virtual restoration drawing

References

1. Rasmussen, K.L., et al., *Mapping diagenesis in archaeological human bones.* Heritage Science, 2019. **7**(1): p. 41.
2. Chen, G., et al., *MOF-818 nanoparticles as radical scavengers to improve the aging resistance of silk fabric.* Scientific Reports, 2024. **14**(1): p. 22289.
3. Karetzky, P.E., *The Art of Women in Contemporary China: Both Sides Now*. 2020, Cambridge: Cambridge Scholars Publishing.
4. Ren, H., et al., *Dunhuang murals image restoration method based on generative adversarial network.* Heritage Science, 2024. **12**(1): p. 39.
5. Diao, X., et al., *Oracle bone inscription image restoration via glyph extraction.* npj Heritage Science, 2025. **13**(1): p. 321.
6. Yang, R. and X. Yang, *A study on cultural characteristics of Taoist clothing.* Asian Social Science, 2020. **16**(4): p. 1–70.
7. James, G., et al., *Linear regression*, in *An introduction to statistical learning: With applications in python*. 2023, Springer: Berlin. p. 69–134.
8. Radford, A., L. Metz, and S. Chintala, *Unsupervised representation learning with deep convolutional generative adversarial networks.* arXiv preprint arXiv:1511.06434, 2015.
9. Hua, Y., et al., *Deep learning with long short-term memory for time series prediction.* IEEE Communications Magazine, 2019. **57**(6): p. 114–119.
10. 袁建平, ***中国古代服饰中的深衣研究***. 求索, 2000(02): p. 113–116.
11. Hallmann, A., *Clothing (non-royal), Pharaonic Egypt.* The Encyclopedia of Ancient History, 2017: p. 1–9.
12. Lee, N.H., *A study on the costume of ancient Western Asia.* Journal of the Korean Society of Clothing and Textiles, 1978. **2**(1): p. 117–124.
13. Lee, M.M., *Body, dress, and identity in ancient Greece*. 2015, Cambridge: Cambridge University Press.
14. Li, Y., et al., *Multi-analytical techniques used for the identification of the dyeing techniques of several textile of ancient China.* Microchemical Journal, 2020. **156**: p. 104–123.
15. Żuchowska, M., *Between realism and artistic convention: Woollen mantles in the iconography of Roman Palmyra.* Textiles in Ancient Mediterranean Iconography, 2022: p. 161–199.
16. 赵丰, 周旸, and 刘剑, ***中国纺织考古与科学研究***. 2018: 上海科学技术出版社.

17. Baxromov, U. and B. Xamroxo'jayev, *National fabrics of Fergana valley, methods of preparation, types of fabrics, traditions and modernity.* International Journal of Development and Public Policy, 2021. **1**(5): p. 27–29.
18. 杨道圣, ***沈从文与服饰史研究的三重证据法***. 艺术设计研究, 2021(02): p. 44–48.
19. Franklin, M., *Gender, Clothing Fasteners, and Dress Practices in Houston's Freedmen's Town, ca. 1880–1904.* Historical Archaeology, 2020. **54**(3): p. 556–580.
20. Sha, S., et al., *Image Classification and Restoration of Ancient Textiles Based on Convolutional Neural Network.* International Journal of Computational Intelligence Systems, 2024. **17**(1): p. 11.
21. Liu, K., K. Lin, and C. Zhu, *Research on Chinese traditional opera costume recognition based on improved YOLOv5.* Heritage Science, 2023. **11**(1): p. 40.
22. Wang, Z., et al., *Artistic Characteristics and Fashion Practice of Traditional K'o-ssu in China.* Fibres & Textiles in Eastern Europe, 2021: p. 106–111.
23. Orifjonova, G.R., *Peculiarities of Surkhandarya ethnocultural clothing.* Current research journal of history, 2022. **3**(01): p. 21–25.
24. Hildebrandt, B., *The terminology of silks in texts of the Roman Empire: Qualities, Origins, Products, and Uses.* Acta Via Serica, 2021. **6**(2): p. 117–139.
25. 沙莎, et al., ***基于深度学习的楚国墓葬纺织品图像复原***. 丝绸, 2023. **60**(05): p. 1–7.
26. Zhang, X. and J.J. Tang, *Reinforcing and preserving ancient silk fabrics.* Sciences of conservation and archaeology, 1999. **11**(1): p. 23–30.
27. 孙选铭 and 苏淼, ***基于深度学习的丝绸文物纹样识别应用***. 丝绸, 2023. **60**(08): p. 1–10.
28. Liu, K., et al., *Study on digital protection and innovative design of Qin opera costumes.* Heritage Science, 2022. **10**(1): p. 127.
29. 宋歌, ***从考古资料谈汉代服饰色彩的变化及其原因***. 中原文物, 2021(05): p. 119–123.
30. Liu, J., et al., *Profiling by HPLC-DAD-MSD reveals a 2500-year history of the use of natural dyes in Northwest China.* Dyes and Pigments, 2021. **187**: p. 109–143.
31. Gou, A. and J. Wang, *The development of roof color in ancient China.* Color Research & Application, 2010. **35**(4): p. 246–266.
32. Gribkov, V.S. and V.M. Petrov, *Color elements in national schools of painting: A statistical investigation.* Empirical Studies of the Arts, 1996. **14**(2): p. 165–181.
33. Houston, M.G., *Ancient Egyptian, Mesopotamian & Persian Costume*. 2002, Chicago: Courier Corporation.
34. Finlay, R., *Weaving the rainbow: visions of color in world history.* Journal of World History, 2007: p. 383–431.

35. Guo, R., et al., *Rare colour in medieval China: Case study of yellow pigments on tomb mural paintings at Xi'an, the capital of the Chinese Tang dynasty.* Archaeometry, 2021: p. 1–15.
36. Siddall, R., *Mineral pigments in archaeology: their analysis and the range of available materials.* Minerals, 2018. **8**(5): p. 201–213.
37. Tamburini, D., *Colour Analysis: An Introduction to the Power of Studying Pigments and Dyes in Archaeological and Historical Objects.* Heritage 2021. **4**(4): p. 4366–4371.
38. 赵丰, *纺织**考古***. 2007, 北京: 文物出版社.
39. 何秋菊, ***文物色彩分析与保护***. 2018, 北京: 北京燕山出版社.
40. Szulc, J., et al., *Metabolomics and metagenomics analysis of 18th century archaeological silk.* International Biodeterioration & Biodegradation, 2021. **156**: p. 1–15.
41. Vasileiadou, A., I. Karapanagiotis, and A. Zotou, *Development and validation of a liquid chromatographic method with diode array detection for the determination of anthraquinones, flavonoids and other natural dyes in aged silk.* Journal of Chromatography A, 2021. **1651**: p. 1–20.
42. 寿晨超, et al., ***天然染料**质谱**数据库**的建立与**应用***. 纺织学报, 2023. **44**(11): p. 120–131.
43. 高素芸, et al., ***古代染料及其分析**检测**技术***. 文物保护与考古科学, 2023. **35**(06): p. 164–171.
44. 刘帅, et al., *纺织**品类**文物材**质**与染料分析方法***. 文物保护与考古科学, 2021. **33**(02): p. 110–119.
45. Harris, S., *The sensory archaeology of textiles*, in *The Routledge Handbook of Sensory Archaeology*. 2019, Routledge: London. p. 210–232.
46. 沈从文, ***中国古代服**饰**研究***. 2011, 北京: 商务印书馆.
47. 陶辉, et al., *"披发左衽,华夷之辨"的考辨*. 装饰, 2020(07): p. 90–92.
48. Chai, J., R. Cui, and L. Niu, *Study on the technological process and artistic characteristics of ancient Chinese Zhuanghua silk fabric.* Fibres & Textiles in Eastern Europe, 2021: p. 101–109.
49. 沈华菊, ***步**线**行**针**成**华**章**——*记**中国古代服**饰**文化展***. 美术观察, 2021(05): p. 30–31.
50. Saunier, I., et al., *Making clothes, dressing the deceased: Analysis of 2nd century AD silk clothing from the child mummy of Burgast (Altai Mountains, Mongolia).* Archaeological Research in Asia, 2022. **29**: p. 1–35.
51. Zheng, Y., *Drawing Technology and Method of Digital Restoration of Ancient Chinese Costume Structure—Take Tibetan Silk Robe in the Qing Dynasty as an Example.* Asian Social Science, 2023. **19**(1): p. 46.

52. Lipkin, S., et al., *Textiles: Decay and Preservation in Seventeenth-to Nineteenth-Century Burials in Finland.* Historical Archaeology, 2021. **55**(1): p. 49–64.
53. Polosmak, N., *Clothes from the XiongNu wardrobe (Based on finds from the Noin-Ula Burial Mounds).* Archaeology and Early History of Ukraine, 2020. **36**(3): p. 431–444.
54. Bass-Krueger, M., *Fashion Collections, Collectors, and Exhibitions in France, 1874–1900: Historical imagination, the spectacular past, and the practice of restoration.* Fashion Theory, 2018. **22**(4-5): p. 405–433.
55. Chen, H., et al., *The restoration of garment heritages based on digital virtual technology: A case of the Chinese pale brown lace-encrusted unlined coat.* Industria Textila, 2023. **74**(1): p. 12–20.
56. 尚玉平, et al., ***新疆尼雅墓地出土纺织品文物的数字化信息采集——以95MNIM8:15“五星出东方利中国”织锦护臂为例.*** 文物, 2020(05): p. 80–88.
57. Liu, K., et al., *Virtual simulation of Yue Opera costumes and fashion design based on Yue Opera elements.* Fashion and Textiles, 2022. **9**(1): p. 31.
58. Creswell, A., et al., *Generative adversarial networks: An overview.* IEEE signal processing magazine, 2018. **35**(1): p. 53–65.
59. Goodfellow, I.J., et al., *Generative adversarial nets.* Advances in neural information processing systems, 2014. **27**.
60. Brock, A., J. Donahue, and K. Simonyan, *Large scale GAN training for high fidelity natural image synthesis.* arXiv preprint arXiv:1809.11096, 2018.
61. Gulrajani, I., et al., *Improved training of wasserstein gans.* Advances in neural information processing systems, 2017. **30**.
62. Salimans, T., et al., *Improved techniques for training gans.* Advances in neural information processing systems, 2016. **29**.
63. Heusel, M., et al., *Gans trained by a two time-scale update rule converge to a local nash equilibrium.* Advances in neural information processing systems, 2017. **30**.
64. Wang, Z., et al., *Image quality assessment: from error visibility to structural similarity.* IEEE transactions on image processing, 2004. **13**(4): p. 600–612.
65. Zhu, C., et al., *Research on Archaeology and Digital Restoration of Costumes in DaoLian Painting.* Sustainability, 2022. **14**(21): p. 14054.
66. Liu, K., J. Zhao, and C. Zhu, *Research on Digital Restoration of Plain Unlined Silk Gauze Gown of Mawangdui Han Dynasty Tomb Based on AHP and Human–Computer Interaction Technology.* Sustainability, 2022. **14**(14): p. 8713.
67. Liu, K., et al., *Research on Archaeology and Digital Restoration of Costumes in Spring Outing Painting of Madam Guo.* Sustainability, 2022. **14**(19): p. 12243.

68. Xie, J., et al., *ECLNet: enhancing the CNN-LSTM networks for multivariate long-term time series forecasting: J. Xie et al.* Applied Intelligence, 2025. **55**(10): p. 743.
69. Jogin, M., et al. *Feature extraction using convolution neural networks (CNN) and deep learning*. in *2018 3rd IEEE international conference on recent trends in electronics, information & communication technology (RTEICT)*. 2018. IEEE.
70. Lindemann, B., et al., *A survey on long short-term memory networks for time series prediction.* Procedia CIRP, 2021. **99**: p. 650–655.
71. Tofallis, C., *A better measure of relative prediction accuracy for model selection and model estimation.* Journal of the Operational Research Society, 2015. **66**(8): p. 1352–1362.
72. Willmott, C.J. and K. Matsuura, *Advantages of the mean absolute error (MAE) over the root mean square error (RMSE) in assessing average model performance.* Climate Research, 2005. **30**: p. 79–82.
73. 高丹丹 and 贾荣林, *浅谈"敬天惜物"造物思想在中国传统服饰中的应用.* 文物鉴定与鉴赏, 2017(11): p. 70–72.
74. 刘瑞璞 and 陈静洁, *中华民族服饰结构图考+汉族编.* 2013, 北京: 中国纺织出版社.
75. 湖南省博物馆 and 中国科学院考古研究所, *长沙马王堆一号汉墓（下）*. 1973, 北京: 文物出版社.
76. 范盈, *唐代襦裙装的研究及其设计应用.* 福建师范大学.
77. 卿源 and 梁惠娥, *宋代服饰"褙子"的形制及其功能考释.* 丝绸, 2021.
78. 福建省博物馆, *福州南宋黄升墓*. 1982, 北京: 文物出版社.
79. 山东博物馆, *鲁荒王墓*. 2014, 北京: 文物出版社.
80. 沈玉, 吴欣, and 付燕妮, *清代龙纹袍的袖部形制特点及内涵.* 服装学报, 2020. **5**(02): p. 134–138,155.
81. 林化煦, *圆领袍:从另类衣冠到流行服饰.* 贵阳文史, 2014(05): p. 84.
82. 吕丽, *古代冠服礼仪的法律规制.* 法制与社会发展, 2004(06): p. 55–59.
83. 孙汝洁, *周代冕服与周礼.* 管子学刊, 2006(04): p. 97–99.
84. 李采姣, *从冕服制度看中国服饰美术的寓意.* 文艺研究, 2013(03): p. 156–158.
85. 吴雨 and 王强, *历代冕服考略——"古礼"传统与王朝制度的互动.* 艺术传播研究, 2022(04): p. 70–78.
86. 骆浩, *西周朝服制度研究.* 艺术探索, 2024. **38**(01): p. 6–13.
87. 吴爱琴, *从先秦人物形象看服制阶级性的形成.* 中原文物, 2015(03): p. 45–51+62.
88. 夏添, *先秦至汉代荆楚服饰考析*. 2020.
89. 阎步克, *服周之冕:《周礼》六冕礼制的兴衰变异*. 2009, 北京: 中华书局.

90. 罗茜尹 and 王亚蓉, *复制的纹理——从战国织锦看中国交织的早期原理*. 南方文物, 2021. **000**(004): p. 198–205.
91. 李超德, *试论先秦染织纹样*. 丝绸, 2004(08): p. 38–39.
92. 宋金英 and 刘国联, *"阴阳五行"对先秦服饰色彩的影响*. 管子学刊, 2010(01): p. 88–91.
93. 湖北省荆州地区博物馆, *江陵马山一号楚墓*. 1985, 北京: 文物出版社.
94. 包铭新, *西域异服:丝绸之路出土古代服饰艺术复原研究*. 2007, 上海: 东华大学出版社.
95. 徐蕊, *汉代服饰的发展轨迹及其变化动因分析*. 中原文物, 2011(04): p. 63–68.
96. 范强, *汉代服饰风格及其成因探析*. 南京艺术学院学报(美术与设计版), 2008(04): p. 109–111.
97. 付野, *从长沙马王堆汉墓文物看汉代服饰艺术*. 兰台世界, 2014(12): p. 149–150.
98. 胡嫔, *论汉代服饰图案融入时装艺术的审美价值*. 装饰, 2010(08): p. 140–141.
99. 王树金, *马王堆汉墓服饰研究*. 湖南博物馆藏品研究大系, ed. 陈建明. 2016, 北京: 中华书局.
100. 苏日娜 and 李娟, *多民族服饰融合与中华文化认同——以魏晋南北朝时期为中心的考察*. 中南民族大学学报(人文社会科学版), 2021. **41**(09): p. 27–33.
101. 周兆望，侯永惠, *魏晋南北朝妇女的服饰风貌与个性解放*. 中国史研究, 1995(03): p. 13–20.
102. 张妍, *胡汉交融背景下的"袴褶"服饰研究——以魏晋南北朝时期为例*. 丝绸, 2017. **54**(02): p. 67–72.
103. 陈丽君, *魏晋南北朝褠裆衫研究*. 2012, 北京服装学院.
104. 吴山, *中国纹样全集(全4卷)*. 2009, 济南: 山东美术出版社.
105. 王芙蓉, *魏晋南北朝时期玄学对当时服饰的影响*. 兰台世界, 2007(18): p. 60–61.
106. 李源, *魏晋南北朝时期女性服饰中的五色研究*. 2023, 湖北美术学院.
107. 孙机, *唐代妇女的服装与化妆*. 文物, 1984. **4**: p. 011.
108. 刘睿佳 and 邵新艳, *唐代半臂中的肩部拼接与历史渊源探析*. 丝绸, 2022. **59**(11): p. 143–149.
109. 张玲, *南宋女装形制风格研究*. 2018, 北京服装学院.
110. 蔡欣, 朱小行, and 陈晓风, *南宋墓葬出土男性服饰植物纹样研究*. 装饰, 2019(12): p. 126–127.
111. Ying, Q. and Z. Xiaohong, *Research on the Color Culture of Red in Chinese Traditional Costume*. Journal of the Color Science Association of Japan, 2020. **44**(3+): p. 186.

112. 吴灵姝, 倪沈键, and 吴元新, *南宋至民国时期有关药斑布的记载与研究*. 南京艺术学院学报(美术与设计版), 2020(06): p. 102–105+210.

113. 乌云, *元代蒙古族服饰的动态特征*. 装饰, 2008(08): p. 126–127.

114. 姚进, *元代服饰设计史料研究*. 2013.

115. 黄蓉, *基于上都扈从诗文本可视化的元代服饰研究*. 2024.

116. 李甍, *历代《舆服志》图释. 元史卷*. 2017, 东华大学出版社: 历代舆服志图释. 元史卷.

117. 宋春会, *艺术考古视域下明代男袍考析与结构复原研究*. 2021, 江南大学.

118. 牛犁 and 林鹏飞, *明末江南地区士族墓出土马面裙考析*. 艺术设计研究, 2023(06): p. 42–48.

119. 祁姿妤, *史更几兴废,物华常流传——马面裙的始末、解构与重组*. 艺术设计研究, 2015(02): p. 84–93.

120. 李理, *清代官制与服饰*. 2009, 沈阳: 辽宁民族出版社.

121. 房宏俊, 严勇, and 万钧, *对清代八团彩云金龙纹吉服的再认识*. 故宫博物院院刊, 2007(02): p. 80–93+157.

122. 李俞霏, 范卓雅, and 王云飞, *清代服饰中三多纹艺术特征分析*. 服装学报, 2024. **9**(03): p. 243–249.

123. 王明杰 and 孙成成, *清代宫廷服饰纹样元素的内涵特征与形成原因*. 兰台世界, 2013(13): p. 100–101.

124. 王渊, *《苏州织造局志》载清代补服信息考*. 丝绸, 2018. **55**(05): p. 91–95.

125. 常卓, *以"样"为媒:清代宫廷衣物织造之"样"式考析*. 丝绸, 2025. **62**(07): p. 108–115.

126. 梁文昱, *元明清《舆服志》服饰色彩研究*. 2021.

127. 张毓雯, *满族宝蓝色暗花绸五彩绣挽袖夹氅衣*. 艺术设计研究, 2020(06): p. 2+129.

128. 张雪飞, *人衣关系视域下的晚清民国女性服饰变革研究*. 2021.

129. 杨渝 and 杨悦, *清末旗装艺术与民国旗袍的传承关系*. 民族艺术, 2013(03): p. 159–160.

130. 张成义 and 李群英, *中国旗袍造型艺术元素的审美演变及其文化传承*. 艺术百家, 2020. **36**(04): p. 62–67.

131. Wu, H., et al., *Archaeological and digital restoration of straight-front robe of Mawangdui Han Dynasty Tomb based on 3D reverse engineering and man-machine interactive technologies.* Industria Textila, 2022. **73**(6): p. 635–644.

Academic research during doctoral studies

[1] **Zhu Chun**, Liu Kaixuan, Wang Ruolin, Wang Jianping, Bruniaux Pascal, Zeng Xianyi. The mathematical model of men's garment prototype [J]. Int J Cloth Sci Technol, 2022, 34(6): 892-904. (**SCI**)

[2] **Zhu Chun**, Liu Kaixuan, Lin Kai, Wang Jianping. Research on the functional pattern-making of men's windbreaker [J]. Int J Cloth Sci Technol, 2022, 34(4): 516-31. (**SCI**)

[3] **Zhu Chun**, Liu Kaixuan, Li Xiaoning, Zeng Qingwei, Wang Ruolin, Zhang Bin, Lü Zhao, Chen Chen, Xin Xiaoyu, Wu Yunlong, Zhang Junjie, Zeng Xianyi. Research on Archaeology and Digital Restoration of Costumes in DaoLian Painting [J]. Sustainability, 2022, 14(21): 14054. （**SSCI/SCI**）

[4] **Zhu Chun**, Gao Yuanyuan, Wang Jianping, Zeng Xianyi, Bruniaux Pascal, Liu Kaixuan. Study and restoration of the costume of the HuoLang (Peddler) in the Ming Dynasty of China [J]. AUTEX Research Journal, 2025, 25(1). (**SCI**)

[5] Liu Kaixuan, **Zhu Chun**, Xuyuan Tao, Bruniaux Pascal, Xianyi Zeng, Wang Jianping. A novel evaluation technique for human body perception of costume fit [J]. Multimedia Tools and Applications, 2023, 82: 21057–69. (**SCI**)

[6] Liu Kaixuan, Wu Hanhan, Gao Yuanyuan, **Zhu Chun,** Ji Yanbo, Zhao Lü. Archaeology and Virtual Simulation Restoration of Costumes in the Han Xizai Banquet Painting [J]. Autex Research Journal, 2023, 23(2): 238-52. (**SCI**)

[7] Liu Kaixuan, Wang Ruolin, Hao Xinyue, **Zhu Chun**, Zhou Shunmuzi, Zeng Xianyi, Tao Xuyuan, Bruniaux Pascal, Wang Jianping. Garment fit evaluation using neural networks technology [J]. The Journal of The Textile Institute, 2023: 1-11. (**SCI**)

[8] Liu Kaixuan, Lin Kai, **Zhu Chun**. Research on Chinese traditional opera costume recognition based on improved YOLOv5 [J]. Heritage Science, 2023, 11(1): 40. (**AHCI/SCI**)

[9] Wu Hanhan, Liu Kaixuan, Ji Yanbo, **Zhu Chun**, Lü Zhao. Archaeological and digital restoration of straight-front robe of Mawangdui Han Dynasty Tomb based on 3D reverse engineering and man-machine interactive technologies [J]. Industria Textila, 2022, 73(6): 635–44. (**SCI**)

[10] Liu Kaixuan, Zhou Shunmuzi, **Zhu Chun**, Lü Zhao. Virtual simulation of Yue Opera costumes and fashion design based on Yue Opera elements [J]. Fashion and Textiles, 2022, 9(1): 31. (**SCI**)

[11] Liu Kaixuan, Zhou Shunmuzi, **Zhu Chun**. Historical changes of Chinese costumes from the perspective of archaeology [J]. Heritage Science, 2022, 10(1): 205. (**AHCI/SCI**)

[12] Liu Kaixuan, Wu Hanhan, **Zhu Chun**, Wang Jianping, Zeng Xianyi, Tao Xuyuan, Bruniaux Pascal. An evaluation of garment fit to improve customer body fit of fashion design costume [J]. The International Journal of Advanced Manufacturing Technology, 2022, 120(3-4): 2685-99. (**SCI**)

[13] Liu Kaixuan, Gao Yuanyuan, Zhang Jiaqi, **Zhu Chun**. Study on digital protection and innovative design of Qin opera costumes [J]. Heritage Science, 2022, 10(1): 127. (**AHCI/SCI**)

[14] Zhang Junjie, Liu Kaixuan, Dong Min, Yuan Hua, **Zhu Chun,** Zeng Xianyi. An intelligent garment recommendation system based on fuzzy techniques [J]. The Journal of The Textile Institute, 2020, 111(9): 1324-30. (**SCI**)

Acknowledgments

As my doctoral thesis is about to be published, my heart is filled with gratitude. Firstly, I would like to sincerely thank my two foreign mentors - Professor Pascal and Professor Xianyi Zeng from ENSAIT in France. Professor Pascal, with his profound academic achievements and rigorous academic attitude, has pointed out the direction of my research and provided me with valuable guidance and encouragement at critical moments. Professor Xianyi Zeng, with his keen insight and rich practical experience, has helped me continuously overcome difficulties in my research and broaden my academic horizons. The careful cultivation and selfless dedication of the two professors have given me endless warmth and strength on my journey of studying in a foreign land.

At the same time, I would like to express my special thanks to my domestic mentor, Professor Wang Jianping from Donghua University. Teacher Wang not only provided me with careful guidance during the selection, writing, and revision process of my doctoral thesis, but also always showed me motherly care and patience when I encountered difficulties and challenges, helping me to solve problems and feel the warmth of home. Teacher Wang's rigorous academic style, noble professional ethics, and selfless dedication will always inspire me to move forward.

Here, I would like to express my sincerest gratitude to the three mentors. It is your careful guidance and selfless dedication that have enabled me to successfully complete my doctoral thesis and take a solid step on my academic path. In the days to come, I will remember my teacher's kindness, continue to work hard, and not disappoint your expectations and cultivation.

Zhu Chun at Ensait

October 15, 2025